

INFORMATION TO USERS

This manuscript has been reproduced from the microfilm master. UMI films the text directly from the original or copy submitted. Thus, some thesis and dissertation copies are in typewriter face, while others may be from any type of computer printer.

The quality of this reproduction is dependent upon the quality of the copy submitted. Broken or indistinct print, colored or poor quality illustrations and photographs, print bleedthrough, substandard margins, and improper alignment can adversely affect reproduction.

In the unlikely event that the author did not send UMI a complete manuscript and there are missing pages, these will be noted. Also, if unauthorized copyright material had to be removed, a note will indicate the deletion.

Oversize materials (e.g., maps, drawings, charts) are reproduced by sectioning the original, beginning at the upper left-hand corner and continuing from left to right in equal sections with small overlaps.

ProQuest Information and Learning
300 North Zeeb Road, Ann Arbor, MI 48106-1346 USA
800-521-0600

UMI[®]

University of Alberta

Identification and characterization of the EmhABC efflux system for polycyclic aromatic hydrocarbons in *Pseudomonas fluorescens* cLP6a

by

Elizabeth M. Hearn



A thesis submitted to the Faculty of Graduate Studies and Research in partial fulfillment of the

requirements for the degree of Doctor of Philosophy

Department of Chemical and Materials Engineering
Department of Biological Sciences

Edmonton, Alberta
Fall 2005



Library and
Archives Canada

Bibliothèque et
Archives Canada

0-494-08655-6

Published Heritage
Branch

Direction du
Patrimoine de l'édition

395 Wellington Street
Ottawa ON K1A 0N4
Canada

395, rue Wellington
Ottawa ON K1A 0N4
Canada

Your file *Votre référence*

ISBN:

Our file *Notre référence*

ISBN:

NOTICE:

The author has granted a non-exclusive license allowing Library and Archives Canada to reproduce, publish, archive, preserve, conserve, communicate to the public by telecommunication or on the Internet, loan, distribute and sell theses worldwide, for commercial or non-commercial purposes, in microform, paper, electronic and/or any other formats.

The author retains copyright ownership and moral rights in this thesis. Neither the thesis nor substantial extracts from it may be printed or otherwise reproduced without the author's permission.

AVIS:

L'auteur a accordé une licence non exclusive permettant à la Bibliothèque et Archives Canada de reproduire, publier, archiver, sauvegarder, conserver, transmettre au public par télécommunication ou par l'Internet, prêter, distribuer et vendre des thèses partout dans le monde, à des fins commerciales ou autres, sur support microforme, papier, électronique et/ou autres formats.

L'auteur conserve la propriété du droit d'auteur et des droits moraux qui protègent cette thèse. Ni la thèse ni des extraits substantiels de celle-ci ne doivent être imprimés ou autrement reproduits sans son autorisation.

In compliance with the Canadian Privacy Act some supporting forms may have been removed from this thesis.

Conformément à la loi canadienne sur la protection de la vie privée, quelques formulaires secondaires ont été enlevés de cette thèse.

While these forms may be included in the document page count, their removal does not represent any loss of content from the thesis.

Bien que ces formulaires aient inclus dans la pagination, il n'y aura aucun contenu manquant.

Canada

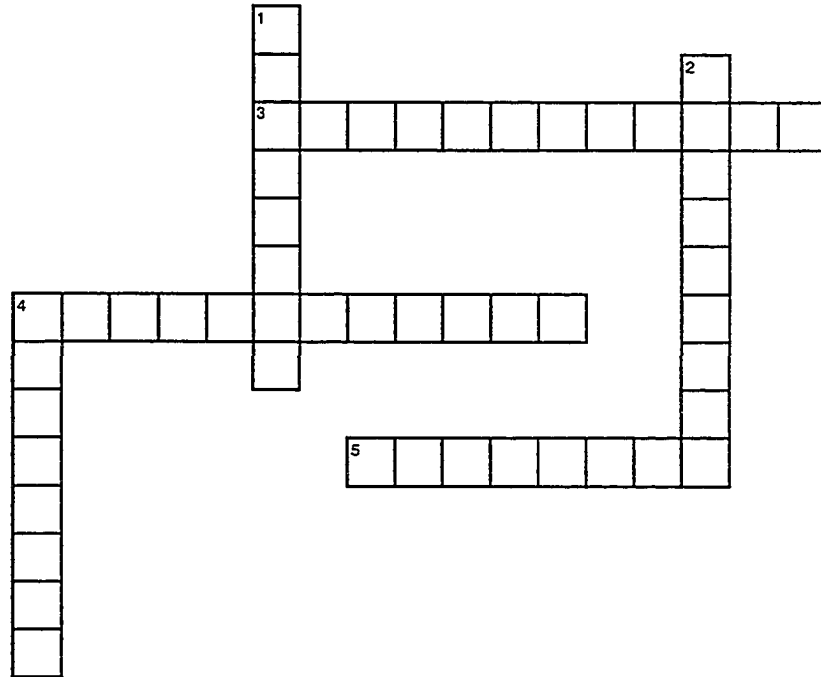
ABSTRACT

Efflux systems belonging to the resistance-nodulation-cell division, or RND, family are prevalent in pseudomonads where they contribute to the resistance of these bacteria to a wide range of toxic, hydrophobic compounds, including antibiotics and solvents. Studies with the polycyclic aromatic hydrocarbon-degrading bacterium *Pseudomonas fluorescens* cLP6a demonstrated that the non-toxic aromatic hydrocarbons phenanthrene, anthracene and fluoranthene were substrates of an active efflux system. An RND efflux system designated EmhABC for efflux of multicyclic hydrocarbons, which showed high homology to antibiotic and solvent efflux pumps, was identified in *P. fluorescens* and was responsible for the efflux of polycyclic aromatic hydrocarbons. The EmhABC efflux system consists of a periplasmic membrane fusion protein (EmhA), an inner membrane RND pump (EmhB) and an outer membrane factor protein (EmhC). These proteins are predicted to form a complex spanning the inner and outer membrane and to expel substrates directly to the extracellular medium. In addition to phenanthrene, anthracene and fluoranthene, the EmhABC efflux system recognizes and exports a number of structurally diverse antibiotics, including tetracycline, chloramphenicol, nalidixic acid, rhodamine 6G, dequalinium, ciprofloxacin, and erythromycin, as well as the monoaromatic solvent toluene. Although the EmhABC efflux system is expressed constitutively in *P. fluorescens*, *emhABC* gene expression is inducible by tetracycline and chloramphenicol, but not by other substrates of the efflux pump, suggesting that there is a complex relationship between pump substrates and expression. Site-directed mutagenesis experiments were designed to elucidate the mechanism for the broad substrate specificity of the RND efflux pump EmhB. These studies highlighted the roles of several key

structural features of the pump protein, including the central cavity and a putative hydrophobic substrate access channel, in substrate binding and translocation. A model for substrate transport through RND efflux pumps is proposed. Finally, polycyclic aromatic hydrocarbon efflux was observed in clinical and environmental strains of several gram-negative bacteria, indicating that the specificity of the EmhABC efflux system for aromatic hydrocarbons is not unique. The studies with the *P. fluorescens* EmhABC system have provided insight into the evolution and function of this transporter family.

ACKNOWLEDGEMENTS

My Acknowledgements Cryptic Crossword



Across

- 3** Doctor sounded happy reading thesis between black and white (2,6,4)
4 Forget I had Jule thankfully rearranging the missing points (2,5,5)
5 Thanks to professor who questioned a road from Saskatchewan (2,6)

Down

- 1** Appreciate professor sinned reading thesis backwards (2,6)
2 Thanks to doctor to select a rare degree initially (2,6)
4 Grateful to professor who ate some pickles, kiwis (2,6)

See answers below

I was fortunate to receive generous funding throughout my degree and would like to thank the following for their financial support: the Natural Science and Engineering Research Council (PGS A and B); the Izaak Walton Killam Memorial Scholarship, the Province of Alberta Graduate Fellowship; the Luscar Environmental Engineering Scholarship; the Department of Chemical and Materials Engineering; and the Faculty of Engineering.

To my supervisors, Dr. Julia Foght (4 across) and Dr. Murray Gray (3 across), your support, encouragement, and insight throughout this endeavor were greatly appreciated. I am grateful to you both for the opportunity to work on this project and for the freedom to approach the project from a different direction.

I'd like to thank my supervisory committee, Dr. Dennis (1 down) and Dr. Pickard (2 down), for their suggestions and encouragement throughout my research. Also, I'd like to thank the members of my examination committee Dr. Leskiw (4 down) and Dr. Howard (5 across) for their thoughtful review of my thesis.

I am grateful to Trevor Bugg, who started the efflux pump project in *P. fluorescens* LP6a, to Ruth Eckford, who provided helpful training on the transport assays, to Peggy Law, who constructed the promoter-reporter plasmids, to Brienne Borlé, who spent her summer doing numerous transport assays and antibiotic sensitivity assays on the pump mutants, and especially to the Jensen lab (Cecilia Anders, Annie Wong, Dr. Perrin Beatty and Dr. Kapil Tahlan), who shared their vast experience in molecular biology with me.

To everyone in the fourth floor microbiology wing with whom I have worked (and spent numerous lunch hours studying cryptic crossword clues) – Sara Ebert, Kathy Semple, Annie Wong, Cecilia Anders, Debbi Coy, Stephanie Cheng, Tara Penner, Rozlyn Young, Maya Bhatia, Kathlyn Kirkwood, Jonathan Klassen, Melissa Haveroen, Perrin Beatty, Jonathan van Hamme, Seena Farea, and Leah Kirkpatrick. Thank you to this great group of people for making my time in the lab a truly enjoyable experience (even when the research wasn't going so well). As well, I'd like to thank the other residents of the Biological Sciences Building, especially Jerry the cockroach and Mickey and his mouse family, for really livening up the place.

And my acknowledgements would not be complete without a huge thank you to my family, especially for living with me during the (often agonizing) writing process and allowing me to share the past six years with my (sometimes obedient, but always devoted) dog, Sandy.

Table of Contents

1. INTRODUCTION.....	1
1.1. Interactions of hydrophobic compounds with biological membranes	2
1.1.1. The cell membrane acts as a solvent for hydrophobic compounds	2
1.1.2. Hydrophobic compounds disrupt cell membranes.....	4
1.1.3. Cell membranes adapt to the presence of hydrophobic compounds.....	4
1.2. Active efflux as a mechanism of resistance.....	6
1.2.1. Overview of efflux systems	6
1.2.2. Active efflux systems contribute to multidrug resistance in gram-negative bacteria.....	7
1.2.3. Active efflux systems contribute to solvent tolerance	9
1.3. Substrate specificities of antibiotic and solvent efflux systems.....	10
1.4. Regulation of efflux pumps	11
1.4.1. Regulation of expression of solvent efflux pump genes in <i>P. putida</i>	11
1.4.2. Regulation of expression of RND multidrug efflux pump genes	14
1.4.3. Structural basis for the regulation of multidrug efflux systems by hydrophobic compounds	16
1.5. Structure and function of RND efflux systems.....	17
1.5.1. The outer membrane factor protein.....	17
1.5.2. The periplasmic membrane fusion protein	19
1.5.3. The inner membrane RND efflux pump	21
1.6. RND efflux systems in the environment.....	25
1.6.1. Solvent efflux systems are prevalent in the environment	25
1.6.2. An efflux system for polycyclic aromatic hydrocarbons is present in an environmental isolate	26
1.7. Objectives	26
2. MATERIALS AND METHODS.....	28
2.1. Chemicals.....	28
2.2. Bacterial strains, plasmids and growth conditions.....	28

2.3.	Phenotypic analysis of efflux ability.....	32
2.3.1.	Polycyclic aromatic hydrocarbon transport assays	32
2.3.2.	Determination of toluene tolerance.....	33
2.3.3.	Antibiotic sensitivity assays.....	33
2.4.	DNA techniques.....	34
2.4.1.	DNA isolation, cloning and transformation.....	34
2.4.2.	Polymerase chain reaction	35
2.4.3.	DNA sequencing.....	35
2.4.4.	Sequence analysis	36
2.5.	Identification of the <i>emhABC</i> genes	36
2.5.1.	Detection and inactivation of <i>emh</i>	36
2.5.2.	Sequencing the <i>emh</i> genes	37
2.5.3.	Nucleotide accession number	37
2.5.4.	Complementation of <i>emhABC</i> in <i>P. fluorescens</i> cLP6a-1	37
2.6.	Regulation of the <i>emhABC</i> efflux system.....	38
2.6.1.	Construction of <i>emh</i> promoter-reporter plasmids	38
2.6.2.	Determination of <i>emh</i> promoter activity.....	41
2.6.2.1.	Growth phase dependence	41
2.6.2.2.	Effect of hydrocarbons and metabolites	41
2.6.2.3.	Effect of antibiotics.....	42
2.6.3.	Measurement of β -galactosidase activity.....	42
2.7.	Site-directed mutagenesis of EmhB.....	43
2.7.1.	Construction of histidine-tagged EmhB.....	43
2.7.2.	Construction of site-directed mutations in EmhB _{his}	44
2.7.3.	SDS-polyacrylamide gel electrophoresis and western immunoblotting.....	47
2.7.4.	Chemical cross-linking of EmhB _{his} protein complexes	48
2.7.5.	Protein modeling.....	48
2.8.	Complementation of <i>srpABC</i> and <i>arpABC</i> in <i>P. fluorescens</i> cLP6a-1.....	48
2.9.	Measurement of growth rates of <i>P. fluorescens</i> cLP6a and cLP6a-1	49

3.	RESULTS AND DISCUSSION.....	51
3.1.	Identification of the EmhABC efflux system in <i>Pseudomonas fluorescens</i> cLP6a	51
3.1.1.	Detection and insertional inactivation of the efflux pump gene	51
3.1.2.	Cloning and sequence analysis of the Emh efflux system.....	57
3.1.3.	Phenanthrene efflux is restored by complementation.....	62
3.1.4.	The EmhABC efflux system transports polycyclic aromatic hydrocarbons... ..	64
3.1.5.	Comparison of the <i>emhABC</i> genes with other RND efflux systems	64
3.2.	Substrate specificity of the EmhABC efflux system	67
3.2.1.	EmhABC is involved in antibiotic resistance	68
3.2.2.	EmhABC is required for survival in the presence of toluene	71
3.2.3.	EmhABC is not involved in naphthalene transport	74
3.2.4.	Comparison of the substrate specificity of EmhABC with other RND efflux systems.....	76
3.3.	Regulation of the EmhABC efflux system in <i>P. fluorescens</i> cLP6a	85
3.3.1.	Sequence analysis of EmhR.....	85
3.3.2.	Identification of regulatory elements in the <i>emhR-emhA</i> intergenic region	88
3.3.3.	Transcription of the <i>emhABC</i> and <i>emhR</i> genes is growth-phase dependent... ..	91
3.3.4.	Transcription of the <i>emhABC</i> and <i>emhR</i> genes is not induced by aromatic hydrocarbons or by metabolites of hydrocarbon degradation.....	95
3.3.5.	Transcription of the <i>emhABC</i> and <i>emhR</i> genes is induced by some antibiotics.....	97
3.3.6.	Comparison of the regulation of the EmhABC efflux system with other RND systems.....	99
3.4.	Evidence for a substrate translocation pathway in EmhB	104
3.4.1.	Homology modeling of the EmhB efflux pump	105
3.4.2.	Construction of site-directed mutants in EmhB _{his}	108
3.4.3.	The histidine-tagged EmhB _{his} is functional in <i>P. fluorescens</i> cLP6a-1	110
3.4.4.	The central cavity provides a flexible binding pocket for substrates during transport	114
3.4.5.	The periplasmic pore domain.....	122

3.4.5.1.	Mutations in the central pore did not affect efflux activity	124
3.4.5.2.	Amino acids lining the vestibules in the pore domain affect efflux activity.....	124
3.4.5.3.	Evidence for a phenylalanine-lined substrate access pathway in the EmhB pore domain	128
3.4.6.	A mutation in the outer membrane protein docking domain enhances efflux activity.....	136
3.4.7.	A model for substrate translocation by RND efflux pumps that describes substrate selectivity and capture from the periplasm or inner membrane	140
3.4.8.	Comparison of the model for transport in RND efflux pumps to other families of multidrug efflux pumps	144
3.4.9.	Future work to elucidate the substrate translocation pathway in RND efflux pumps.....	146
3.5.	Prevalence and significance of polycyclic aromatic hydrocarbon efflux	148
3.5.1.	Phenanthrene efflux is found in other bacteria	148
3.5.2.	Specificity of the ArpABC and SrpABC efflux systems for phenanthrene..	150
3.5.3.	Significance of polycyclic aromatic hydrocarbon efflux in <i>P. fluorescens</i> ..	152
3.5.4.	Significance of the EmhABC efflux system in <i>P. fluorescens</i>	154
4.	CONCLUSIONS AND FUTURE WORK.....	156
5.	REFERENCES.....	158

List of Tables

Table 1.1. Physical properties of aromatic hydrocarbons.....	3
Table 1.2. Comparison of substrate specificities of selected RND efflux systems	12
Table 2.1. Bacterial strains and plasmids used in this study.....	29
Table 2.2. List of EmhB mutations generated by site-directed mutagenesis.....	45
Table 3.1. Comparison of the <i>P. fluorescens</i> cLP6a EmhABC efflux proteins with other three-component RND efflux systems	60
Table 3.2. Antibiotic sensitivities of <i>P. fluorescens</i> strains expressing the EmhABC, ArpABC or SrpABC RND efflux systems.....	69
Table 3.3. Toluene tolerance of <i>P. fluorescens</i> strains expressing the EmhABC, ArpABC or SrpABC RND efflux systems	73
Table 3.4. Accumulation of naphthalene in <i>P. fluorescens</i> and <i>P. putida</i> strains before and after azide addition, as a test for efflux	75
Table 3.5. Comparison of the putative efflux pump regulator EmhR from <i>P. fluorescens</i> cLP6a with homologous TetR-family repressors.....	87
Table 3.6. Effect of mutations on the function of the efflux protein EmhB for polycyclic aromatic hydrocarbon transport, toluene tolerance and antibiotic sensitivity	111
Table 3.7. Conservation of amino acids in the central cavity among RND multidrug and solvent efflux pumps	118
Table 3.8. Conservation of amino acid residues targeted for mutation in the pore domain of EmhB	125
Table 3.9. Conservation of phenylalanine residues in RND multidrug and solvent efflux pumps corresponding to the putative substrate access pathway in EmhB.	135
Table 3.10. Conservation of amino acid residues in the outer membrane protein docking domain of RND efflux pumps	139
Table 3.11. Accumulation of phenanthrene in bacterial strains before and after azide addition, as a test for efflux.....	149
Table 3.12. Specificity of the ArpABC and SrpABC efflux systems for phenanthrene	151

List of Figures

Figure 1.1. Schematic of a three-component RND efflux system	8
Figure 1.2. Three-dimensional structure of the <i>E. coli</i> outer membrane factor protein TolC.....	18
Figure 1.3. Three-dimensional structure of the <i>P. aeruginosa</i> membrane fusion protein MexA.....	20
Figure 1.4. Three-dimensional structure of the <i>E. coli</i> RND efflux pump AcrB	22
Figure 2.1. Schematic of plasmid pBH5 containing the <i>emhABC</i> genes.....	39
Figure 2.2. Schematic of the promoter-reporter transcriptional fusion plasmids	40
Figure 2.3. Schematic of plasmids pBH63(srp) and pBH64(arp).....	50
Figure 3.1. Alignment of conserved regions in RND efflux pump proteins.....	52
Figure 3.2. Amplification of efflux pump genes from <i>P. fluorescens</i> cLP6a genomic DNA	53
Figure 3.3. Confirmation of the efflux pump gene disruption in <i>P. fluorescens</i> cLP6a-1 by Southern blotting and hybridization	55
Figure 3.4. Accumulation of [9- ¹⁴ C]phenanthrene in cell pellets of <i>P. fluorescens</i> cLP6a and the <i>emhB</i> disruption mutant cLP6a-1 over time	56
Figure 3.5. Schematic representation of the <i>emh</i> gene cluster in <i>P. fluorescens</i> cLP6a and cLP6a-1	58
Figure 3.6. Phylogenetic relationship of EmhB to other RND efflux pumps.....	59
Figure 3.7. Distribution of radiolabeled substrates in the cell pellets of <i>P. fluorescens</i> cLP6a strains at steady state before and after addition of 30 mM azide.....	63
Figure 3.8. Partitioning of phenanthrene and naphthalene between <i>P. fluorescens</i> cLP6a cells and the aqueous phase.....	77
Figure 3.9. Chemical structures of the antibiotics tested for resistance in <i>P. fluorescens</i> cLP6a and the efflux mutant cLP6a-1	78
Figure 3.10. Alignment of TetR-family regulatory proteins involved in the regulation of RND efflux systems	86
Figure 3.11. Sequence comparison of the <i>emhR-emhA</i> intergenic region	89
Figure 3.12. Comparison of the <i>emhR-emhABC</i> and <i>ttgR-ttgABC</i> intergenic regions	90

Figure 3.13. Growth phase dependence on expression of β -galactosidase from the $P_{emhA}::lacZ$ and $P_{emhR}::lacZ$ transcriptional fusions	92
Figure 3.14. Effect of hydrocarbons on expression of β -galactosidase from the $P_{emhA}::lacZ$ and $P_{emhR}::lacZ$ transcriptional fusions	96
Figure 3.15. Effect of metabolites from phenanthrene degradation on expression of β -galactosidase from the $P_{emhA}::lacZ$ and $P_{emhR}::lacZ$ transcriptional fusions.	98
Figure 3.16. Effect of antibiotics on expression of β -galactosidase from the $P_{emhA}::lacZ$ and $P_{emhR}::lacZ$ transcriptional fusions	100
Figure 3.17. Homology model of the EmhB monomer	106
Figure 3.18. Homology model of the EmhB trimer.....	107
Figure 3.19. Expression of mutant EmhB _{his} proteins in <i>P. fluorescens</i> cLP6a-1	109
Figure 3.20. Insertion of histidine tag into <i>emhB</i>	115
Figure 3.21. Predicted model of the central cavity in EmhB.....	117
Figure 3.22. Predicted structure of the pore domain of EmhB	123
Figure 3.23. The vestibule region of EmhB.....	126
Figure 3.24. Cross-linking of EmhB in intact cells	129
Figure 3.25. Putative substrate translocation pathway in the periplasmic pore domain of EmhB.....	132
Figure 3.26. Phenylalanine clusters predicted to be involved in substrate access pathways in cytochrome P450 monooxygenases	133
Figure 3.27. Predicted structure of the outer membrane protein docking domain of EmhB	138
Figure 3.28. Proposed model for substrate translocation in RND efflux pumps.....	141
Figure 3.29. Comparison of growth rates of <i>P. fluorescens</i> cLP6a and the EmhB-disruption mutant cLP6a-1 in the presence of phenanthrene	153

List of Abbreviations

DSP, dithiobis(succinimidyl propionate)

K_{ow} , octanol water partition coefficient

MIC, minimum inhibitory concentration

OD₆₀₀, optical density at 600 nm

ONPG, *o*-nitrophenyl- β -D-galactosidase

PCR, polymerase chain reaction

RND, resistance-nodulation-division superfamily

SDS, sodium dodecyl sulfate

SDS-PAGE, sodium dodecyl sulfate-polyacrylamide gel electrophoresis

TMS, transmembrane segment

TSB, tryptic soy broth medium

1. INTRODUCTION

Polycyclic aromatic hydrocarbons are prevalent and persistent environmental contaminants. Found in petroleum, polycyclic aromatic hydrocarbons are also produced by incomplete combustion of organic compounds in fuels (Johnsen *et al.* 2005). Contamination of soil and water with these pollutants is a health concern due to their classification as carcinogens. Microorganisms able to degrade polycyclic aromatic hydrocarbons have been isolated, and the degradation pathways have been studied extensively and have been reviewed by Cerniglia (1992) and van Hamme *et al.* (2003). The chemical and physical properties of polycyclic aromatic hydrocarbons, including the number of fused aromatic rings and their low aqueous solubility, limit the bioavailability of these compounds for microorganisms (Johnsen *et al.* 2005). The principal factor affecting the bioavailability of hydrocarbons is transport, which includes the movement of the contaminant to the microbial cell and its subsequent transfer into the cell. Due to their hydrophobic nature, hydrocarbons readily partition into cell membranes and this may result in toxic effects.

In this chapter, adaptations that allow bacteria to survive in the presence of toxic, hydrophobic compounds are discussed, with an emphasis on transport systems involved in active efflux of hydrophobic compounds. The three-component efflux systems responsible for solvent tolerance and multidrug resistance in gram-negative bacteria are reviewed. These efflux systems are broadly specific for hydrophobic compounds and are controlled by diverse regulatory mechanisms, which include regulatory proteins that directly interact with hydrophobic substrates. The structural basis for the regulation of efflux systems by hydrophobic compounds, as well as structural studies on the efflux pump proteins, are described to provide a better understanding of the mechanism by which these proteins achieve their broad specificity. Recent studies showing the widespread occurrence of efflux systems in hydrocarbon-contaminated environments are presented, and the presence of an efflux system for polycyclic aromatic hydrocarbons in the hydrocarbon-degrading bacterium *Pseudomonas fluorescens* LP6a, which was discovered previously by Bugg *et al.* (2000), is described. The research presented in the following chapters of the thesis describes the efflux system in *P. fluorescens* LP6a, its regulation and substrate specificity.

1.1. Interactions of hydrophobic compounds with biological membranes

1.1.1. The cell membrane acts as a solvent for hydrophobic compounds

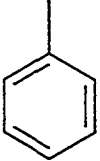
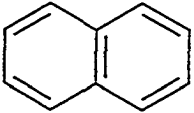
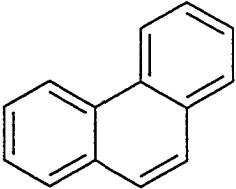
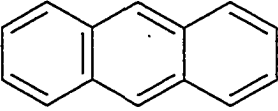
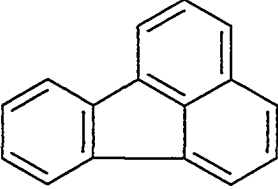
The gram-negative bacterial cell envelope is composed of a bilayer of lipopolysaccharide and phospholipid in the outer membrane and by a phospholipid bilayer in the inner, or cytoplasmic, membrane. Although small molecules, such as gases, can diffuse through the lipid bilayers, the cell envelope presents a permeability barrier to the diffusion of larger, hydrophilic molecules. A variety of membrane-bound proteins, including porins in the outer membrane and passive or active transporters in the inner membrane, facilitate the transport of compounds across the cell envelope. Passive transport is an energy-independent process that uses a membrane-bound protein to mediate the movement of a molecule down its concentration gradient until equilibrium across the membrane is attained. In contrast, active transport is an energy-dependent process that uses inner membrane proteins to move molecules against their concentration gradient, from an area of low concentration to an area of higher concentration. Primary active transporters utilize a primary energy source, such as ATP hydrolysis, light absorption or electrical energy, while secondary active transporters utilize energy stored in ion gradients, such as the proton gradient across bacterial inner membranes.

Although hydrophilic solutes do not pass readily through biological membranes, the hydrophobic interior of the lipid bilayer acts as a solvent for hydrophobic compounds. Sikkema *et al.* (1994) observed a greater accumulation of nonpolar hydrocarbons, including naphthalene and phenanthrene, in phospholipid bilayers compared to polar compounds, such as 4-toluenesulfonic acid and 4-chlorobenzoic acid. The octanol-water partition coefficient, K_{ow} , describes the relative hydrophobicity of a compound and is defined as

$$K_{ow} = \frac{C_{oct}}{C_{aq}} \quad [1]$$

where C_{oct} and C_{aq} are the equilibrium concentrations in the octanol and aqueous phases, respectively. The partition coefficients of various hydrocarbons are presented in Table 1.1. Sikkema *et al.* (1994) found that the membrane accumulation of aromatic hydrocarbons, including toluene, naphthalene and phenanthrene, correlated with the compound's octanol-water partition coefficient and, thus, its hydrophobicity.

Table 1.1. Physical properties of aromatic hydrocarbons^a

Compound	Chemical formula	Structure	Water solubility (mg L ⁻¹) ^b	Octanol-water partition coefficient (logK _{ow})
Toluene	C ₇ H ₈		579	2.65
Naphthalene	C ₁₀ H ₈		30.6	3.35
Phenanthrene	C ₁₄ H ₁₀		1.18	4.57
Anthracene	C ₁₄ H ₁₀		0.0731	4.54
Fluoranthene	C ₁₆ H ₁₀		0.263	5.22

^a Data from Eastcott *et al.* (1988).

^b Water solubilities were measured at 25°C.

1.1.2. Hydrophobic compounds disrupt cell membranes

The partitioning of hydrophobic compounds into biological membranes results in a number of deleterious effects on the cell membrane. Dissolution of hydrophobic compounds into lipid bilayers alters membrane structure, resulting in expansion of the bilayer and an increase in membrane fluidity (Sikkema *et al.* 1994, Sikkema *et al.* 1995). Coupled with these changes to membrane structure, hydrophobic compounds increase membrane permeability and dissipate the proton gradient and electrical potential across the membrane, thereby disrupting membrane function (Sikkema *et al.* 1994).

The toxicity of hydrocarbons towards bacterial cells is related to their octanol-water partition coefficient. Compounds with $\log K_{ow}$ values between 1.5 and 3 are highly toxic, causing an increase in membrane fluidity and an increase in membrane permeability (Sikkema *et al.* 1995, Weber and de Bont 1996). Thus, it was surprising when bacteria were isolated that were able to grow in the presence of high concentrations of toluene, whose $\log K_{ow}$ of 2.65 is within the toxic range. *Pseudomonas putida* S12 was isolated due to its ability to grow in a two-phase styrene-water system and subsequently was found to tolerate, but not to metabolize, high levels of toluene (Weber *et al.* 1993). Similarly, *P. putida* DOT-T1E was isolated from wastewater, and, in addition to its ability to metabolize toluene, the strain is able to grow in the presence of normally toxic concentrations of toluene (Mosqueda *et al.* 1999). Several adaptations may contribute to the unusual ability of microorganisms, including *P. putida* S12 and *P. putida* DOT-T1E, to tolerate high concentrations of toxic solvents (Segura *et al.* 1999): an increased rate of degradation of the compound; a decrease in the permeability of the cell envelope to hydrophobic compounds; and the presence of a transport system that removes the compound from the cell. Since *P. putida* S12 does not metabolize toluene (Weber *et al.* 1993), the latter two mechanisms were explored to elucidate their roles in solvent tolerance.

1.1.3. Cell membranes adapt to the presence of hydrophobic compounds

Because hydrocarbons affect biological membranes, studies with solvent-tolerant bacteria initially focused on adaptations to the cell envelope to explain this phenotype. Comparison of the outer membrane compositions of solvent-tolerant and solvent-

sensitive bacteria revealed differences in the amount of lipopolysaccharide present, with the solvent-tolerant bacterium having a lower cell surface hydrophobicity due to higher amounts of lipopolysaccharide (Aono and Kobayashi 1997). As well, higher proportions of *trans*-unsaturated fatty acids, primarily palmitoleic acid (C16:1) and oleic acid (C18:1), were present in the inner membranes of the solvent-tolerant *P. putida* S12 grown in the presence of toluene compared to cultures grown in the absence of solvent (Weber *et al.* 1994). In addition to the *cis-trans* fatty acid isomerization, an increase in the synthesis of saturated fatty acids and a change in the phospholipid headgroup composition occurred in bacteria exposed to solvents (Segura *et al.* 1999). These adaptations decrease the fluidity of the membrane and counteract the fluidizing effects of solvents on the membrane (Segura *et al.* 1999).

Solvent-sensitive *P. putida* strains also underwent similar changes in membrane composition upon brief exposure to solvents, although these bacteria cannot thrive in the presence of solvents (Pinkart and White 1997, Ramos *et al.* 1997). These adaptations in solvent-sensitive bacteria suggest that the changes to membrane composition upon exposure to organic solvents represent a stress response and are not specific to the solvent-tolerant phenotype (de Bont 1998, Segura *et al.* 1999). Furthermore, membrane adaptations are believed to be an immediate response to organic solvents (Segura *et al.* 1999), since levels of *trans*-fatty acids in *P. putida* liquid cultures increased within the first five minutes after addition of 0.3% (vol/vol) toluene (Ramos *et al.* 1997). Changes to the cell envelope, however, do not eliminate the partitioning and toxic effects of solvents in the membrane. Accordingly, active removal of hydrophobic compounds from the membrane using a membrane-bound protein transport system would provide a better defense against the toxic effects of solvents. Numerous examples of active transport systems that expel toxic substances from cells, including the multidrug transporters in eukaryotic and prokaryotic organisms (Saier *et al.* 1998), serve as precedents for the involvement of an efflux mechanism in solvent tolerance.

1.2. Active efflux as a mechanism of resistance

1.2.1. Overview of efflux systems

Five superfamilies of transport proteins, the ATP-binding cassette superfamily, the major facilitator superfamily, the drug-metabolite transporter superfamily, the multi-antimicrobial exclusion family, and the resistance-nodulation-division (RND) superfamily, contain members that are involved in multidrug efflux (Saier and Paulsen 2001). A common feature of the multidrug efflux pumps within these superfamilies is their unusually broad substrate specificity. Multidrug efflux pumps recognize and expel a wide range of structurally diverse hydrophobic compounds and, thus, are the principal contributor to drug resistance in a variety of organisms (Saier and Paulsen 2001). Examples of multidrug efflux pumps include the ATP-binding cassette transporter P-glycoprotein, which exports doxorubicin, taxol and other chemotherapy drugs in mammalian cancer cells (Loo and Clarke 1999), the major facilitator superfamily transporter Bmr, which exports hydrophobic drugs in *Bacillus subtilis* (Neyfakh *et al.* 1991), the drug-metabolite transporter EmrE, which exports ethidium and other lipophilic cations in *Escherichia coli* (Schuldiner *et al.* 1997), the multi-antimicrobial exclusion family transporter VmrA, which exports ethidium and acriflavin in *Vibrio parahaemolyticus* (Chen *et al.* 2002), and the RND efflux pump AcrB, which exports acriflavin and other hydrophobic antibiotics in *E. coli* (Nikaido 1996). While members of the ATP-binding cassette transporter, the major facilitator, the drug-metabolite transporter and the multi-antimicrobial exclusion families are involved in uptake as well as efflux, RND transporters are involved exclusively in efflux (Saier and Paulsen 2001) and are partly responsible for the increased prevalence of antibiotic resistance among bacteria.

RND efflux pumps are secondary active transporters that catalyze proton:substrate antiport. Within the RND superfamily, five families are present in Prokaryotes, one family is present in Eukaryotes and one family is found in Archaea (Saier and Paulsen 2001). Members of the RND superfamily include the SecDF protein translocation system found in *B. subtilis*, the Niemann-Pick C1 disease protein implicated in cholesterol transport in mammals and several putative efflux pumps found in *Methanococcus jannaschii* and other Archaea (Tseng *et al.* 1999). In addition to these

examples, the largest number of RND efflux pumps that have been identified and characterized functionally is found in gram-negative bacteria (Tseng *et al.* 1999). The gram-negative RND transporters include the heavy metal efflux family, the putative nodulation factor exporter family, and the hydrophobe-amphiphile efflux-1 family, which includes the multidrug efflux pumps AcrB in *E. coli* and MexB in *Pseudomonas aeruginosa* (Tseng *et al.* 1999).

The gram-negative bacterial cell envelope presents a challenging situation with regard to transport, as substrates must cross both the inner and outer membranes. To expel substrates efficiently into the extracellular medium, gram-negative efflux pumps form a complex with two accessory proteins. These proteins belong to the outer membrane factor family and the periplasmic membrane fusion protein family (Paulsen *et al.* 1996) and, together with the inner membrane pump, prevent accumulation of compounds in the cell (Figure 1.1). The best-studied three-component RND efflux systems are the multidrug exporters MexAB-OprM in *P. aeruginosa* and AcrAB-TolC in *E. coli*, where MexB and AcrB are the inner membrane RND pumps, MexA and AcrA are the periplasmic membrane fusion proteins, and OprM and TolC are the outer membrane proteins.

1.2.2. Active efflux systems contribute to multidrug resistance in gram-negative bacteria

The MexAB-OprM efflux system is expressed constitutively in *P. aeruginosa* and is responsible for the intrinsic resistance of this organism to a wide range of hydrophobic antibiotics (Nikaido 1996). Tetracycline, chloramphenicol, norfloxacin and β -lactam antibiotics were shown to be substrates of the MexAB-OprM efflux pump, and overexpression of the *mexAB-oprM* genes enhanced bacterial resistance to these drugs (Li *et al.* 1995). The three genes, *mexA* encoding the membrane fusion protein, *mexB* encoding the RND efflux protein, and *oprM* encoding the outer membrane protein, are located within an operon on the chromosome of *P. aeruginosa*. In addition to MexAB-OprM, genome sequencing has identified ten other genetically distinct RND efflux systems in *P. aeruginosa* PA01 (Stover *et al.* 2000). The roles of several of these systems, designated MexCD-OprJ (Poole *et al.* 1996a), MexEF-OprN (Köhler *et al.* 1997), MexJK-OprM (Chuanchuen *et al.* 2002), MexXY-OprM (Aires *et al.* 1999) and

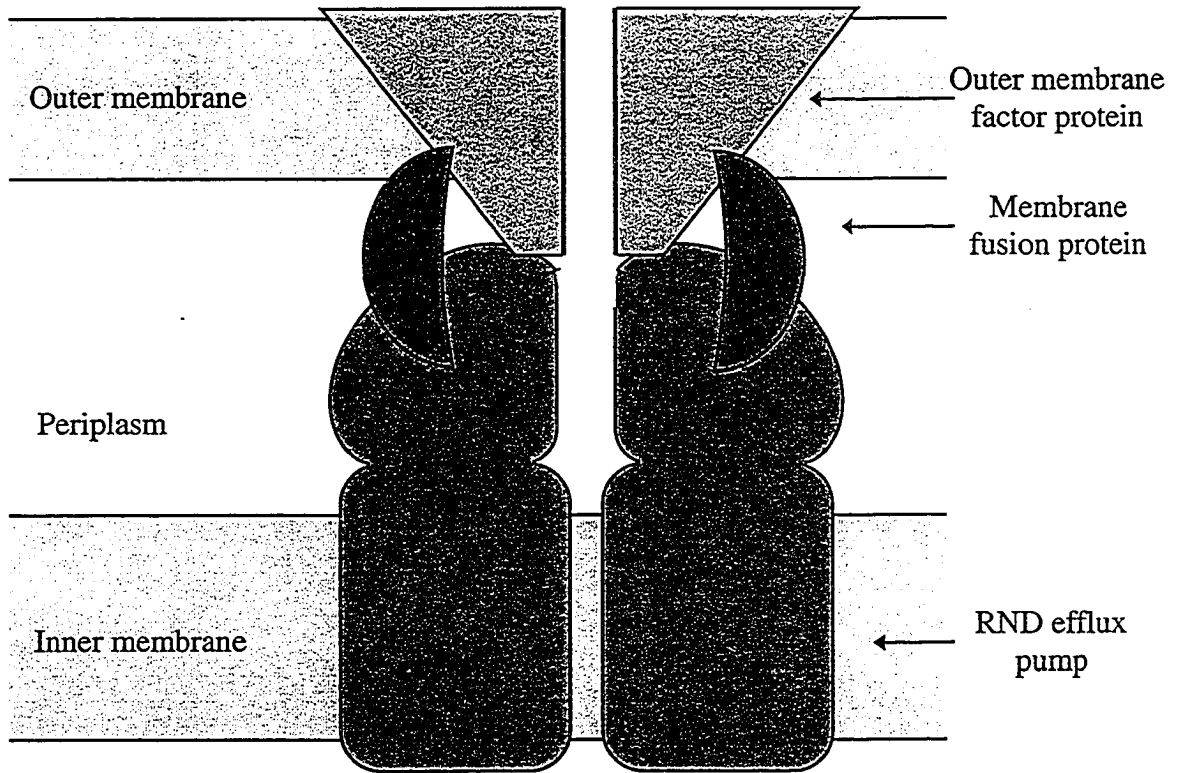


Figure 1.1. Schematic of a three-component RND efflux system. The inner membrane RND pump interacts with the periplasmic membrane fusion protein and the outer membrane factor protein. This three-component protein complex is believed to expel hydrophobic compounds from the inner membrane or periplasm directly into the extracellular medium.

MexVW-OprM (Li *et al.* 2003), in multidrug efflux have been confirmed. These RND efflux systems show a high degree of homology to MexAB-OprM and are believed to play an important role in the adaptability of *P. aeruginosa* to the presence of many antibiotics. For example, Llanes *et al.* (2004) reported the presence of MexAB-OprM and MexXY-OprM in antibiotic-resistant clinical isolates of *P. aeruginosa*, and Beinlich *et al.* (2001) observed increased expression of MexAB-OprM and MexEF-OprN in *P. aeruginosa* strains isolated from canine infections.

Several three-component efflux systems homologous to MexAB-OprM are also encoded on the *E. coli* chromosome, with the most notable being AcrAB-TolC. The membrane fusion protein AcrA and the RND efflux pump AcrB, which are encoded in the *acrAB* operon, function with the outer membrane channel TolC to increase antibiotic resistance to a wide range of compounds, including acriflavin, tetracycline, chloramphenicol, fluoroquinolones and β -lactams (Nikaido 1996). In addition to *P. aeruginosa* and *E. coli*, RND efflux systems involved in the export of hydrophobic antibiotics have been identified in *Burkholderia cepacia*, *Campylobacter jejuni* and *Neisseria meningitidis* (Poole 2004).

1.2.3. Active efflux systems contribute to solvent tolerance

Isken and de Bont (1996) reported the first evidence for the involvement of an active efflux mechanism contributing to solvent tolerance in *P. putida* S12. When grown in the presence of toluene, *P. putida* S12 cells accumulated twice the level of radiolabeled toluene upon addition of the energy inhibitors cyanide and carbonyl cyanide *m*-chlorophenylhydrazone compared to uninhibited cells (Isken and de Bont 1996). The increased cellular accumulation of toluene after addition of cyanide and carbonyl cyanide *m*-chlorophenylhydrazone, which both act to dissipate the proton gradient across the inner membrane, indicates inhibition of an active efflux system. Genetic analysis of a solvent-sensitive mutant of *P. putida* S12 identified three genes within an operon, designated *srpABC* for solvent resistance pump, responsible for toluene tolerance in the parental organism (Kieboom *et al.* 1998a). The *srpA*, *srpB* and *srpC* genes encode proteins that are homologous to members of the membrane fusion protein family, the

RND family of transport proteins and the outer membrane factor family, respectively (Kieboom *et al.* 1998a).

Homologous efflux systems were subsequently found in the toluene-tolerant bacterium *P. putida* DOT-T1E. Three RND efflux systems were identified in *P. putida* DOT-T1E and were labeled *ttgABC*, *ttgDEF* and *ttgGHI* for toluene tolerance genes (Ramos *et al.* 1998, Mosqueda and Ramos 2000, Rojas *et al.* 2001). Both the *ttgABC* and *ttgGHI* efflux systems are able to export toluene, styrene, *m*-xylene, propylbenzene and ethylbenzene, as well as hydrophobic antibiotics, from the cell (Ramos *et al.* 1998, Mosqueda and Ramos 2000, Rojas *et al.* 2001). The *ttgDEF* efflux system, in contrast, recognizes toluene and styrene but not other aromatic hydrocarbons or hydrophobic antibiotics (Rojas *et al.* 2001). The narrow substrate specificity observed for TtgDEF in *P. putida* DOT-T1E represents an unusual property of this toluene efflux pump compared to other RND homologues, and its significance is not known.

1.3. Substrate specificities of antibiotic and solvent efflux systems

A distinguishing feature of multidrug efflux systems compared to other transport proteins is their ability to recognize and export a variety of structurally diverse compounds. The list of compounds recognized and transported by members of the RND hydrophobe-amphiphile efflux-1 family is extensive and includes hydrophobic dyes, detergents, fatty acids, bile salts and homoserine lactones, in addition to organic solvents and antibiotics (Poole 2004). For example, the *E. coli* AcrAB system conveys resistance to neutral hydrophobic compounds such as erythromycin and chloramphenicol, cationic hydrophobic compounds such as acriflavin and ethidium, and anionic hydrophobic compounds such as sodium dodecyl sulfate (Nikaido 1996). The only common characteristic among the efflux pump substrates is their hydrophobic nature.

Notwithstanding their classification as broad specificity efflux pumps, individual RND pumps have been shown to display an unusual degree of substrate selectivity. Masuda *et al.* (2000) compared the antibiotic resistance profiles of the *P. aeruginosa* efflux pumps MexAB-OprM, MexCD-OprJ and MexXY-OprM. Interestingly, the three efflux systems, MexAB-OprM, MexCD-OprJ and MexXY-OprM, had overlapping yet distinct substrate specificities. All three of the efflux systems contributed to resistance to

chloramphenicol, quinolones, macrolides and tetracyclines, whereas acquired resistance to aminoglycosides was mediated solely by MexXY-OprM (Masuda *et al.* 2000). Among the β -lactam antibiotics tested, none of the efflux systems conferred resistance to the carbapenems (Masuda *et al.* 2000). Furthermore, MexCD-OprJ and MexXY-OprM showed specificity for penicillin-G and cloxacillin but not for carbenicillin, while the *P. aeruginosa* strain expressing MexAB-OprM was resistant to all three of these β -lactams (Masuda *et al.* 2000). These efflux pumps, therefore, must possess a level of substrate recognition beyond hydrophobicity.

Analysis of the substrate specificities of the solvent efflux systems in *P. putida* strains supported the hypothesis for a mechanism of substrate recognition provided by the efflux system proteins. In the toluene-tolerant bacterium *P. putida* S12, the SrpABC efflux pump is specific for organic solvents (Isken and de Bont 1996), and a second efflux system, designated ArpABC for antibiotic resistance pump, was responsible for antibiotic resistance (Kieboom and de Bont 2001). Similarly, the toluene efflux pumps in *P. putida* DOT-T1E showed an unusual selectivity; TtgABC and TtgGHI exported both solvents and antibiotics, whereas TtgDEF showed specificity for organic solvents only (Rojas *et al.* 2001). In view of these findings, Kieboom and de Bont (2001) proposed defining three types of efflux systems based on selectivity – solvent-specific, antibiotic-specific, and nonspecific solvent and antibiotic pumps. Table 1.2 summarizes the RND efflux systems discussed throughout this thesis and their substrate specificities.

1.4. Regulation of efflux pumps

1.4.1. Regulation of expression of solvent efflux pump genes in *P. putida*

Corresponding with their substrate specificity profiles, the toluene efflux genes in *P. putida* DOT-T1E are expressed under different conditions. The TtgABC efflux pump is expressed constitutively, while the TtgDEF efflux pump is only expressed when the bacterium is grown in the presence of toluene (Mosqueda and Ramos 2000). Toluene also induces expression of the TtgGHI efflux system, which is constitutively produced at low levels in cells grown in the absence of toluene (Rojas *et al.* 2003). The differential expression of the three toluene efflux pumps in *P. putida* DOT-T1E offers a convenient opportunity to study the regulation of RND efflux systems.

Table 1.2. Comparison of substrate specificities of selected RND efflux systems

Efflux system	Phenotype	Substrate specificity^a
<i>P. aeruginosa</i>		
MexAB-OprM	antibiotic resistance	tetracyclines, chloramphenicol, macrolides, quinolones, β -lactams (except carbapenems)
MexCD-OprJ	antibiotic resistance	tetracyclines, chloramphenicol, macrolides, quinolones, β -lactams (except carbapenems and carbenicillin)
MexXY-OprM	antibiotic resistance	tetracyclines, chloramphenicol, macrolides, quinolones, β -lactams (except carbapenems and carbenicillin), aminoglycosides
<i>P. putida</i> S12		
SrpABC	solvent resistance	toluene, <i>p</i> -xylene, ethylbenzene
ArpABC	antibiotic resistance	tetracycline, chloramphenicol, macrolides, β -lactams
<i>P. putida</i> DOT-T1E		
TtgABC	antibiotic, solvent resistance	tetracycline, chloramphenicol, β -lactams, toluene, styrene, <i>m</i> -xylene, ethylbenzene, propylbenzene
TtgDEF	solvent resistance	toluene, styrene
TtgGHI	solvent, antibiotic resistance	toluene, styrene, <i>m</i> -xylene, ethylbenzene, propylbenzene, tetracycline, chloramphenicol, β -lactams
<i>E. coli</i>		
AcrAB-TolC	antibiotic resistance	tetracycline, chloramphenicol, macrolides, fluoroquinolones, β -lactams, detergents

^a Data from Masuda *et al.* (2000), Kieboom *et al.* (1998a), Kieboom and de Bont (2001), Rojas *et al.* (2001) and Nikaido (1996).

Duque *et al.* (2001) identified the *ttgR* gene, encoding a protein belonging to the tetracycline repressor (TetR) family of transcriptional regulators, upstream of the constitutively expressed TtgABC toluene efflux pump in *P. putida* DOT-T1E. TetR-like proteins are characterized by a helix-turn-helix DNA-binding motif, and TetR acts by binding to operator sites in the DNA, thereby preventing transcription of the *tetA* efflux pump gene (Berens and Hillen 2003). Gene regulation by TetR family proteins is an inducible system; when inducers bind to the TetR repressor protein, a conformational change in the protein causes it to dissociate from the DNA and allows transcription of the *tetA* gene (Berens and Hillen 2003). Consistent with its classification as a TetR transcriptional regulator, TtgR was shown to repress expression of the *ttgABC* operon as well as its own expression (Duque *et al.* 2001). Interestingly, toluene did not affect expression of the *ttgABC* genes (Duque *et al.* 2001), but the antibiotics chloramphenicol and tetracycline, which are also substrates of TtgABC, induced efflux pump gene expression by three- to four-fold compared to normal levels (Terán *et al.* 2003).

Toluene is an inducer for the TtgDEF and TtgGHI efflux systems in *P. putida* DOT-T1E. Expression of the *ttgGHI* operon, while constitutive at low levels in the absence of toluene, increases three- to four-fold in the presence of toluene (Rojas *et al.* 2001) and is controlled by the gene products from the *ttgVW* operon (Rojas *et al.* 2003). TtgV shows homology to the isocitrate lyase regulator (IclR) family of transcriptional repressors. Other members of the IclR family include IclR, which regulates the glyoxylate shunt biochemical pathway in *E. coli* (Sunnarborg *et al.* 1990), and PcaR and CatR, which regulate the protocatechuate and catechol branches in the biochemical pathway for aromatic hydrocarbon degradation (Romero-Steiner *et al.* 1994, Eulberg and Schlömann 1998). In *P. putida* DOT-T1E, the IclR-type regulator TtgV binds to the operator site and represses expression of the TtgGHI efflux system (Guazzaroni *et al.* 2004). Repression of the *ttgGHI* operon was alleviated by efflux pump substrates, including the aromatic hydrocarbons toluene and styrene (Guazzaroni *et al.* 2004). The TtgW protein, encoded in the *ttgVW* operon located upstream of the *ttgGHI* genes, shows homology to a TetR family transcriptional repressor; however, the role of TtgW in the regulation of the TtgGHI efflux system is unknown.

The mechanism by which expression of the TtgDEF efflux system is regulated by toluene in *P. putida* DOT-T1E is less understood. An additional regulatory factor belonging to the leucine-responsive regulatory protein (Lrp) family was identified in *P. putida* DOT-T1E, and TtgDEF was not expressed in the absence of this Lrp-like gene in *P. putida* DOT-T1E cells grown in the presence of toluene (Duque *et al.* 2001). Proteins in the Lrp family are global regulators that affect the expression of many genes (Brinkman *et al.* 2003). These studies with the toluene efflux pumps in *P. putida* DOT-T1E reveal a wide diversity and complexity of regulatory mechanisms involved in controlling the expression of RND efflux systems.

1.4.2. Regulation of expression of RND multidrug efflux pump genes

The regulation of multidrug efflux systems in gram-negative bacteria is also varied and multifaceted. In *E. coli*, expression of the RND efflux system AcrAB-TolC is induced by antibiotics as well as by general stress conditions, such as ethanol and high salt concentrations (Grkovic *et al.* 2001). The *acrAB* operon is regulated by global regulatory mechanisms, including the multiple antibiotic resistance *marRAB* operon, and by a local repressor AcrR, belonging to the TetR family of transcriptional regulators (Grkovic *et al.* 2001). Induction of the *acrAB* operon in response to antibiotics and stress conditions is mediated by the *marRAB* operon, where MarR is a repressor of the *marRAB* operon, MarA is a global transcriptional activator and MarB is a protein of unknown function (Grkovic *et al.* 2001). Under inducing conditions, repression of the *marRAB* operon by the MarR protein is alleviated, allowing expression of the MarA protein, which activates a number of genes including *acrAB* (Grkovic *et al.* 2001). Regulation of the *acrAB* operon by the local repressor AcrR is not affected by antibiotics or general stress conditions (Grkovic *et al.* 2001). The AcrR repressor is believed to prevent excessive expression of the AcrAB proteins under normal growth conditions (Grkovic *et al.* 2001).

Local transcriptional regulators have also been identified adjacent to the *mex* operons in *P. aeruginosa*. MexR is a MarR family transcriptional repressor that regulates expression of the MexAB-OprM efflux system (Poole *et al.* 1996b), MexT is a LysR family transcriptional activator that regulates expression of the MexEF-OprN efflux system (Köhler *et al.* 1997), and MexZ is a TetR family transcriptional repressor that

regulates expression of the MexXY efflux system (Matsuo *et al.* 2004). As yet, a direct interaction between the Mex regulatory proteins and the antibiotic substrates of their corresponding efflux systems has not been established. Terán *et al.* (2003), however, demonstrated that the TtgR repressor protein directly binds antibiotic substrates of the multidrug and solvent efflux system TtgABC in *P. putida* DOT-T1E.

From these examples of the regulation of solvent and multidrug efflux pump genes, it is evident that the expression of RND efflux systems is controlled by a complex network of local and global regulatory mechanisms. Furthermore, gram-negative bacteria that have multiple RND efflux systems possess mechanisms to regulate the number and type of efflux systems expressed. In *P. aeruginosa*, for example, MexAB-OprM is constitutively expressed, while MexCD-OprJ is not normally expressed; however, in a MexAB-OprM-deficient mutant, MexCD-OprJ is expressed to compensate for the lack of MexAB-OprM (Li *et al.* 2000). Microarray analyses may provide a more comprehensive approach for studying the influence of local and global regulatory mechanisms on the transcription of RND efflux pump genes.

Understanding the regulatory mechanisms affecting RND efflux pump expression is important from a clinical perspective, since mutations in regulatory elements often give rise to enhanced multidrug resistance due to overexpression of efflux pump genes. As well, identification of inducers or repressors of efflux pump gene expression may provide clues to the physiological role of the efflux system. For instance, both the TtgABC and TtgGHI efflux systems contribute to antibiotic resistance and solvent tolerance in *P. putida* DOT-T1E (Rojas *et al.* 2001). Yet, the regulation of *ttgABC* gene expression by antibiotics and the regulation of *ttgGHI* gene expression by solvents suggest that TtgABC may be more important for antibiotic resistance, while the primary role of the TtgGHI system is solvent tolerance. The finding that the *P. fluorescens* DOT-T1E TtgR repressor protein binds antibiotic substrates of the TtgABC efflux system (Terán *et al.* 2003) indicates that the regulatory protein and the efflux pump proteins share a common ability to recognize and bind structurally diverse hydrophobic compounds. Structural studies examining the substrate-binding capacity of the transcriptional regulators may provide insight into the mechanism for the broad specificity of RND efflux systems.

1.4.3. Structural basis for the regulation of multidrug efflux systems by hydrophobic compounds

Regulatory proteins for other efflux pump families have also been shown to bind hydrophobic substrates. BmrR and QacR are transcriptional regulators of the major facilitator superfamily multidrug efflux pumps Bmr in *B. subtilis* and QacA in *Staphylococcus aureus* (Saier and Paulsen 2001), and both bind hydrophobic compounds. The crystal structure of the *B. subtilis* BmrR transcriptional activator revealed a drug-binding pocket that accommodated a hydrophobic ligand (Zheleznova *et al.* 1999). Nonpolar and aromatic amino acids lined the drug-binding pocket and formed van der Waals and aromatic stacking interactions with the ligand. The large size of the substrate-binding site, coupled with the relatively nonspecific interactions between the protein and the ligand, contributed to the broad substrate specificity of the BmrR regulator (Zheleznova *et al.* 1999).

Similarly, crystal structures of the QacR transcriptional repressor in *S. aureus* were solved in the presence of two hydrophobic compounds, ethidium and proflavin (Schumacher *et al.* 2004). As in BmrR, the drug-binding pocket of QacR contains nonpolar and aromatic amino acids. Within the large binding region, several smaller pockets identified in QacR were postulated to bind different compounds, allowing the regulator to interact with structurally diverse drugs. The QacR drug-binding pocket accommodated both ethidium and proflavin molecules simultaneously, providing evidence of a flexible drug-binding site that establishes multiple interactions with substrates (Schumacher *et al.* 2004).

The structural studies with BmrR and QacR provided valuable clues regarding the ability of proteins to recognize and bind a wide range of structurally diverse hydrophobic compounds. Similar studies with the local regulators of RND efflux pumps, such as the antibiotic-binding TtgR and solvent-binding TtgV repressors, may provide additional information on the regulation of these systems by hydrophobic compounds. Because regulatory proteins are soluble, they are more amenable to protein crystallography than the efflux pump proteins and, as a result, may be easier for studying the structural basis of multidrug and solvent recognition. Recent structural and functional studies of the efflux

system proteins, however, have provided further insight into the mechanism for their unusually broad substrate specificity.

1.5. Structure and function of RND efflux systems

The clinical importance of the multidrug efflux systems in *P. aeruginosa* and *E. coli* has prompted numerous structural and functional studies of the protein components. The best-studied RND efflux systems are MexAB-OprM in *P. aeruginosa* and AcrAB-TolC in *E. coli*, where MexB and AcrB are the inner membrane RND pumps, MexA and AcrA are the periplasmic membrane fusion proteins, and OprM and TolC are the outer membrane components. Crystal structures of all three components have been solved and have provided a greater understanding of how the proteins interact with each other and with their substrates.

1.5.1. The outer membrane factor protein

The outer membrane components of the multidrug efflux systems in gram-negative bacteria were believed to be porins; however, the three-dimensional crystal structure of the *E. coli* TolC protein (Koronakis *et al.* 2000) indicated that these proteins have unique features (Figure 1.2). The functional TolC form is a homotrimer consisting of three domains – a β -barrel domain, an α -helical domain and a mixed α,β -domain (Koronakis *et al.* 2000). Each TolC monomer provides four membrane-spanning β -strands to form a 12-stranded β -barrel in the outer membrane, comparable to other porins. Unlike other porins, the α -helical domain also forms a long 12-stranded cylinder, which extends into the periplasmic space and is closed at the tip (Koronakis *et al.* 2000). The mixed α,β -domain links the β -barrel to the α -helices (Koronakis *et al.* 2000). The distinguishing α -helical domain is believed to be important for the interaction between TolC and the inner membrane transporters and may form a tunnel through which substrates pass (Koronakis *et al.* 2000). TolC acts not only with the AcrAB efflux system for hydrophobic antibiotics but also with the ABC transporter HlyB in the secretion system for hemolysin in *E. coli* (Nikaido 2000). Probably due to its involvement in multiple efflux systems, the *tolC* gene is distinct from the *acrAB* operon (Nikaido 1996).

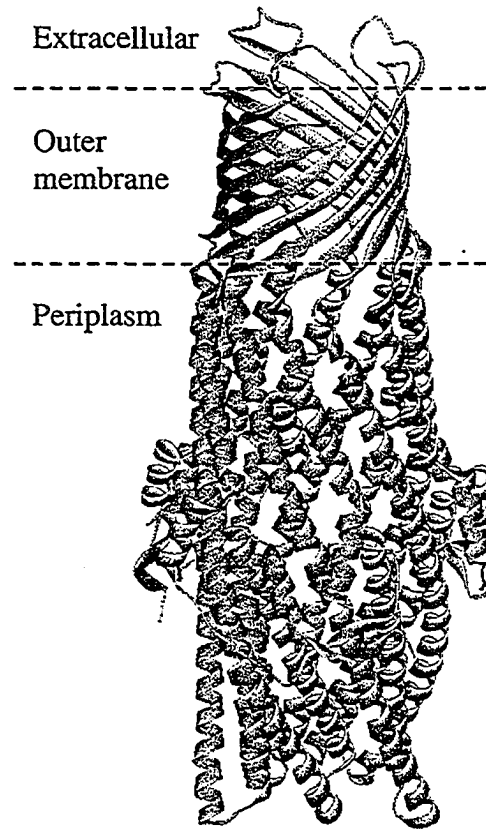


Figure 1.2. Three-dimensional structure of the *E. coli* outer membrane factor protein TolC. The functional homotrimer is shown, and the predicted boundary of the outer membrane is indicated. The structure was redrawn from the Protein Data Bank (PDB) entry 1EK9 (Koronakis *et al.* 2000).

In contrast to TolC, the *oprM* gene is located within the *mexAB-oprM* operon in the *P. aeruginosa* genome (Li *et al.* 1995). Also, OprM is a lipoprotein (Li and Poole 2001), predicted to have a thioether-linked diacylglycerol moiety and an N-acyl fatty acid attached to the N-terminal cysteine residue. The N-terminal lipid modification in OprM was believed to help stabilize the protein in the outer membrane (Akama *et al.* 2004), although Li and Poole (2001) demonstrated that OprM lacking the lipid modification was functional for antibiotic efflux with the membrane fusion protein MexA and the RND efflux pump MexB. The crystal structure of OprM, solved by Akama *et al.* (2004), established that OprM has the same overall structure as TolC and suggested a similar mechanism as a conduit that accepts substrates from the inner membrane efflux pump and facilitates substrate transport across the outer membrane. Further studies are required to elucidate the interactions between the outer membrane protein and the periplasmic and inner membrane components of the efflux complex, as well as the mechanism by which the funnel-shaped periplasmic domain of the outer membrane protein opens to allow substrate entry.

1.5.2. The periplasmic membrane fusion protein

The periplasmic components of the efflux complexes, AcrA in *E. coli* and MexA in *P. aeruginosa*, have a lipoyl-biotinyl and coiled-coil motif characteristic of the paramyxoviral membrane fusion protein family (Zgurskaya and Nikaido 2000a). Subunit swapping experiments conducted by Yoneyama *et al.* (1998) showed that the periplasmic membrane fusion proteins were not functionally interchangeable among different efflux systems. Recently, MexA was crystallized (Figure 1.3) and shown to be an elongated protein with a β -barrel domain, a lipoyl domain and an α -helical hairpin (Higgins *et al.* 2004). The β -barrel domain, containing both the N- and C-termini of the protein, likely interacts with the inner membrane pump since mutations in this region prevented interaction between MexA and MexB (Nehme *et al.* 2004). The membrane fusion proteins are lipoproteins (Zgurskaya and Nikaido 1999), and Higgins *et al.* (2004) postulated that nine MexA monomers form a ring anchored in the inner membrane by the N-terminal lipid modification and enclose the periplasmic α -helical barrel of the outer membrane protein. The quaternary structure of MexA, however, was unclear from the

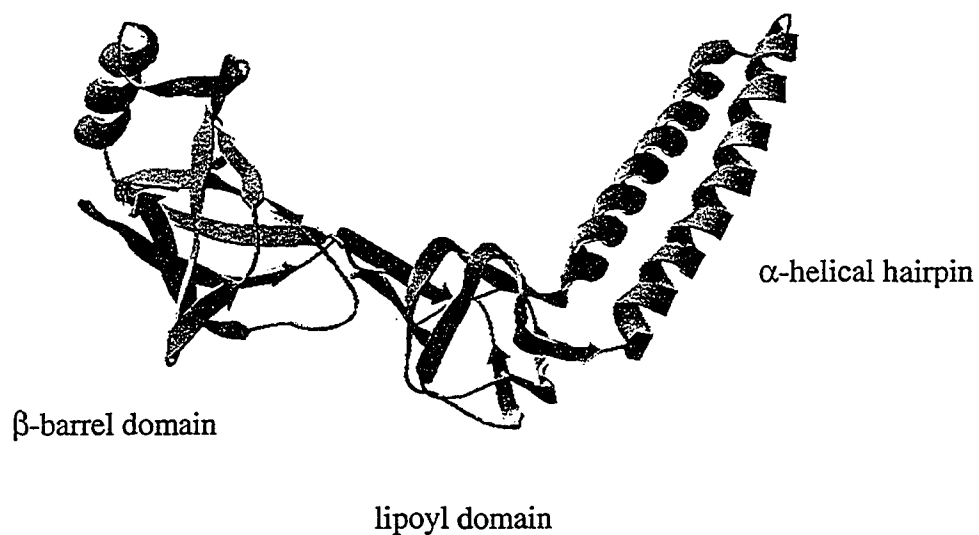


Figure 1.3. Three-dimensional structure of the *P. aeruginosa* membrane fusion protein MexA. The β -barrel domain, lipoyl domain and α -helical hairpin are indicated. The structure was redrawn from the PDB entry 1T5E (Higgins *et al.* 2004).

crystallography data (Higgins *et al.* 2004), and additional research is needed to clarify the role of the membrane fusion protein in the efflux system and its assembly with the outer membrane protein and the inner membrane RND efflux pump.

1.5.3. The inner membrane RND efflux pump

The inner membrane RND protein is the energy-dependent pump and functions as a proton:drug antiporter (Nikaido 1996). Membrane topology analyses identified the presence of 12 transmembrane segments (TMS) and two large periplasmic domains located between TMS1 and 2 and TMS7 and 8, which are a unique feature of the RND family compared to other families of multidrug exporters (Paulsen *et al.* 1996). The crystal structure of the *E. coli* RND protein AcrB (Figure 1.4) showed that the pump exists as a homotrimer and confirmed the presence of a large periplasmic region extending 70 Å above the transmembrane domain (Murakami *et al.* 2002). The top of the periplasmic headpiece forms a funnel believed to interact with the outer membrane channel, TolC, while three α -helices, one from each AcrB monomer, form a pore at the centre of the headpiece (Murakami *et al.* 2002). Channels, or vestibules, extending from the exterior of the protein lead into a central cavity at the bottom of the pore, above the transmembrane domain (Murakami *et al.* 2002). The structure of AcrB has implications for its function in both proton translocation and drug transport.

A previous study with the AcrB homologue, MexB, in *P. aeruginosa* identified three conserved amino acids, D407 and D408 in TMS4 and K939 in TMS10, whose charged side chains were essential for antibiotic resistance to negatively charged and neutral drugs (Guan and Nakae 2001). Guan and Nakae (2001) speculated that the aspartate and lysine residues form a channel for proton translocation. The crystallography data, showing the proximity of these residues in AcrB (Murakami *et al.* 2002), supports this hypothesis. Furthermore, the aspartate residue D408 is conserved in the RND pump CzcA, which is responsible for divalent metal cation efflux in *Ralstonia* sp. (Goldberg *et al.* 1999). Mutation of the aspartate to a neutral amino acid resulted in a mutant CzcA protein that was able to promote facilitated diffusion of metal cations, but did not exhibit proton:metal antiport (Goldberg *et al.* 1999). The conserved aspartate residues played the same role in the antibiotic efflux pumps and metal efflux pumps,

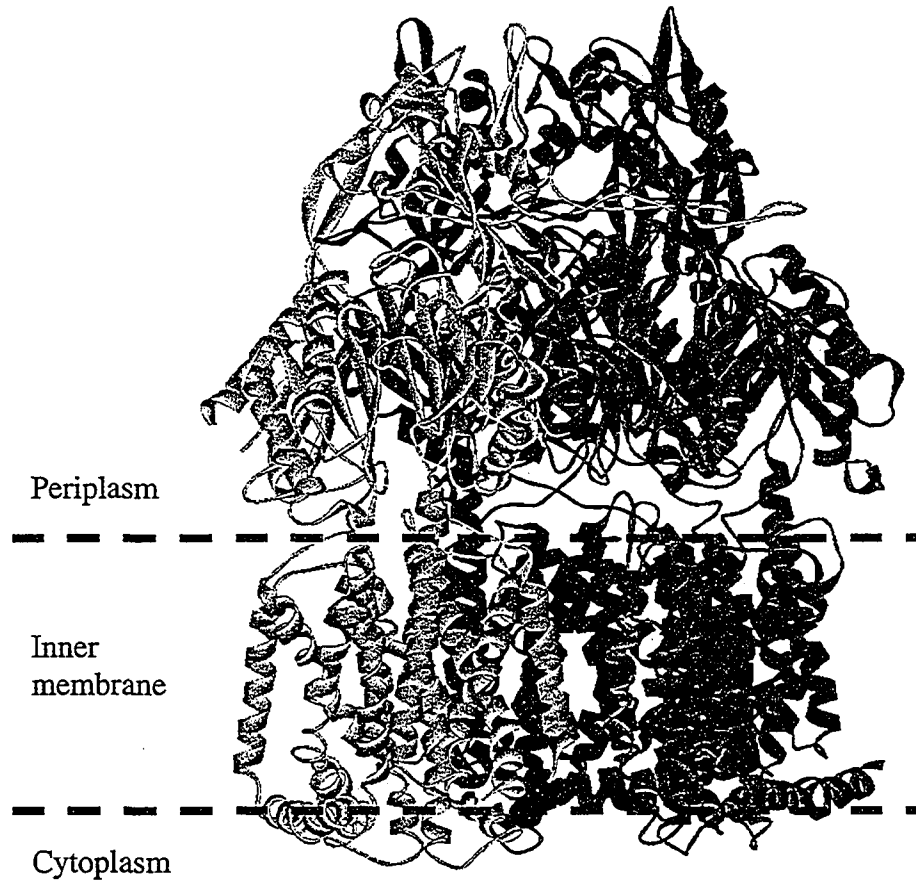


Figure 1.4. Three-dimensional structure of the *E. coli* RND efflux pump AcrB. The protein exists as a trimer, and the individual subunits are coloured in different shades of gray. The predicted boundary of the inner membrane is indicated. The structure was redrawn from PDB entry 1IWG (Murakami *et al.* 2002).

suggesting the presence of two distinct channels, a proton-conducting channel formed by TMS4 and TMS10 and a substrate-conducting channel, in RND proteins.

The AcrB crystal structure provides two possible mechanisms for substrate transport (Murakami *et al.* 2002). Drug substrates may enter the RND pump through the membrane and traverse through the central cavity and pore in the periplasmic domain to reach the outer membrane channel (Murakami *et al.* 2002). Alternatively, substrates may enter the pump from the periplasmic space through the vestibules, which lead into the central cavity and pore (Murakami *et al.* 2002). These models suggest that substrate-protein interactions occur in the periplasmic domain encompassing the central cavity, pore-forming helices and, possibly, the vestibule region.

Evidence for the involvement of the central cavity in substrate binding was provided by the crystallization of AcrB in the presence of drug substrates (Yu *et al.* 2003a). The four structurally dissimilar compounds (rhodamine 6G, ethidium, dequalinium and ciprofloxacin) were located in the central cavity region of the AcrB pump and interacted primarily with hydrophobic amino acids (Yu *et al.* 2003a). Each compound bound to a different set of amino acids within the central cavity, prompting Yu *et al.* (2003a) to propose that the wide substrate range of RND efflux pumps is due to the presence of a large binding pocket that can form hydrophobic interactions with different substrates.

The role of the pore-forming helices was studied by using cysteine-scanning mutagenesis of AcrB (Murakami *et al.* 2004). Mutations at several residues (D101, V105, N109, Q112 and P116) located on the inner face of the pore yielded a pump with reduced activity for a number of antibiotics. Cross-linking studies revealed that the pore is normally closed and indicated that a conformational change of the pore is required for substrate translocation (Murakami *et al.* 2004). Although direct passage of substrates through the central pore was not demonstrated, the pore presents a feasible pathway for substrate translocation from the central cavity to the upper funnel domain of the RND pump.

The structural and mutational studies by Yu *et al.* (2003a) and Murakami *et al.* (2004) implicated the central cavity and pore regions of the RND pump in substrate binding and transport, yet other interactions between the substrates and the protein likely

occur and influence substrate selectivity. Two studies using chimeric constructs of the *E. coli* AcrB and AcrD efflux pumps (Elkins and Nikaido 2002) and of the *E. coli* AcrB and *P. aeruginosa* MexB efflux pumps (Tikhonova *et al.* 2002) exploited the differing substrate specificities of these efflux pumps and demonstrated the involvement of the periplasmic domains in determining substrate specificity. Replacement of both periplasmic loops of AcrD, which does not pump the AcrB substrates ciprofloxacin, chloramphenicol, erythromycin and tetracycline, with the corresponding loops from AcrB yielded a chimeric efflux pump with an AcrB-like substrate range (Elkins and Nikaido 2002). However, the substrate specificity of AcrD was preserved in a chimeric construct that replaced the transmembrane domains of AcrD with the AcrB transmembrane domains, indicating that the periplasmic loops, and not the transmembrane domains, influenced substrate specificity (Elkins and Nikaido 2002). Chimeras of the AcrB and MexB efflux pumps constructed by Tikhonova *et al.* (2002) further implicated the involvement of the second periplasmic loop between TMS7 and 8 in substrate specificity for ethidium and macrolide antibiotics, while the first periplasmic loop between TMS1 and 2 was suggested to play a role in interactions with other drug substrates. However, misfolding of the chimeric pumps could not be discounted as an explanation for the observed effects on transport activity (Tikhonova *et al.* 2002).

In addition to the chimeric studies, Middlemiss and Poole (2004) used random mutagenesis of the *P. aeruginosa* MexB pump to isolate mutants that showed selective activity for one or more of the antibiotics chloramphenicol, carbenicillin, nalidixic acid and novobiocin. For example, *P. aeruginosa* expressing a T60I mutation in MexB showed a decrease in antibiotic resistance for chloramphenicol only, while a G754D mutation affected antibiotic resistance for nalidixic acid only (Middlemiss and Poole 2004). The T60I and G754D mutations, as well as several others identified in the study, mapped to regions predicted to be involved in protein-protein interactions between the MexB subunits and were not believed to interact directly with the substrates (Middlemiss and Poole 2004). However, the basis for the selectivity displayed by mutations affecting pump assembly is unclear.

Despite the recent crystallization and mutagenesis studies, the substrate transport pathway through RND efflux pumps remains largely unclear. The avenue through which

the substrates enter the central cavity has not been elucidated and may involve the vestibules leading into the cavity from the periplasm. Moreover, while the drug-bound AcrB crystal structures demonstrated how the pump accommodates structurally diverse compounds, the mechanism by which these pumps achieve their unusual substrate selectivity is still unknown.

1.6. RND efflux systems in the environment

1.6.1. Solvent efflux systems are prevalent in the environment

Whereas the MexAB-OprM and AcrAB-TolC efflux systems in *P. aeruginosa* and *E. coli* are significant from a medical viewpoint, the solvent efflux pumps, such as the SrpABC and Ttg systems in *P. putida*, may be valuable for their application in bioremediation of contaminated environments. Assessment of the occurrence of solvent efflux systems in bacteria present in toxic environments is important to predict the successful outcome of bioremediation. Segura *et al.* (2003) probed the genomes of solvent-tolerant and solvent-sensitive *P. putida* strains for homologues of the *P. putida* DOT-T1E toluene efflux pumps. Only the highly solvent-tolerant strains possessed homologues of the toluene-inducible TtgGHI pump, suggesting that this pump is the primary resistance mechanism. However, RND efflux pump genes homologous to the nonspecific solvent and antibiotic efflux pump TtgABC were found in all of the *P. putida* strains, regardless of their level of solvent tolerance (Segura *et al.* 2003). The authors did not correlate the antibiotic resistance profiles of the various *P. putida* strains with the presence of the efflux pump homologues, which may have provided a better indication of the role of the TtgABC system. Also, expression of the efflux pump genes in these *P. putida* strains was not determined, and, therefore, a direct involvement of the efflux pumps in solvent tolerance cannot be confirmed. The study by Segura *et al.* (2003), nevertheless, demonstrated the prevalence of RND efflux systems in environmental isolates.

Genome sequencing projects have also identified RND efflux systems in a number of other environmental isolates. For example, putative RND efflux systems are found in the genomes of *Agrobacterium tumefaciens*, *Thiobacillus denitrificans* and *Geobacter* species. The roles of these efflux systems have not been characterized, and

the significance of the apparent ubiquity of RND efflux systems in gram-negative bacteria is unclear.

1.6.2. An efflux system for polycyclic aromatic hydrocarbons is present in an environmental isolate

Recently, an efflux mechanism for polycyclic aromatic hydrocarbons was observed in *P. fluorescens* LP6a (Bugg *et al.* 2000). *P. fluorescens* LP6a was isolated from petroleum-contaminated soil for its ability to degrade naphthalene, as well as the polycyclic aromatic hydrocarbons phenanthrene and anthracene (Foght and Westlake 1996), which makes it an ideal candidate for studying the transport of hydrocarbons across the cell envelope. Bugg *et al.* (2000) noted the presence of an active efflux mechanism in *P. fluorescens* LP6a for the polycyclic aromatic hydrocarbons phenanthrene, anthracene and fluoranthene. Surprisingly, toluene and naphthalene were not exported from the cell. The discovery of this transport system and its unexpected selectivity prompted further examination of the polycyclic aromatic hydrocarbon efflux pump in *P. fluorescens* LP6a.

1.7. Objectives

Given the prevalence of RND efflux systems in gram-negative bacteria and their involvement in the transport of hydrophobic compounds, it was hypothesized that the efflux mechanism for polycyclic aromatic hydrocarbons in *P. fluorescens* LP6a was an RND family pump. Accordingly, the objectives of this thesis were as follows:

- (1) To identify a gene, or genes, encoding an RND efflux pump in *P. fluorescens* LP6a, and to determine the role of the gene product in polycyclic aromatic hydrocarbon efflux by using gene disruption techniques to create an efflux-deficient mutant;
- (2) To characterize further the substrate specificity of the efflux system by comparing the antibiotic resistance profiles of the wild-type and efflux-deficient mutant;
- (3) To examine the regulation of the efflux pump in response to various conditions, including growth phase, the presence of aromatic hydrocarbons, and antibiotics, by using a promoter-reporter system;

(4) To investigate the roles of the central cavity, pore and vestibule regions of RND efflux pumps in determining substrate specificity by generating site-directed mutants of the polycyclic aromatic hydrocarbon efflux pump and analyzing the ability of the mutant pumps to export hydrocarbons and antibiotics; and

(5) To survey the prevalence of polycyclic aromatic hydrocarbon efflux in other gram-negative bacteria.

The efflux genes identified in *P. fluorescens* LP6a in the course of this study were designated *emhABC* for efflux of *multicyclic hydrocarbons*. The overall aim of this study was to gain a better understanding of both the role of transport processes in hydrocarbon metabolism by *P. fluorescens* LP6a and the mechanism of action of RND efflux systems in gram-negative bacteria.

2. MATERIALS AND METHODS¹

2.1. Chemicals

Phenanthrene (98% pure), anthracene (99% pure), fluoranthene (98% pure) and naphthalene (99% pure) were purchased from Aldrich Chemical Co. (Milwaukee, Wisconsin). Toluene (99.8% pure) was obtained from Fisher Scientific (Nepean, Ontario). For the transport assays, the following radiolabeled compounds were used: [9-¹⁴C]phenanthrene (96.5% radiochemical purity; 19.3 mCi mmol⁻¹; Amersham, Arlington Heights, Illinois), [side ring U-¹⁴C]anthracene (98% pure; 45 mCi mmol⁻¹; Amersham), [3-¹⁴C]fluoranthene (97% pure; 45 mCi mmol⁻¹; Sigma Chemical Co., St. Louis, Missouri); and [U-¹⁴C]naphthalene (49.8 mCi mmol⁻¹; Sigma Chemical Co.). The compounds used in the antibiotic sensitivity assays were tetracycline, chloramphenicol, erythromycin, nalidixic acid, dequalinium chloride, rhodamine 6G and streptomycin from Sigma Chemical Co. and ciprofloxacin from Fisher Scientific (Nepean, Ontario). All other chemicals used were reagent or molecular biology grade.

2.2. Bacterial strains, plasmids and growth conditions

The bacterial strains and plasmids used are listed in Table 2.1, and many of the bacterial strains and plasmids, as well as their growth conditions, have been described previously. The cured strain *P. fluorescens* cLP6a, which lacks the 63-kb catabolic plasmid pLP6a carrying the polycyclic aromatic hydrocarbon degradation genes found in the parental strain *P. fluorescens* LP6a (Foght and Westlake 1996), was used to facilitate analysis of hydrocarbon transport in the absence of metabolism. *P. fluorescens*, *P. aeruginosa*, *P. putida* and *B. cepacia* strains were maintained on plate count agar (Difco Laboratories, Detroit, Michigan) or Luria-Bertani agar supplemented with the appropriate antibiotics. Liquid cultures of the *P. fluorescens*, *P. aeruginosa*, *P. putida* and *B. cepacia* strains used in the hydrocarbon transport and antibiotic sensitivity assays were grown from a 0.5% (vol/vol) inoculum of an overnight, 10-mL seed culture in 200 mL tryptic soy broth (TSB, Difco Laboratories), containing the appropriate antibiotic, at 28°C with

¹ Portions of this section have been published previously by Hearn *et al.* (2003).

Table 2.1. Bacterial strains and plasmids used in this study

Strains and plasmids	Characteristics ^a	Reference or Source
<i>P. fluorescens</i> strains		
LP6a (pLP6a)	Wild-type containing pLP6a	Foght and Westlake (1996)
cLP6a	Wild-type derivative lacking pLP6a	Foght and Westlake (1996)
cLP6a-1	Km ^r , EmhABC ⁻	This study
LP6a-D1	Km ^r , LP6a with transposon insertion in <i>nahB</i> on pLP6a	J. Foght, University of Alberta
LP6a-8	Km ^r , LP6a with transposon insertion in <i>nahC</i> on pLP6a	J. Foght, University of Alberta
LP6a-21-41	Km ^r , LP6a with transposon insertion in <i>nahE</i> on pLP6a	J. Foght, University of Alberta
<i>P. putida</i> strains		
S12	Solvent tolerant, Srp ⁺ Arp ⁺	Weber <i>et al.</i> (1993)
G7	Naphthalene degrader carrying plasmid NAH7	Dunn and Gunsalus (1973)
mt-2	Toluene degrader carrying TOL plasmid pWW0	Williams and Murray (1974)
KT2440	mt-2 derivative lacking pWW0	Bagdasarian <i>et al.</i> (1981)
<i>P. aeruginosa</i> strains		
PAO1	Type strain	Holloway (1969)
Strain A	Clinical isolate from cystic fibrosis patient	LCDC ^b
Strain B	Clinical isolate from cystic fibrosis patient	LCDC ^b
<i>B. cepacia</i> strains		
DB01	Soil isolate	Walsh and Ballou (1983)
K56-2	Clinical isolate	Mahenthalingam <i>et al.</i> (2000)
<i>A. vinelandii</i> UW	Wild-type	W. Page, University of Alberta

Table 2.1. Continued

Strains and plasmids	Characteristics ^a	Reference or Source
<i>E. coli</i> strains		
DH5 α	F ⁻ ϕ 80 <i>dlacZ</i> Δ M15 Δ (<i>lacZYA-argF</i>)U169 <i>deoR recA1 endA1 hsdR17</i> ($\tau_K^- m_K^-$) <i>supE44 λ^- thi-1 gyrA96 relA1</i>	Sambrook <i>et al.</i> (1989)
TOP10F'	F' { <i>lacI^q</i> , Tn10(Tc ^r)} <i>mcrA</i> Δ (<i>mrr-hsdRMS-mcrBC</i>) ϕ 80 <i>lacZ</i> Δ M15 Δ <i>lacX74 recA1 deoR araD139</i> Δ (<i>ara-leu</i>)7697 <i>galU galK rpsL</i> (Str ^r) <i>endA1 nupG</i>	Invitrogen Canada
XL10Gold	Tc ^r Δ (<i>mcrA</i>)183 Δ (<i>mcrCB-hsdSMR-mrr</i>)173 <i>endA1 supE44 thi-1 recA1 gyrA96 relA1 lac Hte</i> [F' <i>proAB lacI^qZ</i> Δ M15 Tn10 (Tc ^r) Amy Chl ^r] ^a	Stratagene
Plasmids		
pUC19	Ap ^r <i>lacZ</i> α , cloning vector	Sambrook <i>et al.</i> (1989)
pCR2.1	Ap ^r Km ^r <i>lacZ</i> α , cloning vector for PCR products	Invitrogen Canada
pUCP26	Tc ^r <i>lacZ</i> α , broad-host range vector	West <i>et al.</i> (1994)
p34S-Sm3	Str ^r , plasmid carrying a streptomycin resistance cassette, used to construct the pTZ110 plasmids	J.J. Dennis, University of Alberta
pCR17	Ap ^r Km ^r , pCR2.1 with 2.2-kb <i>emhB</i> fragment	This study
p251	Ap ^r , pUC19 with 9.6-kb <i>Bam</i> HI insert of cLP6a DNA	This study
pBH5	Tc ^r , pUCP26 with 6.8-kb <i>Bam</i> HI insert encompassing the <i>emh</i> genes and promoter region from p251	This study
pBH5-EmhB _{his}	Tc ^r , pBH5 with a hexahistidine tag inserted in-frame into the 3'-end of the <i>emhB</i> gene	This study

Table 2.1. Continued

Strains and plasmids	Characteristics^a	Reference or Source
pTZ110	Ap ^r , broad-host range, promoterless <i>lacZ</i> operon fusion vector	Schweizer and Chuanchuen (2001)
pTZ110-P _{emhA}	Str ^r , pTZ110 with 290-bp region upstream of the <i>emhA</i> gene inserted into the <i>Bam</i> HI- <i>Hind</i> III sites adjacent to the <i>lacZ</i> gene and with the streptomycin resistance cassette from p34S-Sm3 inserted into the <i>Pst</i> I site	This study
pTZ110-P _{emhR}	Str ^r , pTZ110 with 290-bp region upstream of the <i>emhR</i> gene inserted into the <i>Bam</i> HI- <i>Hind</i> III sites adjacent to the <i>lacZ</i> gene and with the streptomycin resistance cassette from p34S-Sm3 inserted into the <i>Pst</i> I site	This study
pTZ110-str	Str ^r , pTZ110 with the streptomycin resistance cassette from p34S-Sm3 inserted into the <i>Pst</i> I site	This study
pBH10	Km ^r , pCR2.1 with a 3.8-kb fragment of the <i>emhA</i> and <i>emhB</i> genes used for site-directed mutagenesis	This study
pJD105	Gm ^r , broad-host range plasmid carrying the <i>srpABC</i> operon from <i>P. putida</i> S12	J.J. Dennis, University of Alberta
pBH63-srp	Tc ^r , pUCP26 with 6.5-kb <i>Sac</i> I insert encompassing the <i>srpABC</i> operon from pJD105	This study
pBH64-arp	Tc ^r , pUCP26 with 6.5-kb <i>Hind</i> III insert encompassing the <i>arpABC</i> operon from <i>P. putida</i> S12	This study

^a Km^r, kanamycin resistance; Tc^r, tetracycline resistance; Ap^r, ampicillin resistance; Chl^r, chloramphenicol resistance; Str^r, streptomycin resistance; Gm^r, gentamycin resistance.

^b LCDC, Laboratory Centre for Disease Control, Health Canada.

shaking (200 rpm). *Azotobacter vinelandii* UW was grown at 28°C in Burke's buffer with glucose and nitrogen, which contained 0.2 g L⁻¹ KH₂PO₄, 0.8 g L⁻¹ K₂HPO₄, 0.2 g L⁻¹ MgSO₄·7H₂O, 0.1 g L⁻¹ CaSO₄·2H₂O, 5 mg L⁻¹ FeSO₄·7H₂O, 0.25 mg L⁻¹ NaMoO₄·2H₂O, 10 g L⁻¹ glucose and 1.1 g L⁻¹ ammonium acetate as described previously (Bugg *et al.* 2000). *E. coli* strains were cultured in LB medium at 37°C. Ampicillin (100 µg mL⁻¹), kanamycin (50 µg mL⁻¹ for *E. coli* and 25 µg mL⁻¹ for *P. fluorescens*), tetracycline (10 µg mL⁻¹), streptomycin (25 µg mL⁻¹) and gentamycin (10 µg mL⁻¹) were added as required.

2.3. Phenotypic analysis of efflux ability

2.3.1. Polycyclic aromatic hydrocarbon transport assays

The accumulation of radiolabeled hydrocarbon substrate in the various strains was measured by using the rapid centrifugation method described by Bugg *et al.* (2000). For all transport experiments, cultures were grown to an OD₆₀₀ ~4 in 200 mL TSB, harvested by centrifugation at 8000 × *g* and 4°C in a Sorvall RC-5B refrigerated superspeed centrifuge (Dupont Instruments, Newtown, Connecticut), washed twice in 0.1 M potassium phosphate buffer (pH 7.2) and resuspended to a final optical density (OD₆₀₀) of 1 in the same buffer. Glassware was treated with chromic acid to reduce absorption of the hydrocarbon to the glass (Bugg *et al.* 2000). For phenanthrene, anthracene and fluoranthene, transport assays with 20 mL of cell suspension were carried out in 250-mL shake flasks. The radiolabeled hydrocarbon substrates were mixed with unlabeled compound and added to the cell suspensions at final concentrations of 6.4 µM for phenanthrene, 0.26 µM for anthracene and 1.2 µM for fluoranthene, which corresponded to 90% of the aqueous solubility limit for these compounds. For naphthalene, transport assays with 20 mL cell suspension were conducted in 35-mL serum bottles sealed with Teflon stoppers, and sampling was done via syringe. Naphthalene was routinely used at final concentrations of 5.7 µM or 50 µM, which corresponded to 2.5% and 22% of its aqueous solubility limit. To determine the accumulation of radiolabeled substrate in the cells, 1-mL samples of the cell suspension were removed to 1.5-mL microcentrifuge tubes and centrifuged at 16 000 × *g* in a microcentrifuge for 20 s. The amount of

radioactivity in the aqueous phase was measured by placing a 0.5-mL aliquot of the supernatant in 10 mL of aqueous scintillation fluor (ACS; Amersham) and counting using a Beckman LS3801 liquid scintillation counter. The remaining supernatant was removed, and the cell pellet was resuspended in 1 mL of 0.1 M potassium phosphate buffer (pH 7.2). The radioactivity in a 0.5-mL aliquot of the remaining cell suspension was measured by liquid scintillation counting. Time course experiments were performed in which the accumulation of substrate in the cells was followed before and after addition of sodium azide to a final concentration of 30 mM to inhibit active transport processes. For steady-state measurements, samples taken in duplicate were analyzed after the transport process had reached steady-state following addition of the substrate to the cell suspension (approximately 10 min) and following addition of 30 mM sodium azide (approximately 10 min). The time periods required to reach steady-state were based on the results of time course experiments. All transport assays were conducted at room temperature.

2.3.2. Determination of toluene tolerance

Growth on solid media in the presence of vapour-phase toluene (Kieboom *et al.* 1998a) was used to assess toluene tolerance resulting from the presence or absence of the EmhABC efflux system. Toluene (about 5 mL) was placed in a glass Petri dish in the bottom of a sealed container and incubated at 28°C overnight to allow the air in the container to become saturated with toluene. The test strains were streaked onto LB agar containing the appropriate antibiotics, placed inside the toluene-saturated container and incubated at 28°C. As a control, duplicate plates were incubated in the absence of toluene. After 4 days, the plates were removed from the toluene container, scored for growth and further incubated for 4 days in the absence of toluene to assess the viability of the cultures.

2.3.3. Antibiotic sensitivity assays

The minimum inhibitory concentrations (MICs) of tetracycline, chloramphenicol, nalidixic acid, rhodamine 6G, dequalinium chloride, ciprofloxacin, erythromycin and streptomycin were determined for the *P. fluorescens* strains in TSB by the microtiter broth dilution method (Jorgensen *et al.* 1999). In microtiter plates, two-fold serial

dilutions of the test antibiotics were prepared in TSB to give the following maximum concentrations: 32 $\mu\text{g mL}^{-1}$ tetracycline; 256 $\mu\text{g mL}^{-1}$ chloramphenicol; 512 $\mu\text{g mL}^{-1}$ nalidixic acid; 128 $\mu\text{g mL}^{-1}$ rhodamine 6G; 32 $\mu\text{g mL}^{-1}$ dequalinium chloride; 1 $\mu\text{g mL}^{-1}$ ciprofloxacin; 1024 $\mu\text{g mL}^{-1}$ erythromycin; and 64 $\mu\text{g mL}^{-1}$ streptomycin. Cell cultures were grown to a density of 10^8 colony-forming units (cfu) mL^{-1} or $\text{OD}_{600} \sim 0.3$, diluted 100-fold in fresh TSB and inoculated into an equal volume of medium containing antibiotic in the microtiter plates to yield an inoculum of 5×10^5 cfu mL^{-1} per well. The microtiter plates were incubated at 28°C for 24 h. The OD_{600} of the microtiter cultures was measured by using a SpectraMax Plus³⁸⁴ microplate reader (Molecular Devices Corporation, Sunnyvale, California) and compared to a positive control grown in the absence of antibiotic. The MIC was defined as the lowest concentration of antibiotic that inhibited growth by more than 50% compared with a control grown in the absence of antibiotic.

2.4. DNA techniques

2.4.1. DNA isolation, cloning and transformation

Genomic DNA was prepared using the phenol:chloroform method as described by Maloy (1990). Plasmid DNA was isolated either by the alkaline lysis method (Sambrook *et al.* 1989) or with a QIAprep Spin Miniprep kit (Qiagen, Mississauga, Ontario). Restriction digestion and ligation reactions were performed according to the supplier's directions (Roche Applied Science, Laval, Quebec). DNA fragments separated on agarose gels were purified by using a QIAquick gel extraction kit (Qiagen) for DNA fragments less than 6 kb long and a QIAEX II gel extraction kit (Qiagen) for DNA fragments more than 6 kb long. Plasmid DNA was introduced into competent *E. coli* by heat shock at 42°C and into electrocompetent *P. fluorescens* by electroporation with a Gene Pulser by using a resistance of 200 Ω , an electric charge of 25 μF , and a voltage of 2.5 kV across a 0.2-cm cuvette (Bio-Rad Laboratories, Mississauga, Ontario). Competent *E. coli* DH5 α cells were prepared by using the 18°C procedure described by Inoue *et al.* (1990), while competent *E. coli* TOP10F' and XL10-Gold cells were purchased from Invitrogen Canada (Burlington, Ontario) and Stratagene (La Jolla,

California). Cultures for preparation of electrocompetent *P. fluorescens* cells were grown with shaking in TSB at 28° to an OD₆₀₀ of 0.4-0.6, harvested at 4°C by centrifugation at 3000 × g, washed twice in cold 10% (vol/vol) glycerol, and finally concentrated 50-fold in 10% (vol/vol) glycerol. Electrocompetent cells were stored at -80°C.

2.4.2. Polymerase chain reaction

The polymerase chain reaction (PCR) was performed with either a Flexigene thermal cycler (Techne, Princeton, New Jersey) or an Eppendorf Mastercycler (Fisher Scientific, Nepean, Ontario). Oligonucleotide primers used for adding the histidine tag to the *emhB* gene and for site-directed mutagenesis were synthesized by Invitrogen Canada, while all other primers were synthesized by the Molecular Biology Services Unit at the University of Alberta (Edmonton, Alberta). Unless otherwise specified, PCR reactions (20 µL) contained 10-50 ng template DNA, 200mM Tris-HCl (pH 8.8), 20 mM MgSO₄, 100 mM KCl, 100 mM (NH₄)₂SO₄, 1% (vol/vol) TritonX-100, 1 mg mL⁻¹ bovine serum albumin (nuclease free, non-acetylated; Roche Applied Science), 0.2 mM of each deoxynucleoside triphosphate (Roche Applied Science), 0.6 µM of each primer, and 5 U *Taq* DNA polymerase. For high-fidelity PCR, 2 U *Pfu* polymerase was used in the reaction instead of the *Taq* polymerase. When required, PCR products were cloned into *E. coli* TOP10F' by using a TOPO TA cloning kit (Invitrogen Canada).

2.4.3. DNA sequencing

Nucleotide sequencing reactions were performed with either a DYEnamic ET Terminator Cycle Sequencing kit (Amersham Biosciences) or a BigDye® Terminator Cycle Sequencing kit (Applied Biosystems Inc., Foster City, California), and the results were analyzed with a model 373A automated DNA sequencer (Applied Biosystems Inc.) by the Molecular Biology Services Unit (University of Alberta, Edmonton, Alberta). Sequence data were analyzed with the GeneTool 1.0 software package (BioTools Inc., Edmonton, Alberta).

2.4.4. Sequence analysis

The BLAST program (Altschul *et al.* 1990) was used for sequence homology searches in the National Center for Biotechnology Information GenBank database (<http://www.ncbi.nlm.nih.gov/>). Nucleotide and protein sequence alignments were generated with the ClustalX program (Thompson *et al.* 1997). Phylogenetic trees were constructed by using the Jones-Taylor-Thornton distance matrix and neighbor-joining methods in the Phylip programs (Felsenstein 2004) and were drawn with the Treeview program (Page 1996). Percent sequence identities and similarities were determined by using the Sequence Manipulation Suite version 2 (Stothard 2000). Protein secondary structure was predicted by using the Proteus Structure Prediction Server on the Canadian Bioinformatics Help Desk website (<http://129.128.185.59/~scott/proteus/index.shtml>).

2.5. Identification of the *emhABC* genes

2.5.1. Detection and inactivation of *emh*

PCR was performed with *P. fluorescens* cLP6a genomic DNA by using the following degenerate oligonucleotide primers corresponding to conserved regions of RND efflux pumps: forward primer BHN6, 5'-CGGA(C/T)GG(C/T)TCICAGGT(A/G)CG-3', and reverse primer BHN7, 5'-A(A/G)G(A/G)TGAAIGC(G/C)AGIGAGGTC-3', where the nucleotides in parentheses represent degenerate sites and I represents inosine. The PCR mixture (100 μ L) contained 500 ng of genomic DNA from *P. fluorescens* cLP6a, 75 mM Tris-HCl, 20 mM (NH₄)₂SO₄, 2 mM MgCl₂, 0.1% (vol/vol) Tween 20, 0.2 mM of each deoxynucleoside triphosphate, 0.6 μ M of each primer, and 5 U *Taq* polymerase. The PCR program consisted of an initial denaturation at 95°C for 5 min, followed by 25 cycles of 95°C for 30 s, 50°C for 30 s, and 72°C for 90 s, and a final extension step at 72°C for 5 min. A 2.2-kb PCR product was isolated and cloned into pCR2.1 by TA cloning, producing plasmid pCR17 (Table 2.1). The 2.2-kb insert in pCR17 was sequenced to verify its identity as a putative RND efflux pump gene. The plasmid pCR17 was introduced into *P. fluorescens* cLP6a by electroporation, and transformants in which the plasmid was integrated into the chromosome by homologous recombination were selected on Luria-Bertani agar containing kanamycin. One transformant, designated *P. fluorescens* cLP6a-1, was selected for further study.

Insertion of pCR17 into the *emhB* gene in *P. fluorescens* cLP6a-1 was confirmed by Southern blotting and hybridization. For Southern blotting and hybridization, DNA from agarose gels was transferred to Hybond N membranes (Amersham Biosciences, Baie D'Urfe, Quebec), and hybridization was performed according to the manufacturer's protocol (Amersham Biosciences). The 2.2-kb efflux gene fragment and plasmid pCR2.1 were used as probes and labeled with [α - 32 P]dCTP (3000 Ci mmol $^{-1}$; Amersham Biosciences) by random primer labeling (Roche Applied Science).

2.5.2. Sequencing the *emh* genes

To locate the chromosomal region containing the efflux pump gene, restriction digests of *P. fluorescens* cLP6a genomic DNA were analyzed by Southern blotting and hybridization using the 2.2-kb *emhB* gene fragment as a probe. The *emhB* gene hybridized to a 9.7-kb *Bam*HI fragment. Genomic DNA from *P. fluorescens* cLP6a was digested with *Bam*HI, and the 7- to 14-kb fragments were ligated to *Bam*HI-linearized pUC19 and transformed into *E. coli* DH5 α . About 300 ampicillin-resistant transformants were screened by colony PCR using primers specific for the *emhB* gene sequence (BHN 10 5'-CTTGCTCTGTGCCCGCCATG-3' and BHN11 5'-ACCGTGGCGTCAAAAGC TAC). One positive colony, harbouring plasmid p251 carrying a 9653-bp insert, was identified, and the nucleotide sequence of the insert was determined.

2.5.3. Nucleotide accession number

The nucleotide sequence of the 9653-bp insert of plasmid p251 containing the *emhABC* genes has been deposited in the GenBank database under accession number AY349612.

2.5.4. Complementation of *emhABC* in *P. fluorescens* cLP6a-1

A 6789-bp fragment containing the *emhABC* genes and their upstream region was amplified from p251 using the Expand Long Template PCR system (Roche Applied Science). The forward primer BHN49, 5'-TTACAGGATCCCGGCTTTTGTAACGATG TGGG-3', corresponding to nucleotide positions 767 to 787 in the nucleotide sequence (accession number AY349612), and reverse primer BHN50, 5'-GTTCAGGATCCCACC

CTTTCCCGCAGCCAAC-3', corresponding to positions 6731 to 6751 in the nucleotide sequence, contained *Bam*HI sites (underlined) for cloning the PCR product into the broad-host-range vector pUCP26. The resulting plasmid pBH5 contained the *emhABC* genes in the opposite orientation as the *lacZ* promoter (Figure 2.1). Plasmid pBH5 was introduced into *P. fluorescens* cLP6a-1 by electroporation, and one transformant, designated *P. fluorescens* cLP6a-1(pBH5), was selected for analysis. As a vector control, pUCP26 was electroporated into *P. fluorescens* cLP6a-1 to obtain *P. fluorescens* cLP6a-1(pUCP26).

2.6. Regulation of the *emhABC* efflux system

2.6.1. Construction of *emh* promoter-reporter plasmids

The intergenic region between *emhR* and *emhA* genes was amplified from p251 by PCR by using primers BHN55 (5'-TAAGACGAAAGCTTGGCAGTACAACCTCAATCAGGGTGC-3', with the *Hind*III site underlined) and BHN56 (5'-CCAGAGGGATCCAGCTGGCTTGAATTGCATGAAA-3', with the *Bam*HI site underlined) corresponding to positions 656 to 680 and positions 919 to 940 in the nucleotide sequence (accession number AY349612). The PCR product was cloned upstream of the promoterless *lacZ* gene in plasmid pTZ110, and the streptomycin resistance cassette from plasmid p34S-Sm3 was inserted into the ampicillin resistance gene on plasmid pTZ110 at the unique *Pst*I site to generate the promoter-reporter plasmid pTZ110-P_{emhA} (Figure 2.2A). A reporter plasmid in which the intergenic region between the *emhA* and *emhR* genes was oriented in the opposite direction was constructed in a similar fashion by using primers BHN72 (5'-TAAGACTAAAGCTTCAGCTGGCTTGAATTGCATGA-3', with the *Hind*III site underlined) and BHN73 (5'-TCACATGGATCCGGCAGTACAACCTCAATCAG-3', with the *Bam*HI site underlined) corresponding to positions 920 to 940 and positions 656 to 675 in the nucleotide sequence (accession number AY349612). The resulting plasmid, pTZ110-P_{emhR}, has the intergenic region in the same orientation as the *emhR* gene (Figure 2.2B). A control plasmid, pTZ110-str, was constructed by inserting the streptomycin resistance cassette into the *Pst*I site of pTZ110. The reporter plasmids and the control plasmid were electroporated into *P. fluorescens* cLP6a to generate strains cLP6a(pTZ110-P_{emhA}), cLP6a(pTZ110-P_{emhR}) and cLP6a(pTZ110-str).

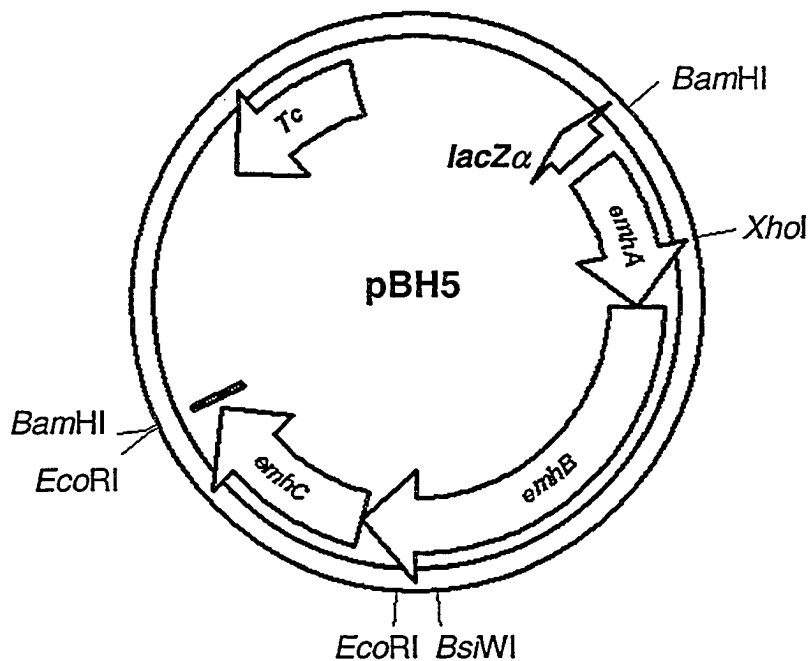


Figure 2.1. Schematic of plasmid pBH5 containing the *emhABC* genes. Plasmid pBH5 was constructed by cloning the *emhABC* genes into the *Bam*HI site on the broad-host-range vector pUCP26. The *emhABC* genes were inserted in the opposite orientation of the *lacZα* gene on the vector. The tetracycline resistance marker (*Tc*) and the locations of the *Bam*HI, *Eco*RI, *Bsi*WI and *Xho*I restriction sites are indicated.

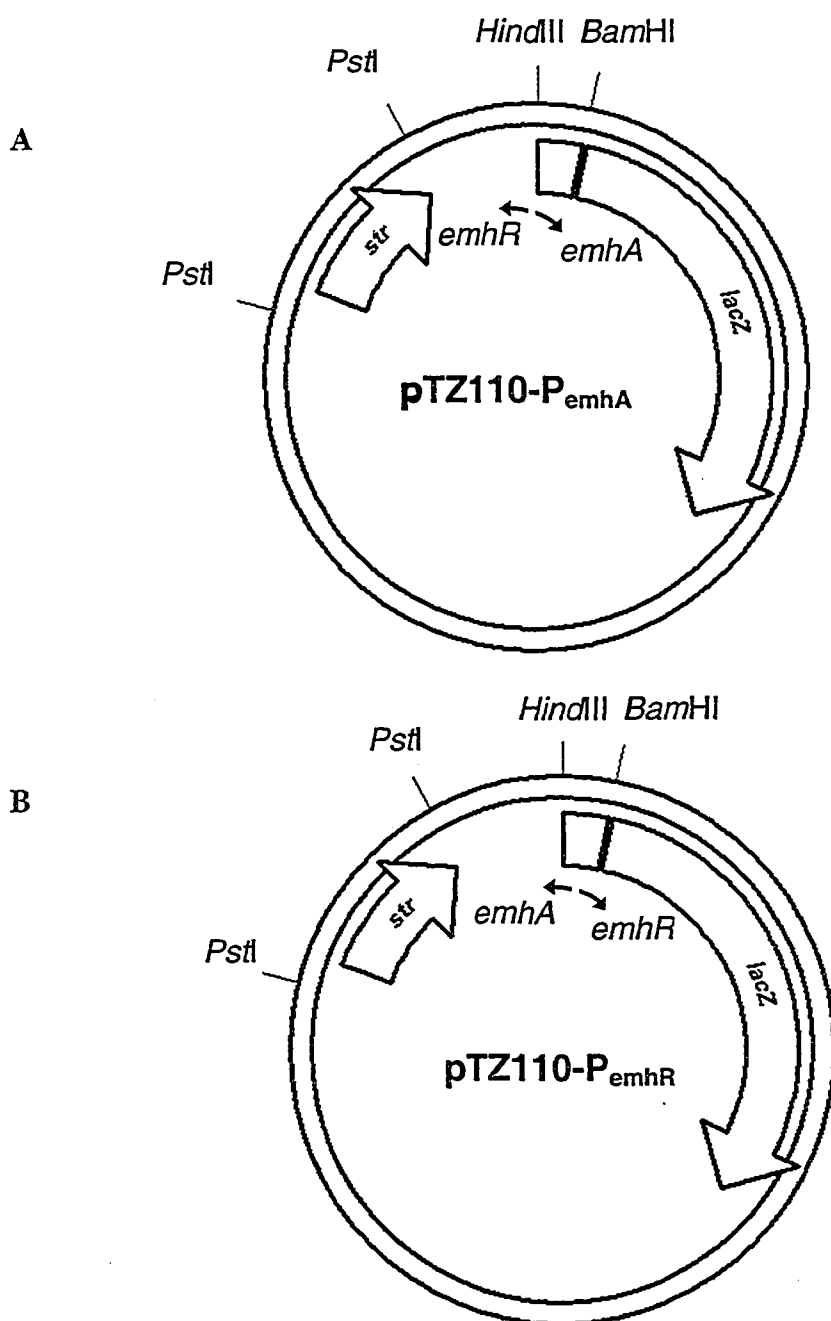


Figure 2.2. Schematic of the promoter-reporter transcriptional fusion plasmids. The *emhA-emhR* intergenic region was fused upstream of the promoterless *lacZ* gene on plasmid pTZ110. Plasmid pTZ110-P_{emhA} (A) was constructed with the *emhA-emhR* intergenic region inserted such that the *emhA* and *lacZ* genes are in the same direction. In plasmid pTZ110-P_{emhR} (B), the intergenic region was inserted such that the *emhR* and *lacZ* genes are in the same direction. The directions of the *emhA* and *emhR* genes are indicated. The streptomycin resistance marker (*str*) and the *Hind*III, *Bam*HI and *Pst*I restriction sites are indicated.

2.6.2. Determination of *emh* promoter activity

2.6.2.1. Growth phase dependence

Growth curves were generated for *P. fluorescens* strains cLP6a(pTZ110-P_{emhA}), cLP6a(pTZ110-P_{emhR}) and cLP6a(pTZ110-str) grown at 28°C in 500-mL flasks containing 200 mL TSB with shaking (200 rpm) and in test tubes containing 10 mL TSB with aeration on a tube roller. At various time intervals, samples were removed for OD₆₀₀ and β-galactosidase activity measurements (section 2.6.3). For consistency, the same mass of cells, which corresponded to an OD₆₀₀ ~0.5 in a 1-mL volume, was removed at each time point.

2.6.2.2. Effect of hydrocarbons and metabolites

To determine the effects of various hydrocarbons on expression of the *lacZ* reporter gene, *P. fluorescens* strains cLP6a(pTZ110-P_{emhA}), cLP6a(pTZ110-P_{emhR}) and cLP6a(pTZ110-str) were grown in 10 mL TSB in the presence of 0.5 g L⁻¹ of phenanthrene, 0.5 g L⁻¹ of anthracene, 0.5 g L⁻¹ fluoranthene, 0.5 g L⁻¹ naphthalene or 0.02% (vol/vol) toluene to an OD₆₀₀ of ~2.5. A mass of cells corresponding to an OD₆₀₀ ~0.5 in a 1-mL volume was harvested for measurement of β-galactosidase activity.

Metabolites of phenanthrene degradation were also tested to determine their effect on the regulation of the *emh* genes. Crude metabolite samples were prepared from the *P. fluorescens* LP6a strains D1, 8 and 21-41, which have the 1,2-dihydroxy-1,2-dihydronaphthalene dehydrogenase (*nahB*), 1,2-dihydroxynaphthalene dioxygenase (*nahC*) and *trans*-*o*-hydroxybenzylidene pyruvate hydratase-aldolase (*nahE*) genes on plasmid pLP6a disrupted by transposon mutagenesis (Table 2.1). The genes for polycyclic aromatic hydrocarbon degradation were induced by addition of 0.5 mM salicylate to *P. fluorescens* LP6a strains, which had been grown in 100 mL TSB to an OD₆₀₀ ~4. After 4 h of induction at 28°C, the cells were washed in 0.1 M potassium phosphate buffer (pH 7.2), resuspended in 100 mL of the same buffer, and 50 μL of a 1M phenanthrene solution in dimethyl formamide was added to yield a final concentration of 0.5 mM. The cell suspensions were incubated at 28°C for 16 h to allow for metabolism of the phenanthrene. Cells were removed by centrifugation, and the supernatant was

collected. The presence of metabolites in the supernatants was confirmed by measuring the absorbance from 200 nm to 400 nm using a Philips PU8740 ultraviolet-visible scanning spectrophotometer (Fisher Scientific). The supernatants were diluted 2-fold in 2× TSB containing 25 $\mu\text{g mL}^{-1}$ streptomycin to which was added a 0.5% (vol/vol) inoculum of *P. fluorescens* cLP6a(pTZ110- P_{emhA}), cLP6a(pTZ110- P_{emhR}) or cLP6a(pTZ110-str). Salicylate and 2-aminobenzoate at concentrations of 2 mM in 10 mL TSB were also tested with the reporter strains. The reporter strains were grown to an OD_{600} of ~ 2.5 , and a mass of cells corresponding to an $\text{OD}_{600} \sim 0.5$ in a 1-mL volume was harvested for measurement of β -galactosidase activity.

2.6.2.3. Effect of antibiotics

The reporter strains *P. fluorescens* cLP6a(pTZ110- P_{emhA}), cLP6a(pTZ110- P_{emhR}) and cLP6a(pTZ110-str) were grown in the presence of tetracycline, chloramphenicol, erythromycin, and nalidixic acid at concentrations of $\frac{1}{4}\times\text{MIC}$ (section 2.3.3) to an $\text{OD}_{600} \sim 2.5$ to determine the effect of these compounds on the expression of the *emh* genes. A mass of cells corresponding to an $\text{OD}_{600} \sim 0.5$ in a 1-mL volume was harvested for measurement of β -galactosidase activity.

2.6.3. Measurement of β -galactosidase activity

The β -galactosidase activities of the samples were determined by permeabilizing the cells according to the Miller assay method (Miller 1972) and measuring the hydrolysis of *o*-nitrophenyl- β -D-galactosidase (ONPG, Sigma) using the microplate assay method described by Griffith and Wolf (2002). The harvested cells were resuspended in 0.85% (wt/vol) sodium chloride, and an aliquot was removed to determine the OD_{600} using a SpectraMax Plus³⁸⁴ microplate reader (Molecular Devices Corporation). To measure the enzyme activity, the resuspended cells were diluted 10-fold in Z-buffer containing 60 mM Na_2HPO_4 , 40 mM NaH_2PO_4 , 10 mM KCl, 1mM $\text{MgSO}_4 \cdot 7\text{H}_2\text{O}$ and 50 mM β -mercaptoethanol. Cells were permeabilized in the Z-buffer by addition of sodium dodecylsulfate (SDS) and chloroform to final concentrations of 0.002% (wt/vol) and 0.04% (vol/vol), respectively. Aliquots (100 μL) of the permeabilized cells were placed

in triplicate into a 96-well microplate, and 20 μL of ONPG was added to a final concentration of 0.67 mg mL^{-1} . After 15 min, the reaction was quenched by addition of 50 μL Na_2CO_3 to a final concentration of 0.3 M. The absorbance at 420 nm (A_{420}) and the absorbance at 550 nm (A_{550}) were measured, and the specific activity of β -galactosidase was calculated according to equation [2]:

$$\beta\text{-galactosidase activity} = \frac{1000 \times (A_{420} - 1.75A_{550})}{t \text{ (min)} \times V \text{ (ml)} \times OD_{600}} \quad [2]$$

where t is the assay time in minutes and V is the volume of cells used in the assay in mL (Griffith and Wolf 2002).

2.7. Site-directed mutagenesis of *EmhB*

2.7.1. Construction of histidine-tagged *EmhB*

An oligonucleotide encoding a six-histidine tag was introduced in-frame at the 3'-end of the *emhB* gene using the overlap extension PCR method (Horton *et al.* 1989) such that the histidines will be located on the cytoplasmic C-terminus of the *EmhB* protein. A 1-kb fragment at the 3'-end of the *emhB* gene was amplified from pBH5 by PCR with the forward primer EMH1, 5'-GGACTGAACGACGAGCCGCAATAT-3', corresponding to positions 4234 to 4257 in the nucleotide sequence (accession number AY349612), and the reverse primer EMH2, 5'-ATTAGTGATGGTGATGGTGGTGGCCAGCCTCTTTAGAAGGTTCAATAGC-3', corresponding to positions 5200 to 5229 in the nucleotide sequence (accession number AY349612) with the additional codons for the six-histidine tag underlined. Similarly, a 1.6-kb fragment at the 5'-end of the *emhC* gene was amplified from pBH5 by PCR with the forward primer EMH3, 5'-GGCCACCACCATCACCATCACTAATGAGCAAGTCGCTACTCTCCATCG-3', corresponding to positions 5227 to 5253 in the nucleotide sequence (accession number AY349612) with the additional codons for the six-histidine tag underlined, and the reverse primer EMH4, 5'-CAGGAAACAGCTATGACCATGATTACGA-3'. In the overlap PCR step, the 1-kb and 1.6-kb PCR products were mixed in equimolar amounts without additional primers and subjected to the following PCR cycles: an initial denaturation at 94°C for 2 min, five cycles of 94°C for 30 s, 50°C for 3 min and 72°C for 2.5 min, and a final extension at 72°C for 5 min. The extension PCR step contained 5 μL of the overlap PCR mixture and

the forward and reverse primers EMH1 and EMH4. The extension PCR consisted of an initial denaturation at 94°C for 2 min, 25 cycles of 94°C for 30 s, 55°C for 30 s and 72°C for 2.5 min, and a final extension at 72°C for 5 min. The resulting 2.6-kb PCR product was digested with *EcoRI*, and the 1.8-kb *EcoRI* fragment was ligated into *EcoRI*-digested pBH5 to replace the corresponding region in the plasmid. The new plasmid carrying the histidine-tagged *emhB* gene was designated pBH5-EmhB_{his} and was transformed into *P. fluorescens* cLP6a-1 by electroporation. Nucleotide sequencing of the 1.8-kb *EcoRI* region in plasmid pBH5-EmhB_{his} confirmed the in-frame addition of six histidines at the 3'-end of the *emhB* gene and the absence PCR-introduced errors or other mutations.

2.7.2. Construction of site-directed mutations in EmhB_{his}

Mutations in the *emhB*_{his} gene were introduced by PCR using the QuikChange® II XL Site-directed Mutagenesis kit (Stratagene). To facilitate the QuikChange reaction, a 3.8-kb fragment of the *emhA* and *emhB* genes spanning the unique *BsiWI* and *XhoI* restriction sites was amplified from pBH5-EmhB_{his} by PCR with primers BHN20 5'-GGTCGACGAACAGGCGGTGAG-3' and BHN38 5'-CCCAGAAGATCGCCAGAACC-3', corresponding to positions 1287 to 1307 and 5118 to 5137 in the nucleotide sequence (accession number AY349612). The 3.8-kb PCR product was cloned into pCR2.1 by TA cloning, and the resulting plasmid, pBH10, was used as the template in the QuikChange reaction. The QuikChange reaction (50µL) contained 20 or 100 ng of pBH10 template DNA, 1×QuikChange buffer, 3 µL Quiksolution, 1 µL dNTP mix, 1 µL *PfuUltra*, and forward and reverse primers at a concentration of 12 µM each. The PCR cycles consisted of an initial denaturation at 95°C for 1 min, 18 cycles of 95°C for 50 s, 60°C for 50 s, and 68°C for 8 min, and a final extension at 68°C for 7 min. Following the PCR, the parental plasmids were digested with *DpnI*, and the mutated pBH10 plasmids were transformed into *E. coli* DH5α. To replace the wild-type *emhB*_{his} gene on plasmid pBH5-EmhB_{his}, the 3-kb *BsiWI-XhoI* fragments from the mutated pBH10 plasmids were ligated into *BsiWI-XhoI* digested pBH5-EmhB_{his}. The resulting plasmids, carrying the mutated *emhB*_{his} genes, were transformed into *P. fluorescens* cLP6a-1 by electroporation. Twenty-one mutations were introduced into the *emhB*_{his} gene in this manner (Table 2.2), and one

Table 2.2. List of EmhB mutations generated by site-directed mutagenesis

Mutation	Plasmid	Mutagenic primer sequence ^a
F386A	pBH13	GGCATCCTCGCGGCGGCCGGTTTCAGCATCAACACC GGTGTGATGCTGAAACCGGCCCGCCGAGGATGCC
A385Y	pBH14	CGTTCGGCATCCTCGCGTACTTCGGTTTCAGCATC GATGCTGAAACCGAAGTACGCGAGGATGCCGAACG
A384P	pBH16	TGGGTACGTTCCGGCATCCTCCCGCGTTCCGGTTTCAGCATCAA TTGATGCTGAAACCGAACGCCGGGAGGATGCCGAACGTACCCA
A384P/A385Y	pBH18	ACGTTCCGGCATCCTCCCGTACTTCGGTTTCAGCATCAA TTGATGCTGAAACCGAAGTACGGGAGGATGCCGAACGT
F458A	pBH20	ATTGCTGCCGATGGCGGCCTTCAGTGGCTCCACGGGTGT ACACCCGTGGAGCCACTGAAGGCCGCCATCGGCAGCAAT
F459A	pBH22	ATTGCTGCCGATGGCGTTCGCCAGTGGCTCCACGGGTGT ACACCCGTGGAGCCACTGGCGAACGCCATCGGCAGCAAT
N99A	pBH24	CGAGCAAGGCACCGCCTCCGATACCGCG CGCGGTATCGGAGGCCGGTGCCTTGCTCG
D101A	pBH26	TCGAGCAAGGCACCAACTCCGCTACCGCGCAGGTCCAGGTCCA GGACCTGGACCTGCGCGGTAGCCGGAGTTGGTGCCTTGCTCGA
N112A	pBH28	GGTCCAGAACAAGCTGGCCCTGGCCACCCCGCTGCT GCAGCGGGGTGGCCAGGGCCAGCTTGTTCTGGACC
Y157A	pBH32	ACCTGTCCAACGCCATCGTGTGAACATG GCATGTTGACACGATGGCGTTGGACAGGTC
F281A	pBH36	ATCAACGCTCAGGCCAACGGTGCACCGGCTTCC CGGAAGCCGGTGCACCGTTGGCCTGAGCGTTGA
F316A	pBH38	CATTAACACGCTCAAGCCAGCCTTCCCGLAAG CTTGCGGAAGGCTGGCTTGAGCGTGTTAATG
F682A	pBH40	TTTCGATGTGGCCCTGCAAGACCGCGCCGG GGCGCGGTCTTGACAGGGCCACATCGAAAC
F325A	pBH44	GGGATGGAAGTGGTGGCCCCGTATGACACCAC GTGGTGTGATACGGGGCCACCACTTCCATCCC
S608A	pBH46	GCGCCGTGGCGGCCGGTGTTTACCG CGGTAAACACCGCCGCCACGGCGC
N282A	pBH48	TCAACGCTCAGTTCGCCGGTGCACCGGC GCCGGTGCACCGGCCAACTGAGCGTTGA
Q104A	pBH50	CTCCGATACCGCGGCCGGTCCAGGTCCAG CTGGACCTGGACCGCCCGGTATCGGAG
K131A	pBH52	CGTGACCAAGTCAGTGGCGAACTTCTGCTGGTG CACCAGCAGGAAGTTCGCCACTGACTTGGTCACG

Table 2.2. Continued

Mutation	Plasmid	Mutagenic primer sequence ^a
D101E	pBH56	TCGAGCAAGGCACCAACTCC <u>GAA</u> ACCGCGCAGGTCCAGGTCCA GGACCTGGACCTGCGCGGTT <u>TC</u> GGAGTTGGTGCCTTGCTCGA
D101N	pBH58	TCGAGCAAGGCACCAACTCC <u>AAT</u> ACCGCGCAGGTCCAGGTCCA GGACCTGGACCTGCGCGGTA <u>TT</u> GGAGTTGGTGCCTTGCTCGA
F317A	pBH60	CGCTCAAGCCATT <u>CGCC</u> CCGCAAGGGATGG CCATCCCTTGCGGG <u>GCG</u> AATGGCTTGAGCG

^a Primer sequences are shown in 5' to 3' direction, and the mutated codon is underlined.

mutation (A206S) was generated by a PCR-introduced error. Nucleotide sequencing confirmed the successful introduction of the mutations.

2.7.3. SDS-polyacrylamide gel electrophoresis and western immunoblotting

To confirm expression of the mutated EmhB_{his} proteins in *P. fluorescens* cLP6a-1, SDS-polyacrylamide gel electrophoresis (SDS-PAGE) and western immunoblotting was performed on whole cell extracts. Cultures were grown in 200 mL TSB from a 0.5% (vol/vol) inoculum of an overnight 10-mL pre-culture, and two 100- μ L aliquots were harvested by centrifugation. One sample was used to measure the total protein content with the BCA protein assay kit (Pierce Chemical Co., Rockford, Illinois). Cells in the second sample were resuspended in 100 μ L SDS-PAGE gel loading buffer, which contained 0.225 M Tris-HCl (pH 6.8), 5% (wt/vol) SDS, 0.05% (wt/vol) bromophenol blue, 0.25 M dithiothreitol and 50% (vol/vol) glycerol, and were heated for 10 min at 95°C to lyse the cells. Samples containing 10 μ g of total cell protein were analyzed by SDS-PAGE as described by Sambrook *et al.* (1989). The stacking and resolving gels consisted of 4% and 6% (wt/vol) acrylamide (29:1 acrylamide: N,N'-methylene bisacrylamide; Bio-Rad Laboratories), respectively. Electrophoresis was performed in a Bio-Rad Mini-Protein III cell (Bio-Rad Laboratories) containing SDS-PAGE running buffer (50 mM Tris-HCl (pH 8.3), 384 mM glycine and 0.1% (wt/vol) SDS). Following electrophoresis, the proteins were transferred to Hybond-P membranes (Amersham Biosciences) by electroblotting using a Mini-Protean 3 Electrophoretic Transfer cell (Bio-Rad Laboratories). The electroblotting transfer buffer contained 25 mM Tris-HCl (pH 8.3), 192 mM glycine and 20% (vol/vol) methanol and the transfer was conducted at 100V and 350 mA for 1-2 h at 4°C. Immunoblotting with the Penta-HisTM HRP conjugate (Qiagen) was performed according to the manufacturer's protocols, and detection was carried out using the ECL chemiluminescence kit (Amersham Biosciences). A 6 \times His protein ladder (Qiagen) was included on the SDS-PAGE gels as a molecular weight marker for visualization on the western immunoblots.

2.7.4. Chemical cross-linking of EmhB_{his} protein complexes

In vivo cross-linking of the EmhB_{his} protein in *P. fluorescens* cLP6a-1 strains carrying the *emhB_{his}* wild-type and mutated genes was performed as described by Zgurskaya and Nikaido (2000b). Cultures were grown to an OD₆₀₀ ~ 4 in TSB containing 10 µg mL⁻¹ tetracycline, and 100 µL of cells were harvested by centrifugation at 16 000 × g for 2 min. The cells were washed in 0.1 M potassium phosphate buffer (pH 7.2), collected by centrifugation and resuspended in the same buffer to a final volume of 500 µL. The cell suspensions were split, and the cross-linking reagent dithiobis(succinimidyl propionate) (DSP; Sigma) was added to one-half of the cell suspension at a final concentration of 0.4 mM. The cells were incubated for 30 min at room temperature before terminating the cross-linking reaction by addition of Tris-HCl (pH 7.5) to a final concentration of 100 mM. Cross-linked and control cells were harvested and resuspended in SDS-PAGE gel loading buffer with or without 0.25 M dithiothreitol. Samples were heated at 95°C for 10 min prior to electrophoresis on SDS-PAGE gels and western immunoblotting with an anti-His₆ antibody was performed on the cross-linked samples as described above (section 2.7.3).

2.7.5. Protein modeling

The SWISS-MODEL protein structure homology-modeling server (Guex and Peitsch 1997) was used to predict the three-dimensional structure of EmhB by homology modeling with AcrB (Murakami *et al.* 2002) (Protein Data Bank (PDB) entry 1IWG (<http://www.pdb.org>)). Structural representations of proteins were generated by using the DS ViewerPro version 6.0 software (Accelrys, San Diego, California).

2.8. Complementation of *srpABC* and *arpABC* in *P. fluorescens* cLP6a-1

To characterize the substrate specificities of the SrpABC and ArpABC efflux systems for polycyclic aromatic hydrocarbons, toluene and antibiotics, these efflux proteins were expressed in the efflux-deficient mutant *P. fluorescens* cLP6a-1. Plasmid pJD105 containing the *srpABC* operon was digested with *SacI*, and the 6.5-kb *SacI* restriction fragment carrying the *srpABC* operon was cloned into pUCP26. The resulting plasmid pBH63-srp, which has the *srpABC* operon in the same orientation as the *lacZ*

promoter in pUCP26 (Figure 2.3A), was introduced by electroporation into *P. fluorescens* cLP6a-1. The *arpABC* operon, plus 137 nucleotides upstream of the *arpA* gene, was amplified by PCR from *P. putida* S12 genomic DNA by using the primers ARP-F2 5'-TTACT**AAGCTT**CAGCAGTATTTACAAACAACCATGA-3' and ARP-R2 5'-GTTCAA**AAGCTT**AGGGTGGGCTTGTGCTGTAAC-3', where the added *Hind*III restriction sites are indicated in bold. The PCR reaction consisted of an initial denaturation at 95°C for 5 min, 25 cycles of 95°C for 50 s, 55°C for 50s and 72°C for 5 min, and a final extension of 72°C for 7 min. The PCR product was cloned into the *Hind*III sites in pUCP26, and the resulting plasmid pBH64-arp, which has the *arpABC* operon in the opposite orientation as the *lacZ* promoter (Figure 2.3B), was introduced into *P. fluorescens* cLP6a-1 by electroporation.

2.9. Measurement of growth rates of *P. fluorescens* cLP6a and cLP6a-1

Growth rates of *P. fluorescens* cLP6a and cLP6a-1 were determined in TSB cultures containing 50 mg mL⁻¹ phenanthrene or in the absence of phenanthrene. The OD₆₀₀ was used to monitor growth, and plate counts were done by spreading 0.1-mL aliquots of ten-fold dilutions on Luria-Bertani agar plates in triplicate.

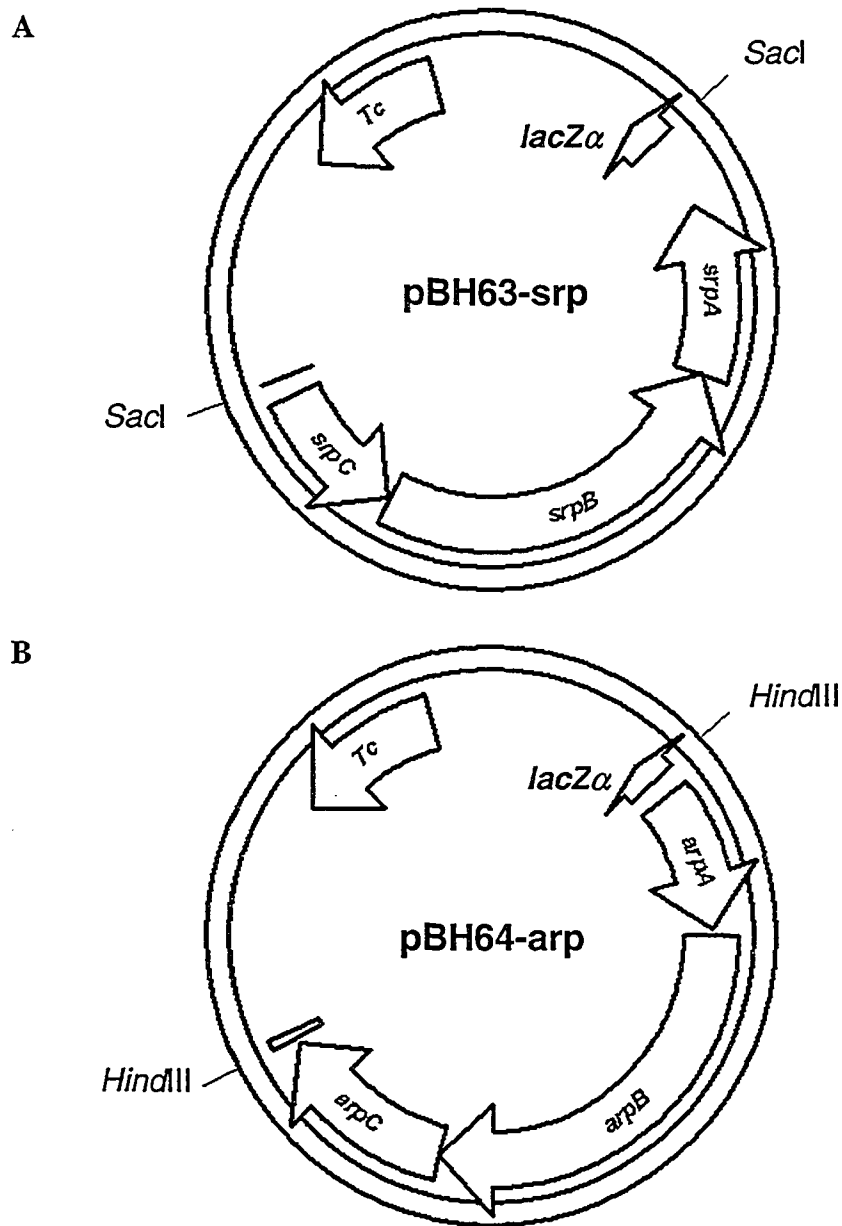


Figure 2.3. Schematic of plasmids pBH63-srp and pBH64-arp. Plasmid pBH63-srp (A) was constructed by cloning *srpABC* operon into the *SacI* restriction site in the broad-host-range plasmid pUCP26. The *srpABC* genes were inserted in the same orientation as the *lacZα* peptide gene. Plasmid pBH64-arp (B) was constructed by cloning the *arpABC* operon into the *HindIII* restriction site in pUCP26. The *arpABC* genes were inserted in the opposite orientation as the *lacZα* peptide gene. The tetracycline resistance marker (*Tc*) on plasmid pUCP26 is indicated.

3. RESULTS AND DISCUSSION

The discovery of an active efflux mechanism for polycyclic aromatic hydrocarbons in *P. fluorescens* cLP6a (Bugg *et al.* 2000) prompted the identification and characterization of the RND efflux system EmhABC reported herein. Following identification of the genes encoding the hydrocarbon efflux system, the objectives of this thesis included further characterization of the substrate specificity of the efflux pump, investigation of the regulation of efflux pump expression in *P. fluorescens*, exploration of the mechanism for substrate recognition and translocation through the efflux pump protein, and a survey of the prevalence of polycyclic aromatic hydrocarbon efflux in gram-negative bacteria. The results of these studies are discussed with respect to the significance of an efflux system for polycyclic aromatic hydrocarbons in *P. fluorescens*.

3.1. Identification of the EmhABC efflux system in *Pseudomonas fluorescens* cLP6a²

3.1.1. Detection and insertional inactivation of the efflux pump gene

In order to identify the genes encoding the efflux system for polycyclic aromatic hydrocarbons observed by Bugg *et al.* (2000) in *P. fluorescens* LP6a, it was hypothesized that the transport protein was homologous to efflux pumps belonging to the RND family. Degenerate PCR primers were designed from conserved sequences in the antibiotic efflux pump MexB from *P. aeruginosa* and in the toluene efflux pumps TtgB and TtgE from *P. putida* DOT-T1E and SrpB from *P. putida* S12 (Figure 3.1) and were used to amplify homologous genes from *P. fluorescens* cLP6a genomic DNA (Figure 3.2). The PCR product corresponding to the expected size (2.2 kb) was cloned, and 6 of 20 recombinant plasmids were selected randomly for partial DNA sequencing. The partial sequences of the six inserts were identical indicating that only one pump gene in *P. fluorescens* cLP6a had been amplified. A BLAST search of the translated sequence revealed a high degree of identity (60 to 80%) to gram-negative bacterial RND pumps in the GenBank database.

² Portions of this section have been published previously by Hearn *et al.* (2003).

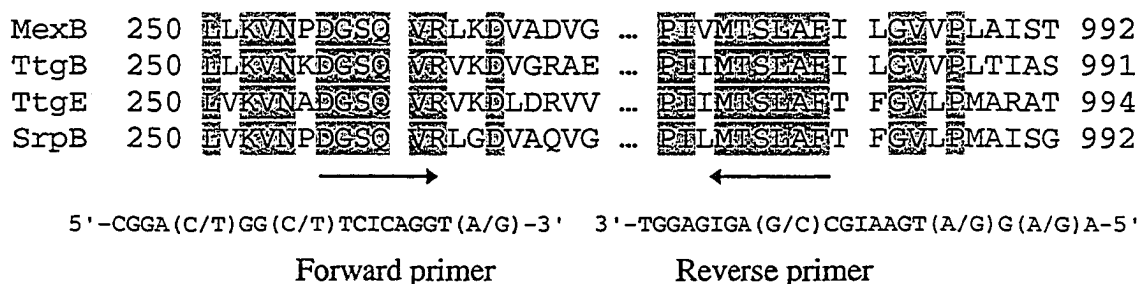


Figure 3.1. Alignment of conserved regions in RND efflux pump proteins. The proteins are MexB from *P. aeruginosa* PA01 (accession number NP_249117), TtgB from *P. putida* DOT-T1E (AAC38671), TtgE from *P. putida* DOT-T1E (CAB72259), and SrpB from *P. putida* S12 (AAD12176). The arrows indicate the conserved regions used to design primers for PCR amplification of homologous efflux pumps in *P. fluorescens* cLP6a, and the primer sequences are indicated with degenerate sites given in parentheses.

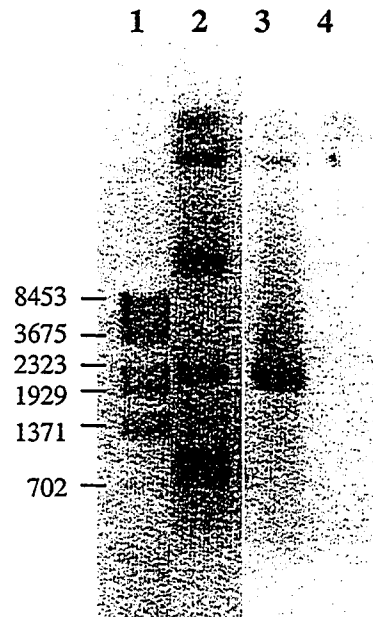


Figure 3.2. Amplification of efflux pump genes from *P. fluorescens* cLP6a genomic DNA. Degenerate PCR primers were used to amplify genes homologous to RND efflux pumps in *P. fluorescens* cLP6a-1 genomic DNA. Lane 1, λ DNA *Bst*EII digest (size of fragments in kb is indicated); lane 2, PCR products from *P. fluorescens* cLP6a genomic DNA as template; lane 3, PCR product from plasmid pJD105, which carries the *srpB* gene; lane 4, PCR negative control.

Plasmid pCR17, containing the 2.2-kb PCR product, was introduced into *P. fluorescens* cLP6a by electroporation such that integration of the plasmid into the chromosome by homologous recombination would disrupt the efflux pump gene. A disruption mutant, *P. fluorescens* cLP6a-1, was obtained, and the presence of the insertion was confirmed by Southern blotting and hybridization by using the 2.2-kb efflux gene fragment and the plasmid pCR2.1 as probes (Figure 3.3). The efflux gene fragment hybridized to a 8 to 10-kb *Bam*HI fragment, a 4.6-kb *Eco*RI fragment, a 3-kb *Pst*I fragment and a 5-kb *Sal*I fragment of the wild-type *P. fluorescens* cLP6a genomic DNA. The hybridization pattern of the mutant *P. fluorescens* cLP6a-1 genomic DNA with the efflux gene probe was different from the wild-type pattern and corresponded to insertion of the plasmid pCR2.1 within the efflux gene. DNA fragments from the mutant *P. fluorescens* cLP6a-1, but not from the wild-type cLP6a, hybridized to the pCR2.1 probe, indicating the correct insertion of the plasmid into the efflux pump gene.

To test the role of the gene product in the efflux of polycyclic aromatic hydrocarbons, the cellular accumulation of [¹⁴C]phenanthrene by *P. fluorescens* cLP6a and by the disruption mutant *P. fluorescens* cLP6a-1 was measured before and after addition of the energy inhibitor azide (Figure 3.4). The cellular accumulation, which represented both the intracellular and membrane-associated hydrocarbon, was the amount of phenanthrene in the cell pellet after centrifugation and was expressed as the fractional amount of the total ¹⁴C added. For *P. fluorescens* cLP6a, the fractional amount of [¹⁴C]phenanthrene in the cells rapidly reached a steady-state level of 0.12 ± 0.07 in the absence of azide. Upon addition of the energy inhibitor azide, the fraction of phenanthrene in the cells increased to 0.32 ± 0.01 . This significant increase ($P < 0.005$) is consistent with inhibition of an active efflux process. In contrast, the disruption mutant *P. fluorescens* cLP6a-1 displayed a significantly higher steady-state level of phenanthrene (0.29 ± 0.02 ; $P < 0.01$) prior to azide addition than the wild-type *P. fluorescens* cLP6a strain. The fraction of phenanthrene in the mutant cells did not increase significantly above the steady-state level when azide was added and was equivalent to the final cellular level in the azide-treated wild-type strain. These results indicate that the gene for polycyclic aromatic hydrocarbon efflux had been disrupted. This gene was designated *emhB*.

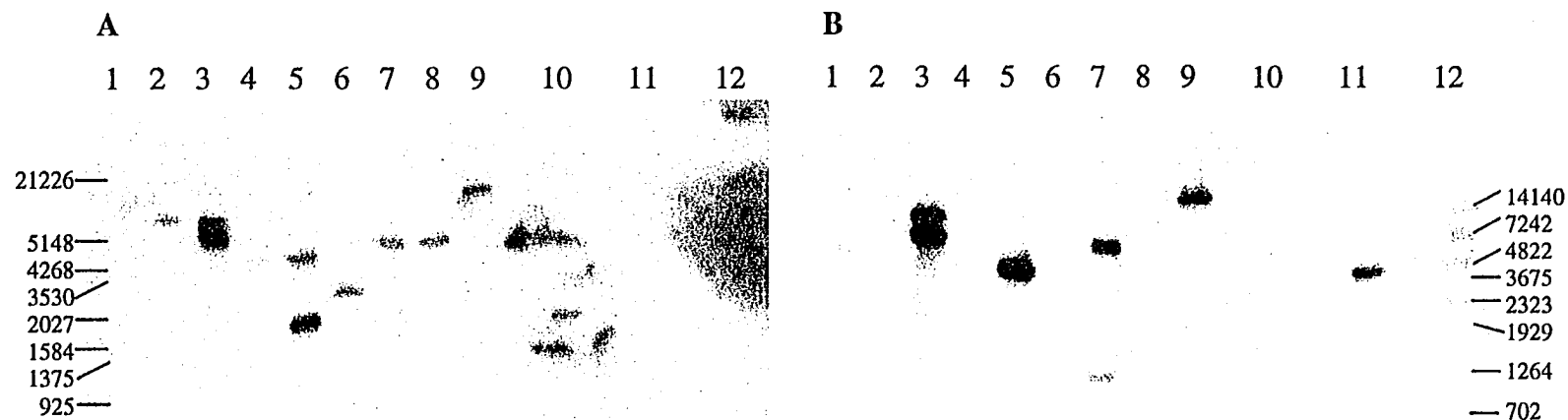


Figure 3.3. Confirmation of the efflux pump gene disruption in *P. fluorescens* cLP6a-1 by Southern blotting and hybridization. Restriction digests of *P. fluorescens* cLP6a or cLP6a-1 genomic DNA were run on a 0.8% (wt/vol) agarose gel at 30V in Tris-acetate-EDTA running buffer and transferred to nylon membrane by Southern blotting. Membranes were probed with the 2.2-kb efflux pump gene fragment (gel A) or the plasmid pCR2.1 (gel B). Lane 1, λ DNA *Hind*III/*Eco*RI double digest (size of fragments in kb is indicated at left); lane 2, cLP6a *Bam*HI digest; lane 3, cLP6a-1 *Bam*HI digest; lane 4, cLP6a *Eco*RI digest; lane 5, cLP6a-1 *Eco*RI digest; lane 6, cLP6a *Pst*I digest; lane 7, cLP6a-1 *Pst*I digest; lane 8, cLP6a *Sal*I digest; lane 9, cLP6a-1 *Sal*I digest; lane 10, 2.2-kb efflux pump gene fragment; lane 11, pCR2.1 *Eco*RI digest; lane 12, λ DNA *Bst*EII digest (size of fragments in kb is indicated at right).

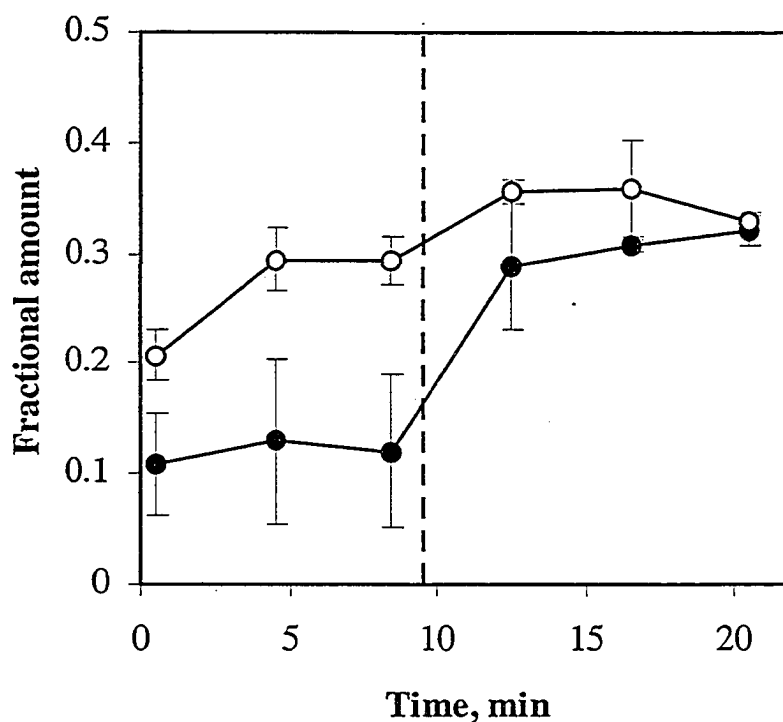


Figure 3.4. Accumulation of [$9\text{-}^{14}\text{C}$]phenanthrene in cell pellets of *P. fluorescens* cLP6a (closed circles) and the *emhB* disruption mutant cLP6a-1 (open circles) over time. The fractional amount of radiolabeled phenanthrene in the cells was measured by using the rapid centrifugation method (Bugg *et al.* 2000). The dashed line indicates the time at which 30 mM azide was added. The data points are the means of three independent experiments, and the error bars indicate one standard deviation. Taken from Hearn *et al.* (2003).

3.1.2. Cloning and sequence analysis of the Emh efflux system

The 8 to 10-kb *Bam*HI fragment of *P. fluorescens* cLP6a genomic DNA, which hybridized to the *emhB* gene fragment (Figure 3.3), was cloned into pUC19, and its nucleotide sequence, which was 9.7 kb in length, revealed seven complete open reading frames (ORFs) (Figure 3.5). ORF3 (nucleotides 2083 to 5229) corresponded to the *emhB* gene, whose deduced protein sequence showed a close phylogenetic relationship to RND pumps in *P. fluorescens* Pf0-1, *P. putida*, *P. aeruginosa* and *E. coli* (Figure 3.6). Interestingly, EmhB clustered phylogenetically with the known antibiotic and toluene efflux pump TtgB in *P. putida* DOT-T1E, as well as with the antibiotic efflux pumps ArpB and MexB in *P. putida* S12 and *P. aeruginosa* PA01, respectively. The solvent efflux pumps SepB, TtgE, SrpB and TtgH that have been characterized in various *P. putida* strains formed a distinct clade on the phylogenetic tree (Figure 3.6).

Adjacent to *emhB* (Figure 3.5), ORF2 (nucleotides 922 to 2079) and ORF4 (nucleotides 5229 to 6689) encoded the putative membrane fusion protein and the outer membrane factor protein, respectively, of the efflux system; these genes were designated *emhA* and *emhC*, which is consistent with the nomenclature for three-component efflux systems. The deduced protein sequences encoded by the *emhA* and *emhC* genes showed high homology to their counterparts in RND three-component efflux systems identified in other pseudomonads and in *E. coli* (Table 3.1). Consistent with the phylogenetic analysis of EmhB (Figure 3.6), the EmhABC system in *P. fluorescens* cLP6a exhibited a high degree of identity to the TtgABC, ArpABC and MexAB-OprM three-component efflux systems, which have been demonstrated to be involved in antibiotic resistance in *P. putida* and *P. aeruginosa* strains (Rojas *et al.* 2001, Kieboom and de Bont 2001, Li *et al.* 1995). The solvent efflux systems SrpABC, TtgDEF and TtgGHI showed lower degrees of identity to EmhABC, but were more similar than the MexCD-OprJ and MexXY efflux systems in *P. aeruginosa* PA01. Finally, the *E. coli* AcrA and AcrB proteins showed high homology to the EmhA and EmhB proteins, although the outer membrane factor proteins TolC and EmhC were less similar.

An additional ORF was located on the 9.7-kb fragment upstream of the *emhABC* genes but in the opposite orientation (Figure 3.5). The deduced amino acid sequence encoded by ORF1 (nucleotides 23 to 655) exhibited homology to sequences of

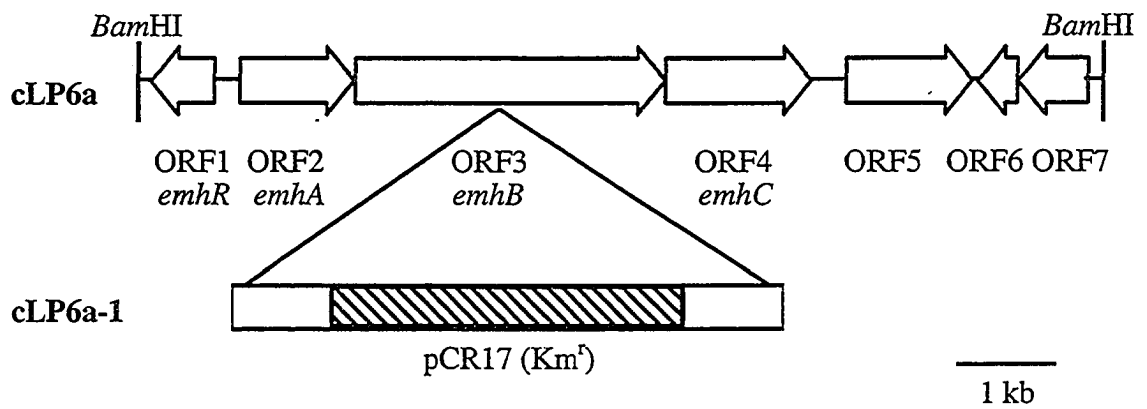


Figure 3.5. Schematic representation of the *emh* gene cluster in *P. fluorescens* *cLP6a* and *cLP6a-1*. In pCR17, the sequence of plasmid pCR2.1, which confers kanamycin resistance (Km^R), is cross-hatched, while the flanking regions homologous to *emhB* are not. Taken from Hearn *et al.* (2003).

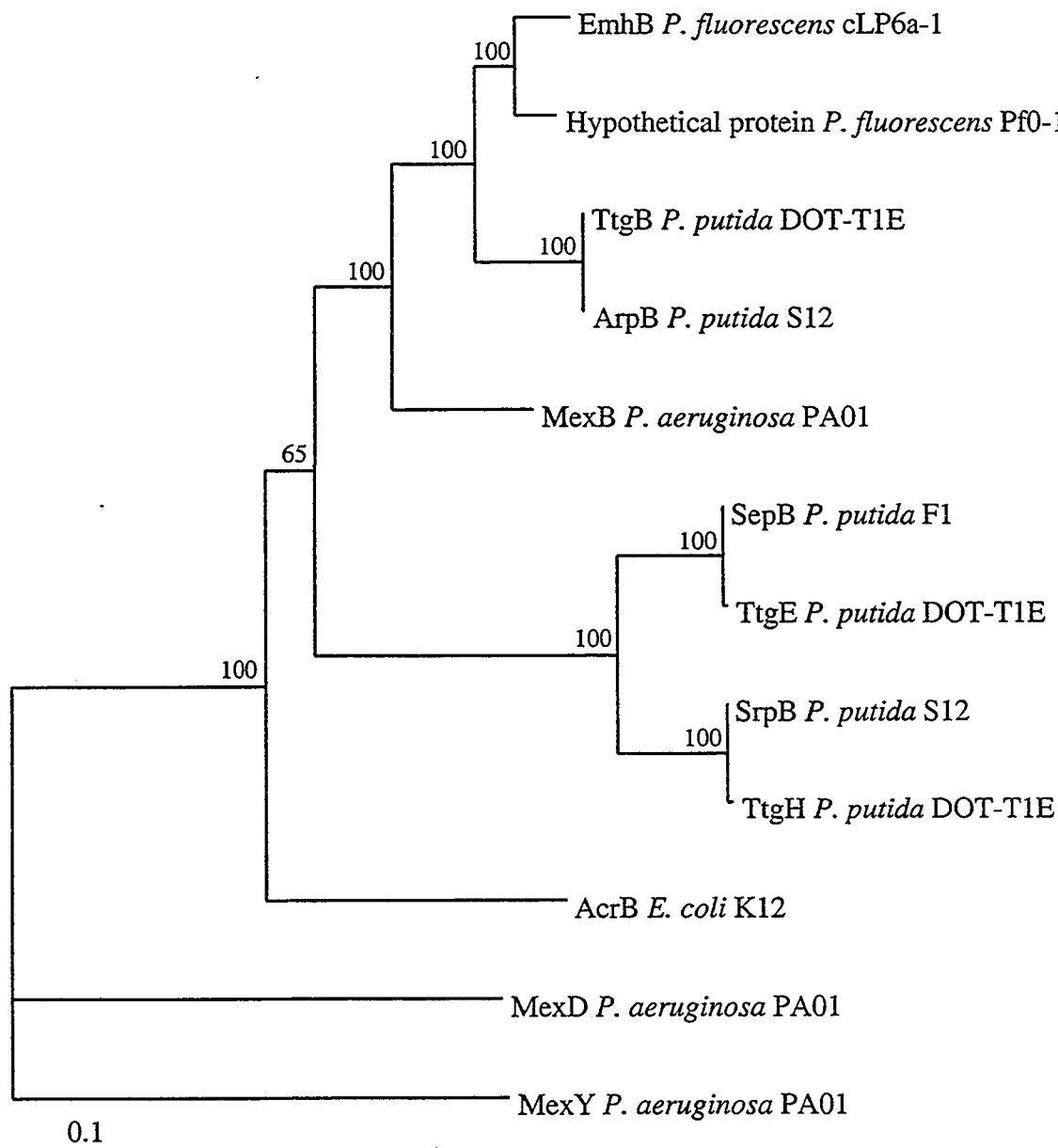


Figure 3.6. Phylogenetic relationship of EmhB to other RND efflux pumps. The tree was generated by using the Jones-Taylor-Thornton distance matrix and the neighbour-joining methods in PHYLIP (Felsenstein 2004) and was drawn by using Treeview (Page 1996). The tree was rooted with MexY as the outgroup, and the scale bar represents 0.1 substitutions per amino acid. Bootstrapping was carried out using PHYLIP (Felsenstein 2004), and the bootstrap values, indicating the number of times the partitioning of the sequences occurred out of 100 trees, are shown at the nodes. The accession numbers are as follows: EmhB, AAQ92181; hypothetical protein *P. fluorescens* Pf0-1, ZP_00266637; TtgB, AAC38671; ArpB, AAF73832; MexB, NP_249117; SepB, AAO49779; TtgE, CAB72259; SrpB, AAD12176; TtgH, AAK69564; AcrB, NP_414995; MexD, NP_253288; and MexY, NP_250708.

Table 3.1. Comparison of the *P. fluorescens* cLP6a EmhABC efflux proteins with other three-component RND efflux systems

Organism	Protein	Function	% Protein identity ^a		
			EmhA ^b	EmhB ^b	EmhC ^b
<i>P. fluorescens</i> Pf0-1 ^c	MFP	unknown	95		
	RND			92	
	OMC				95
<i>P. putida</i> DOT-T1E	TtgA	antibiotic, solvent resistance	78		
	TtgB			86	
	TtgC				76
<i>P. putida</i> S12	ArpA	antibiotic resistance	74		
	ArpB			86	
	ArpC				76
<i>P. aeruginosa</i> PA01	MexA	antibiotic resistance	67		
	MexB			80	
	OprM				69
<i>P. putida</i> S12	SrpA	solvent tolerance	57		
	SrpB			63	
	SrpC				54
<i>P. putida</i> DOT-T1E	TtgG	solvent, antibiotic resistance	55		
	TtgH			63	
	TtgI				53
<i>P. putida</i> DOT-T1E	TtgD	solvent tolerance	54		
	TtgE			62	
	TtgF				54
<i>E. coli</i> K12	AcrA	antibiotic resistance	52		
	AcrB			67	
	TolC				16
<i>P. aeruginosa</i> PA01	MexC	antibiotic resistance	40		
	MexD			50	
	OprJ				44
<i>P. aeruginosa</i> PA01	MexX	antibiotic resistance	31		
	MexY			48	

^a Percent identities were calculated by using the Sequence Manipulation Suite version 2 (Stothard 2000).

^b In *P. fluorescens* cLP6a, EmhA is the membrane fusion protein, EmhB is the RND efflux pump and EmhC is the outer membrane component.

^c Hypothetical membrane fusion protein (MFP; accession number ZP_00266638), RND efflux pump (accession number ZP_00266637) and outer membrane channel (OMC; accession number ZP_00266636) based on the genome sequence of *P. fluorescens* Pf0-1.

transcriptional repressors belonging to the TetR family, including TtgR (71% identity) in *P. putida* DOT-T1E and ArpR (71% identity) in *P. putida* S12. Although the role of ORF1 has not been determined, the gene product is believed to regulate the *emhABC* genes and has been designated *emhR*.

Downstream of the *emhABC* genes, three ORFs were identified on the 9.7-kb *Bam*HI fragment (Figure 3.5). The deduced protein encoded by ORF5 (nucleotides 7041 to 8300) showed homology to porins that are selective for specific substrates, such as BenF (44% identical to ORF5) involved in benzoate uptake (Cowles *et al.* 2000) and PhaK (38% identical to ORF5) required for phenylacetic acid uptake (Olivera *et al.* 1998). ORF6 (nucleotides 8368 to 8760) and ORF7 (nucleotides 8772 to 9458) encode putative proteins similar to carboxymuconolactone decarboxylases and 3-oxoadipate enol-lactone hydrolases involved in the β -keto adipate pathway for metabolism of catechol and protocatechuate (Harwood and Parales 1996), which are intermediates in the degradation of aromatic compounds. Genes similar to ORF5, ORF6, and ORF7 are located in the same arrangement adjacent to the antibiotic and solvent efflux operon *ttgABC* (nucleotide accession number AF031417) in *P. putida* DOT-T1E.

3.1.3. Phenanthrene efflux is restored by complementation

To confirm the role of the Emh efflux system, the *emhABC* genes and their upstream putative promoter region were ligated into the broad-host-range vector pUCP26, and the resulting plasmid, pBH5, was transformed into *P. fluorescens* cLP6a-1. The transformant, *P. fluorescens* cLP6a-1(pBH5), accumulated levels of phenanthrene similar to the levels accumulated by the wild-type strain in both the absence and the presence of azide (Figure 3.7). As a control, pUCP26 was transformed into *P. fluorescens* cLP6a-1 to ensure that the tetracycline resistance gene for tetracycline efflux on the vector did not affect the complementation results. There was no change in the amount of cell-associated phenanthrene in *P. fluorescens* cLP6a-1(pUCP26) after azide addition (Figure 3.7), and the levels of phenanthrene were comparable to those in mutant *P. fluorescens* cLP6a-1, within the error typically observed for the assay. Thus, the increased accumulation of phenanthrene observed in *P. fluorescens* cLP6a-1(pBH5) upon azide addition resulted from inhibition of the restored EmhABC efflux system.

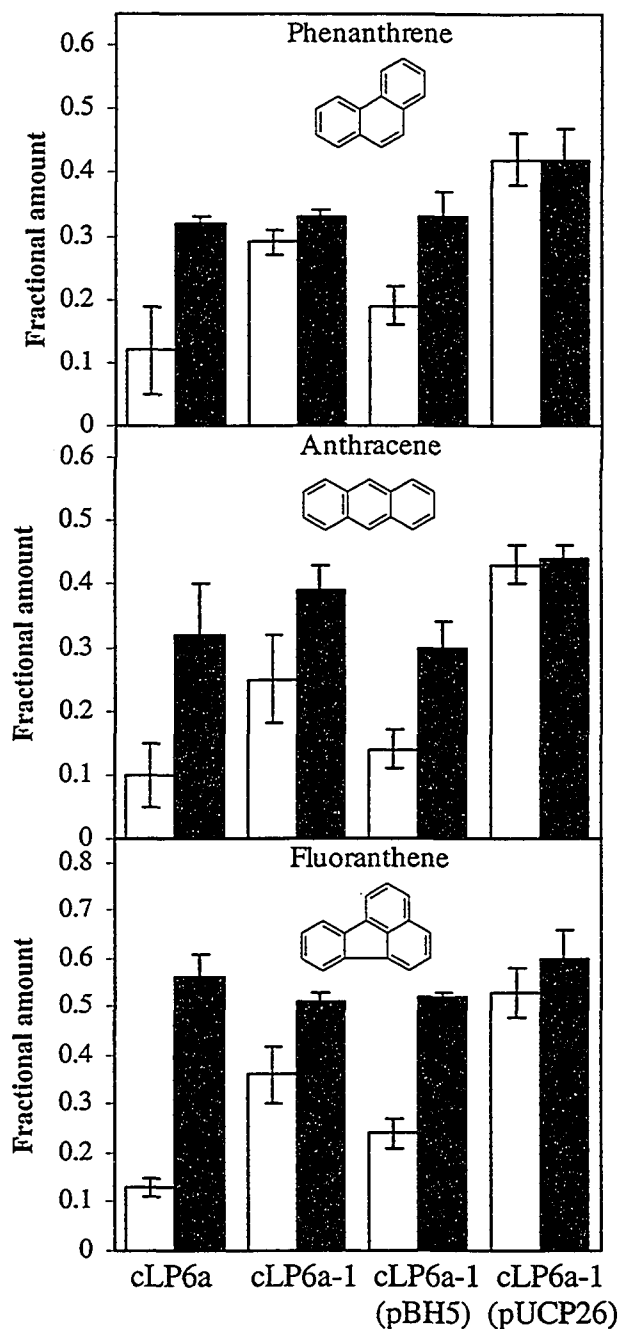


Figure 3.7. Distribution of radiolabeled substrates in the cell pellets of *P. fluorescens* cLP6a strains at steady state before (open bars) and after (solid bars) addition of 30 mM azide. The fractional amounts of phenanthrene, anthracene and fluoranthene in the cells were measured by the rapid centrifugation method (Bugg *et al.* 2000). *P. fluorescens* cLP6a is the wild-type strain, cLP6a-1 is the *emhB* disruption mutant, cLP6a-1(pBH5) is the disruption mutant complemented with the *emhABC* genes, and cLP6a-1(pUCP26) is the vector negative control. The bars indicate the means of three independent experiments, and the error bars indicate one standard deviation. Taken from Hearn *et al.* (2003).

3.1.4. The EmhABC efflux system transports polycyclic aromatic hydrocarbons.

Since it was shown previously that anthracene and fluoranthene are also subject to active efflux in *P. fluorescens* cLP6a (Bugg *et al.* 2000), the involvement of the *emhABC* genes in the efflux of these polycyclic aromatic hydrocarbons was investigated. Transport assays were performed by using radiolabeled anthracene or fluoranthene and *P. fluorescens* cLP6a, cLP6a-1, cLP6a-1(pBH5), and cLP6a-1(pUCP26). Figure 3.7 compares the steady-state levels of these substrates for the four strains in the absence and in the presence of azide. As observed with phenanthrene, disruption of the *emhB* gene in *P. fluorescens* cLP6a-1 caused accumulation of cellular levels of anthracene and fluoranthene before azide addition that were higher than the levels in the wild-type *P. fluorescens* cLP6a strain ($P < 0.025$). However, the fractional amounts of anthracene and fluoranthene increased significantly after azide treatment of cLP6a-1 cells, suggesting that there may be additional efflux mechanisms for these hydrocarbons. Complementation of the *emhB* insertion mutant with pBH5 restored the level of accumulated hydrocarbon to the levels in the unmodified strain cLP6a. As a control, transport of anthracene and fluoranthene was measured in *P. fluorescens* cLP6a-1(pUCP26) and, as expected, was comparable to transport in the mutant cLP6a-1. Although the fractional amounts of anthracene and fluoranthene after azide addition were similar for the two strains, a higher level of hydrocarbon accumulated prior to azide addition in the vector control cLP6a-1(pUCP26) than in cLP6a-1 (Figure 3.7). The presence of plasmid pUCP26 seemed to affect the residual anthracene and fluoranthene efflux activity observed in mutant cLP6a-1. Possibly, expression of the tetracycline resistance gene on pUCP26, which encodes an inner membrane tetracycline-specific efflux pump, affected the expression of other efflux systems in *P. fluorescens* cLP6a-1. However, these results do not contradict the hypothesis that EmhABC is involved in anthracene and fluoranthene efflux, as indicated by the data obtained with *P. fluorescens* cLP6a-1 and cLP6a-1(pBH5).

3.1.5. Comparison of the *emhABC* genes with other RND efflux systems

The *emhABC* gene cluster encoding a three-component RND efflux system was identified in *P. fluorescens* cLP6a and proved to be responsible for the proton-dependent

efflux of phenanthrene (Figure 3.4). The EmhABC system also is involved in the active efflux of anthracene and fluoranthene, although additional active efflux systems may be present in *P. fluorescens* cLP6a to transport these hydrocarbons since disruption of *emhB* did not completely eliminate their efflux (Figure 3.7). Eleven RND efflux pump genes have been identified in the genome of *P. fluorescens* Pf0-1 (http://genome.jgi-psf.org/draft_microbes/psefl/psefl.home.html) and in *P. aeruginosa* PA01 (Stover *et al.* 2001); therefore, *P. fluorescens* cLP6a likely possesses more than one efflux system.

Since gram-negative bacteria commonly possess multiple RND efflux systems, it was surprising that only one RND efflux pump gene was amplified by using PCR with degenerate primers in *P. fluorescens* cLP6a. The PCR primers were designed based on conserved regions in only four RND proteins, MexB, TtgB, TtgE and SrpB (Figure 3.1). The regions selected for primer design are not as highly conserved among other RND pumps. Thus, the PCR was likely biased for the detection of the closest homologue of MexB, TtgB, TtgE and SrpB. As expected, the protein sequence of EmhB was closely related to these efflux pumps (Table 3.1 and Figure 3.6).

The deduced protein sequences encoded by the *emhA*, *emhB* and *emhC* genes showed a high degree of homology to membrane fusion proteins, RND efflux pumps and outer membrane factor proteins of three-component efflux systems (Figure 3.6). Although it has not been verified, the homology of the *emh* genes to the *ttgABC* and *mexAB-oprM* efflux operons strongly suggests that the *emhA*, *emhB* and *emhC* genes form an operon. EmhB is closely related to a putative RND efflux pump in *P. fluorescens* Pf0-1, a strain which was isolated from soil (Compeau *et al.* 1998), to the TtgB efflux pump, which transports antibiotics and solvents in *P. putida* DOT-T1E (Ramos *et al.* 1998), to the ArpB antibiotic efflux pump in *P. putida* S12 (Kieboom and de Bont 2001), and to the MexB antibiotic efflux pump in *P. aeruginosa* (Li *et al.* 1995). Accordingly, the EmhABC efflux system may share a functional relationship with these antibiotic efflux systems. Interestingly, the efflux pumps SepB, TtgE, SrpB and TtgH, which are implicated in high solvent tolerance levels in *P. putida* strains, clustered phylogenetically in a clade distinct from the EmhB, ArpB, TtgB and MexB group (Figure 3.6). Both the *sepABC* and *ttgABC* toluene efflux pump operons in *P. putida* F1 and *P. putida* DOT-T1E are located adjacent to the chromosomal *tod* operons, which encode

genes for toluene metabolism, and are only expressed in the presence of toluene (Phoenix *et al.* 2003, Mosqueda and Ramos 2000). In contrast, the *srpABC* and *ttgGHI* efflux operons are not linked to toluene metabolism genes, but are responsible for the high level of solvent tolerance observed in *P. putida* S12 and *P. putida* DOT-T1E (Kieboom *et al.* 1998a, Rojas *et al.* 2001). Although more distantly related, EmhB and the *E. coli* antibiotic efflux pump AcrB share significant protein sequence identity (Table 3.1). Finally, EmhB showed the least homology to the antibiotic efflux pumps MexD, which is not expressed normally in *P. aeruginosa* (Poole *et al.* 1996a), and MexY, which shows specificity for aminoglycosides in *P. aeruginosa* (Aires *et al.* 1999). In the following section, the substrate specificity of the EmhABC efflux system for antibiotics and solvents is investigated and discussed further with respect to the phylogenetic relationship of the RND efflux pumps.

Interestingly, three genes (ORF5, 6 and 7), whose deduced protein sequences show similarity to proteins implicated in the uptake and degradation of aromatic compounds, were identified downstream of the *emhABC* efflux genes on the 9.7-kb *Bam*HI fragment (Figure 3.5). ORF6 and ORF7 putatively encode enzymes of the β -keto adipate pathway for the metabolism of aromatic compounds. As reviewed by Harwood and Parales (1996), the β -keto adipate pathway is chromosomally encoded in a wide variety of soil bacteria and fungi and converts the aromatic compounds catechol and protocatechuate to tricarboxylic acid cycle intermediates. The β -keto adipate pathway can be involved in the degradation of environmental contaminants, such as aromatic hydrocarbons; however, its primary function is the metabolism of naturally-occurring aromatic compounds such as lignin and other plant-derived material (Harwood and Parales 1996). Although catechol is an intermediate in naphthalene and phenanthrene degradation, the parental strain *P. fluorescens* LP6a carries plasmid-encoded genes for catechol degradation via the *meta*-cleavage pathway (Foght and Westlake 1996), and the chromosomally-encoded β -keto adipate pathway likely is not involved in aromatic hydrocarbon degradation in *P. fluorescens* LP6a. It is unclear whether there is a significant relationship between the efflux genes and the β -keto adipate pathway; however, the efflux pump and β -keto adipate pathway may be involved in a general mechanism for the detoxification of aromatic compounds.

The presence of genes similar to ORF5, 6 and 7 downstream of the *ttgABC* operon in *P. putida* DOT-T1E (nucleotide accession number AF031417) lends support to the hypothesis that EmhABC represents the corresponding efflux system in *P. fluorescens* cLP6a. Moreover, the putative regulatory protein EmhR encoded by ORF1 upstream of the *emhABC* genes (Figure 3.5) showed high homology to the transcriptional repressor encoded by the *ttgR* gene adjacent to the *ttgABC* operon in *P. putida* DOT-T1E. The presence of the *emhR* gene suggests that the EmhABC efflux system is regulated in *P. fluorescens* cLP6a. In the following sections, the EmhABC efflux system in *P. fluorescens* cLP6a is characterized further with respect to its substrate specificity and regulation.

3.2. Substrate specificity of the EmhABC efflux system

Given the protein sequence similarities between the EmhABC efflux system in *P. fluorescens* cLP6a and the well-characterized antibiotic and solvent efflux pumps in *P. putida* and *P. aeruginosa*, the substrate specificity of EmhABC with respect to hydrophobic antibiotics and toluene was explored further.

The assays employed to study the substrate specificity of the EmhABC efflux system in *P. fluorescens* cLP6a can be classified into two categories: the transport assays as in Figure 3.4, which directly measure the amount of substrate accumulation in the cells, and growth-based assays, which indirectly measure the effect of cellular substrate accumulation on growth. The *in vivo* transport assay requires the use of, and thus is dependent upon the availability of, radiolabeled substrates. Growth-based assays are limited to substrates that are toxic to bacterial cells, and the presence of an active efflux system reduces the intracellular substrate concentration sufficiently to allow growth in the presence of normally toxic concentrations. Identification of the genes encoding the efflux system and subsequent construction of the EmhB-deficient *P. fluorescens* cLP6a-1 strain enabled a more comprehensive analysis of the substrate specificity of the EmhABC efflux system by comparing the antibiotic resistant and toluene tolerant phenotypes of the wild-type and mutant strains using growth-based assays.

3.2.1. EmhABC is involved in antibiotic resistance

Growth-based assays are commonly employed to assess the role of an efflux system in antibiotic efflux. A four-fold or greater reduction in the antibiotic resistance, or MIC, of a mutant strain lacking an efflux pump compared to that of the wild-type strain expressing the pump is considered as an indication of active efflux. For example, Li *et al.* (1995) observed a 16-fold reduction in tetracycline resistance, a four-fold reduction in chloramphenicol resistance and a 20-fold reduction in ciprofloxacin resistance in a MexAB-OprM-deficient *P. aeruginosa* strain compared to the wild-type and concluded, on this basis, that all three antibiotics were substrates of the MexAB-OprM efflux system. To corroborate their conclusions, *in vivo* transport assays using radiolabeled tetracycline and chloramphenicol, similar to the transport assay used to determine polycyclic aromatic hydrocarbon efflux in *P. fluorescens* cLP6a, demonstrated the MexAB-OprM-mediated active efflux of these antibiotics (Li *et al.* 1995). In the transport assay, the cellular accumulation of tetracycline increased only three-fold, compared to the observed 16-fold reduction in tetracycline resistance, in the MexAB-OprM-deficient strain over the wild-type levels (Li *et al.* 1995). Since the MIC is influenced by the intracellular concentration of the drug, small changes in the total cellular accumulation of the drug may have large effects on growth inhibition. Nonetheless, antibiotic sensitivity assays provide an indication of substrates transported by an efflux system.

The substrate specificity of the EmhABC system for antibiotics, which are known substrates of other RND efflux systems, was evaluated by comparing the antibiotic susceptibilities of the *P. fluorescens* cLP6a, cLP6a-1 and complemented strains. Table 3.2 shows that sensitivity to tetracycline, chloramphenicol, nalidixic acid, rhodamine 6G, dequalinium, ciprofloxacin and erythromycin was affected by disruption of the *emhB* gene in *P. fluorescens* cLP6a-1, since the MICs were at least eight-fold higher for *P. fluorescens* cLP6a than for the mutant cLP6a-1. In contrast, MICs of streptomycin for *P. fluorescens* cLP6a and cLP6a-1 were comparable. These data indicate that the EmhABC efflux system recognizes tetracycline, chloramphenicol, nalidixic acid, rhodamine 6G, dequalinium, ciprofloxacin and erythromycin, but not streptomycin.

Complementation of the EmhABC efflux system in *P. fluorescens* cLP6a-1(pBH5) restored resistance to chloramphenicol, nalidixic acid, rhodamine 6G,

Table 3.2. Antibiotic sensitivities of *P. fluorescens* strains expressing the EmhABC, ArpABC or SrpABC RND efflux systems

<i>P. fluorescens</i> strain ^a	MIC ($\mu\text{g mL}^{-1}$) of: ^b							
	Tc	Chl	Nal	R6G	Dq	Cip	Ery	Str
cLP6a	1	16	16	>128	4	0.031	32	8
cLP6a-1	0.125	2	1	4	0.5	0.004	4	4
cLP6a-1(pBH5)	ND ^c	32	128	>128	8	0.063	16	1
cLP6a-1(pUCP26)	ND ^c	0.5	1	8	1	0.004	4	1
cLP6a-1(pBH64-arp)	ND ^c	8	32	>128	16	0.031	16	2
cLP6a-1(pBH63-srp)	ND ^c	32	16	>128	8	0.031	16	2

^a The strains tested were the wild-type cLP6a, the *emhB* disruption mutant cLP6a-1, the mutant complemented with the *emhABC* genes cLP6a-1(pBH5), the vector negative control cLP6a-1(pUCP26), and the mutant complemented with either the *arpABC* genes cLP6a-1(pBH64-arp) or the *srpABC* genes cLP6a-1(pBH63-srp).

^b Abbreviations: Tc, tetracycline; Chl, chloramphenicol; Nal, nalidixic acid; R6G, rhodamine 6G; Dq, dequalinium; Cip, ciprofloxacin; Ery, erythromycin; and Str, streptomycin.

^c ND, not determined due to tetracycline resistance gene encoded on vector pUCP26.

dequalinium, ciprofloxacin and erythromycin, confirming that these antibiotics are substrates of the pump. For chloramphenicol, nalidixic acid, dequalinium and ciprofloxacin resistance was enhanced by complementation of the EmhABC system on plasmid pBH5 compared to the wild-type *P. fluorescens* cLP6a. MICs for the vector control, *P. fluorescens* cLP6a-1(pUCP26), were comparable to the disruption mutant cLP6a-1, indicating that the tetracycline resistance gene encoding a tetracycline-specific efflux pump on the vector did not interfere with the assay. Possibly, the efflux genes were expressed at higher levels from the multi-copy plasmid pBH5 than from the chromosome in the wild-type *P. fluorescens* cLP6a, and increased expression of the pump may have led to enhanced antibiotic resistance in the complemented mutant. Similarly, Li *et al.* (1995) observed two- to eight-fold increases in MICs for a *P. aeruginosa* strain overexpressing MexAB-OprM compared to the wild-type.

Although the complemented mutant *P. fluorescens* cLP6a-1(pBH5) exhibited enhanced antibiotic resistance compared to the wild-type *P. fluorescens* cLP6a (Table 3.2), the complemented mutant and the wild-type displayed the same steady-state levels of polycyclic aromatic hydrocarbon accumulation in the cells (Figure 3.7). Since antibiotic resistance is influenced by the intracellular concentration of the drug, small changes in the total cellular accumulation of the drug may have large effects on growth inhibition. For example, a 16-fold reduction in tetracycline resistance corresponded to only a three-fold increase in the cellular accumulation of tetracycline in a MexAB-OprM deficient *P. aeruginosa* strain compared to the wild-type (Li *et al.* 1995). The increased antibiotic resistance of *P. fluorescens* cLP6a-1(pBH5) compared to the wild-type *P. fluorescens* cLP6a (Table 3.2) may reflect a small decrease in the total cellular accumulation of antibiotics, possibly due to higher expression of the EmhABC efflux system from the plasmid pBH5. The transport assay employed with the polycyclic aromatic hydrocarbons is unable to detect small changes in cellular accumulation within the experimental error associated with the rapid centrifugation method. Consequently, the wild-type *P. fluorescens* cLP6a and the complemented mutant *P. fluorescens* cLP6a-1(pBH5) showed no significant difference in polycyclic aromatic hydrocarbon accumulation, while the antibiotic resistance levels were different.

To compare the substrate specificity of EmhABC for antibiotics with other RND efflux systems, MICs were determined for the *P. fluorescens* cLP6a-1 mutant complemented with plasmids carrying either the *arpABC* genes or the *srpABC* genes encoding the antibiotic and solvent efflux systems from *P. putida* S12 (Kieboom and de Bont 2001, Kieboom *et al.* 1998a). The presence of either the ArpABC or the SrpABC efflux systems significantly increased antibiotic resistance for chloramphenicol, nalidixic acid, rhodamine 6G, dequalinium, ciprofloxacin and erythromycin compared to the vector control *P. fluorescens* cLP6a-1(pUCP26) (Table 3.2). The MICs for streptomycin were comparable among the strains expressing ArpABC and SrpABC and the vector control (Table 3.2), indicating that the ArpABC and SrpABC efflux systems do not recognize streptomycin. Thus, EmhABC, ArpABC and SrpABC exhibited identical substrate specificities for antibiotics.

3.2.2. EmhABC is required for survival in the presence of toluene

Bugg *et al.* (2000) reported that *P. fluorescens* cLP6a did not possess an active efflux mechanism for naphthalene; however, the transport assay with toluene was hampered by the low specific activity of the radiolabeled hydrocarbon. Thus, the limitations of the transport assay with toluene precluded a definitive conclusion regarding the active efflux of toluene.

Like antibiotic efflux, toluene efflux is typically assessed by measuring toluene tolerance with growth-based assays. One method for determining the role of toluene efflux pumps in solvent tolerance measures bacterial survival under solvent shock conditions, in which the cells are exposed to toluene for a short period (Ramos *et al.* 1998, Rojas *et al.* 2001). However, membrane adaptations, such as increased fatty acid biosynthesis and *cis-trans* fatty acid isomerization, occur quickly after solvent exposure (Pinkart *et al.* 1996, Segura *et al.* 1999) and may be more likely to affect bacterial survival to solvent shock than efflux pumps. For this reason, measuring growth as a whole in the presence of toluene may provide a better indication of the role of efflux pumps in solvent tolerance. For example, Kieboom *et al.* (1998a) observed that the solvent-sensitive *P. putida* PPO200 was unable to grow on solid medium in the presence of vapour-phase toluene, whereas introduction of a plasmid carrying the *srpABC* efflux

pump genes into *P. putida* PPO200 enabled growth in the presence of toluene vapours. Thus, analysis of growth in the presence of vapour-phase toluene was the method chosen to assess toluene tolerance, mediated by an efflux system, in this study.

The toluene tolerance of *P. fluorescens* cLP6a, cLP6a-1, cLP6a-1(pBH5) and cLP6a-1(pUCP26) were assessed by monitoring growth on solid medium in the presence of vapour-phase toluene (Table 3.3). As a positive control, growth in the presence of toluene was observed for the known solvent-tolerant bacterium *P. putida* S12, which possesses the SrpABC toluene efflux pump. *P. fluorescens* cLP6a was unable to grow on solid medium in the presence of vapour-phase toluene. However, upon removal from the toluene environment and further incubation, growth of *P. fluorescens* cLP6a recovered, suggesting that the solvent limits growth but is not lethal to the bacterium. The *emhB* disruption mutant *P. fluorescens* cLP6a-1 also did not grow in the presence of toluene vapours. In contrast to the wild-type *P. fluorescens* cLP6a, toluene was lethal to the *EmhB*-deficient mutant strain cLP6a-1, which did not recover upon removal of the toluene. These data imply that, although the *EmhABC* efflux system does not confer toluene tolerance to *P. fluorescens* cLP6a, it does play a role in the ability of *P. fluorescens* cLP6a to remain viable in the presence of toluene. Toluene is, therefore, a substrate of the *EmhABC* efflux system.

Surprisingly, *P. fluorescens* cLP6a-1 complemented with the *EmhABC* efflux system on plasmid pBH5 was able to grow in the presence of toluene (Table 3.3). Consistent with the increased antibiotic resistance of the complemented mutant (Table 3.2), the enhanced ability of *P. fluorescens* cLP6a(pBH5) to tolerate toluene may have been due to increased expression of the efflux genes from the multi-copy plasmid. The strain carrying the vector control, *P. fluorescens* cLP6a-1(pUCP26), showed the same growth pattern on toluene as the disruption mutant *P. fluorescens* cLP6a-1, verifying that the observed toluene tolerance in *P. fluorescens* cLP6a-1(pBH5) was due to the *emhABC* genes and was not an artifact due to the presence of the plasmid pUCP26.

Complementation of the efflux pump-deficient mutant *P. fluorescens* cLP6a-1 with the *P. putida* S12 ArpABC antibiotic efflux system resulted in enhanced survival upon removal of the toluene vapours (Table 3.3), similar to the *EmhABC* efflux system, indicating that ArpABC is also involved in toluene efflux. As expected, *P. fluorescens*

Table 3.3. Toluene tolerance of *P. fluorescens* strains expressing the EmhABC, ArpABC or SrpABC RND efflux systems

Strain ^a	Efflux system	Toluene tolerance ^b	
		Growth	Survival
<i>P. fluorescens</i> strain			
cLP6a	EmhABC ⁺	–	+
cLP6a-1	EmhABC [–]	–	–
cLP6a-1(pBH5)	EmhABC ⁺	+	NA
cLP6a-1(pUCP26)	EmhABC [–]	–	–
cLP6a-1(pBH64-arp)	ArpABC ⁺	–	+
cLP6a-1(pBH63-srp)	SrpABC ⁺	+	NA
<i>P. putida</i> S12	ArpABC ⁺ , SrpABC ⁺	+	NA

^a The following *P. fluorescens* strains were tested: the wild-type cLP6a, the *emhB* disruption mutant cLP6a-1, the mutant complemented with either the *emhABC* genes cLP6a-1(pBH5), the vector negative control cLP6a-1(pUCP26), and the mutant complemented with either the *arpABC* genes cLP6a-1(pBH64-arp) or the *srpABC* genes cLP6a-1(pBH63-srp). *P. putida* S12 was included as a positive control.

^b Toluene tolerance was assessed by monitoring growth on agar plates in the presence of vapour-phase toluene. Growth in the presence of toluene was scored as + (positive for growth) or – (negative for growth). After four days of incubation in the presence of toluene, the plates were removed and incubated for an additional four days in the absence of toluene to assess the ability of the strains to survive toluene exposure. Survival was scored as + (growth upon removal of toluene), – (no growth upon removal of toluene) or NA (not applicable, as these strains were able to grow in the presence of toluene). Two independent experiments were done.

cLP6a-1 became toluene tolerant when complemented with the solvent efflux pump SrpABC (Table 3.3).

3.2.3. EmhABC is not involved in naphthalene transport

As mentioned above, Bugg *et al.* (2000) did not observe an active efflux system for naphthalene in *P. fluorescens* LP6a. Given that the tricyclic aromatic hydrocarbons phenanthrene, anthracene and fluoranthene and the monocyclic toluene were shown to be substrates of the EmhABC efflux system in *P. fluorescens* (Figure 3.7 and Table 3.3) the inability to observe active efflux of bicyclic naphthalene was curious. To confirm that the EmhABC efflux system in *P. fluorescens* cLP6a does not pump naphthalene, transport assays using radiolabeled naphthalene were performed with the efflux-pump deficient mutant *P. fluorescens* cLP6a-1 complemented either with the plasmid pBH5 carrying the *emhABC* genes or with the vector negative control pUCP26. In *P. fluorescens* cLP6a-1(pBH5) expressing the EmhABC efflux system, the fraction of naphthalene that accumulated in the cells was 0.059 ± 0.002 ($n = 2$) in the absence of the energy inhibitor azide and increased only slightly to 0.070 ± 0.008 ($n = 2$) in the presence of azide (Table 3.4). The cellular accumulation of naphthalene in *P. fluorescens* cLP6a-1(pUCP26), which does not express a functional EmhB efflux pump, was constant in the absence and in the presence of azide (Table 3.4). The failure to observe a significant increase in the cellular accumulation of naphthalene upon addition of the energy inhibitor to the *P. fluorescens* strain expressing the EmhABC efflux system, as well as the similar naphthalene accumulation profile in the mutant strain lacking EmhB, confirms that naphthalene is not a substrate of the efflux system.

The concentration of naphthalene used in the transport assays ($5.66 \mu\text{mol L}^{-1}$) corresponded to 2.5% of its aqueous solubility ($240 \mu\text{mol L}^{-1}$) and was chosen to ensure rapid dissolution of the substrate in the aqueous cell suspension (Bugg *et al.* 2000). Phenanthrene, for comparison, was used at a concentration of $6.36 \mu\text{mol L}^{-1}$, or 90% of its aqueous solubility ($7 \mu\text{mol L}^{-1}$). Although the concentrations of naphthalene and phenanthrene were comparable, the K_{ow} for naphthalene is approximately an order of magnitude lower than that of phenanthrene (Table 1.1). Thus, the cellular accumulation of naphthalene is expected to be significantly lower than that of phenanthrene, and the

Table 3.4. Accumulation of naphthalene in *P. fluorescens* and *P. putida* strains before and after azide addition, as a test for efflux

Strain	Efflux system	Naphthalene concentration (μM)	Accumulation of naphthalene ^a	
			Uninhibited (before azide)	Inhibited (after azide)
<i>P. fluorescens</i> strain				
cLP6a-1(pBH5)	EmhABC ⁺	5.66	0.059 \pm 0.002	0.070 \pm 0.008
cLP6a-1(pUCP26)	EmhABC ⁻	5.66	0.07 \pm 0.01	0.07 \pm 0.01
cLP6a	EmhABC ⁺	50	0.06	0.06
<i>P. putida</i> S12	ArpABC ⁺ SrpABC ⁺	50	0.04	0.05

^a The fractional amount of radiolabeled naphthalene was measured at steady state for both the uninhibited cells (before azide addition) and inhibited cells (after azide addition). For *P. fluorescens* cLP6a-1(pBH5) and cLP6a-1(pUCP26) the fractional amounts reported are the averages \pm standard deviations of two independent experiments. For *P. fluorescens* cLP6a and *P. putida* S12, the fractional amounts reported are from single experiments.

effect of the naphthalene concentration on the ability to detect active transport was investigated by measuring the partitioning of the hydrocarbon into *P. fluorescens* cLP6a over a range of aqueous concentrations (Figure 3.8). As expected from the K_{ow} values, the cellular accumulation of naphthalene was 10-fold lower than the cellular accumulation of phenanthrene in the absence of active transport in azide-inhibited *P. fluorescens* cLP6a cells (Figure 3.8). In uninhibited *P. fluorescens* cLP6a cells, which have an active EmhABC efflux system, the accumulation of phenanthrene was lower than in the inhibited cells, whereas the cellular accumulation of naphthalene was unchanged for all aqueous concentrations tested (Figure 3.8). The partitioning data confirm the presence of an active efflux system for phenanthrene but not for naphthalene.

To test the involvement of other efflux systems in naphthalene transport, the transport assay was performed with *P. putida* S12 using an initial naphthalene concentration of 50 μ M (Table 3.4). As with the transport assay with *P. fluorescens* cLP6a and 50 μ M naphthalene, only a small fraction of the naphthalene accumulated in the *P. putida* S12 cells, and this amount did not change significantly upon addition of the energy inhibitor azide (Table 3.4).

3.2.4. Comparison of the substrate specificity of EmhABC with other RND efflux systems

The *P. fluorescens* EmhABC efflux system was shown to be broadly specific for a number of structurally dissimilar, hydrophobic antibiotics, including tetracycline, chloramphenicol, rhodamine 6G, the quinolone antibiotics nalidixic acid, ciprofloxacin and dequalinium, and the macrolide erythromycin, whose structures are given in Figure 3.9. Tetracycline, chloramphenicol, nalidixic acid, ciprofloxacin and erythromycin are also substrates of the *P. aeruginosa* MexAB-OprM, MexCD-OprJ and MexXY-OprM efflux systems (Masuda *et al.* 2000), and the *E. coli* AcrAB-TolC system enhanced resistance for these antibiotics as well as for rhodamine 6G (Murakami *et al.* 2004). Additionally, rhodamine 6G and dequalinium were shown to bind to the *E. coli* RND efflux pump AcrB (Yu *et al.* 2003a), indicating that these compounds are substrates of the AcrAB-TolC efflux system. The TtgABC efflux system in *P. putida* DOT-T1E and the ArpABC efflux system in *P. putida* S12 expel tetracycline and chloramphenicol as

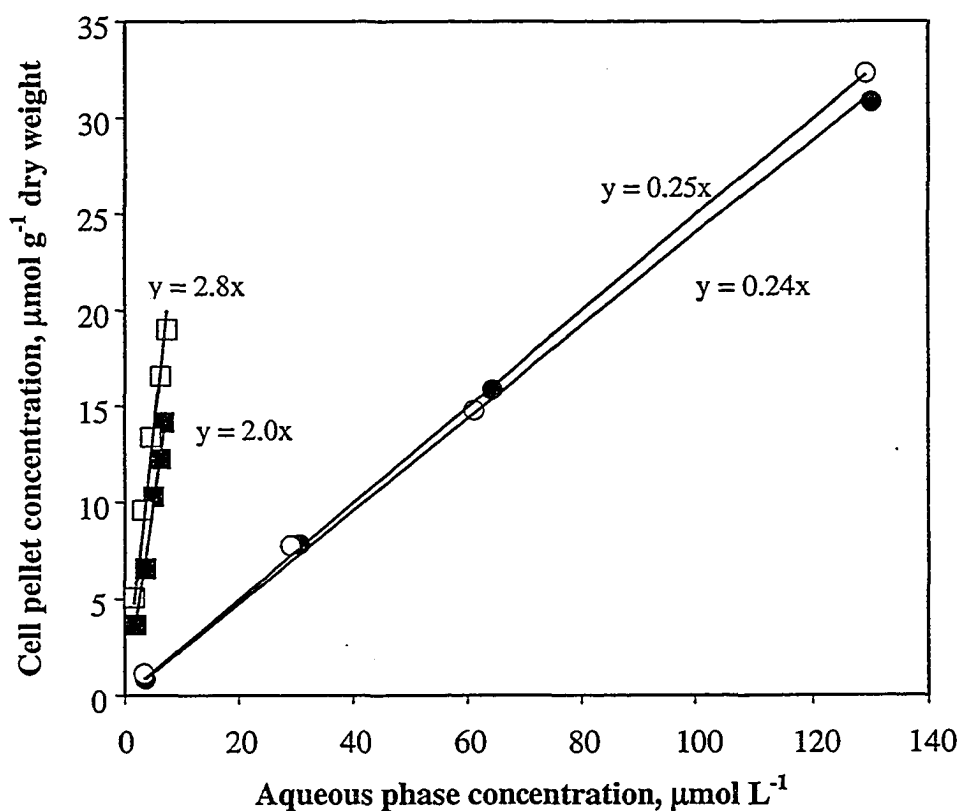


Figure 3.8. Partitioning of phenanthrene (squares) and naphthalene (circles) between *P. fluorescens* cLP6a cells and the aqueous phase. Radiolabeled phenanthrene or naphthalene was added to a cell suspension of *P. fluorescens* cLP6a, which were either preinhibited with 30 mM azide (open symbols) or uninhibited (closed symbols). Samples were removed after the system reached steady-state, and the amount of radiolabeled hydrocarbon in *P. fluorescens* cLP6a cells and in the aqueous supernatant was measured by using the rapid centrifugation method over a range of initial phenanthrene and naphthalene concentrations.

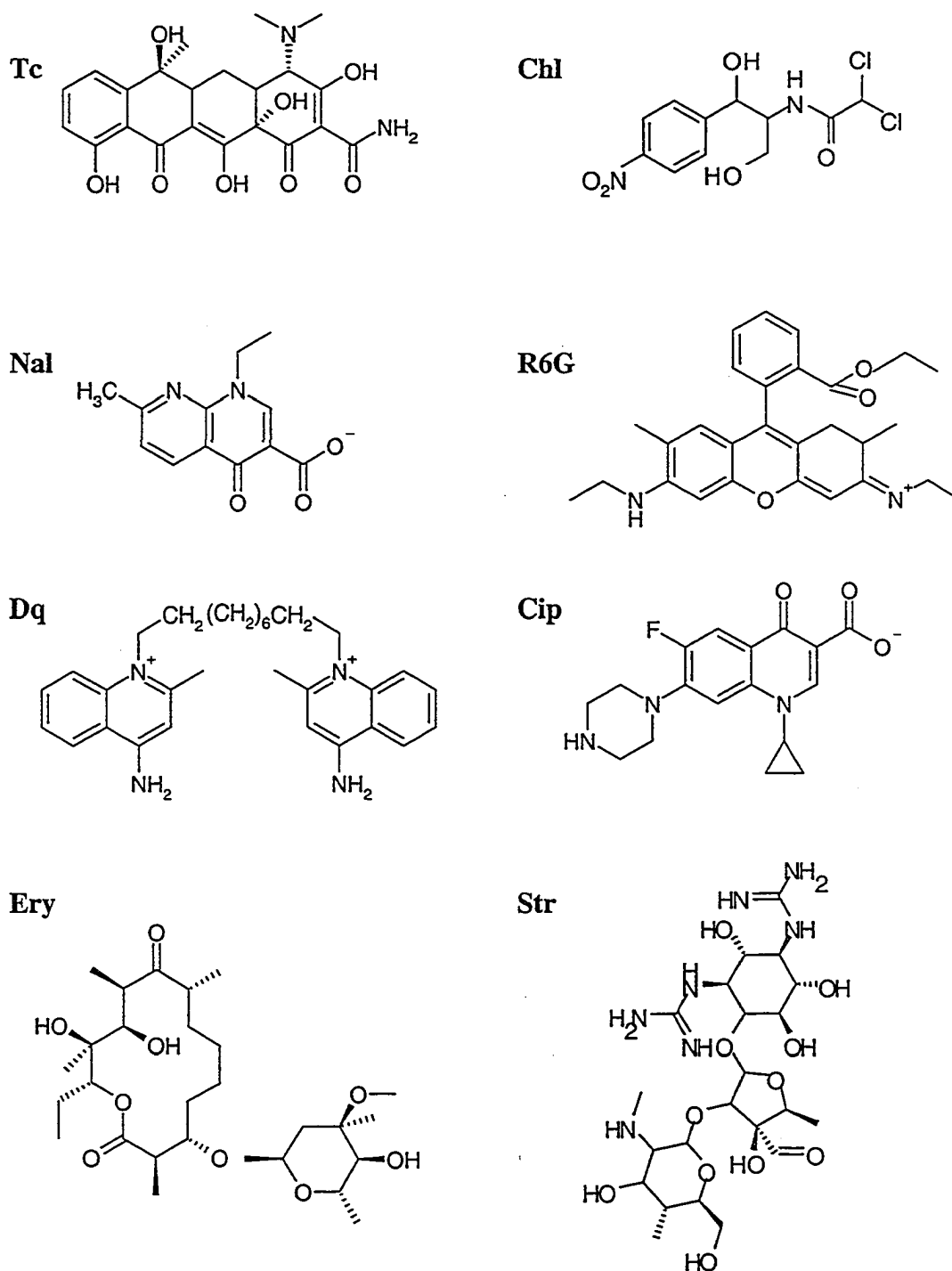


Figure 3.9. Chemical structures of the antibiotics tested for resistance in *P. fluorescens* cLP6a and the efflux mutant cLP6a-1. Tetracycline (Tc), chloramphenicol (Chl), nalidixic acid (Nal), rhodamine 6G (R6G), dequalinium (Dq), ciprofloxacin (Cip) and erythromycin (Ery) were shown to be substrates of the EmhABC efflux system. Streptomycin (Str) was not a substrate of the EmhABC efflux system.

well as other hydrophobic antibiotics (Rojas *et al.* 2001, Kieboom and de Bont 2001). The role of the ArpABC efflux system in antibiotic resistance was confirmed in the *P. fluorescens* cLP6a-1 mutant background (Table 3.2). Like EmhABC, ArpABC pumps chloramphenicol, nalidixic acid, rhodamine 6G, ciprofloxacin, dequalinium and erythromycin.

The SrpABC efflux system from *P. putida* S12 also showed the same substrate specificity for hydrophobic antibiotics as EmhABC and ArpABC when expressed in the *emhB* disruption mutant *P. fluorescens* cLP6a-1 (Table 3.2). A previous study suggested that SrpABC was not involved in antibiotic efflux, because an *srp*-negative mutant and the wild-type *P. putida* S12 showed comparable antibiotic resistance levels (Isken and de Bont 2000). At that time, however, the *arpABC* operon in *P. putida* S12 had not been discovered, and the presence of the ArpABC system in the *srp*-negative mutant likely masked the contribution of SrpABC to antibiotic resistance. Comparable to SrpABC, the closely related efflux system TtgGHI also was involved in the active efflux of tetracycline, chloramphenicol and nalidixic acid in *P. putida* DOT-T1E (Rojas *et al.* 2001). Despite the lower protein sequence identity between the *P. fluorescens* EmhABC proteins and the *P. putida* SrpABC and TtgGHI proteins (Table 3.1), these efflux systems seem to share a similar substrate specificity for antibiotics.

Streptomycin, an aminoglycoside, was the only antibiotic tested that was not found to be a substrate of the EmhABC, ArpABC or SrpABC efflux systems (Table 3.2). Compared to other RND efflux pump substrates, aminoglycosides are considered hydrophilic and do not partition into lipid bilayers (Rosenberg *et al.* 2000, Aires and Nikaido 2005). In *P. aeruginosa*, the MexXY-OprM efflux system showed specificity for aminoglycoside antibiotics as well as for hydrophobic antibiotics (Aires *et al.* 1999, Masuda *et al.* 2000), whereas the MexAB-OprM and MexCD-OprJ efflux systems do not transport aminoglycosides (Masuda *et al.* 2000). Similarly, in *E. coli*, the RND efflux pump AcrD is specific for aminoglycosides, while AcrB is unable to transport these antibiotics (Rosenberg *et al.* 2000). A recent study indicated that RND efflux pumps transport hydrophilic aminoglycosides from the periplasm (Aires and Nikaido 2005) rather than from the inner membrane as predicted for hydrophobic substrates. The MexY and AcrD efflux pumps likely have distinct regions within their periplasmic domains to

recognize and expel aminoglycosides compared to the RND efflux pumps that strictly transport hydrophobic compounds. Replacement of the periplasmic loops of AcrB with the loops of AcrD yielded a chimeric efflux pump with an AcrD-like substrate profile (Elkins and Nikaido 2002), demonstrating that the periplasmic loops are involved in determining substrate specificity. However, the nature of the aminoglycoside binding site within the periplasmic domains of either AcrD or MexY has not been determined. Moreover, little is known about the structural determinants influencing the specificity for hydrophobic antibiotics displayed by AcrB, MexB and their homologues. The *P. aeruginosa* MexY efflux pump was distantly related to the other RND efflux pumps (Figure 3.6), including EmhB, ArpB, MexB and SrpB, which do not transport streptomycin. Thus, the protein sequence of an RND efflux pump may have a limited ability to predict its substrate specificity, at least for pumps that have an unusual selectivity for aminoglycosides.

Also evident from the phylogenetic relationship of the RND efflux pumps (Figure 3.6), the SrpB, TtgE, TtgH and SepB proteins, which are present in the highly solvent tolerant *P. putida* strains, formed a clade distinct from EmhB and the antibiotic efflux pumps MexB, ArpB and TtgB. Segura *et al.* (2003) correlated solvent tolerance to the types of RND efflux pumps present in several *Pseudomonas* species and found that highly toluene tolerant strains possessed homologues of the TtgGHI efflux pump, while the more sensitive strains possessed only a homologue to the TtgABC efflux system. Based on the close phylogenetic relationship between the EmhB and TtgB proteins, and their more distant relationship to TtgH, it was anticipated that the EmhABC efflux system would not play a significant role in toluene efflux in *P. fluorescens* cLP6a. Not surprisingly, *P. fluorescens* cLP6a is solvent-sensitive as shown by its inability to grow in the presence of toluene vapours (Table 3.3). The EmhABC efflux system, however, is essential for the recovery of *P. fluorescens* cLP6a from toluene exposure (Table 3.3) and, thus, is involved in toluene efflux.

Of the TtgABC, ArpABC and MexAB-OprM efflux systems, which show high homology to EmhABC (Table 3.1), only TtgABC in *P. putida* DOT-T1E has been reported in the literature to be involved in toluene efflux (Ramos *et al.* 1998, Rojas *et al.* 2001). Expression of TtgABC alone supported growth of *P. putida* DOT-T1E in the

presence of vapour-phase toluene, although the cells were unable to survive a sudden toluene shock when the solvent was added directly to liquid cultures (Rojas *et al.* 2001). In contrast, the *P. putida* DOT-T1E expressing the TtgGHI efflux system showed enhanced survival to toluene shock conditions when the cells were previously exposed to the solvent (Rojas *et al.* 2001), confirming that expression of TtgGHI is the principal efflux mechanism responsible for the solvent tolerant phenotype of this organism. Like the *P. fluorescens* EmhABC efflux system, TtgABC likely contributes to a basal level of solvent tolerance, although expression of TtgABC in *P. putida* DOT-T1E supported growth in the presence of vapour-phase toluene (Rojas *et al.* 2001). *P. putida* DOT-T1E possesses additional solvent tolerance mechanisms that may account for its enhanced toluene tolerance compared to *P. fluorescens* cLP6a. *P. putida* DOT-T1E undergoes membrane adaptations in the presence of toluene, including *cis-trans* fatty acid isomerization and an increased rate of fatty acid biosynthesis (Segura *et al.* 2004), which may contribute to its solvent-tolerant phenotype. Pinkart and White (1997) also showed that solvent-tolerant *P. putida* strains had higher rates of phospholipid biosynthesis than solvent-sensitive strains. The presence of additional solvent tolerance mechanisms involving membrane adaptations may make it difficult to assess the contribution of efflux pumps to solvent tolerance. Membrane adaptations in response to solvent exposure have not been examined in *P. fluorescens* cLP6a. However, the reported ability of *P. putida* DOT-T1E expressing only the TtgABC efflux system to grow in the presence of vapour-phase toluene (Rojas *et al.* 2001), whereas *P. fluorescens* cLP6a is unable to grow in similar conditions, suggests that *P. putida* DOT-T1E possesses more effective solvent tolerance mechanisms. *P. putida* DOT-T1E may undergo more effective membrane adaptations in response to toluene than *P. fluorescens* cLP6a, or the TtgABC system may be more efficient at toluene efflux than the *P. fluorescens* EmhABC system. Expression of the TtgABC efflux system in the efflux pump-deficient *P. fluorescens* cLP6a-1 would provide a better background for comparison of toluene tolerance mediated by these efflux pumps.

The *P. putida* S12 ArpABC proteins are nearly identical to the TtgABC components (Kieboom and de Bont 2001); in fact, the ArpB and TtgB proteins differ by only one amino acid, an alanine to glycine substitution at position 544. Hence,

expression of the ArpABC efflux system in *P. fluorescens* cLP6a-1 is likely to yield the same result as expression of the TtgABC system in *P. fluorescens* cLP6a-1. Introduction of the *arpABC* operon into *P. fluorescens* cLP6a-1 demonstrated that the ArpABC and EmhABC efflux systems share the same substrate specificity for toluene. As with the wild-type *P. fluorescens* cLP6a expressing EmhABC, the *P. fluorescens* cLP6a-1 mutant expressing ArpABC was unable to grow in the presence of toluene vapours but was able to recover upon removal of the toluene (Table 3.3). Previous characterization of the substrate specificity of the ArpABC efflux system in *P. putida* S12 indicated that ArpABC was not involved in toluene efflux, because a mutant expressing only ArpABC was sensitive to solvents when grown in a two-phase liquid culture (Kieboom and de Bont 2001). Similarly, *P. aeruginosa* was sensitive to toluene when the solvent was supplied as an overlay on solid media, suggesting that the MexAB-OprM efflux system did not pump toluene (Li *et al.* 1998). However, the use of growth in the presence of liquid phase toluene as an indicator of solvent efflux may have been too stringent to detect a minimal contribution of ArpABC or MexAB-OprM to toluene tolerance. In this study, toluene was shown to be a substrate of the ArpABC efflux system by using the ability to recover from exposure to vapour-phase toluene as an indicator of solvent efflux. The results of the antibiotic sensitivity and toluene tolerance assays presented here (Table 3.2 and Table 3.3) demonstrate that EmhABC and ArpABC, and, likely, TtgABC and MexAB-OprM share a functional similarity for antibiotic and toluene efflux, consistent with their high protein sequence identities (Table 3.1). Although the substrate ranges of these efflux systems are comparable, the affinities and efflux rates of the EmhABC, ArpABC, TtgABC and MexAB-OprM systems for various substrates may differ. A more detailed comparison of substrate specificities would require quantitation of substrate binding and rate constants for these efflux systems.

Kieboom and de Bont (2001) proposed that RND efflux systems could be classified on the basis of substrate specificity into three categories: antibiotic efflux pumps, solvent efflux pumps, and combined antibiotic and solvent efflux pumps. However, hydrophobic antibiotics and toluene appear to be common substrates for many RND efflux systems, including EmhABC, TtgABC, ArpABC, SrpABC and TtgGHI, making such a classification system ambiguous. It may be possible, however, to

categorize the efflux systems as multidrug or solvent pumps based on an inferred physiological function. For example, SrpABC and TtgGHI are essential for solvent tolerance, whereas EmhABC, TtgABC and ArpABC contribute nominally to solvent tolerance. The physiological basis for this difference, though, is unclear. One possibility is that the EmhABC efflux system, for example, may have a lower affinity or a lower pumping rate for toluene than the SrpABC and TtgGHI pumps. Alternatively, the EmhABC efflux system may not be expressed at high enough levels in *P. fluorescens* cLP6a to support the high rate of toluene transport that would be required to achieve solvent tolerance. The latter possibility is supported by the observation that the mutant *P. fluorescens* cLP6a-1 complemented with the *emhABC* genes, which presumably had increased expression of the efflux pump due to the multi-copy nature of the plasmid, displayed enhanced toluene tolerance (Table 3.3). As well, the *P. putida* SrpABC and TtgGHI efflux systems are induced by toluene (Kieboom *et al.* 1998b, Guazzaroni *et al.* 2005), and the increased expression of these pumps in the presence of toluene may result in higher levels of solvent tolerance. To confirm the hypothesis that the pump expression level dictates solvent tolerance, the toluene tolerance of strains expressing equivalent numbers of the EmhABC and SrpABC efflux systems need to be compared. Until the expression levels are determined, the first possibility that the EmhABC efflux pump has a reduced ability to transport toluene, compared to the solvent efflux systems, cannot be discounted.

The efflux system in *P. fluorescens* LP6a was reported to have an unusual selectivity for polycyclic aromatic hydrocarbons; phenanthrene, anthracene and fluoranthene with three aromatic rings were substrates of the efflux system, whereas naphthalene with two aromatic rings was not actively expelled from the cell (Bugg *et al.* 2000). Transport assays performed with *P. fluorescens* cLP6a-1 strains in the presence or absence of the EmhABC efflux system confirmed that naphthalene is not a substrate of the EmhABC efflux system (Table 3.4). Given that the monoaromatic hydrocarbon toluene and three-ring polycyclic aromatic hydrocarbons are substrates of EmhABC, the selectivity against naphthalene is remarkable, but not unprecedented for RND efflux pumps. By comparing the tolerance levels of the wild-type strain and a strain only expressing the TtgDEF system, Rojas *et al.* (2001) suggested that the TtgDEF efflux

system in *P. putida* DOT-T1E pumps toluene and styrene, but not *m*-xylene, ethylbenzene and propylbenzene. To date, naphthalene transport by other RND efflux pumps has not been examined in the literature. As in *P. fluorescens* cLP6a, naphthalene accumulation in *P. putida* S12, which possesses the ArpABC and SrpABC efflux systems, was unaffected by the energy inhibitor azide (Table 3.4). This finding indicates that naphthalene selectivity is not unique to the EmhABC efflux system.

Nevertheless, the substrate specificity of the polycyclic aromatic hydrocarbon efflux system, EmhABC, in *P. fluorescens* cLP6a has now been broadened to include a wide variety of hydrophobic antibiotics as well as toluene. Studies on the substrate specificities of RND efflux pumps in other gram-negative bacteria are often hampered by the presence of multiple efflux systems or multiple mechanisms of resistance. For example, membrane adaptations and efflux systems both contribute to toluene tolerance in *P. putida* DOT-T1E (Segura *et al.* 2004, Rojas *et al.* 2001), making it difficult to distinguish clearly the role of efflux pumps in solvent tolerance. The phenotype of the EmhB-deficient mutant *P. fluorescens* cLP6a-1 compared with the wild-type cLP6a strain suggests that additional resistance mechanisms are not significant in *P. fluorescens* cLP6a. Thus, *P. fluorescens* cLP6a-1 may provide a useful background for the characterization of other RND efflux systems.

The wide substrate specificity of EmhABC was exploited to address the remaining objectives of this thesis. The regulation of efflux pump expression in response to the presence of pump substrates was examined (Section 3.3). As well, the mechanism by which substrates interact with and are transported through the efflux pump was investigated (Section 3.4).

3.3. Regulation of the EmhABC efflux system in *P. fluorescens* cLP6a

The presence of a putative transcriptional regulator located upstream of the *emhABC* genes (Figure 3.5) prompted an investigation into the regulatory mechanisms controlling expression of the EmhABC efflux system in *P. fluorescens* cLP6a. Promoter-reporter transcriptional fusions were constructed to determine the effects of efflux pump substrates and other compounds on the expression of the genes.

3.3.1. Sequence analysis of EmhR

The EmhR protein showed homology to members of the TetR family of transcriptional repressors (Figure 3.10 and Table 3.5). As with the EmhABC proteins, the closest homologues of EmhR are a hypothetical transcriptional repressor located upstream of a putative RND efflux system in *P. fluorescens* Pf0-1, the TtgR repressor protein of the TtgABC efflux system in *P. putida* DOT-T1E, and the ArpR repressor protein of the ArpABC efflux system in *P. putida* S12. More distantly related to EmhR are the AcrR regulator of the AcrAB operon in *E. coli* as well as the TetR-family repressors SrpR and TtgW located upstream of the toluene efflux pumps SrpABC in *P. putida* S12 and TtgGHI in *P. putida* DOT-T1E, respectively.

Secondary structure analysis of EmhR revealed the presence of an N-terminal helix-turn-helix DNA binding motif characteristic of TetR-family proteins (Figure 3.10). The C-terminal region of TetR-family proteins is the ligand-binding domain. Not surprisingly, the N-terminal region of EmhR and its homologues in *P. putida* DOT-T1E and S12 and in *E. coli* was highly conserved with protein identities ranging from 98 to 54%, while the C-terminal domain was much less conserved with protein identities ranging from 89 to 18% (Table 3.5). The C-terminal domains of the putative TetR-family repressor in *P. fluorescens* Pf0-1, TtgR in *P. putida* DOT-T1E and ArpR in *P. putida* S12 showed the highest similarity (80 to 94% similar) to EmhR, suggesting that these transcriptional regulators and their respective efflux systems are controlled by similar mechanisms.

EmhR	<u>MVRRTKEEAQ</u>	<u>ETRSQILEAA</u>	<u>EKAFYERGVV</u>	<u>RTTADTATF</u>	<u>AGVTRGAIYW</u>	50
Pf0-1	<u>MVRRTKEEAQ</u>	<u>ETRSQILEAA</u>	<u>EKAFYERGVV</u>	<u>RTTSDIATF</u>	<u>AGVTRGAIYW</u>	50
TtgR	<u>MVRRTKEEAQ</u>	<u>ETRAQILEAA</u>	<u>ERAFYKRGVA</u>	<u>RTTADTATF</u>	<u>AGVTRGAIYW</u>	50
ArpR	<u>MVRRTKEEAQ</u>	<u>ETRAQILEAA</u>	<u>ERAFYKRGVA</u>	<u>RTTADTATF</u>	<u>AGVTRGAIYW</u>	50
AcrR	<u>MARKTKQEAQ</u>	<u>ETROHLELVA</u>	<u>LRLFSQQGVS</u>	<u>STSHGETAKA</u>	<u>AGVTRGAIYW</u>	50
SrpR	<u>MARKTAAPAE</u>	<u>ETRORELDVA</u>	<u>LEVVAQGVV</u>	<u>DAIEDQARK</u>	<u>AGVTRGAIYW</u>	50
TtgW	<u>MARKTAAPAK</u>	<u>ETRORELDVA</u>	<u>LEVVAQGVV</u>	<u>DAIEDQARK</u>	<u>AGVTRGAIYW</u>	50
EmhR	<u>HFSNKADLVQ</u>	<u>AMLDTHHEPI</u>	<u>DEMAKASESE</u>	<u>DELDPIGCMR</u>	<u>KGLIHLHQQV</u>	100
Pf0-1	<u>HFSNKADLVQ</u>	<u>AMLDTHHEPI</u>	<u>DEMAKASESE</u>	<u>DEPDPIGCMR</u>	<u>KGLIHLHQQV</u>	100
TtgR	<u>HEMNKAELVQ</u>	<u>ALDLSHETH</u>	<u>DHIFARASESE</u>	<u>DEVDPGCMR</u>	<u>KGLLQVENEL</u>	100
ArpR	<u>HEMNKAELVQ</u>	<u>ALDLSHETH</u>	<u>DHIFARASESE</u>	<u>DELDPIGCMR</u>	<u>KGLLQVENEL</u>	100
AcrR	<u>HEKDRSDIFS</u>	<u>EIWELSESNI</u>	<u>GEIELEYQAK</u>	<u>FPGDPISVLR</u>	<u>EIIHLHVLEST</u>	100
SrpR	<u>HENGKLEVLQ</u>	<u>AVIASRQHPF</u>	<u>ELDFTPDLG</u>	-----IERSW	<u>EAVVVMMLDA</u>	94
TtgW	<u>HENGKLEVLQ</u>	<u>AVIASRQHPF</u>	<u>ELDFTPDLG</u>	-----IERSW	<u>EAVVVMMLDA</u>	94
EmhR	<u>AMDEKTRREN</u>	<u>ELIFHKCEFI</u>	<u>DEMCDLROOR</u>	<u>REVSIDGNVR</u>	<u>FGHATSNAVN</u>	150
Pf0-1	<u>AMDEKTRREN</u>	<u>ELIFHKCEFI</u>	<u>DEMCDLROOR</u>	<u>RTASTDGNVR</u>	<u>HAITTSNAIN</u>	150
TtgR	<u>VGDARTRREN</u>	<u>ELIFHKCEFI</u>	<u>DDMGELROOR</u>	<u>QSAVTDCHKG</u>	<u>ITTAATANAVR</u>	150
ArpR	<u>VGDARTRREN</u>	<u>ELIFHKCEFI</u>	<u>DDMGELROOR</u>	<u>QSAVTDCHKG</u>	<u>ITTAATANAVR</u>	150
AcrR	<u>YTEERRLLM</u>	<u>ELIFHKCEEV</u>	<u>GEMAVVQQAQ</u>	<u>RNLCEESYDR</u>	<u>TEQTEKHCIE</u>	150
SrpR	<u>VHSEQSKQFS</u>	<u>ELIYQGL</u>	<u>DESGLEHNRM</u>	<u>VQASDRFLQY</u>	<u>IHQVIRHAVT</u>	142
TtgW	<u>VHSEQSKQFS</u>	<u>ELIYQGL</u>	<u>DESGLEHNRM</u>	<u>VQASDRFLQY</u>	<u>IHQVIRHAVT</u>	142
EmhR	<u>RGQIEDNIDT</u>	<u>ARVAISLHAY</u>	<u>EDGILYQWLF</u>	<u>APDS</u>	-----FOIH	188
Pf0-1	<u>RGQEPADIDT</u>	<u>ARVAISIHAY</u>	<u>EDGELKQWLF</u>	<u>APDS</u>	-----FEIY	188
TtgR	<u>RGQIEGELDA</u>	<u>ERAVAMFAY</u>	<u>VDGILRRWLF</u>	<u>LEDS</u>	-----VDIE	188
ArpR	<u>RGQIEGELDV</u>	<u>ERAVAMFAY</u>	<u>VDGILGRWLF</u>	<u>LEDS</u>	-----VDIE	188
AcrR	<u>AKMPEADIMT</u>	<u>RRAVIMRGY</u>	<u>ISCHMENWLF</u>	<u>AEOS</u>	-----FDEK	188
SrpR	<u>QGEELINIDL</u>	<u>QTSIGVFKGL</u>	<u>ITGELVEGER</u>	<u>SKDQQAQIIK</u>	<u>VALGSEFWALF</u>	192
TtgW	<u>QGEELINIDL</u>	<u>HTSIGVFKGL</u>	<u>ITGELVEGER</u>	<u>SKDQQTQIIK</u>	<u>VALGSFLALF</u>	192
EmhR	<u>TEAERWVDA</u>	<u>EDMRESPESE</u>	<u>RR</u>	-----	210	
Pf0-1	<u>AEAERWVDTG</u>	<u>EDMRESPESE</u>	<u>RR</u>	-----	210	
TtgR	<u>GDVEKVVDTG</u>	<u>EDMRESPESE</u>	<u>RR</u>	-----	210	
ArpR	<u>GDVEKVVDTG</u>	<u>EDMRESPESE</u>	<u>RR</u>	-----	210	
AcrR	<u>KEARDYVAIL</u>	<u>HEMYLCEPTE</u>	<u>RNPATNE</u>		215	
SrpR	<u>REPPRFLLCE</u>	<u>EAQIKQVKSF</u>	<u>E</u>	-----	213	
TtgW	<u>REPPRFLLCE</u>	<u>EAQIKQAKPF</u>	<u>E</u>	-----	213	

Figure 3.10. Alignment of TetR-family regulatory proteins involved in the regulation of RND efflux systems. The proteins are EmhR from *P. fluorescens* cLP6a, a hypothetical regulator from *P. fluorescens* Pf0-1 (ZP_00266639), TtgR from *P. putida* DOT-T1E (AAK15050), ArpR from *P. putida* S12 (AAF73830), AcrR from *E. coli* K12 (NP_414997), SrpR from *P. putida* S12 (AAF16682), and TtgW from *P. putida* DOT-T1E (AAK69561). Amino acids that are identical in at least four of the seven sequences are shaded. Secondary structure was predicted by using the Proteus Structure Prediction Server on the Canadian Bioinformatics Help Desk website (<http://129.128.185.59/~scott/proteus/index.shtml>), and the cylinders indicate the location of predicted α -helices. The first 50 amino acids constitute the putative helix-turn-helix DNA binding motif.

Table 3.5. Comparison of the putative efflux pump regulator EmhR from *P. fluorescens* cLP6a with homologous TetR-family repressors

Organism	Protein	Operon regulated	% Protein identity to EmhR (% similarity) ^a		
			Overall	N-terminus	C-terminus
<i>P. fluorescens</i> Pf0-1	Pf0-1 ^b	Putative ^b	91 (95)	98 (98)	89 (94)
<i>P. putida</i> DOT-T1E	TtgR	TtgABC	71 (83)	90 (94)	64 (80)
<i>P. putida</i> S12	ArpR	ArpABC	71 (83)	90 (94)	65 (80)
<i>E. coli</i> K12	AcrR	AcrAB	41 (61)	60 (84)	35 (53)
<i>P. putida</i> S12	SrpR	SrpABC	28 (47)	54 (70)	18 (40)
<i>P. putida</i> DOT-T1E	TtgW	TtgGHI	28 (46)	54 (68)	18 (40)

^a Percent identities and percent similarities (given in parentheses) were calculated by using the Sequence Manipulation Suite version 2 (Stothard 2000) for the full-length proteins (overall), the first 50 amino acids (N-terminus) and the subsequent amino acids (C-terminus).

^b A putative TetR-family repressor (accession number ZP_00266639) was identified in the genome sequence of *P. fluorescens* Pf0-1 and is located upstream of a putative three-component RND efflux system.

3.3.2. Identification of regulatory elements in the *emhR-emhA* intergenic region

To support the hypothesis that EmhABC, TtgABC, ArpABC and the homologous putative RND efflux system in *P. fluorescens* Pf0-1 are regulated in a similar fashion, the DNA sequences of the intergenic region between the regulatory gene and the membrane fusion protein gene were aligned for the four efflux systems (Figure 3.11). The alignment revealed several highly conserved regions in all four DNA sequences, particularly a 55-nucleotide segment corresponding to positions 148 to 202 in the *emhR-emhA* intergenic region (Figure 3.11).

For the *ttgR-ttgA* intergenic region, Duque *et al.* (2001) mapped the transcription initiation sites for *ttgR* and *ttgABC* by using primer extension analysis. Figure 3.12 shows the alignment of the *ttgR-ttgA* and *emhR-emhA* intergenic regions with the transcription initiation sites for *ttgR* and *ttgABC* and the corresponding putative transcription initiation sites for *emhR* and *emhABC* indicated. The predicted -10 and -35 regions of the putative promoters are also shown (Figure 3.12). The TtgR DNA-binding sites were determined by using DNaseI footprint analysis (Terán *et al.* 2003) and are also shown in Figure 3.12. Both the transcription initiation sites and the repressor protein binding sites are located within the highly conserved region between positions 148 and 202 in the *emhR-emhA* sequence. The similarity of the intergenic regions provides additional evidence that expression of the EmhABC and TtgABC, as well as of the homologous ArpABC and *P. fluorescens* Pf0-1 efflux systems, is regulated by the same mechanisms.

The predicted -10 and -35 regions of the *emhA* promoter show homology to the consensus sequence for the *E. coli* σ^{70} -dependent RNA polymerase. The consensus sequences for the -10 and -35 regions of σ^{70} promoters are TATAAT and TTGACA, respectively (Paget and Helmann 2003), and the corresponding sequences in the *emhA* promoter region (Figure 3.12), TATAAt and TTtACA, differ from the consensus by only one nucleotide (indicated in lower case). As well, the *emhR* promoter region shows some homology to the σ^{70} consensus sequence at the -10 (TATAcT) and -35 (TgGAtA) regions (Figure 3.12). The σ^{70} factor of the RNA polymerase is responsible for transcription initiation in exponentially growing cells (Paget and Helmann 2003).

```

emhR-A  CATGGCAGTACCAAGCTGAATCAGGGTGCTTCAGCGATCCCTCAACAGGCC 50
Pf0-1   CATGGCAGTAAAGCTGAACAGGATGTTTCAGGGATCGCTCAATATCCG 50
ttgR-A  CATGGCAGTACCAAGCTGA-----TCAGCCCCAACCCGCAGC-C 38
arpR-A  CATGGCAGTACCAAGCTGA-----TCAGCCCCAACCCGCAGC-C 38

emhR-A  CTGAATAAAAAGTGGGCCAACCCTCTTGGGTGTCGTCCCGGGCTTACAAT 100
Pf0-1   CTGAATAAAAAGGGTTGATCTCTCGCGGATCGGATCCCGGGCTTACAAT 100
ttgR-A  CGTGCGGGGAACCTCCCGGGGCACCTCTGCCGGGGCCCTCT-CGGATAAG 87
arpR-A  CGGGCGGGGAACCTCCGAGGGCTCTGTGCCGGGGCCCTCT-CGGATGAG 87

emhR-A  TCGAACCTTTCAAACCGCTTTTGTAAAGATGTGGGTAGGCAGCAAGCTA 150
Pf0-1   TTCAGACCTTCGACGACTTTTGTAAAGGGTTCGATAGGACCGCAAGCTG 150
ttgR-A  CT--AATCAAACGCTGAGGCT-GTACC-----TCAGTACCAACCAGCACTA 130
arpR-A  CT--AATCAAACGCTGAGGG-GTACC-----TCAGTACAACCTAGCACTA 129

emhR-A  TTTACAAACAACCATCAATCTAAGTATATTTCCCTTAGCAAGCTATTTATCC 200
Pf0-1   TTTACAAACAACCATCAATCTAAGTATATTTCCCTTAGCAAGCTATTTATCC 200
ttgR-A  TTTACAAACAACCATCAATCTAAGTATATTTCCCTTAGCAAGCTATTTATCC 180
arpR-A  TTTACAAACAACCATCAATCTAAGTATATTTCCCTTAGCAAGCTATTTATCC 179

emhR-A  ACTCAGCGCACATTTTTTA-----CCCTTACACATTTCCTTCTCCG 240
Pf0-1   ACCGGTAACCCTTTTTTTA-----CCCTTCCCACTTCCTTCTCCG 240
ttgR-A  ACCGATAGCATTTTTTCCAGATCAAGATCTCTTCCATTACTTCTTACCC 230
arpR-A  ACCGATAGCATTTTTTCCAGATCAAGATCTCTTCCATTACTTCTTACCC 229

emhR-A  -CAATTTGGCGCCTGAGCCGAGGATTT-----TCATG 272
Pf0-1   -CTTTTCGGCGCCTGAGCCGAGGATCT-----TCATG 272
ttgR-A  TCTCCCTGCTCAGCGACCCGAGGATCCGGATCCTCATG 269
arpR-A  TCTCCCTGCTCAGCGACCCGAGGATCC-----TCATG 262

```

Figure 3.11. Sequence comparison of the *emhR-emhA* intergenic region. The following sequences were compared to the *emhR-emhA* intergenic region: the intergenic region between a putative repressor and RND efflux system in *P. fluorescens* Pf0-1; the intergenic region between the *ttgR* and *ttgABC* genes in *P. putida* DOT-T1E; and the intergenic region between the *arpR* and *arpABC* genes in *P. putida* S12. The start codons of the genes are indicated in bold-face. Nucleotides conserved in all four sequences are indicated by shading.

3.3.3. Transcription of the *emhABC* and *emhR* genes is growth-phase dependent

Promoter-reporter plasmids were constructed to examine the growth-phase dependence of *emhABC* gene expression, as well as to investigate the effects of hydrophobic compounds on efflux pump gene expression. To measure *emhABC* gene transcription, a $P_{emhA}::lacZ$ transcriptional fusion was constructed on plasmid pTZ110- P_{emhA} by cloning the *emhR-emhA* intergenic region in the same orientation as the *emhA* gene upstream of the promoterless *lacZ* gene. Similarly, a $P_{emhR}::lacZ$ transcriptional fusion was constructed on plasmid pTZ110- P_{emhR} by cloning the *emhR-emhA* intergenic region in the opposite orientation as the *emhA* gene and was used as a measure of *emhR* gene transcription. β -galactosidase activity from the promoter-reporter plasmids, as well as from the negative control plasmid pTZ110-str, was measured in *P. fluorescens* cLP6a grown in various conditions.

Transcription of the *emhABC* and *emhR* genes was monitored throughout the growth phases in *P. fluorescens* cLP6a strains carrying the promoter-reporter plasmids. A 0.5% (vol/vol) inoculum of the *P. fluorescens* cLP6a cultures was prepared in 200 mL TSB to reflect the growth conditions used for the hydrocarbon transport assays, and β -galactosidase activity was measured at specified time intervals (Figure 3.13). Both the $P_{emhA}::lacZ$ and the $P_{emhR}::lacZ$ transcriptional fusions showed an initial, rapid decline in β -galactosidase activity, which suggests that expression of both the *emhABC* genes and the *emhR* genes was repressed when the cultures were diluted to a low cell density. An increase in β -galactosidase activity was observed in both cultures during mid-exponential phase, followed by a decline in activity to a steady level as the cultures moved into stationary phase. The growth-phase dependent trend shown in Figure 3.13 was observed repeatedly in three independent experiments. The β -galactosidase activity from the $P_{emhR}::lacZ$ transcriptional fusion was two-fold higher than the activity from the $P_{emhA}::lacZ$ fusion until mid-exponential phase, when the activities of both putative promoter regions reached approximately equivalent levels. The higher activity from the *emhR* transcriptional fusion suggests that the EmhR transcriptional regulator has a higher affinity for the *emhA* operator site than for the *emhR* operator site.

The identical β -galactosidase expression patterns from the *emhR* and *emhABC* promoters (Figure 3.13) are consistent with the role of the *emhR* gene product as a

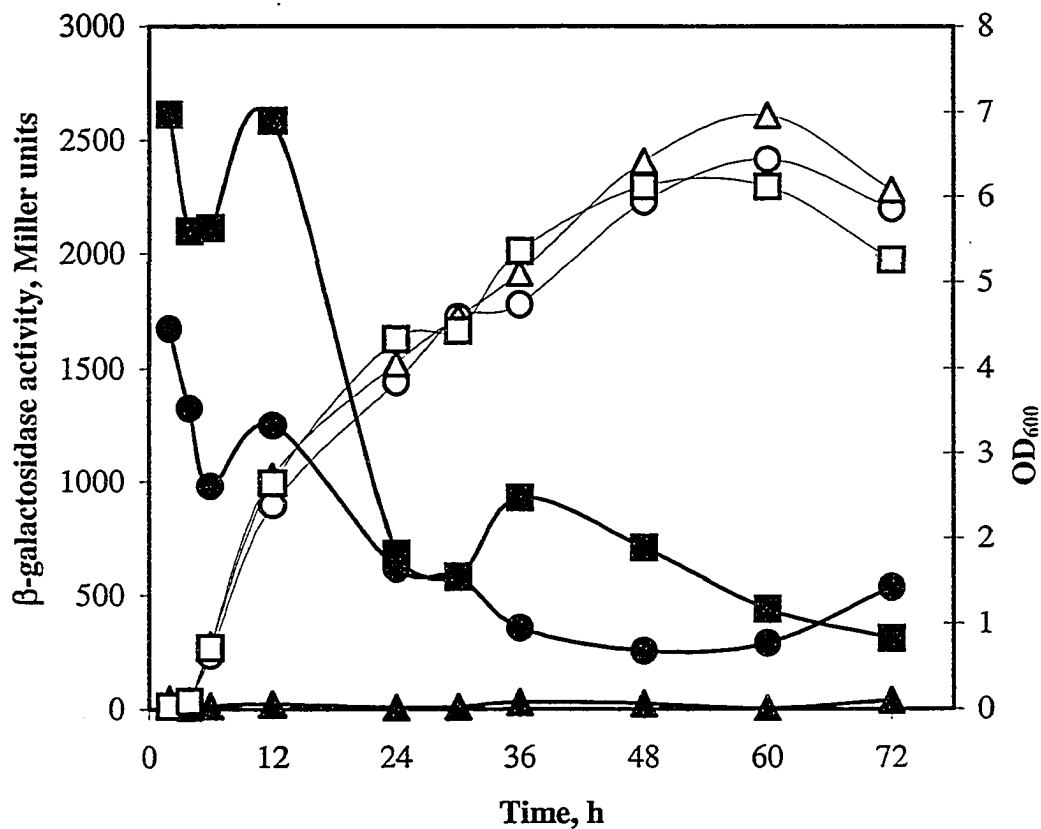


Figure 3.13. Growth phase dependence on expression of β -galactosidase from the $P_{emhA}::lacZ$ and $P_{emhR}::lacZ$ transcriptional fusions. Cultures of *P. fluorescens* cLP6a(pTZ110- P_{emhA}) (circles), *P. fluorescens* cLP6a(pTZ110- P_{emhR}) (squares), and *P. fluorescens* cLP6a(pTZ110-str) (triangles) were grown in 200 mL of TSB with streptomycin, and the OD₆₀₀ was monitored (open symbols). β -galactosidase activity (closed symbols) was measured in permeabilized cells by the method described by Griffith and Wolf (2002). Three independent growth curves were done. Representative data from one experiment are shown.

repressor of its own transcription as well as that of the *emhABC* genes. The EmhR protein was predicted to bind to the *emhR-emhA* intergenic region in an area overlapping the *emhR* and *emhABC* promoters (Figure 3.12). Thus, in the absence of an inducer, EmhR is predicted to bind to the two promoters, thereby preventing the binding of the RNA polymerase, and represses transcription of both the *emhR* and *emhABC* genes. Other proteins belonging to the TetR family of transcriptional regulators are known to repress their own transcription. These include the TtgR regulator of the TtgABC efflux system in *P. putida* DOT-T1E (Terán *et al.* 2003), the SmeT regulator of the SmeDEF efflux system in *Stenotrophomonas maltophilia* (Sánchez *et al.* 2002a), and the TetR regulator of the TetA efflux pump in *E. coli* (Hillen and Berens 1994).

The growth-phase dependent expression of the *P. fluorescens* EmhABC efflux system (Figure 3.13) was similar to the trend observed for the *P. aeruginosa* MexAB-OprM efflux system (Maseda *et al.* 2004). By using a *mexAB-oprM* promoter-reporter plasmid, Maseda *et al.* (2004) observed a decrease in expression upon dilution of the *P. aeruginosa* preculture into fresh medium. Expression from the *mexAB-oprM* promoter increased during exponential phase and subsequently declined after the onset of stationary phase (Maseda *et al.* 2004), comparable to the expression pattern observed from the *emhABC* promoter (Figure 3.13). As well, Northern analysis demonstrated that transcription of the *mexR* gene, which is located adjacent to the *mexAB-oprM* operon in *P. aeruginosa* and encodes a MarR family transcriptional repressor, was greatest during the mid-exponential growth phase and declined as the culture progressed into stationary phase (Sánchez *et al.* 2002b), similar to the expression pattern observed from the *emhR* promoter (Figure 3.13). Thus, expression of the EmhABC efflux system in *P. fluorescens* cLP6a and of the MexAB-OprM efflux system in *P. aeruginosa* appear to be controlled by similar growth-dependent mechanisms, although the EmhR and MexR proteins belong to different families of transcriptional regulators and the promoter regions are dissimilar.

The growth-phase dependent expression of the β -galactosidase reporter gene from the *emhABC* and *emhR* promoters (Figure 3.13) suggests that expression of the *emhABC* and *emhR* genes is dependent either upon the metabolic state of the culture or upon the cell density. At low cell densities, such as upon dilution of a stationary-phase inoculum

into fresh medium, expression of the *emhABC* and *emhR* genes is repressed. Likely, a compound, as yet unidentified, accumulates in the cultures during growth, or as the cell density increases, which relieves the repression of the *emhABC* and *emhR* genes during exponential phase. Acylhomoserine lactones, which are autoinducers controlling quorum-sensing mechanisms in *P. aeruginosa*, accumulate during growth and induce the expression of cell density-dependent factors, including rhamnolipid biosynthesis and exotoxin production (Hardman *et al.* 1998). Moreover, Maseda *et al.* (2004) found that the autoinducer *N*-butyl-L-homoserine lactone enhanced expression of the MexAB-OprM efflux system in *P. aeruginosa* and suggested that accumulation of *N*-butyl-L-homoserine lactone was responsible for the increased expression of the MexAB-OprM efflux system as the cell density increased from mid- to late-exponential phase. Further work demonstrated that the autoinducer enhanced expression of MexAB-OprM in the absence of the MexR repressor protein (Sawada *et al.* 2004). Thus, there are likely global regulatory mechanisms, possibly mediated by quorum sensing systems, which affect the expression of RND efflux pumps. Further research into the regulation of the *P. fluorescens* EmhABC efflux system is required to determine if the expression is cell-density dependent and if quorum sensing may be involved.

The culture conditions used to generate the growth curves in Figure 3.13 were identical to those used to prepare the *P. fluorescens* cLP6a strains for the polycyclic aromatic hydrocarbon transport assays. For the transport assays, the cultures were harvested at 24 h, corresponding to late exponential phase and a low level of EmhABC expression. Although the level of EmhABC expression is not maximal at this time point, clearly there is sufficient expression of the efflux system to observe active transport of polycyclic aromatic hydrocarbons (Figure 3.7). The possibility that aromatic hydrocarbons, which are substrates of the efflux system, induce expression of the *emhABC* genes was explored using the promoter-reporter systems.

A series of *P. fluorescens* cLP6a cultures with the promoter-reporter plasmids were tested to screen the effect of aromatic hydrocarbons and other compounds on the expression of the *emhABC* and *emhR* genes. For the screening, smaller (10-mL) cultures were employed, and the growth curves were repeated with a 0.5% (vol/vol) inoculum of the *P. fluorescens* cLP6a reporter strains to determine the optimum sampling point. The

growth curves and β -galactosidase activities for the $P_{emhA}::lacZ$ and $P_{emhR}::lacZ$ transcriptional fusions in the smaller cultures followed the same trends as in the larger 200-mL cultures (data not shown). The β -galactosidase activity reached a steady level in both cultures at an OD_{600} of 2–2.5. This range was chosen as the optimum cell density to monitor β -galactosidase activity with the test compounds, in order that changes in activity would reflect the effect of the compound and not fluctuations due to growth state or cell density.

3.3.4. Transcription of the *emhABC* and *emhR* genes is not induced by aromatic hydrocarbons or by metabolites of hydrocarbon degradation

To determine if the *emhABC* genes or the *emhR* gene are induced by aromatic hydrocarbons, *P. fluorescens* cLP6a strains carrying the promoter-reporter plasmids pTZ110- P_{emhA} or pTZ110- P_{emhR} were grown in the presence of phenanthrene, anthracene, fluoranthene, naphthalene or toluene. β -galactosidase activities for the negative control *P. fluorescens* cLP6a(pTZ110-str), which has the promoterless *lacZ* gene, were less than 10% of the values for the strains carrying the promoter-reporter plasmids and were unaffected by the presence of hydrocarbon (data not shown). Therefore, any observed changes in β -galactosidase activity for the strains carrying pTZ110- P_{emhA} or pTZ110- P_{emhR} could be attributed to the presence of the putative promoter sequences. Figure 3.14 shows that there was no significant change in the expression level of the *lacZ* reporter gene in the $P_{emhA}::lacZ$ or $P_{emhR}::lacZ$ transcriptional fusions by any of the aromatic hydrocarbons tested (P values > 0.2) compared to the control cells grown in the absence of hydrocarbon. Thus, expression of the EmhABC efflux system and of the putative repressor protein, EmhR, is not affected by aromatic hydrocarbons.

Since the wild-type *P. fluorescens* LP6a possesses plasmid-encoded genes for the degradation of polycyclic aromatic hydrocarbons including naphthalene, phenanthrene and anthracene (Foght and Westlake 1996), the possible role of intermediates of phenanthrene degradation in the expression of the *emhABC* and *emhR* genes was explored. Mutants of *P. fluorescens* LP6a blocked at different stages in the phenanthrene degradation pathway were used to prepare crude metabolite extracts. The *P. fluorescens*

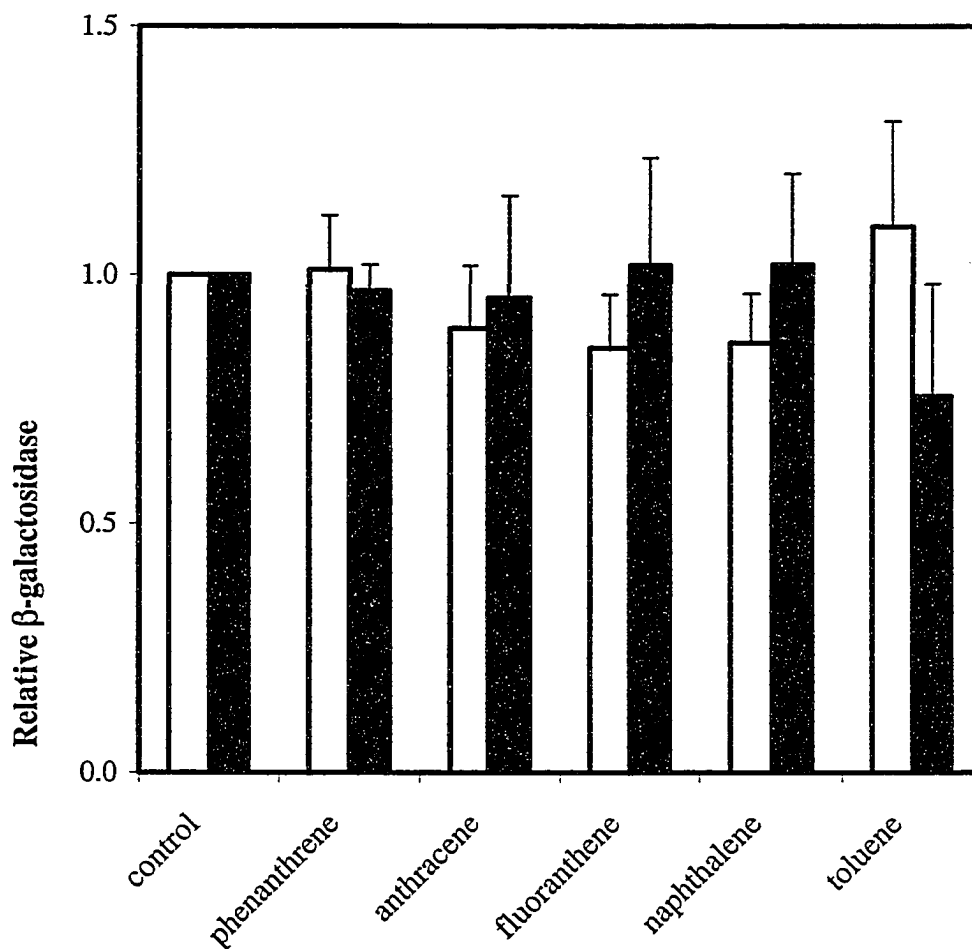


Figure 3.14. Effect of hydrocarbons on expression of β -galactosidase from the $P_{emhA}::lacZ$ (open bars) and $P_{emhR}::lacZ$ (solid bars) transcriptional fusions. *P. fluorescens* cLP6a(pTZ110- P_{emhA}) and *P. fluorescens* cLP6a(pTZ110- P_{emhR}) cells were grown to an $OD_{600} \sim 2$ in TSB with streptomycin in the absence of hydrocarbon (control) or in the presence of 0.5 g L^{-1} phenanthrene, 0.5 g L^{-1} anthracene, 0.5 g L^{-1} fluoranthene, 0.5 g L^{-1} naphthalene or 0.02% (vol/vol) toluene. β -galactosidase activity was measured in permeabilized cells by the method described by Griffith and Wolf (2002). The relative β -galactosidase activity represents the activity in the presence of hydrocarbon relative to the control (in the absence of hydrocarbon). The values are the means \pm standard deviations for three independent experiments.

strains used and the corresponding intermediate compounds present in the crude metabolite extract are shown in Figure 3.15 and were as follows: *P. fluorescens* cLP6a, which does not carry the pLP6a degradation plasmid, contained phenanthrene; *P. fluorescens* LP6a strain D1, which is blocked at the 1,2-dihydroxy-1,2-dihydronaphthalene dehydrogenase (*nahB*) reaction, accumulated *cis*-3,4-dihydroxy-3,4-dihydrophenanthrene; *P. fluorescens* LP6a strain 8, which is blocked at the 1,2-dihydroxynaphthalene dioxygenase (*nahC*) reaction, accumulated 3,4-dihydroxyphenanthrene; and *P. fluorescens* LP6a strain 21-41, which is blocked at the *trans*-*o*-hydroxybenzylidene pyruvate hydratase-aldolase (*nahE*) reaction, accumulated *trans*-4-(1'-hydroxynaphth-2'-yl)-2-oxobut-3-enoate. The promoter-reporter strains *P. fluorescens* cLP6a(pTZ110- P_{emhA}) and cLP6a(pTZ110- P_{emhR}) were grown in the presence of the culture supernatants to determine the effect of phenanthrene metabolites on expression of the *lacZ* gene from the *emhABC* and *emhR* promoters.

Figure 3.15 shows that there was no significant change in the expression level of the *lacZ* reporter gene in the P_{emhA} or P_{emhR} transcriptional fusions by the metabolites tested (P values > 0.2) compared to the control cells grown in the absence of hydrocarbon. Salicylate, which is both an intermediate in the degradation pathway (Foght and Westlake 1996) and an inducer of the degradation genes (Barnsley 1975), and 2-aminobenzoate, which is a non-metabolized gratuitous inducer of the degradation genes (Barnsley 1975), were also tested with the promoter-reporter strains. Neither salicylate nor 2-aminobenzoate produced a significant change in the expression level of the *lacZ* reporter gene (P values > 0.2; Figure 3.15). Thus, expression of the EmhABC efflux system and of its regulator EmhR is not affected by metabolites of phenanthrene degradation or by inducers of the hydrocarbon degradation genes in *P. fluorescens* cLP6a.

3.3.5. Transcription of the *emhABC* and *emhR* genes is induced by some antibiotics

The EmhABC efflux system in *P. fluorescens* cLP6a-1 exports hydrophobic antibiotics as well as polycyclic aromatic hydrocarbons (Table 3.2). To investigate the possible role of these antibiotics in the regulation of pump expression, the promoter-reporter strains *P. fluorescens* cLP6a(pTZ110- P_{emhA}) and cLP6a(pTZ110- P_{emhR}) were

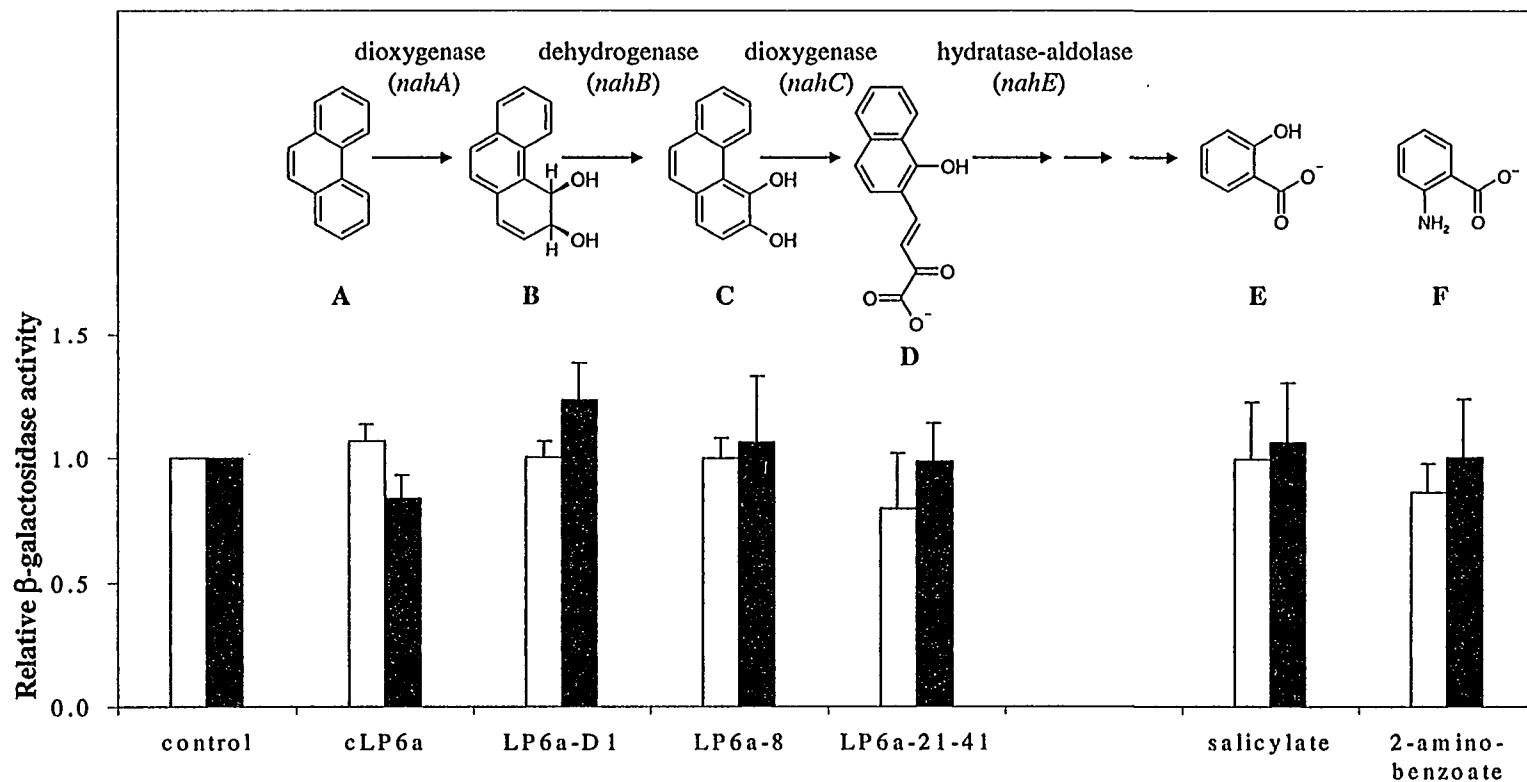


Figure 3.15. Effect of metabolites from phenanthrene degradation on expression of β -galactosidase from the $P_{emhA}::lacZ$ (open bars) and $P_{emhR}::lacZ$ (solid bars) transcriptional fusions. *P. fluorescens* cLP6a(pTZ110- P_{emhA}) and *P. fluorescens* cLP6a(pTZ110- P_{emhR}) cells were grown without treatment (control), with culture supernatants from *P. fluorescens* cLP6a, LP6a-D1, LP6a-8 or LP6a-21-41 grown on TSB with phenanthrene, or with 2 mM salicylate or 2-aminobenzoate. The chemical structures shown above the bars are the major compounds present and are as follows: A, phenanthrene; B, *cis*-3,4-dihydroxy-3,4-dihydrophenanthrene; C, 3,4-dihydroxyphenanthrene; D, *trans*-4-(1'-hydroxynaphth-2'-yl)-2-oxobut-3-enoate; E, salicylate; and F, 2-aminobenzoate. The relative β -galactosidase activities represent the activity in the treated samples relative to the control and are the means \pm standard deviations for three independent experiments.

grown in the presence of tetracycline, chloramphenicol, nalidixic acid or erythromycin. The antibiotic concentrations used were $\frac{1}{4} \times \text{MIC}$, which corresponded to $0.25 \mu\text{g mL}^{-1}$ tetracycline, $4 \mu\text{g mL}^{-1}$ chloramphenicol, $4 \mu\text{g mL}^{-1}$ nalidixic acid and $8 \mu\text{g mL}^{-1}$ erythromycin, to minimize any effects on expression due to growth inhibition. β -galactosidase activities of the *lacZ* reporter were measured for the promoter-reporter strains grown in the presence of antibiotic and compared to the control strains grown in the absence of antibiotic (Figure 3.16). Expression of the *lacZ* reporter from the *emhABC* promoter showed a significant 2.5-fold induction in the presence of tetracycline ($0.005 > P > 0.001$) and a 1.5-fold induction in the presence of chloramphenicol ($0.01 > P > 0.005$). Tetracycline also induced expression from the *emhR* promoter ($0.01 > P > 0.005$), although to a lesser extent (1.4-fold). Chloramphenicol, however, did not significantly induce expression from the *emhR* promoter ($P > 0.2$) at the concentration of $4 \mu\text{g mL}^{-1}$ tested. Neither nalidixic acid nor erythromycin affected expression of the *lacZ* reporter from either the *emhABC* promoter or the *emhR* promoter at the concentrations tested. Thus, the EmhABC efflux system and its regulator are induced by pump substrates, but the induction is selective.

3.3.6. Comparison of the regulation of the EmhABC efflux system with other RND systems

To study the regulation of the *P. fluorescens* EmhABC efflux system, promoter-reporter plasmids were constructed by transcriptional fusion of the intergenic region between the *emhR* and *emhABC* genes to a promoterless *lacZ* gene. Unlike translational fusions, which measure the rates of transcription and translation, expression of the reporter gene from a transcriptional fusion reflects the rate of transcription only (Pessi *et al.* 2001). Thus, the $P_{emhR}::'lacZ$ and $P_{emhA}::'lacZ$ transcriptional fusions constructed in this study were employed to evaluate the *emhR* and *emhABC* promoter strengths and to analyze the effects of hydrophobic compounds on the regulation of the promoters.

Promoter-reporter transcriptional fusions can be introduced into the bacterium either on a replicative plasmid, as was the case in this study, or by integration into the chromosome. Both methods may not provide an accurate representation of the transcriptional rate depending on the site of the fusion (Pessi *et al.* 2001). Plasmid-based

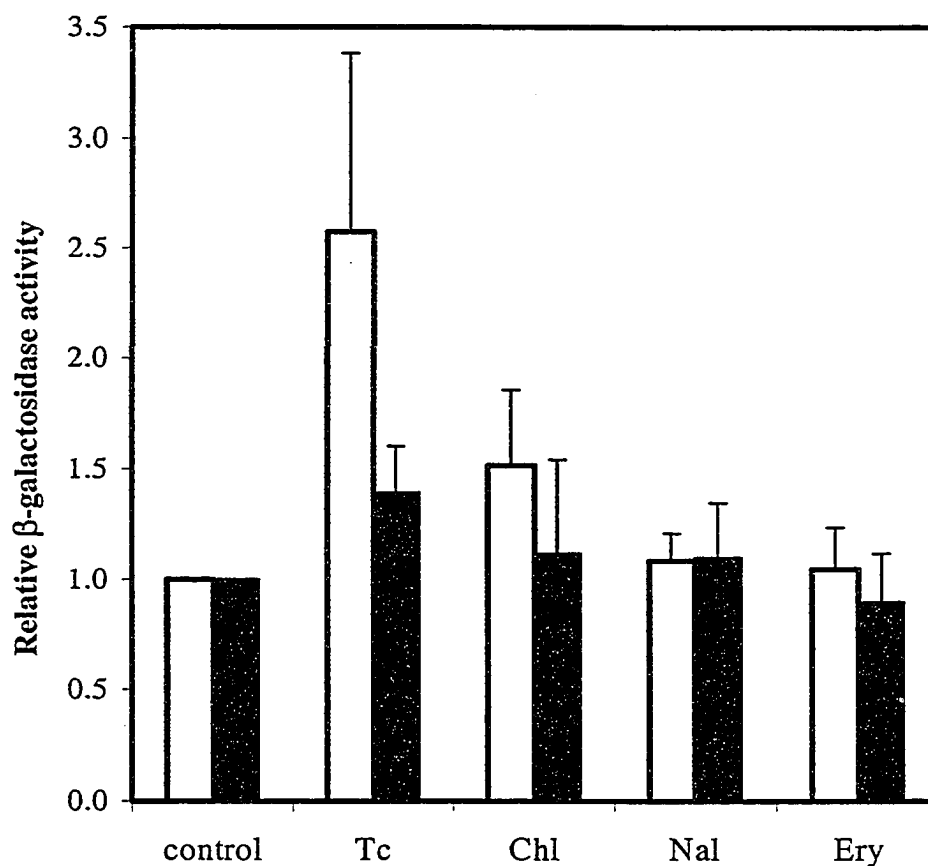


Figure 3.16. Effect of antibiotics on expression of β -galactosidase from the $P_{emhA}::lacZ$ (open bars) and $P_{emhR}::lacZ$ (solid bars) transcriptional fusions. *P. fluorescens* cLP6a(pTZ110- P_{emhA}) and *P. fluorescens* cLP6a(pTZ110- P_{emhR}) cells were grown to an $OD_{600} \sim 2.5$ in TSB in the absence of antibiotic (control) or in the presence of $0.25 \mu\text{g mL}^{-1}$ tetracycline (Tc), $4 \mu\text{g mL}^{-1}$ chloramphenicol (Chl), $4 \mu\text{g mL}^{-1}$ nalidixic acid (Nal), or $8 \mu\text{g mL}^{-1}$ erythromycin (Ery). β -galactosidase activity was measured in permeabilized cells by the method described by Griffith and Wolf (2002). The relative β -galactosidase activity represents the activity in the presence of antibiotic relative to the control (in the absence of antibiotic). The values are the means \pm standard deviations for six independent experiments.

promoter-reporter systems suffer from additional drawbacks, including high background levels and artificially higher levels of transcription due to the presence of the reporter gene on a multi-copy plasmid rather than a single copy on the chromosome (Schweizer 2001). To minimize the problems associated with plasmid-based promoter-reporter systems, the low copy number, broad-host range plasmid pTZ110, which has a low background of β -galactosidase activity (Schweizer and Chuanchuen 2001), was used to construct the *emhR* and *emhABC* transcriptional fusions. The *P. fluorescens* cLP6a strains carrying the promoter-reporter plasmids provided a simple and rapid method for assessing transcriptional levels and were amenable to high through-put screening for analyzing a variety of growth conditions.

The promoter sequences for the *emhABC* and *emhR* genes showed homology to the consensus sequence for the σ^{70} -dependent *E. coli* RNA polymerase. Consistent with the role of the σ^{70} factor in the initiation of transcription during exponential phase, transcription from the *emhABC* and *emhR* promoters increased during exponential phase (Figure 3.13). Studies with the MexAB-OprM efflux system in *P. aeruginosa* (Maseda *et al.* 2004, Sawada *et al.* 2004) suggested that the accumulation of an *N*-acylhomoserine lactone autoinducer was responsible for the increased expression of the efflux pump in exponential phase. A similar global mechanism involving the quorum sensing system may regulate the EmhABC efflux system in *P. fluorescens* cLP6a. Interestingly, the *N*-butyl-L-homoserine lactone autoinducer that was shown to increase MexAB-OprM expression in *P. aeruginosa* (Maseda *et al.* 2004) was not a substrate of the efflux system (Pearson *et al.* 1999). Another autoinducer molecule produced by *P. aeruginosa*, *N*-(3-oxododecanoyl)-L-homoserine lactone, did not affect MexAB-OprM expression (Maseda *et al.* 2004), but was demonstrated to be a substrate of the efflux system (Pearson *et al.* 1999). This example with the MexAB-OprM system illustrates that regulators of the efflux pump expression cannot be predicted based on the pump specificity.

The dichotomy between efflux pump substrates and inducers of the pump was demonstrated further by examination of the roles of EmhABC substrates on the expression of the efflux system in *P. fluorescens* cLP6a. Aromatic hydrocarbons, including phenanthrene, anthracene, fluoranthene, naphthalene and toluene did not affect transcription from the *emhABC* or *emhR* promoters (Figure 3.14). Furthermore,

metabolites of phenanthrene degradation and inducers of the degradation genes did not affect the expression of the EmhABC efflux system or of the EmhR regulator protein (Figure 3.15). These data contrast several reports of the induction of solvent efflux pumps by aromatic hydrocarbons. The SrpABC efflux pump for toluene in *P. putida* S12 was induced by the aromatic solvents toluene, styrene and xylene as well as by aliphatic and aromatic alcohols (Kieboom *et al.* 1998b). Recently, expression of the solvent efflux system TtgGHI in *P. putida* DOT-T1E was shown to be induced two- to four-fold by toluene, xylene, naphthalene and the naphthalene degradation product 2,3-dihydroxynaphthalene (Guazzaroni *et al.* 2005). Guazzaroni *et al.* (2005) demonstrated a direct binding of these compounds to the TtgV repressor protein by using isothermal titration calorimetry. In addition, electrophoretic mobility shift assays showed that binding of the inducers to TtgV released the TtgV protein from the operator region of the DNA, thereby alleviating repression of the TtgGHI efflux system (Guazzaroni *et al.* 2005).

Not surprisingly, expression of the EmhABC efflux system in *P. fluorescens* cLP6a was not affected by the presence of aromatic hydrocarbons, while the solvent efflux systems SrpABC and TtgGHI are induced by solvents, given that the regulators of these efflux systems are quite dissimilar. The EmhR protein showed homology to the TetR family of transcriptional repressors, whereas the SrpS and TtgV proteins, which are the local regulators of the SrpABC and TtgGHI systems, respectively, belong to the IclR family of transcriptional repressors (Wery *et al.* 2001, Rojas *et al.* 2003). Furthermore, both SrpS and TtgV are located in operons with a downstream gene, SrpR or TtgW, encoding a TetR-family transcriptional repressor whose function in the regulation of the solvent efflux system is unknown (Wery *et al.* 2001, Rojas *et al.* 2003). The SrpR and TtgW proteins showed low homology to EmhR (28% protein sequence identity), particularly in the C-terminal ligand-binding domain (18% protein sequence identity; Table 3.5), and these proteins likely recognize different effectors. Therefore, the regulation of the solvent efflux systems SrpABC and TtgGHI in *P. putida* S12 and *P. putida* DOT-T1E is distinct from that of the EmhABC efflux system in *P. fluorescens* cLP6a. The induction of the SrpABC and TtgGHI by toluene could explain the enhanced toluene tolerance of *P. putida* S12 and DOT-T1E compared to *P. fluorescens* cLP6a.

Although aromatic hydrocarbons did not affect expression of the EmhABC efflux system, the hydrophobic antibiotics tetracycline and chloramphenicol were shown to induce gene expression from the *emhABC* promoter (Figure 3.16). Terán et al. (2003) also showed that tetracycline and chloramphenicol induced expression of the *P. putida* DOT-T1E TtgABC efflux system by two- to four-fold. The induction of the TtgABC system by chloramphenicol and tetracycline was shown to involve the direct binding of these antibiotics to the TtgR transcriptional repressor (Terán *et al.* 2003), which shows high homology to the EmhR protein (Table 3.5). Nalidixic acid and carbenicillin, which are also substrates of the TtgABC efflux system, did not induce the efflux pump (Terán *et al.* 2003), nor did nalidixic acid and erythromycin induce the EmhABC efflux system (Figure 3.16). Like RND efflux pumps, the repressor proteins are capable of recognizing and binding structurally dissimilar hydrophobic compounds. However, the substrate specificity of the repressor protein appears to be more selective than that of the efflux system, and there does not appear to be a clear relationship between the substrate specificities of the efflux pump and its local regulator. The regulator's specificity may provide a better indication of the physiological role of the efflux system.

The promoter-reporter system employed to study the regulation of the EmhABC efflux system can be adapted easily for high through-put screening of potential inducer compounds. However, the search for additional inducers of the EmhABC efflux system is not promising due to the inability to predict which compounds might induce the efflux system. Furthermore, identifying inducers of the efflux system in *P. fluorescens* cLP6a may be insignificant since the constitutive level of expression appears to be sufficient for polycyclic aromatic hydrocarbon transport (Figure 3.7), for antibiotic resistance (Table 3.2) and for maintaining viability in the presence of toluene (Table 3.3). It would be of interest, however, to explore further the relationship between the level of efflux pump expression and solvent tolerance. For example, it would be useful to evaluate the toluene tolerance of *P. fluorescens* cLP6a-1 expressing the EmhABC or the SrpABC efflux systems under control of the *emhABC* promoter, such that equivalent levels of pump expression could be compared. Such studies would address the question of whether the toluene sensitivity of *P. fluorescens* cLP6a is due to a lower level of EmhABC expression or to a lower affinity of the EmhABC efflux system for toluene compared to SrpABC.

Future work to investigate the structure of the repressor protein and its ligand-binding domain may be valuable to understand how these proteins have adapted to bind structurally diverse, hydrophobic compounds. Structural studies with transcriptional regulators of multidrug efflux systems in *B. subtilis* and *S. aureus* have identified hydrophobic substrate-binding pockets capable of accommodating diverse substrates (Zheleznova *et al.* 1999, Schumacher *et al.* 2004). Similar studies with the EmhR protein as well as with the TtgV protein, which has a broader substrate specificity for aromatic hydrocarbons (Guazzaroni *et al.* 2005), may provide a better understanding of how hydrophobic compounds interact with the repressor proteins and may provide insight into the interactions between hydrophobic compounds and the RND efflux pump.

3.4. Evidence for a substrate translocation pathway in EmhB³

The recent crystallization of an RND efflux pump, the AcrB protein from *E. coli*, by Murakami *et al.* (2002) was a major advancement in the field of multidrug efflux pumps. The structure of the AcrB trimer provided insights into the possible roles of the various protein domains in intermolecular interactions with the periplasmic and outer membrane proteins and in substrate recognition and translocation. Yet, more detailed structure-function analyses are required to identify the path taken by substrates through the pump and to understand the structural basis for the substrate selectivity of these efflux systems. One approach that can be employed to study structure-function relationships is mutagenesis, and this strategy was applied to the EmhB protein from *P. fluorescens* cLP6a to fulfill the fourth objective of this thesis.

In this section, the rationale used to design the site-directed mutations in EmhB is discussed along with the results of the mutagenesis studies and their implications. The data were used to develop a model describing the mechanism of substrate binding and translocation in RND efflux pumps. The results from other studies with RND efflux pumps are discussed in the context of the proposed model.

³ Portions of this section have been submitted for publication.

3.4.1. Homology modeling of the EmhB efflux pump

The three-dimensional structure of the EmhB efflux protein was predicted by homology modeling with the known crystal structure of the *E. coli* RND efflux pump AcrB (PDB entry 1IWG, Murakami *et al.* 2002) using the SWISS-MODEL protein structure homology-modeling server (Guex and Peitsch 1997). Because EmhB and AcrB share 67% protein sequence identity (Table 3.1), homology modeling of the EmhB protein sequence onto the AcrB crystal structure provided a reliable estimation of the EmhB structure. Like other RND proteins, the EmhB monomeric subunit, shown in Figure 3.17, is predicted to have 12 α -helical transmembrane segments (TMS) and a large periplasmic domain formed by the loops between TMS1 and 2 and TMS7 and 8.

The functional RND efflux pump has been shown to be a trimer (Murakami *et al.* 2002), and the trimeric form of EmhB was modeled (Figure 3.18). By comparison to the published structure of AcrB (Murakami *et al.* 2002), three domains were identified in the EmhB trimer: the transmembrane domain, which is comprised of the 12 TMS from each monomer; the pore domain, which is located in the periplasm and is a mixture of β -strands and α -helices; and the putative outer membrane channel docking domain, which is a mixed β -sheet structure located at the top of the trimer. The transmembrane domain anchors the protein in the inner membrane and has been implicated in proton translocation (Guan and Nakae 2001, Aires *et al.* 2002). A cavity that has been implicated in substrate binding in AcrB (Yu *et al.* 2003) is evident between the transmembrane domain and the pore domain in the center of the molecule. When viewed from a perspective perpendicular to the plane of the membrane, a pore is observed through the center of the trimer (Figure 3.18A). Three α -helices (one contributed by each monomer) are visible in the center of the pore and are located in the periplasmic pore domain. This pore connects the central cavity to the outer membrane protein docking domain.

Murakami *et al.* (2002) proposed a model in which substrates pass through channels in the periplasmic pore domain to reach the central cavity and are then pumped through the pore to the outer membrane protein. The exact details of the substrate translocation pathway through the RND efflux pump, however, have not been determined. Mutations were introduced into the central cavity, the central pore, the

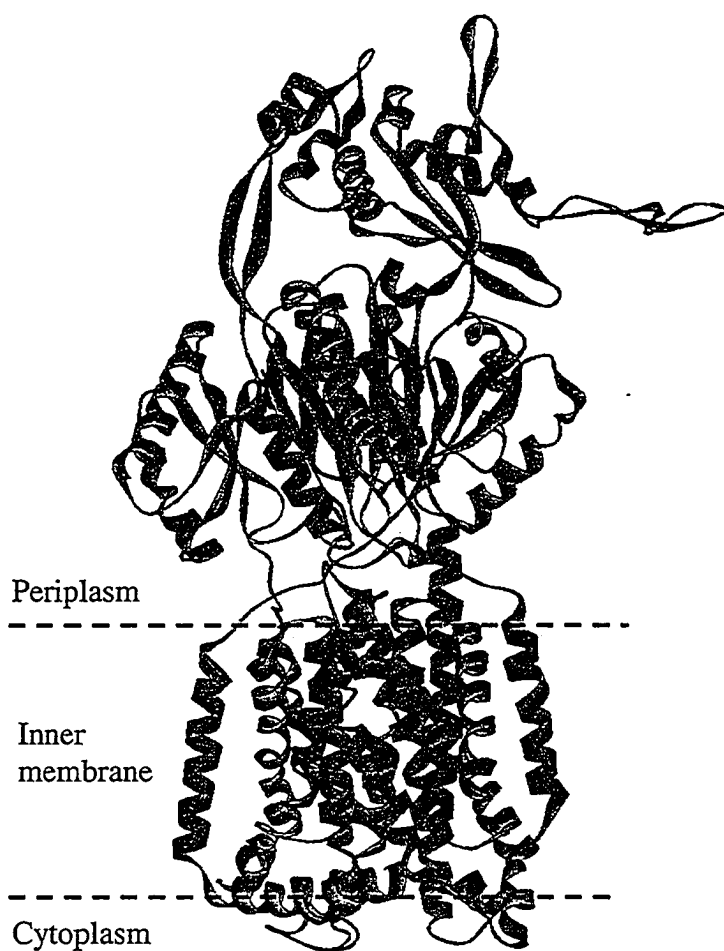


Figure 3.17. Homology model of the EmhB monomer. The EmhB pump was modeled using the known crystal structure of the *E. coli* AcrB pump (PDB entry 1IWG; Murakami *et al.* 2002). The putative boundary of the inner membrane is indicated by the dashed lines. This figure and all subsequent protein models were drawn using the DS ViewerPro version 6.0 software (Accelrys).

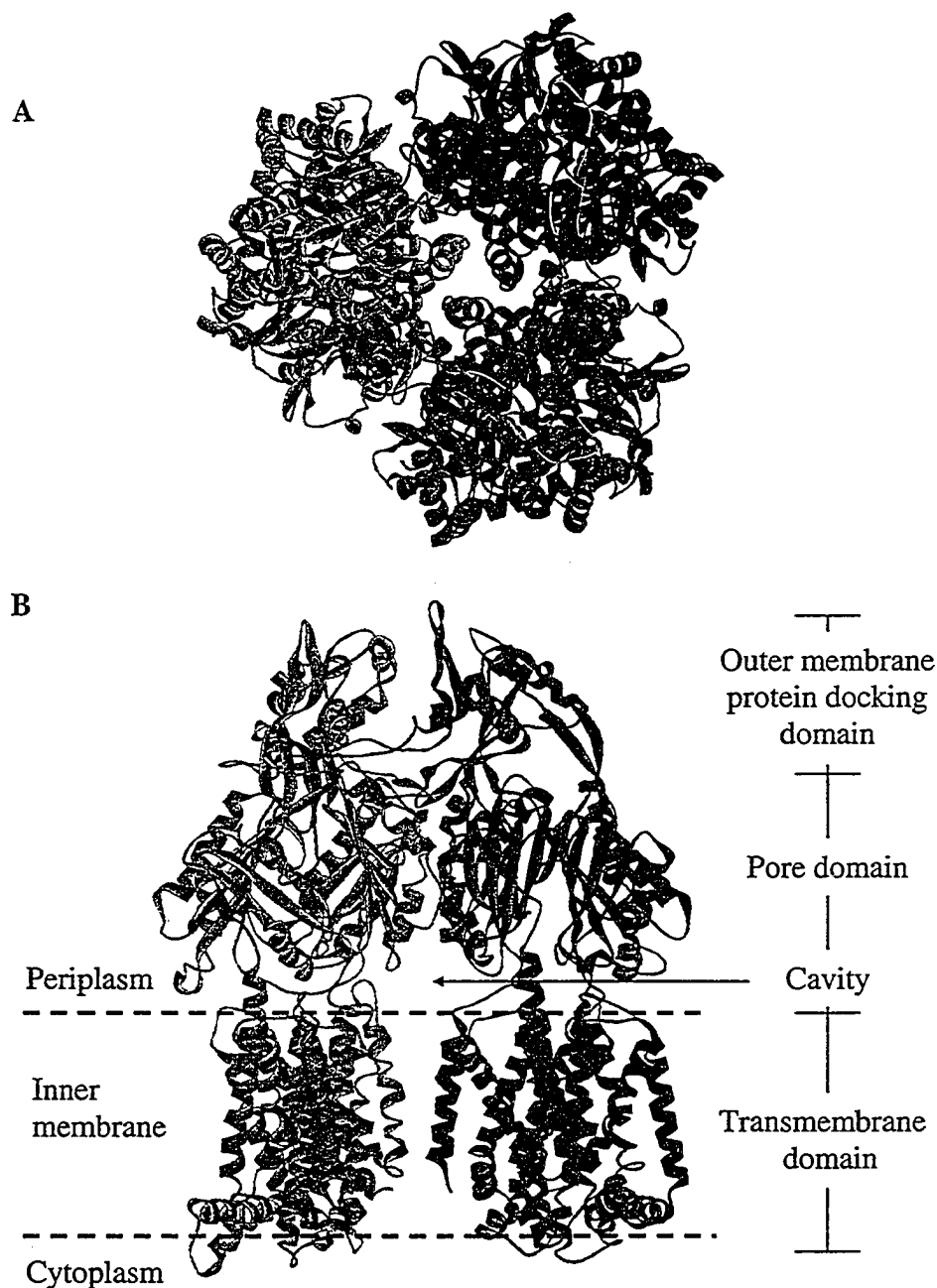


Figure 3.18. Homology model of the EmhB trimer. The EmhB pump was modeled using the known crystal structure of the *E. coli* pump AcrB (PDB entry 1IWG, Murakami *et al.* 2002). (A) The view of the predicted EmhB trimer from above the plane of the inner membrane shows the presence of a pore extending through the pump. (B) The transmembrane domain, pore domain and outer membrane protein docking domain are indicated on the side view of the EmhB trimer, with the rear monomer removed to facilitate viewing. A central cavity is evident at the center of the pump above the transmembrane domain.

periplasmic pore domain and the outer membrane protein docking domain of the *P. fluorescens* EmhB efflux pump to elucidate the roles of these domains on efflux activity. Data from the crystal structure of the *E. coli* AcrB pump with and without bound substrates (Yu *et al.* 2003a, Murakami *et al.* 2002) were considered in the construction of several mutations. In addition to the structural analyses, sequence alignments of the homologous antibiotic and solvent efflux pumps, including ArpB and SrpB from *P. putida* S12, TtgB, TtgE and TtgH from *P. putida* DOT-T1E, MexB from *P. aeruginosa* PA01, and AcrB from *E. coli*, aided in the design of the mutations.

3.4.2. Construction of site-directed mutants in EmhB_{his}

Twenty-two mutations were constructed in the histidine-tagged EmhB_{his} protein by using site-directed mutagenesis. The mutations were confirmed by DNA sequencing and were as follows: nine single mutations (A384P, A385Y, F386A, F458A, F459A, N99A, D101A, D101N and D101E) and one double mutation (A384P/A385Y) were introduced in the central cavity region; three mutations (Q104A, N112A, K131A) were introduced in the central pore; and eight mutations (Y157A, F316A, F317A, F682A, F281A, F325A, N282A and S608A) were constructed in the periplasmic pore domain (excluding the pore-forming helix). One mutation (A206S) in the outer membrane protein docking domain of EmhB_{his} was obtained by a PCR-introduced error. The mutations were constructed in a histidine-tagged EmhB_{his} to facilitate analysis of their expression in the *emhB* disruption mutant *P. fluorescens* cLP6a-1. The mutated *emhB_{his}* genes were introduced with the *emhA* and *emhC* genes on the complementation plasmid pBH5 into *P. fluorescens* cLP6a-1.

Western immunoblotting using an antibody specific for the histidine tag was performed on the membrane fractions obtained from the *P. fluorescens* cLP6a-1 strains carrying the mutated *emhB_{his}* genes to assess the expression levels of the mutated pump proteins (Figure 3.19). EmhB_{his} migrated on the SDS-PAGE gel with an estimated molecular weight of 105 kDa, which is comparable to the size predicted by the amino acid sequence and to the size of the MexB efflux pump (Middlemiss and Poole 2004). Two mutant proteins, A385Y in the central cavity (Figure 3.19) and Q104A (data not shown) in the central pore, were not expressed in *P. fluorescens* cLP6a-1. Expression of

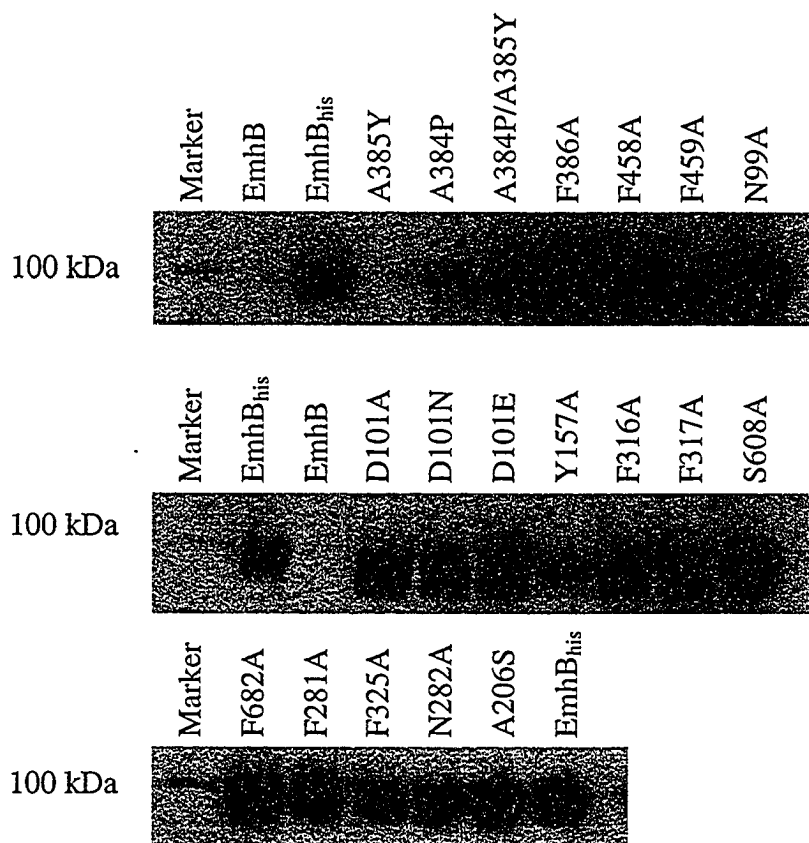


Figure 3.19. Expression of mutant EmhB_{his} proteins in *P. fluorescens* cLP6a-1. *P. fluorescens* cLP6a-1 cells were harvested, and samples containing 10 µg of protein were separated by SDS-PAGE using a 6% resolving gel. The SDS-PAGE gels were subjected to western immunoblotting using an anti-His antibody. The size of the molecular weight marker in kDa is indicated.

the Y157A mutant pump was significantly lower than that of the control EmhB_{his}, while all other mutant pumps were expressed at levels comparable to EmhB_{his} (Figure 3.19). The N112A and K131A mutants are not shown in Figure 3.19, but their expression was comparable to that of EmhB_{his}.

3.4.3. The histidine-tagged EmhB_{his} is functional in *P. fluorescens* cLP6a-1

Before analyzing the activity of the mutant proteins, the activity of the histidine-tagged EmhB_{his} pump was compared with the wild-type EmhB in *P. fluorescens* cLP6a-1 to ensure that the histidine tag did not affect efflux pump function (Table 3.6). In Table 3.6, the ability to transport the polycyclic aromatic hydrocarbons phenanthrene and anthracene is reported as the ratio of the amounts of hydrocarbon accumulated in the cells prior to (uninhibited) and after (inhibited) addition of the energy inhibitor azide. Previous data (Figure 3.7) indicated that cells possessing an active efflux system for polycyclic aromatic hydrocarbons accumulated approximately two-fold less hydrocarbon in the absence of azide than in the presence of the inhibitor and, thus, have a ratio of uninhibited/inhibited of about 0.5. In contrast, cells that do not have an active efflux system for hydrocarbons showed no change in the cellular accumulation of hydrocarbon in the absence or presence of azide and, thus, have a ratio of uninhibited/inhibited of 1. As expected, the strains expressing both EmhB and EmhB_{his} showed active efflux of phenanthrene and anthracene, while the negative control, which did not express EmhB, did not (Table 3.6).

The ability of EmhB and EmhB_{his} to pump antibiotics was also compared by measuring MICs for a suite of antibiotics. As shown previously (Table 3.2), chloramphenicol, nalidixic acid, rhodamine 6G, dequalinium, ciprofloxacin and erythromycin are substrates of the EmhABC efflux system. Although the MICs for chloramphenicol and nalidixic acid were lower for the *P. fluorescens* cLP6a-1 strain expressing EmhB_{his} compared to the wild-type EmhB, the MICs were still significantly higher than the negative control (Table 3.6). The MICs for rhodamine 6G, dequalinium, ciprofloxacin and erythromycin were comparable for the strains expressing the EmhB_{his} and EmhB pumps (Table 3.6). Streptomycin was not a substrate of either the EmhB efflux pump, as previously demonstrated (Table 3.2), or the EmhB_{his} efflux pump

Table 3.6. Effect of mutations on the function of the efflux protein EmhB for polycyclic aromatic hydrocarbon transport, toluene tolerance and antibiotic sensitivity

Mutation ^a	Hydrocarbon transport (Ratio of uninhibited/inhibited) ^b		Antibiotic sensitivity (MIC, $\mu\text{g mL}^{-1}$) ^c							Toluene tolerance ^d	
	Phenanthrene	Anthracene	Chl	Nal	R6G	Dq	Cip	Ery	Str	Growth	Survival
EmhB _{his}	0.53 ± 0.07 (9)	0.48 ± 0.13 (6)	8	32	128	8	0.031	16	2	–	+
EmhB	0.56 ± 0.08 (3)	0.56 ± 0.07 (3)	32	128	>128	8	0.063	16	1	+	NA
Negative control	1.06 ± 0.05 (9)	0.90 ± 0.11 (6)	0.5	1	8	1	0.004	4	1	–	–
Central cavity											
Lower boundary											
A384P	0.60	0.59	8	16	32	2	0.016	8	1	–	+
A384P/A385Y	0.61	0.67	4	16	32	2	0.016	8	2	–	+
F386A	0.52	0.50	8	32	>128	2	0.016	16	1	–	+
F458A	0.55	0.56	8	16	64	4	0.016	8	1	–	+
F459A	0.60	0.56	8	16	64	4	0.016	8	1	–	+
Upper boundary											
N99A	0.53	0.49	4	32	64	2	0.031	16	1	–	+
D101A	0.84	0.96	1	16	16	1	0.016	4	2	–	+
D101N	0.80	0.70	2	16	32	2	0.016	8	1	–	+
D101E	0.50	0.47	8	32	>128	4	0.016	16	4	–	+
Central pore											
N112A	0.52	0.46	8	32	>128	4	0.031	8	1	–	+
K131A	0.47	0.41	16	16	>128	8	0.031	16	2	–	+

Table 3.6. Continued

Mutation ^a	Hydrocarbon transport (Ratio of uninhibited/inhibited) ^b		Antibiotic sensitivity (MIC, $\mu\text{g mL}^{-1}$) ^c						Toluene tolerance ^d		
	Phenanthrene	Anthracene	Chl	Nal	R6G	Dq	Cip	Ery	Str	Growth	Survival
Periplasmic pore domain											
Vestibule											
Y157A	0.62	0.58	4	16	16	4	0.008	8	4	-	-
F316A	0.52	0.50	16	32	32	4	0.008	8	1	-	+
F317A	0.46	0.48	4	16	64	4	0.016	8	2	-	+
Substrate pathway											
F682A	0.46	0.44	8	32	>128	4	0.008	16	2	-	+
F281A	0.90	0.83	<0.5	8	32	2	0.016	8	4	-	-
F325A	0.88	0.76	2	8	16	2	0.016	8	2	-	-
N282A	0.71	0.74	1	8	32	2	0.016	4	4	-	+
S608A	0.61	0.55	8	16	64	4	0.016	16	1	-	+
Outer membrane protein docking domain											
A206S	0.48	0.53	32	128	>128	16	0.125	64	2	+	NA

^a Mutations were introduced into the gene encoding EmhB_{his} protein by site-directed mutagenesis as described in Materials and Methods. The mutated *emhB* genes, along with the *emhA* and *emhC* genes, were introduced into the efflux-deficient mutant *P. fluorescens* cLP6a-1 on the broad-host range plasmid pUCP26. The negative control was *P. fluorescens* cLP6a-1 carrying the vector (pUCP26) only.

- ^b Polycyclic aromatic hydrocarbon transport was measured using the rapid centrifugation method as described in Materials and Methods. The fractional amount of radiolabeled phenanthrene or anthracene was determined in uninhibited cells and in cells inhibited with 30 mM azide. Values represent the ratio of the fractional amounts of hydrocarbon in the uninhibited and inhibited cells. For the strains expressing the EmhB_{his} and EmhB proteins and for the negative control strain, the number in parentheses indicates the number of independent experiments performed. All other transport data are the averages of duplicate samples taken from single experiments.
- ^c MICs were determined using the microtiter broth dilution method as described in Materials and Methods. Two independent experiments were done, and representative data are shown. Abbreviations: Chl, chloramphenicol; Nal, nalidixic acid; R6G, rhodamine 6G; Dq, dequalinium chloride; Cip, ciprofloxacin; Ery, erythromycin; and Str, streptomycin.
- ^d Toluene tolerance was assessed by monitoring growth on agar plates in the presence of vapour-phase toluene as described in the Materials and Methods. Growth in the presence of toluene was scored as + (positive for growth) or – (negative for growth). After four days of incubation in the presence of toluene, the plates were removed and further incubated for four days in the absence of toluene to assess the ability of the strains to survive toluene exposure. Survival was scored as + (growth upon removal of toluene), – (no growth upon removal of toluene) or NA (not applicable, as these strains were able to grow in the presence of toluene). Two independent experiments were done.

(Table 3.6). Thus the presence of the histidine tag did not alter the specificity of the efflux pump for the antibiotics tested.

Toluene tolerance was also assessed for *P. fluorescens* cLP6a-1 expressing EmhB_{his}. Unlike the strain expressing EmhB, *P. fluorescens* cLP6a-1 expressing EmhB_{his} was unable to grow in the presence of toluene vapours, although it did recover upon removal of the toluene (Table 3.6) similar to *P. fluorescens* cLP6a (Table 3.3). The difference in toluene tolerance, as well as in the antibiotic resistance levels, between EmhB and EmhB_{his} may be the result of a lower level of expression of EmhB_{his} due to the presence of the histidine tag compared to the wild-type EmhB. Alternatively, insertion of the codons for the histidine tag may have had a downstream polar effect on transcription of the *emhC* gene encoding the outer membrane protein, which may have resulted in the expression of fewer functional efflux pump complexes. This latter possibility is likely given the overlap between the start and stop codons of the *emhC* and *emhB* genes (Figure 3.20). Nevertheless, the ability of the strain expressing EmhB_{his} to grow upon removal of the toluene vapours indicated that the histidine-tagged pump was functional for toluene efflux.

Despite the minor differences in efflux activity for antibiotics and toluene, the histidine-tagged EmhB_{his} was shown to be functional for the efflux of polycyclic aromatic hydrocarbons, hydrophobic antibiotics and toluene. In the subsequent sections, the activity of the mutant pumps for polycyclic aromatic hydrocarbons, antibiotics and toluene was compared relative to the activity of EmhB_{his} (Table 3.6). It should be noted that, although the phenanthrene and anthracene transport experiments were performed only once for each mutant, the data for the two hydrocarbons correspond and serve as pseudo-replicates.

3.4.4. The central cavity provides a flexible binding pocket for substrates during transport

The three-dimensional structure of the *E. coli* AcrB efflux pump identified a cavity between the transmembrane domain and the periplasmic domain (Murakami *et al.* 2002), and co-crystallization of AcrB with bound drugs demonstrated the importance of this region in substrate binding (Yu *et al.* 2003a). Accordingly, the central cavity area of

the EmhB pump in *P. fluorescens* cLP6a was investigated by site-directed mutagenesis to determine its role in aromatic hydrocarbon and antibiotic efflux.

A closer view of the central cavity region of the EmhB model is given in Figure 3.21. The cavity is bounded on the bottom (closest to the inner membrane) by residues A384, A385, F386, F458 and F459, which are located at the periplasmic ends of TMS3 and TMS5, and on the top (farthest from the inner membrane) by residues N99 and D101 from the N-terminal ends of the pore-forming helices. Comparison of the protein sequence of EmhB with its closest homologues from Figure 3.6 revealed that F458, F459 and D101 are highly conserved, while A384, A385, F386 and N99 are less well-conserved (Table 3.7). Mutations in EmhB_{his} were designed to target these residues lining the central cavity.

Crystallization studies of the *E. coli* AcrB pump with bound ligands showed that the A385, F386, F458 and F459 residues are involved in the binding of ciprofloxacin, rhodamine 6G and dequalinium (Yu *et al.* 2003a). Hence, these residues were chosen for site-directed mutagenesis in EmhB_{his}. The phenylalanines were mutated to alanines, while A385 was mutated to tyrosine to correspond with the SrpB, TtgH and TtgE sequences. Because the A385Y mutant protein was not expressed in *P. fluorescens* cLP6a-1 (Figure 3.19), a double mutant, A384P/A385Y, and an additional single mutant, A384P, were constructed. Likely, the EmhB protein could not accommodate introduction of the large, aromatic side chain in the A385Y single mutation; however, simultaneous mutation of the adjacent A384 residue to proline enabled the A385Y substitution to be accommodated.

The five mutations targeted to the lower boundary of the central cavity region, A384P, A384P/A385Y, F386A, F458A and F459A, did not affect polycyclic aromatic hydrocarbon transport or toluene tolerance (Table 3.6). Variations in antibiotic sensitivity for some substrates, however, were observed (Table 3.6). Not surprisingly, significant four-fold changes in MICs for rhodamine 6G and dequalinium were observed for the A384P, A384P/A385Y, F386A, F458A and F459A mutations in the central cavity of EmhB_{his} (Table 3.6), as expected from the structural studies with AcrB (Yu *et al.* 2003a).

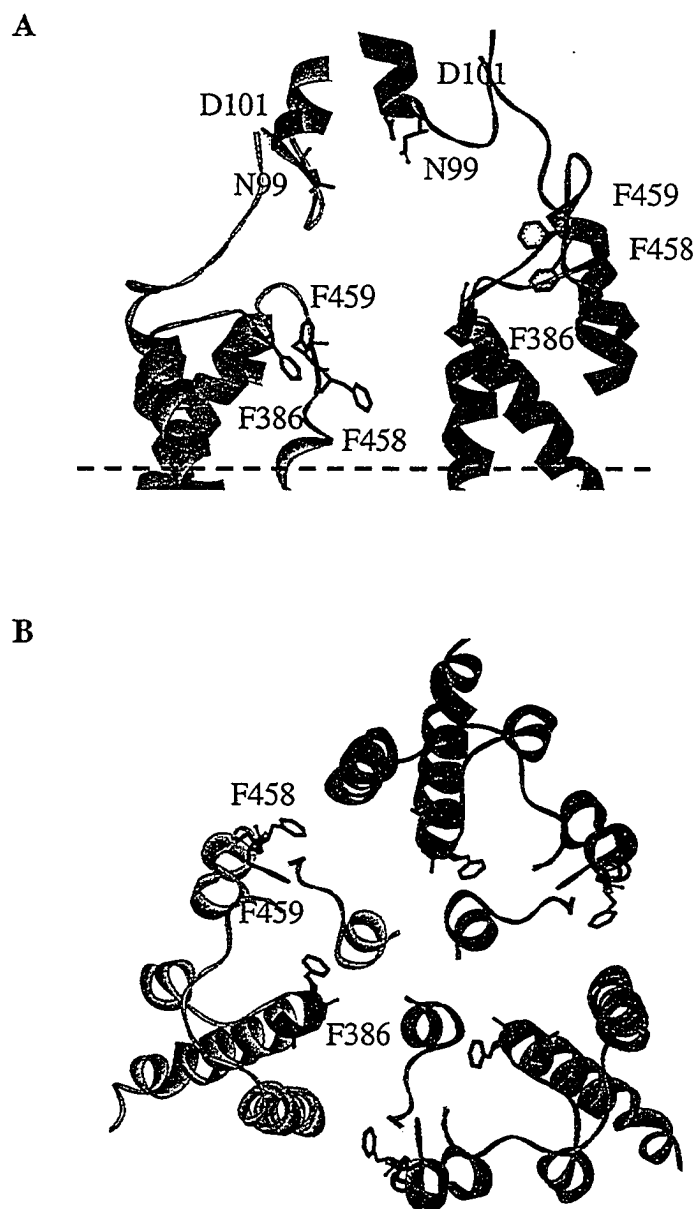


Figure 3.21. Predicted model of the central cavity in EmhB. (A) A side view of the central cavity, with the front monomer removed, shows the positions of the N99, D101, F386, F458 and F459 residues. The A384 and A385 residues adjacent to F386 are not shown for ease of viewing. (B) The top view of the central cavity shows a ring formed by the aromatic side chains of residues F386, F458 and F459.

Table 3.7. Conservation of amino acids in the central cavity among RND multidrug and solvent efflux pumps^a

Efflux pump ^c	Mutated residue in EmhB ^b						
	Lower boundary					Upper boundary	
	A384	A385	F386	F458	F459	N99	D101
ArpB	A	A	A	F	F	N	D
TtgB	A	A	A	F	F	N	D
MexB	A	A	F	F	F	D	D
SrpB	P	Y	F	F	F	D	D
TtgH	P	Y	F	F	F	D	D
TtgE	P	Y	F	F	F	N	D
AcrB	A	A	F	F	F	D	D
MexD	Y	L	L	F	M	D	D
MexY	L	G	L	F	F	N	D

^a Protein sequences were aligned by using ClustalX (Thompson *et al.* 1997).

^b Residues that are identical to the EmhB sequence are indicated in boldface type.

^c The efflux pumps compared to EmhB were ArpB (accession number AAF73832) and SrpB (AAD12176) from *P. putida* S12, TtgB (AAC38671), TtgH (AAK69564) and TtgE (CAB72259) from *P. putida* DOT-T1E, MexB (NP_249117), MexD (NP_253288) and MexY (NP_250708) from *P. aeruginosa*, and AcrB (NP_414995) from *E. coli*.

The crystal structure of the *E. coli* AcrB efflux pump with rhodamine 6G bound in the central cavity identified substrate interactions with A385, F386, L25, K29 and V382 (Yu *et al.* 2003a). With the exception of lysine at position 29, these amino acids have hydrophobic side chains, and van der Waals and hydrophobic interactions were predicted to stabilize the binding of rhodamine 6G (Yu *et al.* 2003a). Investigation of homologous residues in EmhB_{his} corroborated the involvement of A385, and its neighbour A384, in the rhodamine 6G binding site. Both the A384P and A384P/A385Y EmhB_{his} mutants showed four-fold reductions in rhodamine 6G resistance (Table 3.6) when expressed in *P. fluorescens* cLP6a-1, indicating that these mutations affected the ability of the pump to transport the substrate. Introduction of the bulkier proline and tyrosine side chains would cause localized disruption of the central cavity structure (Figure 3.21) making the rhodamine 6G binding unfavourable. In the *E. coli* AcrB protein, Yu *et al.* (2003a) showed that the aromatic side chain of F386 is adjacent to the alkyl tail of rhodamine 6G (Figure 3.9); however, mutation of the corresponding residue in EmhB_{his} did not decrease resistance to this substrate (Table 3.6). The F386A mutation may have enhanced the ability of EmhB_{his} to pump rhodamine 6G, because the MIC for *P. fluorescens* cLP6a-1 expressing this mutated pump was greater than that for the non-mutated EmhB_{his} pump. Although the MIC data do not conclusively indicate a significant increase in rhodamine 6G resistance in the F386A mutant, it is possible that removal of the aromatic side chain created a ligand-binding domain that better accommodated the alkyl group on rhodamine 6G, thereby improving the activity of EmhB_{his} for this substrate.

The F386A mutation in EmhB_{his} decreased the resistance of *P. fluorescens* cLP6a-1 expressing the mutant pump to dequalinium (Table 3.6). The X-ray crystal structure of the *E. coli* AcrB pump with bound dequalinium (Yu *et al.* 2003a) revealed an interaction, likely hydrophobic, between the aromatic side chain of F386 and the quinolinium group at one end of the dequalinium molecule (Figure 3.9). Thus, the experimental evidence presented here supports the role of F386 in dequalinium binding.

Ciprofloxacin was also shown to interact with amino acids in the lower part of the central cavity in the AcrB crystal structure (Yu *et al.* 2003a). The crystal structure of AcrB with bound ciprofloxacin showed the drug in proximity to A385, F458, F459, L25

and K29 (Yu *et al.* 2003). However, the ciprofloxacin MICs for the A384P, A384P/A385Y, F458A and F459A mutations in EmhB_{his} were comparable to those observed when the normal EmhB_{his} protein was expressed in *P. fluorescens* cLP6a-1 (Table 3.6). Surprisingly, the F458A and F459A mutations did not compromise ciprofloxacin resistance, although the phenylalanine side chains were shown to interact with the cyclopropyl group of ciprofloxacin (Figure 3.9) in the *E. coli* AcrB structure (Yu *et al.* 2003a). The failure to observe a significant change in ciprofloxacin resistance for the F458A and F459A single mutations suggests that mutation of only one of the phenylalanines was not sufficient to disrupt the binding of ciprofloxacin, and the unchanged phenylalanine was able to maintain ciprofloxacin binding. Likely, both phenylalanines need to be disrupted simultaneously to observe an effect on ciprofloxacin resistance.

The ligand-bound crystal structures of the *E. coli* AcrB efflux pump determined by Yu *et al.* (2003a) showed the binding of rhodamine 6G, dequalinium and ciprofloxacin to amino acids lining the bottom of the central cavity. The site-directed mutagenesis data with the *P. fluorescens* cLP6a EmhB_{his} efflux pump presented here demonstrated the involvement of these residues for pump activity towards rhodamine 6G and dequalinium. Other substrates of the EmhABC efflux system, including polycyclic aromatic hydrocarbons, toluene and the antibiotics chloramphenicol, nalidixic acid and erythromycin were not affected by mutations in the lower part of the central cavity (Table 3.6). Possibly, these substrates also interact with the amino acids lining the bottom of the central cavity. As suggested for the failure to observe changes in ciprofloxacin resistance in the F458A and F459A mutants, mutation of single residues may not be sufficient to disrupt substrate-binding for polycyclic aromatic hydrocarbons, toluene, chloramphenicol, nalidixic acid and erythromycin. Consequently, efflux activity for these substrates was comparable in the mutated pumps and the EmhB_{his} control (Table 3.6). Site-directed mutagenesis of the residues lining the upper boundary of the central cavity, however, revealed the importance of two amino acids, an asparagine at position 99 and an aspartate at position 101 in EmhB, on the activity of the efflux pump.

Both the N99A and D101A mutations in EmhB_{his} affected dequalinium resistance in *P. fluorescens* cLP6a-1 expressing the mutant proteins (Table 3.6). Yu *et al.* (2003a)

previously demonstrated that dequalinium bridges the lower and upper regions of the central cavity in AcrB and interacts with the residues at positions 99 and 101. In AcrB, the residue at position 99 is an aspartate, which has a negatively charged carboxylic acid side chain, whereas the corresponding residue in EmhB is an asparagine, which has an amino group (Table 3.7). From the crystal structure of AcrB (Yu *et al.* 2003a), it appears that the aspartate side chain points away from the dequalinium molecule. Therefore, the aliphatic chain, rather than the charged functional group, on the amino acid at position 99 must be important for stabilizing dequalinium binding in both AcrB and EmhB_{his}. The carboxylic acid group of D101 is adjacent to the quinolinium moiety of dequalinium in the crystal structure of AcrB (Yu *et al.* 2003a), and, as expected, the D101A mutation in EmhB_{his} diminished antibiotic resistance for dequalinium in *P. fluorescens* cLP6a-1.

Compared to position 99, the aspartate residue at position 101 is highly conserved in RND efflux pumps (Table 3.7). The D101 residue is located at the N-terminal end of the central pore, which extends into the periplasmic domain, and, thus bounds both the central cavity and pore. In addition to its effect on dequalinium resistance, the D101A mutation in EmhB_{his} resulted in significant (more than four-fold) decreases in antibiotic resistance for chloramphenicol, rhodamine 6G, ciprofloxacin and erythromycin, a two-fold decrease in nalidixic acid resistance, and greatly reduced the ability of the efflux pump to transport the polycyclic aromatic hydrocarbons phenanthrene and anthracene (Table 3.6). Mutation of D101 to asparagine also inhibited the function of the EmhB_{his} efflux pump for these substrates. However, conservation of the carboxyl group on the amino acid side chain by mutation to glutamate (D101E) restored function of the efflux pump. Cysteine-scanning mutagenesis studies with the AcrB pump in *E. coli* also demonstrated the importance of D101 in antibiotic resistance for chloramphenicol, nalidixic acid and erythromycin as well as for tetracycline and acriflavin (Murakami *et al.* 2004). Neither the rhodamine 6G nor the ciprofloxacin binding sites were shown to involve the D101 residue (Yu *et al.* 2003a); yet, mutation of D101 in EmhB_{his} to alanine or asparagine compromised efflux activity for these antibiotics, as well as for all other EmhB substrates except toluene. The results of the mutations at position D101 suggest that the carboxyl side chain may be involved in stabilizing protein-protein interactions between the pump subunits or may play a role in the opening of the central pore.

The crystal structure of the *E. coli* AcrB efflux pump with bound ligands (Yu *et al.* 2003a) combined with the cysteine-scanning mutagenesis data of the AcrB pump (Murakami *et al.* 2004) and the site-directed mutagenesis data presented here for the *P. fluorescens* cLP6a-1 EmhB efflux pump demonstrate the importance of the central cavity region of RND efflux pumps in the binding of structurally diverse substrates and in efflux activity. The central cavity appears to be a common residence for substrates during the translocation process. Because of its size and the generally nonspecific hydrophobic interactions with ligands, the central cavity is able to accommodate the structurally diverse substrates transported by these efflux pumps. Although mutations in the EmhB central cavity altered the substrate specificity of the efflux pump, substrate selectivity likely is not dictated solely by the central cavity. Substrates must interact with other areas of the protein prior to reaching the central cavity, and these other interactions likely influence substrate selectivity.

3.4.5. The periplasmic pore domain

RND efflux pumps have a large periplasmic domain, which is distinct from other families of multidrug transporters. Other studies have implicated the periplasmic domain in substrate recognition and specificity, as well as in the interaction between the efflux pump and the membrane fusion protein (Elkins and Nikaido 2002, Tikhonova *et al.* 2002, Mao *et al.* 2002, Eda *et al.* 2003). The crystal structure of the *E. coli* AcrB efflux pump (Murakami *et al.* 2002) and the EmhB model (Figure 3.18) showed two distinct periplasmic domains, which were classified as the pore domain and the outer membrane protein docking domain. Based on the structure of AcrB, Murakami *et al.* (2002) predicted that efflux pump substrates likely passed through the pore domain to reach the central cavity. Thus, the pore domain of EmhB was investigated by site-directed mutagenesis to investigate its role in substrate translocation and selectivity.

Figure 3.22 shows the predicted model for the pore domain of EmhB based on the AcrB crystal structure. Murakami *et al.* (2002) identified three main regions within the AcrB pore domain located above the central cavity: a central pore bounded by an α -helix

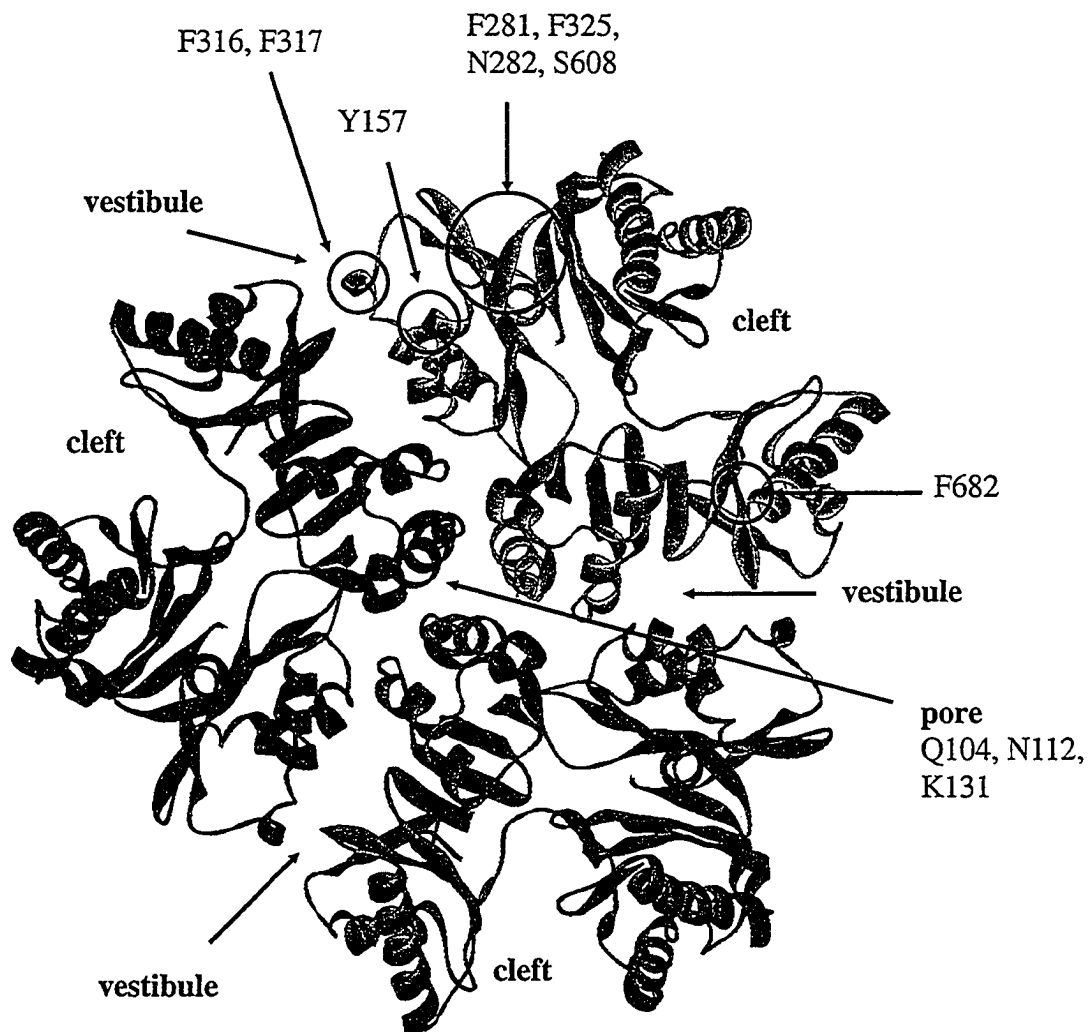


Figure 3.22. Predicted structure of the pore domain of EmhB. The pore domain, viewed from the top of the protein, shows the positions of the central pore, vestibules and clefts. The location of the residues targeted for mutagenesis are indicated.

from each subunit; three channels, or vestibules, located between the subunits; and three clefts in the center of each subunit. Mutations were made in the pore and vestibule regions as well as in other areas of the pore domain to determine the roles of these residues in substrate translocation. The amino acids targeted for mutation in EmhB_{his} are compared to the corresponding residues in other multidrug and solvent efflux pumps in Table 3.8.

3.4.5.1. Mutations in the central pore did not affect efflux activity

Two mutations, Q104A and N112A, were constructed in the pore-forming α -helix, and an additional mutation, K131A, adjacent to the bottom of the pore was constructed. The Q104A mutant EmhB_{his} pump was not expressed in *P. fluorescens* cLP6a-1. This residue is located on the external face of the pore-forming helix and may stabilize the position of the helix in the pore domain. Thus, the Q104A mutant protein likely was unstable and may not have been expressed properly in the inner membrane.

The N112A and K131A mutant EmhB_{his} pumps were expressed, but neither affected the activity of the efflux pump for any of the substrates tested (Table 3.6). Since N112 faces the center of the pore, it was anticipated that the N112A mutation would affect transport of the EmhB substrates. Murakami *et al.* (2004) observed decreased antibiotic resistance upon mutation of the corresponding Q112 residue to cysteine in the *E. coli* AcrB pump. Possibly, the choice of substitution (alanine versus cysteine) at position 112 may have an effect on the preservation of pump function.

3.4.5.2. Amino acids lining the vestibules in the pore domain affect efflux activity

The presence of three vestibules leading into the central cavity suggested that these are involved in substrate recognition and transport (Murakami *et al.* 2002). Compared with the central cavity (Table 3.7) and central pore (Table 3.8), the amino acids lining the vestibules are less conserved (Table 3.8). To examine the role of the vestibules in substrate selectivity, three residues, Y157, F316 and F317, located at the entrance of the channel (Figure 3.23) were targeted for site-directed mutagenesis in

Table 3.8. Conservation of amino acid residues targeted for mutation in the pore domain of EmhB^a

Efflux pump ^c	Mutated residue in EmhB ^b										
	Central pore			Vestibule			Pore domain				
	Q104	N112	K131	Y157	F316	F317	F682	F281	F325	N282	S608
ArpB	Q	N	K	Y	F	F	F	F	F	N	S
TtgB	Q	N	K	Y	F	F	F	F	F	N	S
MexB	Q	Q	K	Y	F	M	F	F	Y	N	S
SrpB	Q	Q	K	L	Y	L	Y	Y	Y	K	H
TtgH	Q	Q	K	L	Y	L	Y	Y	Y	K	H
TtgE	Q	Q	K	L	Y	L	Y	Y	Y	R	H
AcrB	Q	Q	K	Y	F	F	E	F	Y	N	S
MexD	Q	K	Q	Y	F	F	R	L	V	N	S
MexY	A	K	K	I	Y	F	R	V	I	N	Y

^a Protein sequences were aligned by using ClustalX (Thompson *et al.* 1997).

^b Residues that are identical to the EmhB sequence are indicated in boldface type.

^c The efflux pumps compared to EmhB were as listed for Table 3.7.

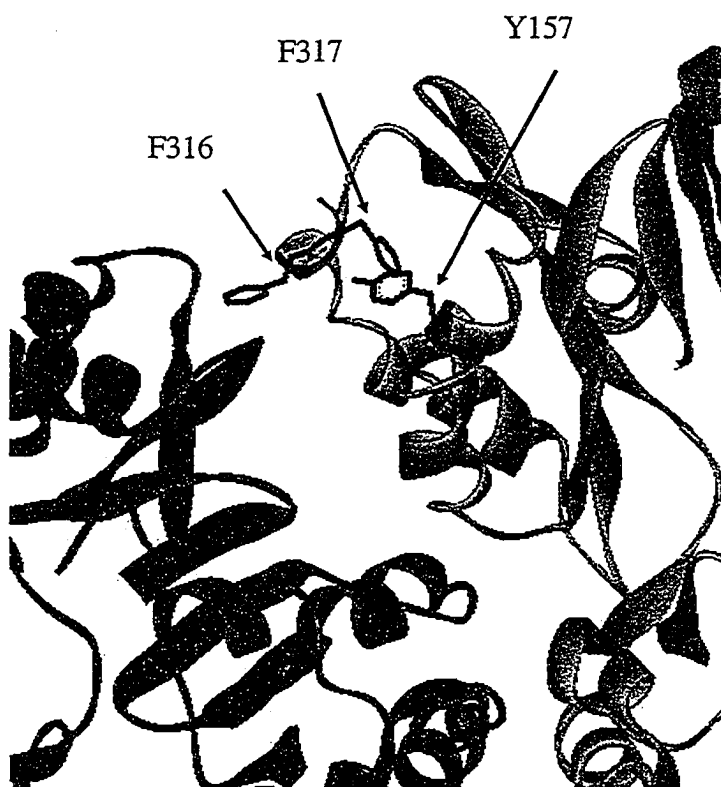


Figure 3.23. The vestibule region of EmhB. A section of the periplasmic domain, viewed from the top of the protein, shows the vestibule between two EmhB subunits. The side chains of the residues F316, F317 and Y157, which were targeted for site-directed mutagenesis, are shown.

EmhB_{his}. *P. fluorescens* cLP6a-1 expressing the Y157A mutant EmhB_{his} pump showed eight-fold and four-fold decreases in resistance to rhodamine 6G and ciprofloxacin, respectively, and was unable to survive in the presence of vapour-phase toluene compared to the control expressing EmhB_{his} (Table 3.6). Resistance to chloramphenicol, nalidixic acid, dequalinium and erythromycin decreased only two-fold and polycyclic aromatic hydrocarbon transport appeared to be unaffected by the Y157A mutation. As noted earlier, a lower level of expression was obtained for the Y157A mutant pump compared to EmhB_{his} (Figure 3.19). Thus, the decreased antibiotic resistance and toluene tolerance caused by the Y157A mutation were likely due to decreased expression of the mutant efflux pump.

Both the F316A and F317A mutant pumps were expressed at levels comparable to EmhB_{his} (Figure 3.19). The F316A mutant EmhB_{his} pump showed significant (four-fold) decreases in resistance to rhodamine 6G and ciprofloxacin and small (two-fold) decreases in resistance to dequalinium and erythromycin compared to the normal EmhB_{his} (Table 3.6). The F317A mutant pump showed small (two-fold) decreases in antibiotic resistance for all antibiotic substrates (Table 3.6). Neither the F316A nor the F317A mutations affected polycyclic aromatic hydrocarbon transport or toluene tolerance. The observations that the F316 side chain points into the vestibule (Figure 3.23) and that the activity of the F316A mutant pump was less active towards rhodamine 6G and ciprofloxacin (Table 3.6) may suggest that this mutation produces a greater conformational change at the rhodamine 6G and ciprofloxacin binding sites than does the F317A mutation. However, without direct binding evidence, speculations about the effect of the mutations on substrate binding are unsubstantiated. Because F316 and F317 are located at the interface between EmhB monomers (Figure 3.23), mutation of these residues more likely disrupted the structure of the EmhB trimer, thereby reducing efflux activity for a number of substrates. Similarly, Middlemiss and Poole (2004) attributed the loss of efflux activity for two mutations in the MexB vestibule region, S462F and E864K, to alterations in the tertiary structure of the pump. Crystallographic analyses of the EmhB F316A and F317A mutant pumps, and other vestibule mutations, are required to assess the impact of the mutations on the structure of the efflux pump. Further studies

of the vestibules demonstrating substrate-binding in EmhB and other RND efflux pumps may provide better evidence linking this region to substrate selectivity.

3.4.5.3. Evidence for a phenylalanine-lined substrate access pathway in the EmhB pore domain

In addition to the vestibule region, other areas of the EmhB pore domain were investigated by site-directed mutagenesis. Because EmhB pumps polycyclic aromatic hydrocarbons, it was hypothesized that amino acids with aromatic side chains may be involved in hydrocarbon recognition and binding. Consequently, two phenylalanine residues (F682 and F281) located near the vestibules were mutated to alanines in EmhB_{his} (Figure 3.22), and the activity of these mutant pumps for EmhB substrates was assessed. One phenylalanine (F682) did not affect the transport of polycyclic aromatic hydrocarbons, antibiotics or toluene (Table 3.6). However, mutation of F281 in EmhB_{his} disrupted efflux activity not only for phenanthrene and anthracene but also for toluene and all of the antibiotics tested, except for streptomycin, which is not a substrate of EmhB (Table 3.6). Mutation of the neighbouring F325 residue also inhibited EmhB_{his} activity for all substrates, and mutation of the neighbouring N282 residue inhibited activity for all substrates except toluene (Table 3.6). Yet, mutation of the adjacent S608 residue yielded a mutant pump that was fully functional for all substrates (Table 3.6).

One possible explanation for the inhibition of the EmhB_{his} pump by the F281A and F325A mutations is that these residues, which are located near the surface of the pore domain, may be involved in intermolecular protein interactions with the membrane fusion protein EmhA. To address this possibility, chemical cross-linking with the cleavable cross-linker dithiobis(succinimidyl propionate), which specifically reacts with the amino group on lysine and has a 12 Å spacer (Zgurskaya and Nikaido 2000b), demonstrated the *in vivo* formation of higher molecular weight complexes for EmhB_{his} and mutant proteins (Figure 3.24). Several major limitations of the cross-linking experiment, however, restricted its usefulness. An inherent problem with cross-linking is the tendency for excessive cross-linking to occur between proteins that do not necessarily interact with each other *in vivo*. The size of the EmhB_{his} protein complex and the identity of the proteins in the complex were not determined. As well, cross-linking does not indicate

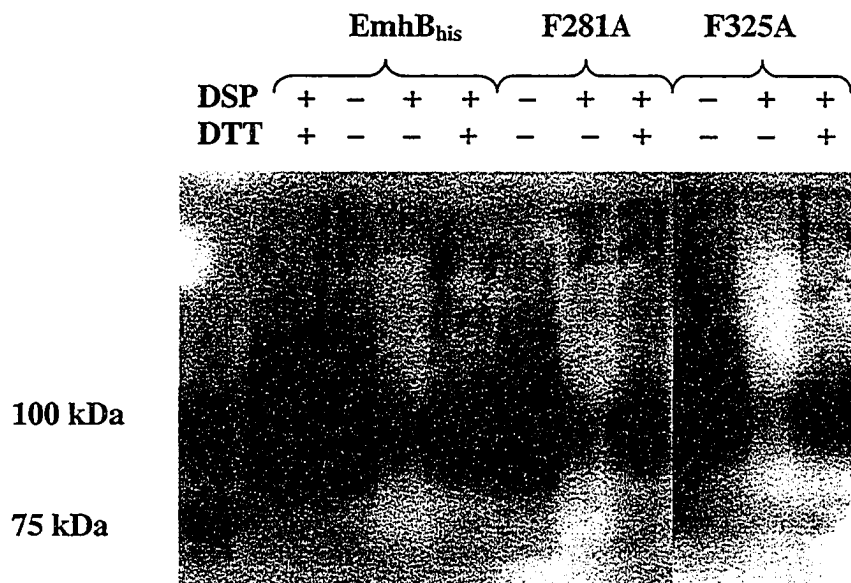


Figure 3.24. Cross-linking of EmhB in intact cells. *P. fluorescens* cLP6a-1 cells expressing EmhB_{his}, EmhB_{his}(F281A) or EmhB_{his}(F325A) were treated with or without the chemical cross-linker DSP as described in Materials and Methods. Following termination of the cross-linking reaction by addition of Tris·HCl (pH 7.5) to a final concentration of 100 mM, cells were harvested, resuspended in SDS-PAGE loading buffer with or without dithiothreitol, and heated to 95°C for 10 min. Samples were run on SDS-PAGE gels using a 6% resolving gel and subjected to western immunoblotting using an anti-His antibody. The sizes of the molecular weight markers are indicated.

that a functional complex has formed. Thus, the *in vivo* cross-linking results with the F281A and F325A mutant pumps are alone insufficient to discount an effect of the mutations on protein-protein interactions.

The protein-protein interactions between the components of the *E. coli* AcrAB-TolC efflux system were modeled recently using the known crystal structures of the AcrB and TolC proteins and a predicted structure of AcrA generated from the MexA crystal structure (Fernandez-Recio *et al.* 2004). In the model, the membrane fusion protein AcrA was predicted to interact with the efflux pump between the AcrB subunits, which corresponds to the vestibule region in the upper part of the pore domain (Fernandez-Recio *et al.* 2004). The region of AcrB corresponding to the location of the F281 and F325 residues in EmhB did not appear to be involved in the AcrA-AcrB interaction. However, precise details of the interaction between RND efflux pumps and their membrane fusion proteins are still unknown, and the possibility that mutation of F281 and F325 in EmhB affected interaction with the membrane fusion protein cannot be discounted.

The F281A and F325A mutations may have caused an indirect effect on the folding of the efflux pump, which resulted in the observed disruption of efflux activity. Notably, the mutant pumps showed intermediate levels of activity between the normal EmhB_{his} and the negative control for some substrates. For the F281A mutant, for example, the MICs for nalidixic acid and rhodamine 6G, while four-fold lower than the positive control EmhB_{his}, were significantly (four-fold) greater than the negative control, whereas the MICs for chloramphenicol and dequalinium were comparable to the negative control (Table 3.6). Additionally, transport of phenanthrene and anthracene by the F325A mutant pump was not completely inhibited (Table 3.6). These data indicate that efflux activity was significantly reduced, but not eliminated, for various substrates in the mutant pumps compared to the normal EmhB_{his}. Therefore, if indirect structural changes induced by the mutations were responsible for the reduced activity, the changes were not severe enough to cause complete inactivation of the pump. Without crystallographic analyses to determine the structures of the mutant proteins, the possibility of indirect structural effects cannot be excluded definitely.

The reduced efflux activity for all substrates by mutation of F281 and F325 in EmhB_{his} strongly suggests protein misfolding or disruption of protein-protein interactions. However, the possibility that these residues may be implicated in substrate translocation through the periplasmic pore domain warrants further investigation. A closer inspection of the EmhB pore domain revealed the presence of several additional phenylalanine residues leading from F325 and F281 at the surface of the periplasmic domain towards the central pore (Figure 3.25). These phenylalanine residues may form a common channel through which substrates reach the central cavity.

The hypothesis that the phenylalanine cluster in EmhB forms a substrate access channel is supported by examples of similar pathways in enzymes that bind hydrophobic compounds. Cytochrome P450 monooxygenases are responsible for the biodegradation of many xenobiotic compounds, drug metabolism, and the biosynthesis of steroids and lipids in prokaryotic and eukaryotic cells. Like multidrug efflux pumps, cytochrome P450 enzymes have a broad substrate specificity for hydrophobic compounds. For example, cytochrome P450cam, a cytosolic enzyme in *P. putida*, catalyzes the oxidation of camphor, its natural substrate, as well as camphor derivatives such as thiocamphor and adamantane, benzene derivatives, styrene and chlorinated aliphatics (Ragg and Poulos 1991, Bell *et al.* 2003). Cytochrome P450cam has been crystallized with various substrates, and the heme-containing active site has been characterized (Schlichting *et al.* 2000). A tyrosine residue (Y96) in the active site was shown to interact via hydrogen bonding with the bound camphor substrate (Schlichting *et al.* 2000). More recently, molecular wires, which are substrate analogues linked to a probe molecule via an alkyl chain, have been employed to characterize the substrate access pathway of cytochrome P450cam (Dunn *et al.* 2001, Hays *et al.* 2004). Crystallization of cytochrome P450cam with the molecular wires revealed the substrate analogue moiety in the active site of the enzyme with the alkyl chain and probe molecule extending from the active site into the substrate access pathway. The amino acids identified in the channel (Figure 3.26), which terminated at Y96 in the active site, were F87, F98 and F193 (Dunn *et al.* 2001, Hays *et al.* 2004). Residues adjacent to the phenylalanines in the access channel were involved in stabilizing the interaction with the substrates (Hays *et al.* 2004). By using a variety of

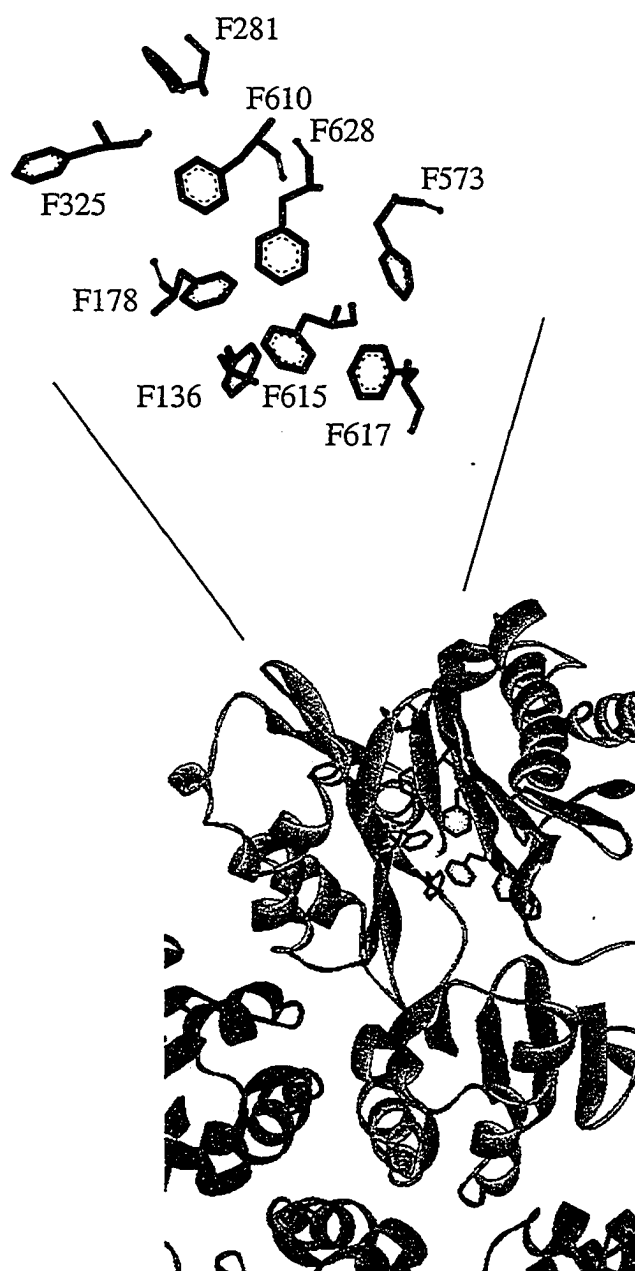


Figure 3.25. Putative substrate translocation pathway in the periplasmic pore domain of EmhB. A segment of the periplasmic domain is viewed from the top of the protein. The position of the phenylalanine residues predicted to be involved in the putative substrate access pathway are shown.

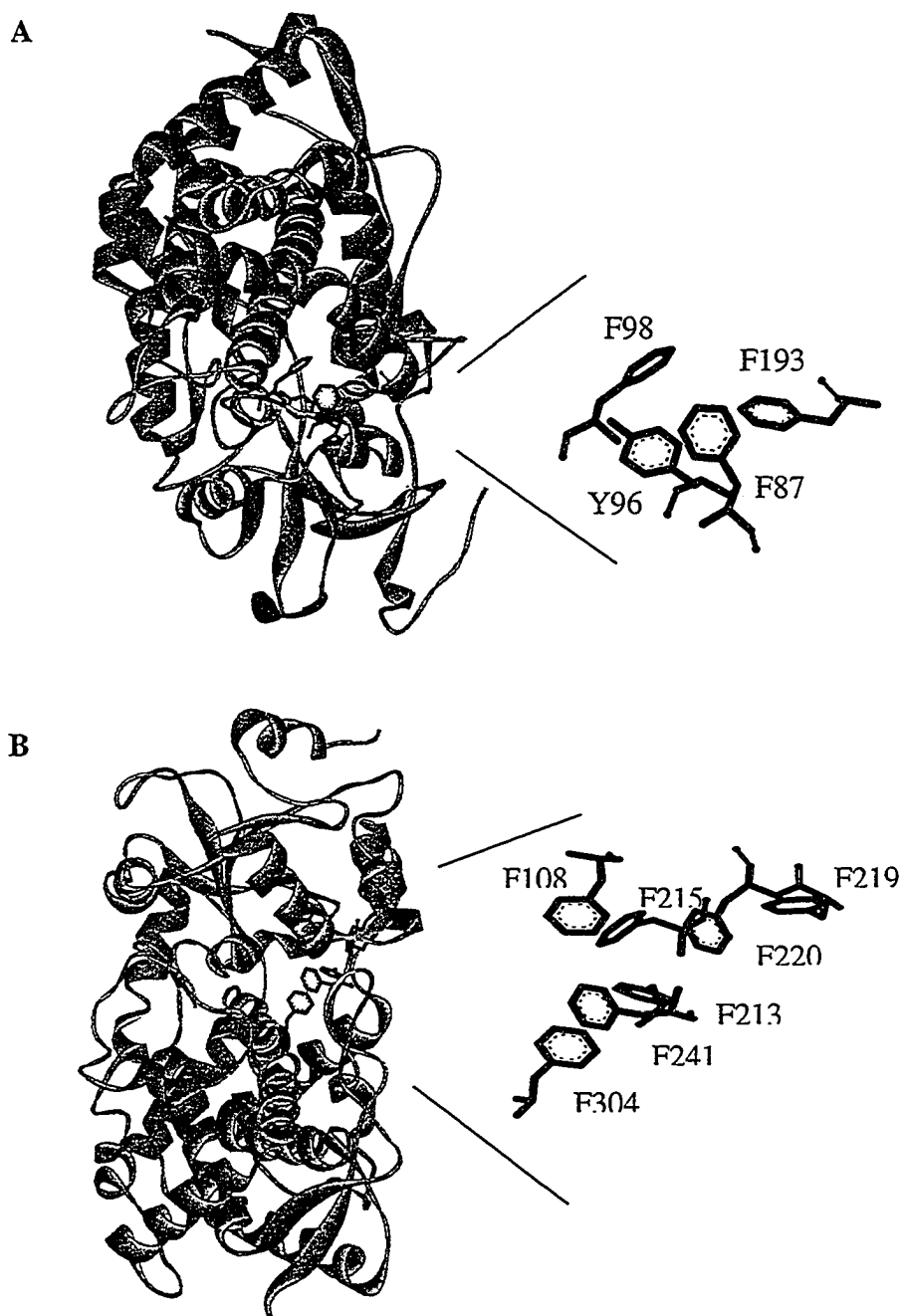


Figure 3.26. Phenylalanine clusters predicted to be involved in substrate access pathways in cytochrome P450 monooxygenases. (A) In cytochrome P450cam (redrawn from PDB entry 1PHC; Poulos *et al.* 1986), the phenylalanine cluster, comprised of F87, F98 and F193, has been shown to be involved in a substrate access pathway leading into the active site residue Y96 (Dunn *et al.* 2001, Hays *et al.* 2004). (B) In cytochrome P450 3A4 (redrawn from PDB entry 1W0E; Williams *et al.* 2004), the phenylalanine cluster, comprised of F108, F215, F219, F220, F213, F241 and F304, is predicted to form a substrate access pathway leading into the active site.

molecular wire compounds, Hays *et al.* (2004) demonstrated the flexibility of the substrate access pathway to accommodate diverse substrates.

A phenylalanine cluster was also observed in the crystal structure of the human cytochrome P450 3A4 isozyme (Williams *et al.* 2004). Cytochrome P450 3A4, a membrane-bound enzyme prevalent in the liver, oxidizes over 100 substrates including estradiol, taxol, lidocaine, cyclosporin A and erythromycin (Josephy 1997). In the cytochrome P450 3A4 structure (Figure 3.26), the aromatic side chains of the phenylalanines (F108, F213, F215, F219, F220, F241 and F304) point towards each other to form a hydrophobic channel leading to the active site (Williams *et al.* 2004). Williams *et al.* (2004) suggested that an initial substrate recognition event on the external surface of cytochrome P450 3A4 triggers a conformational change, widening the phenylalanine channel and allowing substrate passage to the active site.

The presence of phenylalanine clusters in the EmhB efflux pump and in cytochrome P450 monooxygenases suggests that there is a common theme among these broad specificity proteins. The aromatic side chains of the phenylalanine residues likely provide a flexible access channel, whereby a wide variety of hydrophobic compounds can be accommodated by relatively non-specific interactions. Neighbouring amino acid residues may play a role in stabilizing substrate binding in the hydrophobic channel. For example, mutation of the N282 residue, which is adjacent to F281 and F325 in EmhB (Figure 3.22), also reduced the transport of all substrates except toluene (Table 3.6). Mutation of the S608 residue, which is also near F281 and F325 (Figure 3.22), did not affect efflux activity (Table 3.6), perhaps because the serine to alanine substitution did not significantly alter the substrate binding affinity of the EmhB_{his} pump.

Interestingly, of the nine phenylalanine residues identified in the putative substrate access pathway in EmhB (Figure 3.25), only F136, F178, F615 and F617 are highly conserved among the multidrug and solvent efflux pumps (Table 3.9). These four residues lie along one surface of the putative channel and lead into the central cavity (Figure 3.26). The residues corresponding to positions 573, 610 and 628 in EmhB are less conserved. In the toluene efflux pumps SrpB, TtgH and TtgE, the residues corresponding to positions 573, 610 and 628 in EmhB, which are positioned along the side of the putative channel, are methionine or leucine residues rather than phenylalanine

Table 3.9. Conservation of phenylalanine residues in RND multidrug and solvent efflux pumps corresponding to the putative substrate access pathway in EmhB^a

Efflux pump ^b	Residue in EmhB ^c								
	F136	F178	F281 ^d	F325 ^d	F573	F610	F615	F617	F628
ArpB	F	F	F	F	F	F	F	F	F
TtgB	F	F	F	F	F	F	F	F	F
MexB	F	F	F	Y	F	F	F	F	F
SrpB	F	F	Y	Y	M	M	F	F	L
TtgH	F	F	Y	Y	M	M	F	F	L
TtgD	F	F	Y	Y	M	M	F	F	L
AcrB	F	F	F	Y	M	F	F	F	F
MexD	F	F	L	V	V	F	F	F	F
MexY	I	W	V	I	M	Y	F	L	F

^a Protein sequences were aligned by using ClustalX (Thompson *et al.* 1997).

^b The efflux pumps compared to EmhB were as listed for Table 3.7.

^c Residues that are conserved in EmhB are indicated in boldface type.

^d The F281 and F325 residues in EmhB were shown by site-directed mutagenesis to be essential for the efflux of polycyclic aromatic hydrocarbons, antibiotics and toluene (Table 3.6).

(Table 3.9). These residues were not targeted for site-directed mutagenesis in EmhB, and, as a result, their function in the putative substrate access path is unknown. One hypothesis is that the amino acids at positions 573, 610 and 628 may be implicated in substrate selectivity. Alternatively, these residues may not be involved in the putative substrate access channel. Additional site-directed mutations in EmhB, as well as mutagenesis studies with other multidrug and solvent efflux pumps, will help to clarify the roles of F573, F610 and F628. The amino acids at positions 281 and 325 on the surface of the EmhB pore domain are the least conserved among the residues identified in the putative substrate access channel (Table 3.9). These residues may play a role in substrate specificity. Notably, in the toluene efflux pumps SrpB, TtgH and TtgE, tyrosine residues replace the phenylalanines at positions 281 and 325 in EmhB (Table 3.9). The tyrosine substitutions in SrpB, TtgH and TtgE may enhance binding of more polar hydrocarbons, such as toluene, enabling these proteins to be more efficient solvent efflux pumps. Analysis of F281Y and F325Y single and double mutations in EmhB, particularly with respect to toluene tolerance, may clarify their function in substrate recognition and translocation.

The residues lining the putative substrate access pathway (Table 3.9), with the exception of the amino acids on the surface of the protein, are hydrophobic in the EmhB homologues as well as in the *P. aeruginosa* MexD and MexY pumps, which are more distantly related to EmhB (Figure 3.6). The similarity of these amino acids among RND efflux pumps lends support to the hypothesis that this region forms a hydrophobic substrate-binding pocket, which, like the central cavity, is able to accommodate structurally diverse compounds. Based on protein sequence alignments and homology modeling, however, the location of these residues is difficult to know precisely. Thus, further studies are required to confirm the hypothesis that these residues form a hydrophobic substrate access channel leading into the central cavity in RND pumps.

3.4.6. A mutation in the outer membrane protein docking domain enhances efflux activity

One EmhB_{his} mutant protein (A206S) exhibited enhanced efflux activity for antibiotics and toluene. Antibiotic resistance of *P. fluorescens* cLP6a-1 expressing

EmhB_{his}(A206S) was significantly greater (four-fold) compared to the normal EmhB_{his} for all of the antibiotics tested, except for the non-substrate streptomycin (Table 3.6). Most notably, *P. fluorescens* cLP6a-1 expressing EmhB_{his} with the A206S mutation became toluene tolerant as indicated by its ability to grow in the presence of vapour-phase toluene (Table 3.6). The transport of phenanthrene or anthracene, however, appeared to be unaffected by the mutation (Table 3.6). A small decrease in the steady-state levels of hydrocarbon may be undetectable due to the lack of sensitivity of the rapid centrifugation method used to measure the cellular accumulation of phenanthrene and anthracene. Small changes in the cellular accumulation of the antibiotics or toluene, however, have large measurable effects on the growth-based assays used to assess the transport of these substrates.

The A206S mutation responsible for the enhanced efflux activity mapped to the outer membrane protein docking domain of the efflux pump (Figure 3.27), and this residue is highly conserved among the ArpB, SrpB, TtgB, TtgE, TtgH, MexB and AcrB multidrug and toluene efflux pumps (Table 3.10). The outer membrane protein docking domain of RND efflux pumps has been proposed to act as a funnel, which interacts with the outer membrane protein and opens to allow substrates entry into the outer membrane channel (Murakami *et al.* 2002). In the RND pump structure, A206 is located at the interface between the EmhB subunits (Figure 3.27) and may be involved in the funnel structure and function. One possibility is that the A206S mutation may maintain the funnel in a more open state, thus facilitating passage of substrates from the RND pump to the outer membrane channel. Alternatively, the A206S mutation may cause conformational changes in the efflux pump that enhance the interaction between the RND pump and the outer membrane protein, thereby creating a more efficient efflux complex. The two possibilities may not be mutually exclusive; that is, locking the RND funnel in an open state may stabilize the interaction with the open conformation of the outer membrane protein.

Middlemiss and Poole (2004) also identified mutations in the outer membrane protein docking domain of the MexB pump in *P. aeruginosa* that affected efflux activity. A G220S mutation reduced antibiotic resistance levels for all drugs tested (Middlemiss and Poole 2004). The G220 residue is located on the protruding arm of the MexB

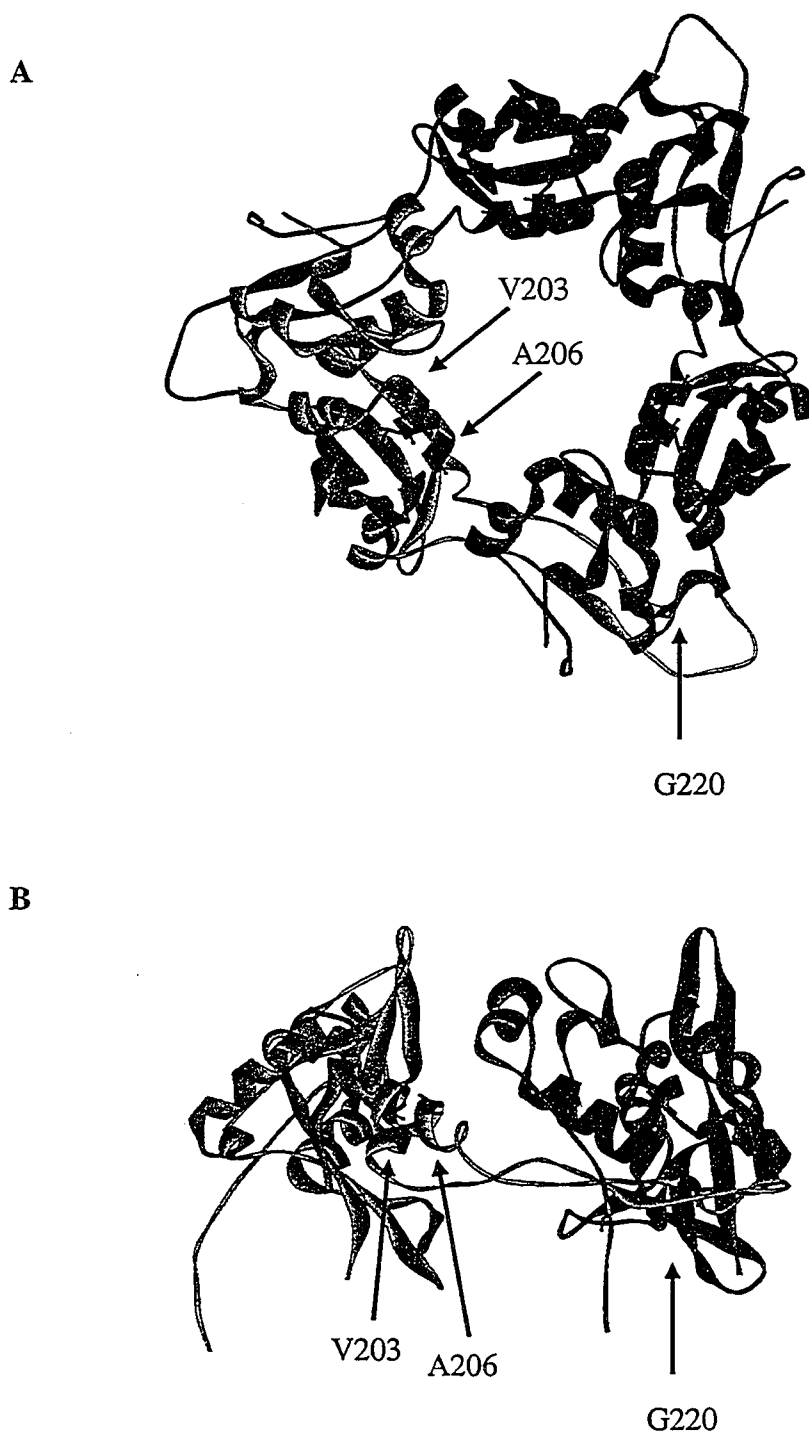


Figure 3.27. Predicted structure of the outer membrane protein docking domain of EmhB. The domain is viewed from the top of the protein perpendicular to the plane of the membrane in (A) and from the side of the protein with the rear monomer removed in (B). The location of the A206, V203 and G220 residues are indicated.

Table 3.10. Conservation of amino acid residues in the outer membrane protein docking domain of RND efflux pumps^a

Efflux pump ^b	Residue in EmhB ^c		
	A206	G220	V203
ArpB	A	G	V
TtgB	A	G	V
MexB	A	G	V
SrpB	A	G	V
TtgH	A	G	V
TtgD	A	G	V
AcrB	A	G	V
MexD	A	G	V
MexY	A	G	L

^a Protein sequences were aligned by using ClustalX (Thompson *et al.* 1997).

^b The efflux pumps compared to EmhB were as listed for Table 3.7.

^c Residues that are conserved in EmhB are indicated in boldface type.

subunit, which inserts into a pocket in the neighbouring subunit, and is conserved among RND efflux pumps (Table 3.10). Middlemiss and Poole (2004) attributed the lack of efflux activity observed for the G220S mutation to an inability of the MexB subunits to assemble into trimers. Alternatively, the protruding arm of the efflux pump may be involved in opening and closing the funnel, and the G220S mutation may lock the efflux pump in a closed state. Several second-site suppressor mutations that restored antibiotic efflux in the G220S mutant pump were isolated and mapped to the outer membrane protein docking domain (Middlemiss and Poole 2004). In particular, a V203M/G581D double mutation restored antibiotic resistance of the G220S mutant pump to wild-type levels (Middlemiss and Poole 2004). Like A206 in EmhB, V203 is highly conserved in RND efflux pumps (Table 3.10), and the V203M mutation may maintain the MexB pump in an open state or enhance the interaction with the outer membrane protein, compensating for the G220S mutation.

The results for the A206S mutation in EmhB presented here, as well as the G220S mutation in MexB reported by Middlemiss and Poole (2004), provide evidence for the role of the outer membrane protein docking domain in the function of RND efflux pumps. Further examination of this region will provide valuable information regarding the mechanism by which the efflux pump opens to allow substrates to enter the outer membrane protein. Since the mechanism is likely a universal feature of RND efflux pumps, the outer membrane protein docking domain provides an excellent target for pump inhibitors. An inhibitor that locks the funnel in a closed state could successfully eliminate efflux pump-mediated antibiotic resistance.

3.4.7. A model for substrate translocation by RND efflux pumps that describes substrate selectivity and capture from the periplasm or inner membrane

Previous models of RND efflux pumps predicted that substrates are captured from the outer leaflet of the inner membrane (Murakami *et al.* 2002, Yu *et al.* 2003b), while a recent study of aminoglycoside transport by the *E. coli* pump AcrD demonstrated substrate capture from the periplasm (Aires and Nikaido 2005). Here, a model for the transport of substrates through RND efflux pumps, which supports both types of substrate capture is proposed (Figure 3.28) based on the results of the mutagenesis studies with

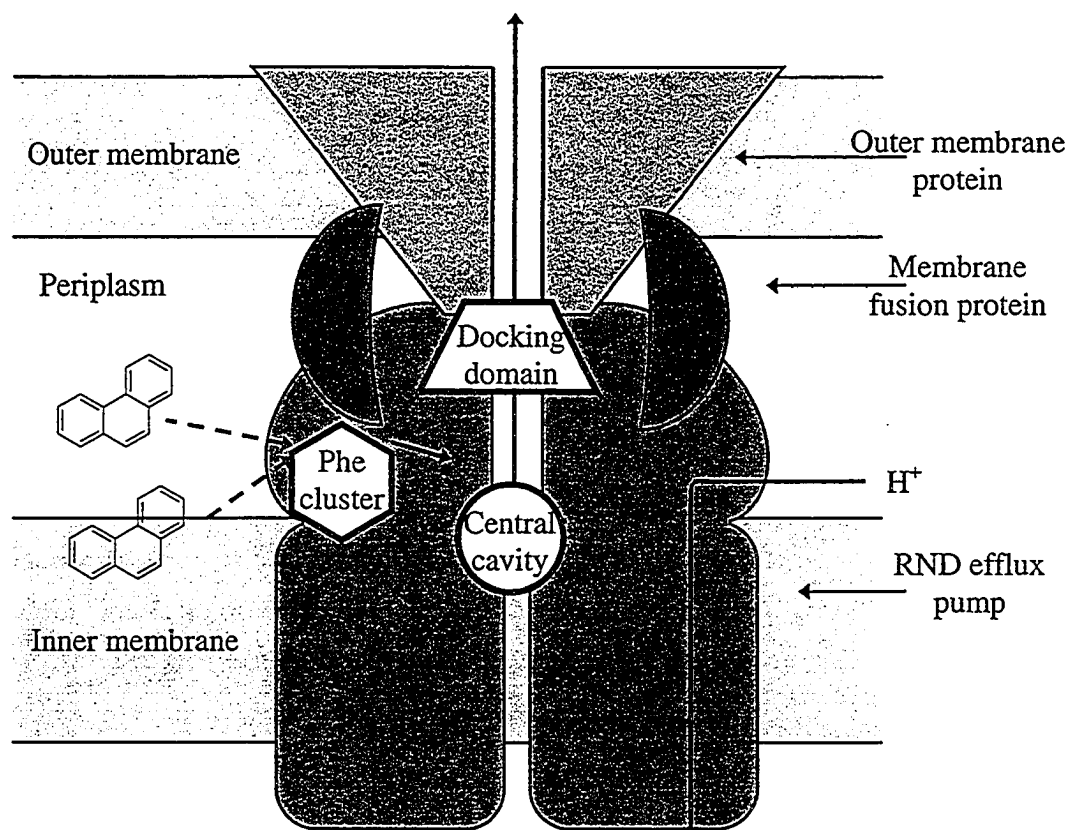


Figure 3.28. Proposed model for substrate translocation in RND efflux pumps. Substrates in the periplasm or in the inner membrane interact with the periplasmic domain of the RND pump and enter a common hydrophobic substrate access pathway, possibly comprised of a phenylalanine cluster in EmhB. From the hydrophobic substrate access pathway, substrates enter a cavity located at the center of the trimer above the inner membrane. Substrates then pass through the central pore, which is formed by three α -helices in the periplasmic domain. The final step involves substrate translocation through the funnel-shaped outer membrane protein docking domain into the outer membrane protein.

EmhB. In this model, substrates are initially recognized at the external surface of the efflux pump pore domain. After the initial recognition event, substrates enter a common access pathway, which may be provided by the phenylalanine cluster in the pore domain leading to the central cavity. The efflux pump likely undergoes a conformational change, induced either by the initial substrate binding or by proton translocation, to open the phenylalanine cluster and facilitate substrate passage. Following residence in the central cavity, substrates are expelled through the central pore into the outer membrane protein docking domain. Another conformational change opens the funnel-shaped outer membrane protein docking domain, resulting in substrate translocation directly to the outer membrane channel.

The initial step of substrate recognition by the efflux pump remains unclear in the proposed model. Several studies have established that the periplasmic domain of RND efflux pumps determines substrate specificity. Chimeric analyses of the *E. coli* AcrB and AcrD efflux pumps (Elkins and Nikaido 2002) and of the *P. aeruginosa* MexB and MexY efflux pumps (Eda *et al.* 2003) showed that the periplasmic loops dictated substrate specificity. Also using chimeric constructs of the *E. coli* AcrB pump and the *P. aeruginosa* MexB pump, Tikhonova *et al.* (2002) demonstrated that the second periplasmic loop conferred specificity for macrolide antibiotics. Moreover, random mutagenesis of MexB identified several amino acids throughout the pore domain, including S462 and E864 in the vestibules and T578, A618 and R716 within the periplasmic cleft, that altered the activity and substrate selectivity of the efflux pump (Middlemiss and Poole 2004). These data suggest that different substrates initially interact with the pump at distinct sites in the pore domain.

Once the initial substrate binding has occurred, the model (Figure 3.28) proposes that substrates reach the central cavity via a hydrophobic channel, possibly lined by phenylalanine residues in EmhB (Figure 3.25), in the pore domain. The proposed substrate access pathway through the pore domain contradicts previous models of substrate entry in RND efflux pumps (Murakami *et al.* 2002, Yu *et al.* 2003b). The presence of vestibules extending from the surface of the pore domain into the central cavity in the crystal structure of AcrB prompted the hypothesis that substrates enter the pump through these channels (Murakami *et al.* 2002, Yu *et al.* 2003b). To date,

experimental evidence has been lacking to confirm the role of the vestibules in a substrate access pathway. Mutational analysis of the EmhB efflux pump, however, demonstrated the importance of F281 and F325 in the efflux of all substrates (Table 3.6) and suggested the existence of a common pathway leading from these residues into the central cavity (Figure 3.28). The presence of similar phenylalanine channels in cytochrome P450 monooxygenases, which also bind hydrophobic compounds (Dunn *et al.* 2001, Hays *et al.* 2004, Williams *et al.* 2004), supports the hypothesis of such a substrate access pathway in RND efflux pumps. Further analyses with EmhB are required to confirm the involvement of the putative phenylalanine cluster in substrate access.

Strong evidence for the involvement of the central cavity in the proposed substrate translocation model was provided by the co-crystallization studies of the *E. coli* AcrB efflux pump with several drug substrates (Yu *et al.* (2003a)). The results from the site-directed mutagenesis of the EmhB central cavity presented here confirmed the importance of several central cavity residues (A384, A385 and F386) for efflux activity. Further, the D101 residue, which bounds the cavity and the central pore, was shown to be essential for efflux activity. Mutagenesis of the D101 residue in EmhB, as well as the cysteine-scanning mutagenesis of other central pore residues by Murakami *et al.* (2004), strongly demonstrated the involvement of the pore in efflux activity.

The final step in the proposed model of substrate translocation through RND efflux pumps is passage through the outer membrane protein docking domain (Figure 3.28). The A206S mutation in the outer membrane protein docking domain of EmhB (Table 3.6), as well as the G220S mutation in MexB (Middlemiss and Poole 2004), demonstrated the involvement of this domain in substrate transport. Substrates may not interact directly with amino acid residues in the outer membrane protein docking domain, but rather this funnel-shaped domain may simply open to expel substrates from the central pore to the outer membrane channel. The mechanism by which the funnel opens likely involves movement of the protruding arm of the pump subunit, which interacts with the neighbouring subunit (Figure 3.27). Structural studies using X-ray crystallography will confirm the model proposed for the opening of the outer membrane protein docking domain by comparing the diameter of the funnel in the wild-type EmhB and the A206S mutant.

While the initial substrate recognition event may be distinct for individual substrates, the remaining steps in the transport model proposed for RND efflux pumps (Figure 3.28) are likely common to all substrates. Thus, these proteins have evolved a number of adaptations to accommodate structurally diverse ligands. As discussed earlier, the central cavity is unusually large, compared to enzyme active sites, and is lined by hydrophobic amino acids, which enables it to accommodate a wide variety of substrates. Like the central cavity, the proposed substrate access channel, involving the phenylalanine cluster identified in EmhB, likely provides a flexible pathway that facilitates passage of the different substrates.

It has been proposed that substrates enter the RND efflux pump from either the inner membrane or the periplasm (Murakami *et al.* 2002, Yu *et al.* 2003b). The model described here, based on the mutagenesis studies with EmhB, supports both types of substrate capture (Figure 3.28). Highly hydrophobic substrates, such as polycyclic aromatic hydrocarbons, may interact with the amino acid residues adjacent to the membrane and gain access to the efflux pump through the membrane. Periplasmic capture may also occur for certain substrates through other sites in the pore domain. Experimental evidence demonstrated periplasmic capture of the hydrophilic aminoglycoside substrates of the *E. coli* AcrD efflux pump (Aires and Nikaido 2005). It should be noted that Aires and Nikaido (2005) also demonstrated the AcrD-mediated transport of aminoglycosides directly from the cytoplasm. However, this route was not investigated in the present study, and the significance of cytoplasmic capture of efflux pump substrates remains unclear. Further studies are required to confirm the proposed model for RND efflux pumps, as well as to elucidate the roles of the membrane fusion protein and the outer membrane protein in substrate transport across the gram-negative cell envelope.

3.4.8. Comparison of the model for transport in RND efflux pumps to other families of multidrug efflux pumps

Multidrug efflux pumps that, like RND efflux pumps, have a broad specificity for hydrophobic substrates are found in several other protein families, including the ATP-binding cassette superfamily and the major facilitator superfamily (Saier and Paulsen

2001). Members of the ATP-binding cassette superfamily and major facilitator superfamily are responsible for multidrug resistance in eukaryotes and gram-positive bacteria. Thus, proteins belonging to these other families of multidrug transporters do not have large extracellular domains, like the periplasmic domain characteristic of RND efflux pumps. Despite their structural dissimilarities, studies with the ATP-binding cassette transporter P-glycoprotein, which is responsible for multidrug resistance to a wide array of hydrophobic chemotherapy drugs in mammalian cells, suggest that these proteins share common features with RND efflux pumps for recognizing and transporting hydrophobic compounds.

Detailed structural data for multidrug efflux pumps belonging to the ATP-binding cassette superfamily are lacking due to the absence of X-ray crystal structures for P-glycoprotein. However, crystal structures of other solute transporters belonging to the ATP-binding cassette superfamily, as well as biochemical structural studies, have provided insight into the structure of P-glycoprotein. The 12 transmembrane α -helices of P-glycoprotein are predicted to form a funnel in the cytoplasmic membrane that, in one conformation, is narrow at the cytoplasmic side and open at the extracellular side (Loo *et al.* 2004). The amino acid sequence of P-glycoprotein predicted two homologous halves of the protein, with TMS1-6 and TMS7-12 forming symmetrical halves of the funnel. Cysteine-scanning mutagenesis studies of P-glycoprotein identified a number of hydrophobic amino acids in the transmembrane segments that contributed to a common drug-binding pocket capable of accommodating two structurally different drugs simultaneously (Loo and Clarke 2000, Loo *et al.* 2003a). These hydrophobic amino acids line the interior of the funnel-shaped protein and, like the central cavity within RND efflux pumps, provide a large and flexible substrate-binding pocket.

Unlike the dual mode of substrate capture from the inner membrane and from the periplasm that is proposed for RND efflux pumps, P-glycoprotein and other multidrug transporters belonging to the ATP-binding cassette and major facilitator superfamilies are believed to capture substrates solely from the membrane. Loo and Clarke (2005) suggested that substrates gain access to the drug-binding pocket of P-glycoprotein through gates formed between adjacent transmembrane segments. Site-directed mutagenesis of hydrophobic amino acid residues on the exterior surfaces of TMS2,

TMS5, TMS8 and TMS11 inhibited drug transport by P-glycoprotein (Loo and Clarke 2005). In the three-dimensional model of P-glycoprotein, TMS2 and TMS11 are adjacent to each other and opposite to TMS5 and TMS8. Thus, the hydrophobic amino acids lining the TMS2/11 and TMS5/8 interfaces were predicted to form gates on opposite sides of the funnel leading into the central drug-binding pocket (Loo and Clarke 2005). Photoaffinity labeling studies with P-glycoprotein confirmed that the initial substrate interaction likely occurs at the transmembrane domain interfaces between the two halves of the transporter (Pleban *et al.* 2005). The hydrophobic nature of the proposed gates represents another adaptation enabling P-glycoprotein to recognize and transport structurally diverse hydrophobic compounds.

The site-directed mutagenesis studies with the RND efflux pump EmhB presented in this study also demonstrated the importance of domain interfaces in substrate recognition and translocation. The central cavity of RND proteins is located at the interface between the membrane and periplasmic domains of the pump. As well, the F281 and F325 residues are located near the surface of the periplasmic domain and were proposed to be involved in a hydrophobic substrate access channel in EmhB (Figure 3.25). The presence of similar hydrophobic gates leading to the central drug-binding pocket in P-glycoprotein lends support to the proposed model for substrate recognition and translocation by RND efflux pumps (Figure 3.28). Binding of substrates at domain interfaces through hydrophobic interactions may represent a universal feature of multidrug efflux pumps that accounts for their broad substrate specificity.

3.4.9. Future work to elucidate the substrate translocation pathway in RND efflux pumps

While X-ray crystallography of the EmhB pump would be beneficial to confirm the effects of site-directed mutations on protein structure, the use of crystallography alone is unlikely to yield significant information on the transport cycle of RND efflux pumps. Co-crystallization studies of the *E. coli* AcrB pump with substrates (Yu *et al.* 2003a) likely revealed the most stable complex with drugs bound in the central cavity. To detect transient substrate-protein complexes, other methods are required. The biochemical studies used to elucidate the drug-binding domain of P-glycoprotein can be applied to the

EmhB transporter and combined with structural analyses to provide valuable insights into the mechanism of action of RND efflux pumps.

To identify residues involved in the drug-binding domain of P-glycoprotein, cysteine-scanning mutagenesis was coupled with cross-linking analysis using thiol-reactive substrate analogues (Loo and Clarke 2002, Loo *et al.* 2003*a, b*). If a residue is involved in substrate binding, mutation to cysteine and cross-linking with a thiol-reactive substrate analogue will inhibit the transport activity of the pump by preventing the binding of additional substrates. For example, methanethiosulfate-rhodamine was used to identify the rhodamine-binding site in P-glycoprotein (Loo and Clarke 2002). Similarly, copper phenanthroline, a zero-length cross-linker, was used to probe the structure of P-glycoprotein (Loo *et al.* 2003*b*). Cysteine-scanning mutagenesis coupled with the use of thiol-reactive substrate analogues, such as methanethiosulfate-rhodamine and copper phenanthroline, could be used to study the role of the phenylalanines in the proposed hydrophobic substrate access pathway in EmhB.

In this study, the broad substrate specificity of the EmhB pump for polycyclic aromatic hydrocarbons, toluene and hydrophobic antibiotics was exploited effectively to identify site-directed mutations affecting the substrate specificity and transport activity of the efflux pump. The growth-based assays employed to assess toluene and antibiotic efflux are amenable to high through-put screening and, thus, could be used to screen mutant pumps generated by random mutagenesis. As indicated by the A206S mutant pump, which was created by a PCR-introduced error, random mutagenesis has the potential to identify important amino acids that might be overlooked using a site-directed mutagenesis strategy. Understanding the mechanism of action of RND efflux pumps will aid in the design of pump inhibitors for clinical applications.

3.5. Prevalence and significance of polycyclic aromatic hydrocarbon efflux⁴

The protein sequence and functional similarities between the *P. fluorescens* EmhABC efflux system and the antibiotic and solvent efflux systems suggested that polycyclic aromatic hydrocarbon efflux might not be unique to *P. fluorescens* cLP6a. To investigate this hypothesis, several gram-negative bacteria, including environmental isolates and clinical strains, were investigated for their ability to transport phenanthrene. As well, the substrate specificities of the *P. putida* S12 antibiotic efflux system ArpABC and solvent efflux system SrpABC for phenanthrene were investigated. The significance of polycyclic aromatic hydrocarbon efflux is discussed.

3.5.1. Phenanthrene efflux is found in other bacteria

Table 3.11 shows that the ability to transport phenanthrene with an active efflux system is not unique to *P. fluorescens* cLP6a. Several *P. putida* strains, including *P. putida* G7, which harbours the NAH7 plasmid encoding naphthalene degradation genes, *P. putida* mt-2, which carries the TOL plasmid pWW0 encoding toluene degradation genes, *P. putida* KT2440, a cured derivative of *P. putida* mt-2 lacking the TOL plasmid, and *P. putida* S12, a solvent-tolerant strain, showed increased cellular accumulation of phenanthrene upon inhibition of an active efflux process. Three *P. aeruginosa* strains, including the type strain PA01 and two clinical isolates, and two *B. cepacia* strains, an environmental isolate and a clinical isolate, also have mechanisms for phenanthrene efflux (Table 3.11). The MexAB-OprM efflux system in *P. aeruginosa* and the ArpABC and SrpABC efflux systems in *P. putida* S12 showed high homology to and shared similar substrate specificities with the EmhABC system, as discussed in sections 3.1 and 3.2. Hence, MexAB-OprM and ArpABC, and possibly SrpABC, likely are responsible for the observed phenanthrene efflux in *P. aeruginosa* and *P. putida* S12. A number of RND efflux systems have been identified by genome sequencing in other *P. putida* strains and *B. cepacia*. Likely, phenanthrene efflux in the *P. putida*, *P. aeruginosa* and *B. cepacia* strains is mediated by RND efflux pumps homologous to the EmhABC system.

⁴ Portions of this section were published previously by Hearn *et al.* (2003).

Table 3.11. Accumulation of phenanthrene in bacterial strains before and after azide addition, as a test for efflux^a

Strain	Accumulation of phenanthrene ^b	
	Uninhibited (before azide addition)	Inhibited (after azide addition)
<i>P. fluorescens</i> strains		
cLP6a	0.12 ± 0.07 (3)	0.32 ± 0.01 (3)
cLP6a-1	0.29 ± 0.02 (3)	0.33 ± 0.01 (3)
<i>P. putida</i> strains		
G7	0.04	0.22
mt-2	0.09	0.25
KT2440	0.07	0.32
S12	0.07	0.34
<i>P. aeruginosa</i> strains		
PA01	0.08	0.36
A	0.11	0.33
B	0.10	0.27
<i>B. cepacia</i> strains		
DB101	0.09	0.21
K56-2	0.07	0.25
<i>A. vinelandii</i> UW	0.27	0.26

^a Table taken from Hearn *et al.* 2003.

^b The fractional amount of radiolabeled phenanthrene was measured at steady-state for both the uninhibited cells (before azide addition) and inhibited cells (after addition of 30 mM azide). For the *P. fluorescens* strains, the fractional amounts given are the averages ± standard deviations for three independent experiments. For all other strains, the data represent single experiments.

Only *A. vinelandii* did not show evidence of an active efflux mechanism for phenanthrene when it was grown in Burke's buffer under iron-rich conditions (Table 3.11), in Burke's buffer under iron-limited conditions, or in TSB (data not shown). Interestingly, genome sequencing of *A. vinelandii* revealed the presence of an RND efflux pump (GenPept accession number ZP_00089531) whose protein sequence is 77% identical to that of EmhB. The efflux system in *A. vinelandii* may recognize a different spectrum of substrates than EmhABC, or it may not have been expressed in *A. vinelandii* under the growth conditions tested. Since the efflux system and its regulation in *A. vinelandii* have not been characterized, conclusions about the lack of observed phenanthrene efflux in *A. vinelandii* cannot be made.

3.5.2. Specificity of the ArpABC and SrpABC efflux systems for phenanthrene

Of the two RND efflux pumps in *P. putida* S12, the ArpABC proteins show greater homology to the EmhABC efflux system than SrpABC (Table 3.1). EmhABC, ArpABC and SrpABC exhibited the same substrate specificity for hydrophobic antibiotics (Table 3.2), and all three efflux systems pump toluene (Table 3.3), although SrpABC is a more efficient toluene efflux system. It was, therefore, of interest to determine which of the efflux systems, ArpABC, SrpABC or both, are responsible for the observed phenanthrene efflux in *P. putida* S12.

The EmhB-disruption mutant *P. fluorescens* cLP6a-1 was complemented with either the *arpABC* operon or the *srpABC* operon, and the ratios of phenanthrene accumulation in the uninhibited and inhibited cells is given in Table 3.12 for the various strains. The ArpABC efflux system pumped phenanthrene as efficiently as the EmhABC efflux system in *P. fluorescens* cLP6a-1, as indicated by the cellular accumulation levels of phenanthrene in the uninhibited and inhibited cells (Table 3.12). This result was not surprising given the high protein sequence identities of the EmhABC and ArpABC components (Table 3.1).

In contrast to ArpABC, *P. fluorescens* cLP6a-1 cells expressing the SrpABC efflux system exhibited a reduced ability to transport phenanthrene (Table 3.12). The SrpB efflux pump appears to have a lower affinity for phenanthrene than the EmhB and ArpB efflux pumps. As discussed in section 3.4.5, the amino acid differences in the

Table 3.12. Specificity of the ArpABC and SrpABC efflux systems for phenanthrene

<i>P. fluorescens</i> strain ^a	Efflux pump	Phenanthrene transport (Ratio of uninhibited/inhibited) ^b
cLP6a-1(pBH5)	EmhABC ⁺	0.56 ± 0.08 (3)
cLP6a-1(pUCP26)	EmhABC ⁻	1.06 ± 0.05 (9)
cLP6a-1(pBH64-arp)	ArpABC ⁺	0.58 (1)
cLP6a-1(pBH63-srp)	SrpABC ⁺	0.85 ± 0.01 (2)

^a The following *P. fluorescens* strains were tested: the wild-type cLP6a, the *emhB* disruption mutant cLP6a-1, the mutant complemented with either the *emhABC* genes cLP6a-1(pBH5), the vector negative control cLP6a-1(pUCP26), and the mutant complemented with either the *arpABC* genes cLP6a-1(pBH64-arp) or the *srpABC* genes cLP6a-1(pBH63-srp).

^b The fractional amount of radiolabeled phenanthrene was determined in uninhibited cells and in cells inhibited with 30 mM azide. Values represent the ratio of the fractional amounts of hydrocarbon in the uninhibited and inhibited cells. When given, the values are the averages ± standard deviations with the number in parentheses indicating the number of independent experiments performed.

protein sequences of EmhB and SrpB are predicted to influence the substrate specificity of the efflux pumps. In particular, the phenylalanines at positions 281 and 325 in EmhB and in ArpB, which inhibited phenanthrene efflux when mutated to alanines in EmhB_{his}, correspond to tyrosine residues in the SrpB sequence (Table 3.9). The presence of tyrosine residues at these positions, which was suggested to improve toluene binding, may reduce the affinity of the SrpB efflux pump for phenanthrene compared to EmhB. Analysis of F281Y and F325Y single and double mutations in the EmhB pump will help to clarify the roles of these residues in polycyclic aromatic hydrocarbon efflux, as well as toluene efflux.

3.5.3. Significance of polycyclic aromatic hydrocarbon efflux in *P. fluorescens*

The polycyclic aromatic hydrocarbons phenanthrene, anthracene and fluoranthene recognized by the EmhABC efflux system differ from the compounds typically exported by multidrug and solvent efflux pumps in that they are not toxic to bacterial cells and are growth substrates for the parental strain *P. fluorescens* LP6a. Comparable growth rates in TSB were measured for the wild-type *P. fluorescens* cLP6a and the efflux pump-deficient mutant cLP6a-1 in the presence and absence of saturating amounts of phenanthrene (Figure 3.29). The growth rates confirmed that phenanthrene is not toxic to *P. fluorescens* cLP6a and, therefore, the EmhABC efflux system is not essential for growth in the presence of polycyclic aromatic hydrocarbons.

Although polycyclic aromatic hydrocarbons are not toxic to bacteria, metabolites formed during aromatic hydrocarbon degradation have a higher toxicity. Studies of naphthalene degradation by a *P. putida* strain demonstrated that the accumulation of catechol and other metabolites resulted in decreased cell viability (Park *et al.* 2004). Catechol was shown to accumulate in the culture medium during naphthalene degradation, reaching a maximum concentration near the onset of stationary phase (Park *et al.* 2004). The study by Park *et al.* (2004) did not address the mechanism by which the catechol was extruded from the cell. Given the prevalence of broad specificity RND efflux pumps in *P. putida* strains and their role in the transport of toluene and polycyclic aromatic hydrocarbons, an RND efflux pump may be responsible for the catechol export observed by Park *et al.* (2004). Interestingly, the growth-phase dependent expression

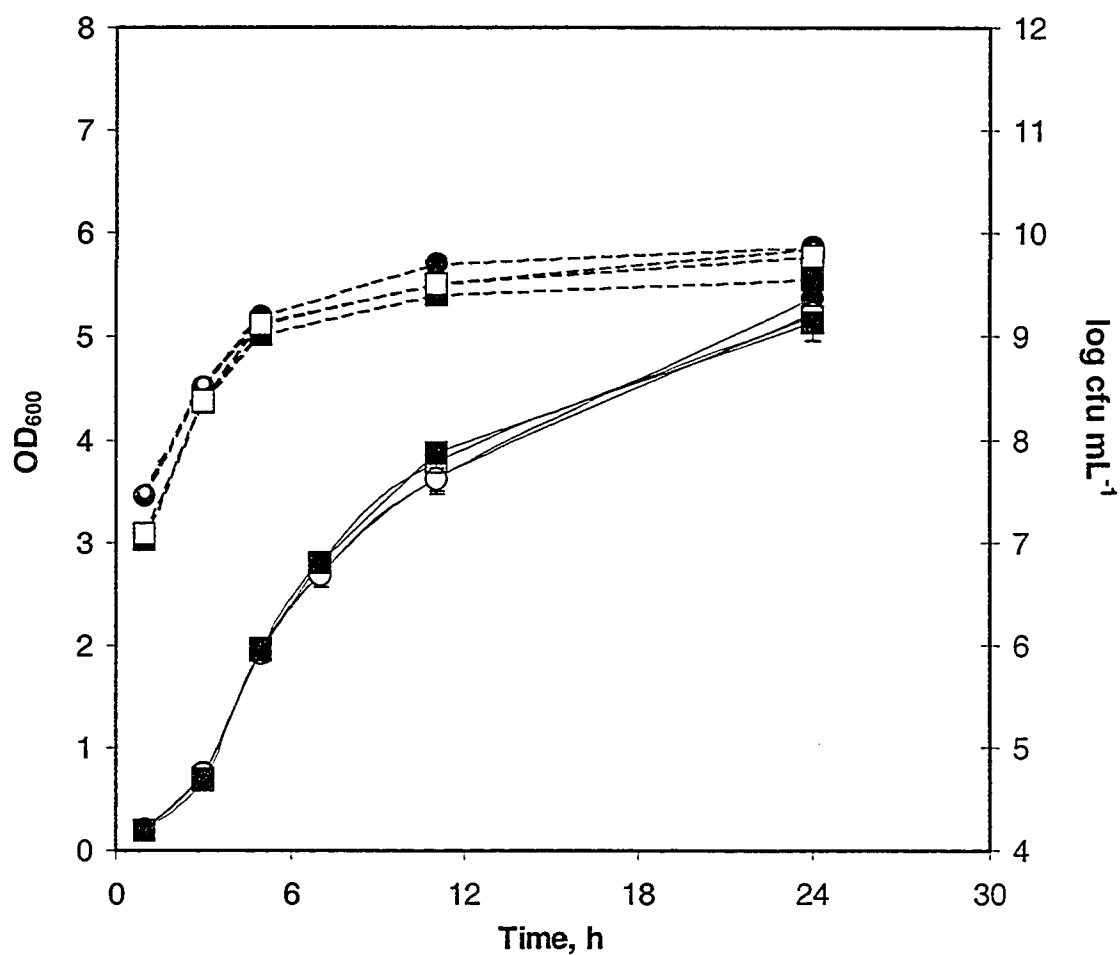


Figure 3.29. Comparison of growth rates of *P. fluorescens* cLP6a (circles) and the EmhB-disruption mutant cLP6a-1 (squares) in the presence of phenanthrene. The strains were grown in TSB in the presence (open symbols) and in the absence (closed symbols) of saturating amounts of phenanthrene. The OD₆₀₀ (solid lines) and number of colony forming units (cfu mL⁻¹) (dashed lines) were measured at various time intervals. Error bars (where visible) represent \pm one standard deviation.

profile of the EmhABC efflux pump (Figure 3.13), which showed a maximum at mid-exponential phase, is consistent with the growth-phase dependent excretion of catechol into the medium in the naphthalene-degrading *P. putida* strain. Further studies examining the specificity of the EmhABC system for metabolites of aromatic hydrocarbon degradation and comparing the rates of phenanthrene degradation by *P. fluorescens* LP6a with and without the EmhABC efflux system are required to resolve the role of the efflux system in hydrocarbon degradation in this organism.

3.5.4. Significance of the EmhABC efflux system in *P. fluorescens*

The function of the EmhABC efflux system in *P. fluorescens* LP6a likely is not solely the removal of toxic metabolites formed during aromatic hydrocarbon degradation, and this hypothesis is supported by several lines of evidence. Phenanthrene efflux is independent of the ability to degrade hydrocarbons, since it was observed in non-degrading species, as well as in toluene and polycyclic aromatic hydrocarbon degraders (Table 3.11). The location of the *emhABC* genes on the chromosome, rather than on the plasmid carrying the hydrocarbon degradation genes in *P. fluorescens* LP6a, strengthens the argument that hydrocarbon efflux and degradation are not linked. Moreover, the efflux genes were not induced either by aromatic hydrocarbons or by inducers of the degradation genes (Figure 3.14 and Figure 3.15).

The EmhABC efflux system, and its homologues in *P. putida* and *P. aeruginosa*, may be part of a general detoxification mechanism for aromatic compounds that is utilized by gram-negative bacteria in the environment. The location of the efflux genes adjacent to genes putatively involved in the β -keto adipate pathway (Figure 3.5), which catabolizes catechol and protocatechuate to tricarboxylic acid cycle intermediates, supports this hypothesis. In soil, bacteria are exposed to a variety of phenolic compounds secreted by plants and from the degradation of lignin, and the β -keto adipate pathway is involved in the detoxification of these compounds (Harwood and Parales 1996). The RND efflux system may play a role in this detoxification process by preventing the accumulation of high levels of catechol and other toxic aromatic substrates, thereby maintaining a balance between the uptake of these toxic substrates into the cell and catabolism via the β -keto adipate pathway. Such a detoxification system would provide

bacteria with a selective advantage in the environment, which may explain the prevalence of RND efflux systems in gram-negative bacteria.

The broad specificity of the EmhABC and homologous RND efflux pumps may also provide a selective advantage to bacteria in environments contaminated with petroleum hydrocarbons or industrially produced toxic solvents. *P. fluorescens* LP6a was isolated from petroleum condensate-contaminated soil (Foght and Westlake 1996), and thus the EmhABC efflux system may have contributed to the survival of *P. fluorescens* LP6a in that environment. Both *P. putida* S12 and *P. putida* DOT-T1E were isolated from solvent-contaminated wastewater (Weber *et al.* 1993, Mosqueda *et al.* 1999). Thus, the evolution of specialized RND pumps for solvent efflux in these *P. putida* strains is not surprising.

While the acquisition of efflux pump-mediated antibiotic resistance by bacteria is detrimental from a clinical perspective, the broad specificity of the EmhABC and other RND efflux pumps for antibiotics may be beneficial for bacterial survival in the environment. A variety of soil bacteria produce antibiotics, and the presence of antibiotics in the environment may create a selection pressure for bacteria that possess these efflux pumps. Additionally, the presence of multidrug efflux pumps in gram-negative bacteria may be advantageous for their survival in the environment given the current trend to incorporate antimicrobial agents in consumer products, which have been identified as contaminants in the water system (Halden and Paull 2005). Thus, RND efflux pumps may be essential for the survival of beneficial bacteria in the environment, as well as contributing to multidrug resistance in pathogenic bacteria.

4. CONCLUSIONS AND FUTURE WORK

The identification and characterization of the EmhABC efflux system in *P. fluorescens* cLP6a provided insight into the evolution and function of RND efflux pumps. Characteristic of RND pumps, EmhABC has a broad substrate specificity for polycyclic aromatic hydrocarbons, toluene and hydrophobic antibiotics. The EmhB pump showed high homology to the *P. putida* and *P. aeruginosa* ArpB, TtgB and MexB multidrug and solvent efflux pumps, as well as to the *E. coli* multidrug efflux pump AcrB. EmhABC also showed homology to the solvent efflux systems SrpABC and TtgGHI that are responsible for high levels of toluene tolerance in *P. putida*. Although EmhABC pumps toluene, it does not confer toluene tolerance to the wild-type *P. fluorescens* cLP6a. Unlike the SrpABC and TtgGHI solvent efflux systems, expression of EmhABC is not induced by aromatic hydrocarbons but is induced by the hydrophobic antibiotics tetracycline and chloramphenicol. The similarities in protein sequence and substrate specificity between the *P. fluorescens* EmhABC system and the multidrug and solvent efflux systems in *P. putida*, *P. aeruginosa* and *E. coli* suggest a common evolutionary origin for these RND efflux systems. The regulation of RND efflux pump expression, however, is more divergent, and the regulatory mechanisms may be related to the physiological significance of the efflux system.

The site-directed mutagenesis studies of the EmhB efflux pump presented here represent a preliminary attempt to characterize the mechanism of action of RND efflux pumps. The efflux pump is able to accommodate structurally diverse substrates in a large central cavity through nonspecific interactions with phenylalanine, alanine and aspartate residues. As well, substrates are predicted to enter the central cavity through a hydrophobic channel leading from two phenylalanine residues (F281 and F325) on the periplasmic surface of the protein and exit the pump through the funnel-shaped outer membrane protein docking domain.

The success of the mutagenesis approach in identifying amino acids in EmhB that are involved in determining substrate specificity and efflux activity demonstrated the effectiveness of the method for probing the structure-function relationships of the efflux pump. Other methods, such as random mutagenesis, cysteine-scanning mutagenesis coupled with the use of thiol-reactive substrate analogues, and X-ray crystallography with

bound substrates, will help to clarify the steps in the proposed model for substrate translocation in RND efflux pumps. The steps in the proposed model of substrate translocation in RND pumps that require further elucidation include confirmation of the hydrophobic substrate access channel leading into the central cavity, additional characterization of the pathway leading from the central cavity to the outer membrane protein, and investigation of the mechanism by which energy is transferred from proton translocation to substrate efflux. As well, the interactions between the RND efflux pump, the outer membrane channel and the membrane fusion protein need to be characterized further to understand how substrates are expelled efficiently to the extracellular environment. These structure-function studies with the RND efflux complex will aid in the design of pump inhibitors that will help to counteract the prevalence of efflux pump-mediated multidrug resistance in clinically important gram-negative bacteria.

In addition to the clinical significance, RND efflux pumps may have valuable applications in biocatalysis. Since many enzymatic reactions occur intracellularly, efflux systems may provide a useful mechanism to separate the desired product from the cells and, thereby, facilitate recycling of the biocatalyst. Future studies examining the role of the EmhABC efflux system on the transport of metabolites from aromatic hydrocarbon degradation will help to elucidate the role of the efflux system in biodegradation, as well as expand the potential of the system for biocatalysis applications. The ability to alter the substrate specificity of the EmhB efflux pump by mutation of single residues suggests that the selectivity of the pump can be optimized for selective separations. Gene shuffling between RND efflux pump genes may generate efflux pumps with novel substrate specificities that may be useful for biocatalysis.

The studies with the *P. fluorescens* EmhABC efflux system presented here, as well as future studies to understand the mechanism of action and the regulation of RND efflux systems in gram-negative bacteria, are significant from a clinical perspective and for biocatalysis applications.

5. REFERENCES

- Aires, J. R., T. Köhler, H. Nikaido and P. Plesiat. 1999. Involvement of an active efflux system in the natural resistance of *Pseudomonas aeruginosa* to aminoglycosides. *Antimicrob. Agents Chemother.* **43**:2624-2628.
- Aires, J. R. and H. Nikaido. 2005. Aminoglycosides are captured from both periplasm and cytoplasm by the AcrD multidrug efflux transporter of *Escherichia coli*. *J. Bacteriol.* **187**:1923-1929.
- Aires, J. R., J.-C. Pechère, C. van Delden and T. Köhler. 2002. Amino acid residues essential for function of the MexF efflux pump protein of *Pseudomonas aeruginosa*. *Antimicrob. Agents Chemother.* **46**:2169-2173.
- Akama, H., M. Kanemaki, M. Yoshimura, T. Tsukihara, T. Kashiwagi, H. Yoneyama, S. Narita, A. Nakagawa and T. Nakae. 2004. Crystal structure of the drug discharge outer membrane protein, OprM, of *Pseudomonas aeruginosa*: dual modes of membrane anchoring and occluded cavity end. *J. Biol. Chem.* **279**:52816-52819.
- Altschul, S. F., W. Gish, W. Miller, E. W. Myers and D. J. Lipman. 1990. Basic local alignment search tool. *J. Mol. Biol.* **215**:403-410.
- Aono, R. and H. Kobayashi. 1997. Cell surface properties of organic solvent-tolerant mutants of *Escherichia coli* K-12. *Appl. Environ. Microbiol.* **63**:3637-3642.
- Bagdasarian, M., R. Lurz, B. Rückert, F. C. Franklin, M. M. Bagdasarian, J. Frey and K. N. Timmis. 1981. Specific-purpose plasmid cloning vectors. II. Broad host range, high copy number, RSF1010-derived vectors, and a host vector system for gene cloning in *Pseudomonas*. *Gene* **16**:237-247.
- Barnsley, E. A. 1975. The induction of the enzymes of naphthalene metabolism in pseudomonads by salicylate and 2-aminobenzoate. *J. Gen. Microbiol.* **88**:193-196.
- Beinlich, K. L., R. Chuanchuen and H. P. Schweizer. 2001. Contribution of multidrug efflux pumps to multiple antibiotic resistance in veterinary clinical isolates of *Pseudomonas aeruginosa*. *FEMS Microbiol. Lett.* **198**:129-134.
- Bell, S. G., X. Chen, F. Xu, Z. Rao and L.-L. Wong. 2003. Engineering substrate recognition in catalysis by cytochrome P450cam. *Biochem. Soc. Trans.* **31**:558-562.
- Berens, C. and W. Hillen. 2003. Gene regulation by tetracyclines: constraints for resistance regulation in bacteria shape TetR for application in eukaryotes. *Eur. J. Biochem.* **270**:3109-3121.

- Brinkman, A. B., T. J. Ettema, W. M. de Vos and J. van der Oost. 2003. The Lrp family of transcriptional regulators. *Mol. Microbiol.* **48**:287-294.
- Bugg, T., J. M. Foght, M. A. Pickard and M. R. Gray. 2000. Uptake and active efflux of polycyclic aromatic hydrocarbons by *Pseudomonas fluorescens* LP6a. *Appl. Environ. Microbiol.* **66**:5387-5392.
- Cerniglia, C. E. 1992. Biodegradation of polycyclic aromatic hydrocarbons. *Biodegradation.* **3**:351-368.
- Chen, J., Y. Morita, M. N. Huda, T. Kuroda, T. Mizushima and T. Tsuchiya. 2002. VmrA, a member of a novel class of Na(+)-coupled multidrug efflux pumps from *Vibrio parahaemolyticus*. *J. Bacteriol.* **184**:572-576.
- Chuanchuen, R., C. T. Narasaki and H. P. Schweizer. 2002. The MexJK Efflux pump of *Pseudomonas aeruginosa* requires OprM for antibiotic efflux but not for efflux of triclosan. *J. Bacteriol.* **184**:5036-5044.
- Compeau, G., B. J. Al-Achi, E. Platsouka and S. B. Levy. 1998. Survival of rifampin-resistant mutants of *Pseudomonas fluorescens* and *Pseudomonas putida* in soil systems. *Appl. Environ. Microbiol.* **54**:2432-2438.
- Cowles, C. E., N. N. Nichols and C. S. Harwood. 2000. BenR, a XylS homologue, regulates three different pathways of aromatic acid degradation in *Pseudomonas putida*. *J. Bacteriol.* **182**:6339-6346.
- de Bont, J. A. M. 1998. Solvent-tolerant bacteria in biocatalysis. *Trends in Biotechnol.* **16**:493-499.
- Dunn, A. R., I. J. Dmochowski, A. M. Bilwes, H. B. Gray and B. R. Crane. 2001. Probing the open state of cytochrome P450cam with ruthenium-linker substrates. *Proc. Natl. Acad. Sci.* **98**:12420-12425.
- Dunn, N. W. and I. C. Gunsalus. 1973. Transmissible plasmids coding early enzymes of naphthalene oxidation in *Pseudomonas putida*. *J. Bacteriol.* **114**:974-979.
- Duque, E., A. Segura, G. Mosqueda and J. L. Ramos. 2001. Global and cognate regulators control the expression of the organic solvent efflux pumps TtgABC and TtgDEF of *Pseudomonas putida*. *Mol. Microbiol.* **39**:1100-1106.
- Eastcott, L., W. Y. Shiu and D. Mackay. 1988. Environmentally relevant physical-chemical properties of hydrocarbons: a review of data and development of simple correlations. *Oil and Chemical Pollution.* **4**:191-216.

- Eda, S., H. Maseda and T. Nakae. 2003. An elegant means of self-protection in Gram-negative bacteria by recognizing and extruding xenobiotics from the periplasmic space. *J. Biol. Chem.* **278**:2085-2088.
- Elkins, C. A. and H. Nikaido. 2002. Substrate specificity of the RND-type multidrug efflux pumps *acrB* and *AcrD* of *Escherichia coli* is determined predominantly by two large periplasmic loops. *J. Bacteriol.* **184**:6490-6498.
- Eulberg, D. and M. Schlömann. 1998. The putative regulator of catechol catabolism in *Rhodococcus opacus* 1CP – an IclR-type, not a LysR-type transcriptional regulator. *Antonie van Leeuwenhoek* **74**:71-82.
- Felsenstein, J. 2004. PHYLIP (Phylogeny Inference Package) version 3.6. Distributed by the author. Department of Genome Sciences, University of Washington, Seattle.
- Fernandez-Recio, J., F. Walas, L. Federici, J. V. Pratap, V. N. Bavro, R. N. Miguel, K. Mizuguchi and B. Luisi. 2004. A model of a transmembrane drug-efflux pump from Gram-negative bacteria. *FEBS Lett.* **578**:5-9.
- Foght, J. M. and D. W. S. Westlake. 1996. Transposon and spontaneous deletion mutants of plasmid-borne genes encoding polycyclic aromatic hydrocarbon degradation by a strain of *Pseudomonas fluorescens*. *Biodegradation* **7**:353-356.
- Goldberg, M., T. Pribyl, S. Juhnke, and D. H. Nies. 1999. Energetics and topology of CzcA, a cation/proton antiporter of the resistance-nodulation-cell division protein family. *J. Biol. Chem.* **274**:26065-26070.
- Griffith, K. L. and R. E. Wolf, Jr. 2002. Measuring β -galactosidase activity in bacteria: cell growth, permeabilization, and enzyme assays in 96-well arrays. *Biochem. Biophys. Res. Commun.* **290**:397-402.
- Grkovic, S., M. H. Brown and R. A. Skurray. 2001. Transcriptional regulation of multidrug efflux pumps in bacteria. *Sem. Cell Dev. Biol.* **12**:225-237.
- Guan, L. and T. Nakae. 2001. Identification of essential charged residues in transmembrane segments of the multidrug transporter MexB of *Pseudomonas aeruginosa*. *J. Bacteriol.* **183**:1734-1739.
- Guazzaroni, M.-E., T. Krell, A. Felipe, R. Ruiz, C. Meng, X. Zhang, M.-T. Gallegos and J. L. Ramos. 2005. The multidrug efflux regulator TtgV recognizes a wide range of structurally different effectors in solution and complexed with target DNA: evidence from isothermal titration calorimetry. *J. Biol. Chem.* **280**:20887-20893.
- Guazzaroni, M.-E., W. Terán, X. Zhang, M.-T. Gallegos and J. L. Ramos. 2004. TtgV bound to a complex operator site represses transcription of the promoter for the multidrug and solvent extrusion TtgGHI pump. *J. Bacteriol.* **186**:2921-2927.

- Guex, N. and M. C. Peitsch. 1997. SWISS-MODEL and the Swiss-PdbViewer: an environment for comparative protein modeling. *Electrophoresis* **18**:2714-2723.
- Halden, R. U. and D. H. Paull. 2005. Co-occurrence of triclocarban and triclosan in U.S. water resources. *Environ. Sci. Technol.* **39**:1420-1426.
- Hardman, A. M., G. S. Stewart and P. Williams. 1998. Quorum sensing and the cell-cell communication dependent regulation of gene expression in pathogenic and non-pathogenic bacteria. *Antonie van Leeuwenhoek* **74**:199-210.
- Harwood, C. S. and R. E. Parales. 1996. The β -ketoacid pathway and the biology of self-identity. *Annu. Rev. Microbiol.* **50**:553-590.
- Hays, A. A., A. R. Dunn, R. Chiu, H. B. Gray, C. D. Stout and D. B. Goodin. 2004. Conformational states of cytochrome P450cam revealed by trapping of synthetic molecular wires. *J. Mol. Biol.* **344**:455-469.
- Hearn, E. M., J. J. Dennis, M. R. Gray and J. M. Foght. 2003. Identification and characterization of the *emhABC* efflux system for polycyclic aromatic hydrocarbons in *Pseudomonas fluorescens* cLP6a. *J. Bacteriol.* **185**:6233-6240.
- Higgins, M. K., E. Bokma, E. Koronakis, C. Hughes and V. Koronakis. 2004. Structure of the periplasmic component of a bacterial drug efflux pump. *Proc. Natl. Acad. Sci.* **101**:9994-9999.
- Hillen, W. and C. Berens. 1994. Mechanisms underlying expression of *Tn10* encoded tetracycline resistance. *Annu. Rev. Microbiol.* **48**:345-369.
- Holloway, B. W. 1969. Genetics of *Pseudomonas*. *Bacteriol. Rev.* **33**:419-443.
- Horton, R. M., H. D. Hunt, S. N. Ho, J. K. Pullen and L. R. Pease. 1989. Engineering hybrid genes without the use of restriction enzymes: gene splicing by overlap extension. *Gene* **77**:61-68.
- Inoue, H., H. Nojima and H. Okayama. 1990. High efficiency transformation of *Escherichia coli* with plasmids. *Gene* **96**:23-28.
- Isken, S. and J. A. M. de Bont. 1996. Active efflux of toluene in a solvent-resistant bacterium. *J. Bacteriol.* **178**:6056-6058.
- Isken, S. and de Bont, J.A.M. 2000. The solvent efflux system of *Pseudomonas putida* S12 is not involved in antibiotic resistance. *Appl. Microbiol. Biotechnol.* **54**:711-714.

- Johnsen, A. R., L. Y. Wick and H. Harms. 2005. Principles of microbial PAH-degradation in soil. *Environ. Pollut.* **133**:71-84.
- Jorgensen, J. H., J. D. Turnridge and J. A. Washington. 1999. Antibacterial susceptibility tests: dilution and disk diffusion methods, p. 1526-1543. *In* P. R. Murray, E. J. Baron, M. A. Tenover and R. H. Tenover (ed.), *Manual of clinical microbiology*, 7th ed. American Society for Microbiology, Washington, D.C.
- Josephy, P. D. 1997. Cytochrome P-450, pp. 209-247. *In* *Molecular Toxicology*. Oxford University Press, New York.
- Kieboom, J. and J. A. M. de Bont. 2001. Identification and molecular characterization of an efflux system involved in *Pseudomonas putida* S12 multidrug resistance. *Microbiology*. **147**:43-51.
- Kieboom, J., J. J. Dennis, J. A. M. de Bont and G. J. Zylstra. 1998a. Identification and molecular characterization of an efflux pump involved in *Pseudomonas putida* S12 solvent tolerance. *J. Biol. Chem.* **273**:85-91.
- Kieboom, J., J. J. Dennis, G. J. Zylstra and J. A. M. de Bont. 1998b. Active efflux of organic solvents by *Pseudomonas putida* S12 is induced by solvents. *J. Bacteriol.* **180**:6769-6772.
- Köhler, T., M. Michea-Hamzehpour, U. Henze, N. Gotoh, L. K. Curty and J. C. Pechere. 1997. Characterization of MexE-MexF-OprN, a positively regulated multidrug efflux system of *Pseudomonas aeruginosa*. *Mol. Microbiol.* **23**:345-354.
- Koronakis, V., A. Sharff, E. Koronakis, B. Luisi and C. Hughes. 2000. Crystal structure of the bacterial membrane protein TolC central to multidrug efflux and protein export. *Nature*. **405**:914-919.
- Li, X.-Z., N. Barre and K. Poole. 2000. Influence of the MexA-MexB-OprM multidrug efflux system on expression of the MexC-MexD-OprJ and MexE-MexF-OprN multidrug efflux systems in *Pseudomonas aeruginosa*. *J. Antimicrob. Chemother.* **46**:885-893.
- Li, X.-Z. and K. Poole. 2001. Mutational analysis of the OprM outer membrane component of the MexA-MexB-OprM multidrug efflux system of *Pseudomonas aeruginosa*. *J. Bacteriol.* **183**:12-27.
- Li, X.-Z., H. Nikaido and K. Poole. 1995. Role of MexA-MexB-OprM in antibiotic efflux in *Pseudomonas aeruginosa*. *Antimicrob. Agents Chemother.* **39**:1948-1953.

- Li, X-Z., L. Zhang and K. Poole. 1998. Role of the multidrug efflux systems of *Pseudomonas aeruginosa* in organic solvent tolerance. *J. Bacteriol.* **180**:2987-2991.
- Li, Y., T. Mima, Y. Komori, Y. Morita, T. Kuroda, T. Mizushima and T. Tsuchiya. 2003. A new member of the tripartite multidrug efflux pumps, MexVW-OprM, in *Pseudomonas aeruginosa*. *J. Antimicrob. Chemother.* **52**:572-575.
- Llanes, C., D. Hocquet, C. Vogne, D. Benali-Baitich, C. Neuwirth and P. Plésiat. 2004. Clinical strains of *Pseudomonas aeruginosa* overproducing MexAB-OprM and MexXY efflux pumps simultaneously. *Antimicrob. Agents Chemother.* **48**:1797-1802.
- Loo, T. W., M. C. Bartlett and D. M. Clarke. 2003a. Simultaneous binding of two different drugs in the binding pocket of the human multidrug resistance P-glycoprotein. *J. Biol. Chem.* **278**:39706-39710.
- Loo, T. W., M. C. Bartlett and D. M. Clarke. 2003b. Substrate-induced conformational changes in the transmembrane segments of human P-glycoprotein: direct evidence for the substrate-induced fit mechanism for drug binding. *J. Biol. Chem.* **278**:13603-13606.
- Loo, T. W., M. C. Bartlett and D. M. Clarke. 2004. The drug-binding pocket of the human multidrug resistance P-glycoprotein is accessible to the aqueous medium. *Biochemistry* **43**: 12081-12089.
- Loo, T. W. and D. M. Clarke. 1999. Molecular dissection of the human multidrug resistance P-glycoprotein. *Biochem. Cell Biol.* **77**:11-23.
- Loo, T. W. and D. M. Clarke. 2000. Identification of residues within the drug-binding domain of the human multidrug resistance P-glycoprotein by cysteine-scanning mutagenesis and reaction with dibromobimane. *J. Biol. Chem.* **275**:39272-39278.
- Loo, T. W. and D. M. Clarke. 2002. Location of the rhodamine-binding site in the human multidrug resistance P-glycoprotein. *J. Biol. Chem.* **277**:44332-44338.
- Loo, T. W. and D. M. Clarke. 2005. Do drug substrates enter the common drug-binding pocket of P-glycoprotein through "gates"? *Biochem. Biophys. Res. Commun.* **329**:419-422.
- Mahenthiralingam, E., T. Coenye, J. W. Chung, D. P. Speert, J. R. Govan, P. Taylor, and P. Vandamme. 2000. Diagnostically and experimentally useful panel of strains from the *Burkholderia cepacia* complex. *J. Clin. Microbiol.* **38**:910-913.

- Maloy, S. R. 1990. Experimental techniques in bacterial genetics. Jones and Bartlett Publishers Inc., Boston, Mass.
- Mao, W., M. S. Warren, D. S. Black, T. Satou, T. Murata, T. Nishino, N. Gotoh and O. Lomovskaya. 2002. On the mechanism of substrate specificity by resistance nodulation division (RND)-type multidrug resistance pumps: the large periplasmic loops of MexD from *Pseudomonas aeruginosa* are involved in substrate recognition. *Mol. Microbiol.* **46**:889-901.
- Maseda, H., I. Sawada, K. Saito, H. Uchiyama, T. Nakae and N. Nomura. 2004. Enhancement of the *mexAB-oprM* efflux pump expression by a quorum-sensing autoinducer and its cancellation by a regulator, MexT, of the *mexEF-oprN* efflux pump operon in *Pseudomonas aeruginosa*. *Antimicrob. Agents Chemother.* **48**:1320-1328.
- Masuda, N., E. Sakagawa, S. Ohya, N. Gotoh, H. Tsujimoto and T. Nishino. 2000. Substrate specificities of MexAB-OprM, MexCD-OprJ, and MexXY-OprM efflux pumps in *Pseudomonas aeruginosa*. *Antimicrob. Agents Chemother.* **44**:3322-3327.
- Matsuo, Y., S. Eda, N. Gotoh, E. Yoshihara and T. Nakae. 2004. MexZ-mediated regulation of *mexXY* multidrug efflux pump expression in *Pseudomonas aeruginosa* by binding on the *mexZ-mexX* intergenic DNA. *FEMS Microbiol. Lett.* **238**:23-28.
- Middlemiss, J. K. and K. Poole. 2004. Differential impact of MexB mutations on substrate selectivity of the MexAB-OprM multidrug efflux pump of *Pseudomonas aeruginosa*. *J. Bacteriol.* **186**:1258-1269.
- Miller, J. H. 1972. Experiments in molecular genetics. Cold Spring Harbor Laboratory Press, Cold Spring Harbor, N.Y.
- Mosqueda, G. and J. L. Ramos. 2000. A set of genes encoding a second toluene efflux system in *Pseudomonas putida* DOT-T1E is linked to the *tod* genes for toluene metabolism. *J. Bacteriol.* **182**:937-943.
- Mosqueda, G., M. I. Ramos-Gonzalez and J. L. Ramos. 1999. Toluene metabolism by the solvent-tolerant *Pseudomonas putida* DOT-T1 strain, and its role in solvent impermeabilization. *Gene.* **232**:69-76.
- Murakami, S., R. Nakashima, E. Yamashita and A. Yamaguchi. 2002. Crystal structure of bacterial multidrug efflux transporter AcrB. *Nature* **419**:587-593.
- Murakami, S., N. Tamura, A. Saito, T. Hirata and A. Yamaguchi. 2004. Extramembrane central pore of multidrug exporter AcrB in *Escherichia coli* plays an important role in drug transport. *J. Biol. Chem.* **279**:3743-3748.

- Nehme, D., X.-Z. Li, R. Elliot and K. Poole. 2004. Assembly of the MexAB-OprM multidrug efflux system of *Pseudomonas aeruginosa*: identification and characterization of mutations in *mexA* compromising MexA multimerization and interaction with MexB. *J. Bacteriol.* **186**:2973-2983.
- Neyfakh, A. A., V. E. Bidnenko and L.B. Chen. 1991. Efflux-mediated multidrug resistance in *Bacillus subtilis*: similarities and dissimilarities with the mammalian system. 1991. *Proc. Natl. Acad. Sci.* **88**:4781-4785.
- Nikaido, H. 1996. Multidrug efflux pumps of Gram-negative bacteria. *J. Bacteriol.* **178**:5853-5859.
- Nikaido, H. 2000. How do exported proteins and antibiotics bypass the periplasm in Gram-negative bacterial cells? *Trends Microbiol.* **8**:481-483.
- Olivera, E. R., B. Minambres, B. Garcia, C. Muniz, M. A. Morena, A. Ferrandez, E. Diaz, J. L. Garcia and J. M. Luengo. 1998. Molecular characterization of the phenylacetic acid catabolic pathway in *Pseudomonas putida* U: the phenylacetyl-CoA catabolon. *Proc. Acad. Natl. Sci.* **95**:6419-6424.
- Page, R. D. 1996. TREEVIEW: An application to display phylogenetic trees on personal computers. *Comput. Appl. Biosci.* **12**:357-358.
- Paget, M. S. and J. D. Helmann. 2003. The σ^{70} family of sigma factors. *Genome Biol.* **4**:203.
- Park, W., C. O. Jeon, H. Cadillo, C. DeRito and E. L. Madsen. 2004. Survival of naphthalene-degrading *Pseudomonas putida* NCIB9816-4 in naphthalene-amended soils: toxicity of naphthalene and its metabolites. *Appl. Microbiol. Biotechnol.* **64**:429-435.
- Paulsen, I. T., M. H. Brown and R. A. Skurray. 1996. Proton-dependent multidrug efflux systems. *Microbiol. Rev.* **60**:575-608.
- Pearson, J. P., C. van Delden and B. H. Iglewski. 1999. Active efflux and diffusion are involved in transport of *Pseudomonas aeruginosa* cell-to-cell signals. *J. Bacteriol.* **181**:1203-1210.
- Pessi, G., C. Blumer and D. Haas. 2001. *lacZ* fusions report gene expression, don't they? *Microbiology* **147**:1993-1995.
- Phoenix, P., A. Keane, A. Patel, H. Bergeron, S. Goshal and P. C. K. Lau. 2003. Characterization of a new solvent-responsive gene locus in *Pseudomonas putida* F1 and its functionalization as a versatile biosensor. *Environ. Microbiol.* **5**: 309-1327.

- Pinkart, H. C. and D. C. White. 1997. Phospholipid biosynthesis and solvent tolerance in *Pseudomonas putida* strains. *J. Bacteriol.* **179**:4219-4226.
- Pleban, K., S. Kopp, E. Csaszar, M. Peer, T. Hrebicek, A. Rizzi, G. F. Ecker and P. Chiba. 2005. P-glycoprotein substrate binding domains are located at the transmembrane domain/transmembrane domain interfaces: a combined photoaffinity labeling-protein homology modeling approach. *Mol. Pharmacol.* **67**:365-374.
- Poole, K. 2004. Efflux-mediated multiresistance in Gram-negative bacteria. *Clin. Microbiol. Infect.* **10**:12-26.
- Poole, K., N. Gotoh, H. Tsujimoto, Q. Zhao, A. Wada, T. Yamasaki, S. Neshat, J. Yamagishi, X. Z. Li and T. Nishino. 1996a. Overexpression of the *mexC-mexD-oprJ* efflux operon in *nfx-B* type multidrug-resistant strains of *Pseudomonas aeruginosa*. *Mol. Microbiol.* **21**:713-724.
- Poole, K., K. Tetro, Q. Zhao, S. Neshat, D. E. Heinrichs and N. Bianco. 1996b. Expression of the multidrug resistance operon *mexA-mexB-oprM* in *Pseudomonas aeruginosa*: *mexR* encodes a regulator of operon expression. *Antimicrob. Agents Chemother.* **40**:2021-2028.
- Poulos, T. L., B. C. Finzel and A. J. Howard. 1986. Crystal structure of substrate-free *Pseudomonas putida* cytochrome P-450. *Biochemistry* **25**:5314-5322.
- Raag, R. and T. L. Poulos. 1991. Crystal structures of cytochrome P-450_{CAM} complexed with camphane, thiocamphor, and adamantane: factors controlling P-450 substrate hydroxylation. *Biochemistry* **30**:2674-2684.
- Ramos, J. L., E. Duque, P. Godoy and A. Segura. 1998. Efflux pumps involved in toluene tolerance in *Pseudomonas putida* DOT-T1E. *J. Bacteriol.* **180**:3323-3329.
- Ramos, J. L., E. Duque, J. J. Rodriguez-Herva, P. Godoy, A. Haidour, F. Reyes and A. Fernandez-Barrero. 1997. Mechanisms for solvent tolerance in bacteria. *J. Biol. Chem.* **272**:3887-3890.
- Rojas, A., E. Duque, G. Mosqueda, G. Golden, A. Hurtado, J. L. Ramos and A. Segura. 2001. Three efflux pumps are required to provide efficient tolerance to toluene in *Pseudomonas putida* DOT-T1E. *J. Bacteriol.* **183**:3967-3973.
- Rojas, A., A. Segura, M. E. Guazzaroni, W. Terán, A. Hurtado, M. T. Gallegos and J. L. Ramos. 2003. In vivo and in vitro evidence that TtgV is the specific regulator of the TtgGHI multidrug and solvent efflux pump of *Pseudomonas putida*. *J. Bacteriol.* **185**:4755-4763.

- Romero-Steiner, S., R. E. Parales, C. S. Harwood and J. E. Houghton. 1994. Characterization of the *pcaR* regulatory gene from *Pseudomonas putida*, which is required for the complete degradation of *p*-hydroxybenzoate. *J. Bacteriol.* **176**: 771-5779.
- Rosenberg, E. Y., D. Ma and H. Nikaido. 2000. AcrD of *Escherichia coli* is an aminoglycoside efflux pump. *J. Bacteriol.* **182**: 1754-1756.
- Saier, M. H. Jr. and I. T. Paulsen. 2001. Phylogeny of multidrug transporters. *Semin. Cell Dev. Biol.* **12**:205-213.
- Saier, M. H. Jr., I. T. Paulsen, M. K. Sliwinski, S. S. Pao, R. A. Skurray and H. Nikaido. 1998. Evolutionary origins of multidrug and drug-specific efflux pumps in bacteria. *FASEB J.* **12**:265-274.
- Sambrook, J., E. F. Fritsch and T. Maniatis. 1989. *Molecular cloning: a laboratory manual*, 2nd ed. Cold Spring Harbor Laboratory Press, Cold Spring Harbor, N.Y.
- Sánchez, P., A. Alonso and J. L. Martínez. 2002a. Cloning and characterization of SmeT, a repressor of the *Stenotrophomonas maltophilia* multidrug efflux pump SmeDEF. *Antimicrob. Agents Chemother.* **46**:3386-3393.
- Sánchez, P., F. Rojo and J. L. Martínez. 2002b. Transcriptional regulation of *mexR*, the repressor of *Pseudomonas aeruginosa mexAB-oprM* multidrug efflux pump. *FEMS Microbiol. Lett.* **207**:63-68.
- Sawada, I., H. Maseda, T. Nakae, H. Uchiyama and N. Nomura. 2004. A quorum-sensing autoinducer enhances the *mexAB-oprM* efflux-pump expression without MexR-mediated regulation in *Pseudomonas aeruginosa*. *Microbiol. Immunol.* **48**:435-439.
- Schlichting, I., J. Berendzen, K. Chu, A. M. Stock, S. A. Maves, D. E. Benson, R. M. Sweet, D. Ringe, G. A. Petsko and S. G. Sligar. 2000. The catalytic pathway of cytochrome P450cam at atomic resolution. *Science* **287**:1615-1622.
- Schuldiner, S., M. Lebendiker and H. Yerushalmi. 1997. EmrE, the smallest ion-coupled transporter, provides a unique paradigm for structure-function studies. *J. Exp. Biol.* **200**:335-341.
- Schumacher, M. A., M. C. Miller and R. G. Brennan. 2004. Structural mechanism of the simultaneous binding of two drugs to a multidrug-binding protein. *EMBO J.* **23**:2923-2930.
- Schweizer, H. P. 2001. Vectors to express foreign genes and techniques to monitor gene expression in pseudomonads. *Curr. Opin. Biotechnol.* **12**:439-445.

- Schweizer, H. P. and R. Chuanchuen. 2001. Small broad-host-range *lacZ* operon fusion vector with low background activity. *Biotechniques*. **31**:1258-1262.
- Segura, A., E. Duque, G. Mosqueda, J. L. Ramos and F. Junker. 1999. Multiple responses of Gram-negative bacteria to organic solvents. *Environ. Microbiol.* **1**:191-198.
- Segura, A., E. Duque, A. Rojas, P. Godoy, A. Delgado, A. Hurtado, J. E. Cronan Jr. and J. L. Ramos. 2004. Fatty acid biosynthesis is involved in solvent tolerance in *Pseudomonas putida* DOT-T1E. *Environ. Microbiol.* **6**:416-423.
- Segura, A., A. Rojas, A. Hurtado, M.-J. Huertas and J. L. Ramos. 2003. Comparative genomic analysis of solvent extrusion pumps in *Pseudomonas* strains exhibiting different degrees of solvent tolerance. *Extremophiles* **7**:371-376.
- Sikkema, J., J. A. M. de Bont and B. Poolman. 1994. Interactions of cyclic hydrocarbons with biological membranes. *J. Biol. Chem.* **269**:8022-8028.
- Sikkema, J., J. A. M. de Bont and B. Poolman. 1995. Mechanisms of membrane toxicity of hydrocarbons. *Microbiol. Rev.* **59**:201-222.
- Stothard, P. 2000. The sequence manipulation suite: JavaScript programs for analyzing and formatting protein and DNA sequences. *Biotechniques* **28**:1102-1104.
- Stover, C. K., X. Q. Pham, A. L. Erwin, S. D. Mizoguchi, P. Warrener, M. J. Hickey, F. S. Brinkman, W. O. Hufnagle, D. J. Kowalik, M. Lagrou, R. L. Garber, L. Goltry, E. Tolentino, S. Westbrook-Wadman, Y. Yuan, L. L. Brody, S. N. Coulter, K. R. Folger, A. Kas, K. Larbig, R. Lim, K. Smith, D. Spenser, G. K. Wong, A. We, I. T. Paulsen, J. Reizer, M. H. Saier, R. E. Hancock, S. Lory and M. V. Olson. 2000. Complete genome sequence of *Pseudomonas aeruginosa* PA01, an opportunistic pathogen. *Nature* **406**:959-964.
- Sunnarborg, A., D. Klumpp, T. Chung and D. C. LaPorte. 1990. Regulation of the glyoxylate bypass operon: cloning and characterization of *iclR*. *J. Bacteriol.* **172**:2642-2649.
- Terán, W., A. Felipe, A. Segura, A. Rojas, J. L. Ramos and M.-T. Gallegos. 2003. Antibiotic-dependent induction of *Pseudomonas putida* DOT-T1E TtgABC efflux pump is mediated by the drug binding repressor TtgR. *Antimicrob. Agents Chemother.* **47**:3067-3072.
- Thompson, J. D., T. J. Gibson, F. Plewniak, F. Jeanmougin and D. G. Higgins. 1997. The ClustalX windows interface: flexible strategies for multiple sequence alignment aided by quality analysis tools. *Nucleic Acids Res.* **25**:4876-4882.

- Tikhonova, E. B., Q. Wang, and H. I. Zgurskaya. 2002. Chimeric analysis of the multicomponent multidrug efflux transporters from Gram-negative bacteria. *J. Bacteriol.* **184**: 6499-6507.
- Tseng T. T., K. S. Gratwick, J. Kollman, D. Park, D. H. Nies, A. Goffeau and M. H. Saier Jr. 1999. The RND permease superfamily: an ancient, ubiquitous and diverse family that includes human disease and development proteins. *J. Mol. Microbiol. Biotechnol.* **1**:107-25.
- Van Hamme, J. D., A. Singh and O. P. Ward. 2003. Recent advances in petroleum microbiology. *Microbiol. Mol. Biol. Rev.* **67**:503-549.
- Walsh, T. A. and D. P. Ballou. 1983. Halogenated protocatechuates as substrates for protocatechuate dioxygenase from *Pseudomonas cepacia*. *J. Biol. Chem.* **258**:14413-14421.
- Weber, J. F. and J. A. M. de Bont. 1996. Adaptation mechanisms of microorganisms to the toxic effects of organic solvents on membranes. *Biochim. Biophys. Acta.* **1286**:225-245.
- Weber, J. F., S. Isken and J. A. M. de Bont. 1994. *Cis/trans* isomerization of fatty acids as a defence mechanism of *Pseudomonas putida* strains to toxic concentrations of toluene. *Microbiology* **140**:2013-2017.
- Weber, J. F., L. P. Ooijkaas, R. M. Schemen, S. Hartmans, and J. A. M. de Bont. 1993. Adaptation of *Pseudomonas putida* S12 to high concentrations of styrene and other organic solvents. *Appl. Environ. Microbiol.* **59**:3502-3504.
- Wery, J., B. Hidayat, J. Kieboom and J. A. M. de Bont. 2001. An insertion sequence prepares *Pseudomonas putida* S12 for severe solvent stress. *J. Biol. Chem.* **276**:5700-5706.
- West, S. E. H., H. P. Schweizer, C. Dall, A. K. Sample, and L. J. Runyen-Janecky. 1994. Construction of improved *Escherichia-Pseudomonas* shuttle vectors derived from pUC18/19 and sequence of the region required for their replication in *Pseudomonas aeruginosa*. *Gene* **148**:81-86.
- Williams, P. A., J. Cosme, D. M. Vinković, A. Ward, H. C. Angove, P. J. Day, C. Vonrhein, I. J. Tickle and H. Jhoti. 2004. Crystal structures of human cytochrome P450 3A4 bound to metyrapone and progesterone. *Science* **305**:683-686.
- Williams, P. A. and K. Murray. 1974. Metabolism of benzoate and methylbenzoates by *Pseudomonas putida* (*arvilla*) mt-2: evidence for the existence of a TOL plasmids. *J. Bacteriol.* **120**:416-423.

- Yoneyama, H.; A. Ocaktan, N. Gotoh, T. Nishino and T. Nakae. 1998. Subunit swapping in the Mex-extrusion pumps in *Pseudomonas aeruginosa*. *Biochem. Biophys. Res. Commun.* **244**: 898-902.
- Yu, E. W., G. McDermott, H. I. Zgurskaya, H. Nikaido and D. E. Koshland Jr. 2003a. Structural basis of multiple drug-binding capacity of the AcrB multidrug efflux pump. *Science* **300**:976-980.
- Yu, E. W., J. R. Aires, and H. Nikaido. 2003b. AcrB multidrug efflux pump of *Escherichia coli*: composite substrate-binding cavity of exceptional flexibility generates its extremely wide substrate specificity. *J. Bacteriol.* **185**:5657-5664.
- Zgurskaya, H. I. and H. Nikaido. 1999. AcrA is a highly asymmetric protein capable of spanning the periplasm. *J. Mol. Biol.* **285**:409-420.
- Zgurskaya, H. I. and H. Nikaido. 2000a. Multidrug resistance mechanisms: drug efflux across two membranes. *Mol. Microbiol.* **37**:219-225.
- Zgurskaya, H. I. and H. Nikaido. 2000b. Cross-linked complex between oligomeric periplasmic lipoprotein AcrA and the inner-membrane-associated multidrug efflux pump AcrB from *Escherichia coli*. *J. Bacteriol.* **182**: 4264-4267.
- Zheleznova, E. E., P. N. Markham, A. A. Neyfakh and R. G. Brennan. 1999. Structural basis of multidrug recognition by BmrR, a transcription activator of a multidrug transporter. *Cell* **96**: 353-362.